Hashemite Kingdom of Jordan

Jordan Journal of Biological Sciences

An International Peer-Reviewed Scientific Journal

Financed by the Scientific Research and Innovation Support Fund

This title is indexed in Scopus

http://jjbs.hu.edu.jo/

المجلة الأردنية للعلوم الحياتية
Jordan Journal of Biological Sciences (JJBS)
http://jjbs.hu.edu.jo

Jordan Journal of Biological Sciences (JJBS) (ISSN: 1995–6673 (Print); 2307-7166 (Online)):

An International Peer- Reviewed Open Access Research Journal financed by the Scientific Research and Innovation Support Fund, Ministry of Higher Education and Scientific Research, Jordan and published quarterly by the Deanship of Scientific Research , The Hashemite University, Jordan.

Submission Address

Professor Abu-Elteen, Khaled H

The Hashemite University
P.O. Box 330127, Zarqa, 13115, Jordan
Phone: +962-5-3903333 ext. 4357
E-Mail: jjbs@hu.edu.jo

المجلة الاردنية للعلوم الحياتية
Jordan Journal of Biological Sciences (JJBS)
http://jjbs.hu.edu.jo

International Advisory Board

Instructions to Authors

Scopes

Study areas include cell biology, genomics, microbiology, immunology, molecular biology, biochemistry, embryology, immunogenetics, cell and tissue culture, molecular ecology, genetic engineering and biological engineering, bioremediation and biodegradation, bioinformatics, biotechnology regulations, gene therapy, organismal biology, microbial and environmental biotechnology, marine sciences. The JJBS welcomes the submission of manuscript that meets the general criteria of significance and academic excellence. All articles published in JJBS are peer-reviewed. Papers will be published approximately one to two months after acceptance.

Type of Papers

The journal publishes high-quality original scientific papers, short communications, correspondence and case studies. Review articles are usually by invitation only. However, Review articles of current interest and high standard will be considered.

Submission of Manuscript

Manuscript, or the essence of their content, must be previously unpublished and should not be under simultaneous consideration by another journal. The authors should also declare if any similar work has been submitted to or published by another journal. They should also declare that it has not been submitted/ published elsewhere in the same form, in English or in any other language, without the written consent of the Publisher. The authors should also declare that the paper is the original work of the author(s) and not copied (in whole or in part) from any other work. All papers will be automatically checked for duplicate publication and plagiarism. If detected, appropriate action will be taken in accordance with International Ethical Guideline. By virtue of the submitted manuscript, the corresponding author acknowledges that all the co-authors have seen and approved the final version of the manuscript. The corresponding author should provide all co-authors with information regarding the manuscript, and obtain their approval before submitting any revisions. Electronic submission of manuscripts is strongly recommended, provided that the text, tables and figures are included in a single Microsoft Word file. Submit manuscript as e-mail attachment to the Editorial Office at: JJBS@hu.edu.jo. After submission, a manuscript number will be communicated to the corresponding author within 48 hours.

Peer-review Process

It is requested to submit, with the manuscript, the names, addresses and e-mail addresses of at least 4 potential reviewers. It is the sole right of the editor to decide whether or not the suggested reviewers to be used. The reviewers' comments will be sent to authors within 6-8 weeks after submission. Manuscripts and figures for review will not be returned to authors whether the editorial decision is to accept, revise, or reject. All Case Reports and Short Communication must include at least one table and/ or one figure.

Preparation of Manuscript

The manuscript should be written in English with simple lay out. The text should be prepared in single column format. Bold face, italics, subscripts, superscripts etc. can be used. Pages should be numbered consecutively, beginning with the title page and continuing through the last page of typewritten material.

The text can be divided into numbered sections with brief headings. Starting from introduction with section 1. Subsections should be numbered (for example 2.1 (then 2.1.1, 2.1.2, 2.2, etc.), up to three levels. Manuscripts in general should be organized in the following manner:

Title Page

The title page should contain a brief title, correct first name, middle initial and family name of each author and name and address of the department(s) and institution(s) from where the research was carried out for each author. The title should be without any abbreviations and it should enlighten the contents of the paper. All affiliations should be provided with a lower-case superscript number just after the author's name and in front of the appropriate address.
The name of the corresponding author should be indicated along with telephone and fax numbers (with country and area code) along with full postal address and e-mail address.

Abstract

The abstract should be concise and informative. It should not exceed **350 words** in length for full manuscript and Review article and **150 words** in case of Case Report and/ or Short Communication. It should briefly describe the purpose of the work, techniques and methods used, major findings with important data and conclusions. No references should be cited in this part. Generally non-standard abbreviations should not be used, if necessary they should be clearly defined in the abstract, at first use.

Keywords

Immediately after the abstract, **about 4-8 keywords** should be given. Use of abbreviations should be avoided, only standard abbreviations, well known in the established area may be used, if appropriate. These keywords will be used for indexing.

Abbreviations

Non-standard abbreviations should be listed and full form of each abbreviation should be given in parentheses at first use in the text.

Introduction

Provide a factual background, clearly defined problem, proposed solution, a brief literature survey and the scope and justification of the work done.

Materials and Methods

Give adequate information to allow the experiment to be reproduced. Already published methods should be mentioned with references. Significant modifications of published methods and new methods should be described in detail. Capitalize trade names and include the manufacturer's name and address. Subheading should be used.

Results

Results should be clearly described in a concise manner. Results for different parameters should be described under subheadings or in separate paragraph. Results should be explained, but largely without referring to the literature. Table or figure numbers should be mentioned in parentheses for better understanding.

Discussion

The discussion should not repeat the results, but provide detailed interpretation of data. This should interpret the significance of the findings of the work. Citations should be given in support of the findings. The results and discussion part can also be described as separate, if appropriate. The Results and Discussion sections can include subheadings, and when appropriate, both sections can be combined

Conclusions

This should briefly state the major findings of the study.

Acknowledgment

A brief acknowledgment section may be given after the conclusion section just before the references. The acknowledgment of people who provided assistance in manuscript preparation, funding for research, etc. should be listed in this section.

Tables and Figures

Tables and figures should be presented as per their appearance in the text. It is suggested that the discussion about the tables and figures should appear in the text before the appearance of the respective tables and figures. No tables or figures should be given without discussion or reference inside the text.

Tables should be explanatory enough to be understandable without any text reference. Double spacing should be maintained throughout the table, including table headings and footnotes. Table headings should be placed above the table. Footnotes should be placed below the table with superscript lowercase letters. Each table should be on a separate page, numbered consecutively in Arabic numerals.

Each figure should have a caption. The caption should be concise and typed separately, not on the figure area. Figures should be self-explanatory. Information presented in the figure should not be repeated in the table. All symbols and abbreviations used in the illustrations should be defined clearly. Figure legends should be given below the figures.

References

References should be listed alphabetically at the end of the manuscript. Every reference referred in the text must be also present in the reference list and vice versa. In the text, a reference identified by means of an author's name should be followed by the year of publication in parentheses (e.g.(Brown,2009)). For two authors, both authors' names followed by the year of publication (e.g.(Nelson and Brown, 2007)). When there are more than two authors, only the first author's name followed by "*et al*." and the year of publication (e.g. (Abu-Elteen *et al*., 2010)). When two or more works of an author has been published during the same year, the reference should be identified by the letters "a", "b", "c", etc., placed after the year of publication. This should be followed both in the text and reference list. e.g., Hilly, (2002a, 2002b); Hilly, and Nelson, (2004). Articles in preparation or submitted for publication, unpublished observations, personal communications, etc. should not be included in the reference list but should only be mentioned in the article text (e.g., Shtyawy,A., University of Jordan, personal communication). Journal titles should be abbreviated according to the system adopted in Biological Abstract and Index Medicus, if not included in Biological Abstract or Index Medicus journal title should be given in full. The author is responsible for the sccuracy and completeness of the references and for their correct textual citation. Failure to do so may result in the paper being withdraw from the evaluation process. Example of correct reference form is given as follows:-

Reference to a journal publication:

Bloch BK. 2002. Econazole nitrate in the treatment of *Candida vaginitis*. *S Afr Med J.* , **58**:314-323.

Ogunseitan OA and Ndoye IL. 2006. Protein method for investigating mercuric reductase gene expression in aquatic environments. *Appl Environ Microbiol.*, **64**: 695-702.

Hilly MO, Adams MN and Nelson SC. 2009. Potential fly-ash utilization in agriculture. *Progress in Natural Sci.*, **19**: 1173-1186.

Reference to a book:

Brown WY and White SR.1985. **The Elements of Style**, third ed. MacMillan, New York.

Reference to a chapter in an edited book:

Mettam GR and Adams LB. 2010. How to prepare an electronic version of your article. In: Jones BS and Smith RZ (Eds.), **Introduction to the Electronic Age**. Kluwer Academic Publishers, Netherlands, pp. 281–304.

Conferences and Meetings:

Embabi NS. 1990. Environmental aspects of distribution of mangrove in the United Arab Emirates. Proceedings of the First ASWAS Conference. University of the United Arab Emirates. Al-Ain, United Arab Emirates.

Theses and Dissertations:

El-Labadi SN. 2002. Intestinal digenetic trematodes of some marine fishes from the Gulf of Aqaba. MSc dissertation, The Hashemite University, Zarqa, Jordan.

Nomenclature and Units

Internationally accepted rules and the international system of units (SI) should be used. If other units are mentioned, please give their equivalent in SI.

For biological nomenclature, the conventions of the *International Code of Botanical Nomenclature, the International Code of Nomenclature of Bacteria*, and the *International Code of Zoological Nomenclature* should be followed.
Scientific names of all biological creatures (crops, plants, insects, birds, mammals, etc.) should be mentioned in parentheses at first use of their English term.

Chemical nomenclature, as laid down in the *International Union of Pure and Applied Chemistry* and the official recommendations of the *IUPAC-IUB Combined Commission on Biochemical Nomenclature* should be followed. All biocides and other organic compounds must be identified by their Geneva names when first used in the text. Active ingredients of all formulations should be likewise identified.

Math formulae

All equations referred to in the text should be numbered serially at the right-hand side in parentheses. Meaning of all symbols should be given immediately after the equation at first use. Instead of root signs fractional powers should be used. Subscripts and superscripts should be presented clearly. Variables should be presented in italics. Greek letters and non-Roman symbols should be described in the margin at their first use.

To avoid any misunderstanding zero (0) and the letter O, and one (1) and the letter l should be clearly differentiated. For simple fractions use of the solidus (/) instead of a horizontal line is recommended. Levels of statistical significance such as: $^{*}P < 0.05$, $^{**}P < 0.01$ and $^{***}P < 0.001$ do not require any further explanation.

Copyright

Submission of a manuscript clearly indicates that: the study has not been published before or is not under consideration for publication elsewhere (except as an abstract or as part of a published lecture or academic thesis); its publication is permitted by all authors and after accepted for publication it will not be submitted for publication anywhere else, in English or in any other language, without the written approval of the copyright-holder. The journal may consider manuscripts that are translations of articles originally published in another language. In this case, the consent of the journal in which the article was originally published must be obtained and the fact that the article has already been published must be made clear on submission and stated in the abstract. It is compulsory for the authors to ensure that no material submitted as part of a manuscript infringes existing copyrights, or the rights of a third party.

Ethical Consent

All manuscripts reporting the results of experimental investigation involving human subjects should include a statement confirming that each subject or subject's guardian obtains an informed consent, after the approval of the experimental protocol by a local human ethics committee or IRB. When reporting experiments on animals, authors should indicate whether the institutional and national guide for the care and use of laboratory animals was followed.

Plagiarism

The JJBS hold no responsibility for plagiarism. If a published paper is found later to be extensively plagiarized and is found to be a duplicate or redundant publication, a note of retraction will be published, and copies of the correspondence will be sent to the authors' head of institute.

Galley Proofs

The Editorial Office will send proofs of the manuscript to the corresponding author as an e-mail attachment for final proof reading and it will be the responsibility of the corresponding author to return the galley proof materials appropriately corrected within the stipulated time. Authors will be asked to check any typographical or minor clerical errors in the manuscript at this stage. No other major alteration in the manuscript is allowed. After publication authors can freely access the full text of the article as well as can download and print the PDF file.

Publication Charges

There are no page charges for publication in Jordan Journal of Biological Sciences, except for color illustrations,

Reprints

Ten (10) reprints are provided to corresponding author free of charge within two weeks after the printed journal date. For orders of more reprints, a reprint order form and prices will be sent with article proofs, which should be returned directly to the Editor for processing.

Disclaimer

Articles, communication, or editorials published by JJBS represent the sole opinions of the authors. The publisher shoulders no responsibility or liability what so ever for the use or misuse of the information published by JJBS.

Indexing

JJBS is indexed and abstracted by:

DOAJ (Directory of Open Access Journals)	CABI
Google Scholar	EBSCO
Journal Seek	CAS (Chemical Abstract Service)
HINARI	ETH- Citations
Index Copernicus	Open J-Gat
NDL Japanese Periodicals Index	SCImago
SCIRUS	Clarivate Analytics (Zoological Abstract)
OAJSE	Scopus
ISC (Islamic World Science Citation Center)	AGORA (United Nation's FAO database)
Directory of Research Journal Indexing (DRJI)	SHERPA/RoMEO (UK)
Ulrich's	

المجلة الأردنية للعلوم الحياتية
Jordan Journal of Biological Sciences (JJBS)
ISSN 1995- 6673 (Print), 2307- 7166 (Online)
http://jjbs.hu.edu.jo

The Hashemite University

Deanship of Scientific Research

TRANSFER OF COPYRIGHT AGREEMENT

Journal publishers and authors share a common interest in the protection of copyright: authors principally because they want their creative works to be protected from plagiarism and other unlawful uses, publishers because they need to protect their work and investment in the production, marketing and distribution of the published version of the article. In order to do so effectively, publishers request a formal written transfer of copyright from the author(s) for each article published. Publishers and authors are also concerned that the integrity of the official record of publication of an article (once refereed and published) be maintained, and in order to protect that reference value and validation process, we ask that authors recognize that distribution (including through the Internet/WWW or other on-line means) of the authoritative version of the article as published is best administered by the Publisher.

To avoid any delay in the publication of your article, please read the terms of this agreement, sign in the space provided and return the complete form to us at the address below as quickly as possible.

Article entitled:----------

Corresponding author: ----------

To be published in the journal: Jordan Journal of Biological Sciences (JJBS)

I hereby assign to the Hashemite University the copyright in the manuscript identified above and any supplemental tables, illustrations or other information submitted therewith (the "article") in all forms and media (whether now known or hereafter developed), throughout the world, in all languages, for the full term of copyright and all extensions and renewals thereof, effective when and if the article is accepted for publication. This transfer includes the right to adapt the presentation of the article for use in conjunction with computer systems and programs, including reproduction or publication in machine-readable form and incorporation in electronic retrieval systems.
Authors retain or are hereby granted (without the need to obtain further permission) rights to use the article for traditional scholarship communications, for teaching, and for distribution within their institution.

☐ **I am the sole author of the manuscript**

☐ **I am signing on behalf of all co-authors of the manuscript**

☐ **The article is a 'work made for hire' and I am signing as an authorized representative of the employing company/institution**

Please mark one or more of the above boxes (as appropriate) and then sign and date the document in black ink.

Signed:_____ Name printed: _____
Title and Company (if employer representative) : _____
Date: _____

Data Protection: By submitting this form you are consenting that the personal information provided herein may be used by the Hashemite University and its affiliated institutions worldwide to contact you concerning the publishing of your article.

Please return the completed and signed original of this form by mail or fax, or a scanned copy of the signed original by e-mail, retaining a copy for your files, to:

Hashemite University
Jordan Journal of Biological Sciences
Zarqa 13115 Jordan
Fax: +962 5 3903338
Email: jjbs@hu.edu.jo

EDITORIAL PREFACE

Jordan Journal of Biological Sciences (JJBS) is a refereed, quarterly international journal financed by the Scientific Research and Innovation Support Fund, Ministry of Higher Education and Scientific Research in cooperation with the Hashemite University, Jordan. JJBS celebrated its 11th commencement this past January, 2019. JJBS was founded in 2008 to create a peer-reviewed journal that publishes high-quality research articles, reviews and short communications on novel and innovative aspects of a wide variety of biological sciences such as cell biology, developmental biology, structural biology, microbiology, entomology, molecular biology, biochemistry, medical biotechnology, biodiversity, ecology, marine biology, plant and animal biology, plant and animal physiology, genomics and bioinformatics.

We have watched the growth and success of JJBS over the years. JJBS has published 11 volumes, 45 issues and 479 articles. JJBS has been indexed by SCOPUS, CABI's Full-Text Repository, EBSCO, Clarivate Analytics- Zoological Record and recently has been included in the UGC India approved journals. JJBS Cite Score has improved from 0.18 in 2015 to 0.60 in 2018.

A group of highly valuable scholars have agreed to serve on the editorial board and this places JJBS in a position of most authoritative on biological sciences. I am honored to have six eminent associate editors from various countries. I am also delighted with our group of international advisory board members coming from 15 countries worldwide for their continuous support of JJBS. With our editorial board's cumulative experience in various fields of biological sciences, this journal brings a substantial representation of biological sciences in different disciplines. Without the service and dedication of our editorial; associate editorial and international advisory board members, JJBS would have never existed.

In the coming year, we hope that JJBS will be indexed in Clarivate Analytics and MEDLINE (the U.S. National Library of Medicine database) and others. As you read throughout this volume of JJBS, I would like to remind you that the success of our journal depends on the number of quality articles submitted for review. Accordingly, I would like to request your participation and colleagues by submitting quality manuscripts for review. One of the great benefits we can provide to our prospective authors, regardless of acceptance of their manuscripts or not, is the feedback of our review process. JJBS provides authors with high quality, helpful reviews to improve their manuscripts.

Finally, JJBS would not have succeeded without the collaboration of authors and referees. Their work is greatly appreciated. Furthermore, my thanks are also extended to The Hashemite University and the Scientific Research and Innovation Support Fund, Ministry of Higher Education and Scientific Research for their continuous financial and administrative support to JJBS.

Professor Khaled H. Abu-Elteen
March, 2019

JJBS

Volume 12, Number 1, March .2019
ISSN 1995-6673

Jordan Journal of Biological Sciences

CONTENTS

Original Articles

Short Communication

JJBS

Volume 12, Number 1,March 2019
ISSN 1995-6673
Pages 1 - 4

Jordan Journal of Biological Sciences

A Comparative Anatomical and Epidermal Analysis of *Physalis angulata* L. and *Physalis micrantha* L. (Solanaceae)

Chimezie Ekeke*, Gordian C. Obute and Chinedum A. Ogazie

Department of Plant Science and Biotechnology, Faculty of Science, University of Port Harcourt, P.M.B. 5323, Port Harcourt, Rivers State, Nigeria.

Received May 12, 2018; Revised June 20, 2018; Accepted June 27, 2018

Abstract

The epidermal and anatomical characteristics of *Physalis angulata* L. and *Physalis micrantha* L. (Solanaceae) are analyzed in this study to determine the taxonomic features of these species. The specimens were peeled or sectioned, stained with safranin O and alcian blue, mounted on slide, and micro-photographed with Optika B-1000 FL LED. The plants are amphistomatic and dorsiventral with anisotricytic, isotricytic, tetracytic, anisocytic, anomocytic and contiguous stomata. *P. micrantha* has calcium oxalate crystals of different forms (prism, rod, cylindrical, and star-shaped or druses), and osteosclereide, while *P. angulata* has only druses and macroscleried occurring in parts of the plants. The similarities in the anatomical features among these species suggest an interspecific relationship between the species while the differences confirm these species as distinct.

Keywords: Amphistomatic, Druses, *Physalis*, Prismatic crystals, Solanaceae.

1. Introduction

Physalis L. belongs to the family Solanaceae. *Physalis* is believed to have originated in Mexico (Kelly *et al*., 2012). Generally, there are at least seventy-five known species of the genus *Physalis* (Whitson and Manos 2005). In West Tropical Africa, only four species are known; namely, *P. angulata* L., *P. peruviana* L., *P. micrantha* L. and *P. pubescens* L. (Burkill, 2000). Among these species, *P. pubescens* is only found in Ghana, and is native to America (Burkill, 2000), while the other three species *P. angulata, P. micrantha* and *P. peruviana* are widely distributed in Nigeria (Olorode *et al*., 2013).

The importance of epidermal, anatomical, morphological and cytological characteristics in taxonomy of vascular plants have been investigated and recognized by several authors (Hutchinson and Dalziel, 1954; Metcalfe and Chalk, 1979; Wahua and Sam, 2013; Olorode *et al.*, 2013; Ekeke and Mensah, 2015; Ekeke and Agogbua, 2017). The anatomical, epidermal and morphological characteristics of the members of Solanaceeae have also been reported (Hutchinson and Dalziel, 1954; Metcalfe and Chalk, 1979; Olorode *et al*., 2013; Wahua and Sam, 2013; Chockpisit and Aree, 2013). The morphological, floral and cytological characteristics of these species have also been described (Olorode *et al*., 2013).

Information on the anatomical features of the studied species is scanty. This research is carried out to outline the epidermal and anatomical characteristics of these species to complement the existing data on the species.

2. Materials and Methods

2.1. Plant Source and Identification

The plant species investigated in this study are *Physalis angulata* L. and *P. micrantha* L. Samples of these plants were collected from various locations in Choba, Nigeria, between April and December of 2016 and November 2017 when the plants were in full bloom and in their optimal conditions. The collected samples were identified at the herbarium of the University of Port Harcourt.

2.2. Epidermal Studies

For the epidermal analysis, foliar sections were collected from fresh plants growing in fields. One square centimeter leaf cuttings were obtained from identical regions of each fresh leaf, generally mid-way between the leaf base and apex of the lamina. The adaxial and abaxial epidermal peels were obtained using sharply pointed forceps. Peels were stained with 1 % safranin O and alcian blue, rinsed with distilled water to remove excessive stain and were then mounted in a drop of pure glycerol on clean glass slides. A cover glass was placed over the drop and sealed with nail varnish to prevent dehydration (Okoli and Ndukwu, 1992). The epidermal features observed included: the organization of the epidermis, the arrangement of the epidermal cells, the nature of trichomes, the shape of epidermal cells, and the nature of the anticlinal cell wall of the leaf epidermis, stomatal types, and stomatal density and index. The stomatal index (SI) was estimated based on (Metcalfe and Chalk, 1979),

* Corresponding author. e-mail: ekeke.uche@uniport.edu.ng.

while the terminology for the stomatal type is based on (Malvey, 2004).

2.3. Anatomical Studies

Fresh samples (petiole, stem and midrib) of the *Physalis* species were fixed in formalin, acetic acid, and alcohol (FAA) for twelve hours, dehydrated in alcohol series (30 %, 50 % 70 %, 95 % and absolute alcohol) for three hours each, cleared in chloroform-alcohol series ((3:1; 1:1; 1:3) v/v for ten minutes in each, wax-embedded and sectioned. Thin sections were selected, de-waxed, stained with Alcian blue, and counterstained with safranin (Okoli and Ndukwu, 1992). Good preparations were mounted on slides; they were viewed and photographed with Optika B-1000 FL LED

3. Results

3.1. Leaf Epidermal Characteristics

The two species are amphistomatic and have dorsiventral leaves. The leaf epidermal characteristics slightly varied among them with the non-glandular, multicellular base, uniseriate trichomes with one-four celled stalk (Fig. 1E) and glandular trichomes; the base is multicellular, the stalk has one-two cells and the globular multicellular head, three-four cells. (Figure 1F) and Table 1.

3.1.1. Physalis micrantha

The upper and lower epidermal cells are irregular in shape with undulating anticlinal cell walls (Figure 1A-B) and stomatal indices of 88.23 and 38.09 on the lower and upper epidermis respectively. The upper epidermis had isotricytic, tetracytic, anisocytic but rarely anomocytic stomata (Figure 1A) while the lower epidermis had isotricytic, tetracytic, tricytic and polar contiguous stomata with glandular trichomes (Figures 1B and 1F).

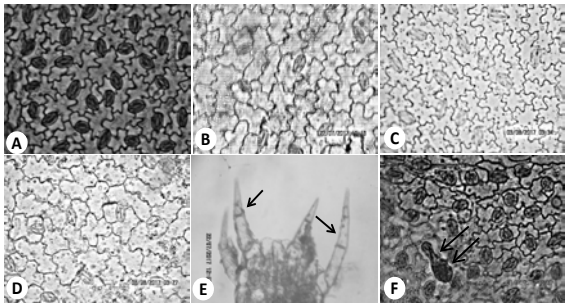

Figure 1. Epidermal characteristics of *Physalis* species: (A-upper and B-lower) *P. micrantha and* (C- upper and D- lower) *P. angulata,* E- arrows show non-glandular multicellular uniseriate trichomes and F- arrows show glandular trichome on *P. micrantha* epidermis.

3.1.2. Physalis angulata

The upper and lower epidermal cells of this species are irregular in shape with undulating anticlinal walls and glandular trichomes (one-two- celled stalk, multicellular base, three-four-celled head). The upper epidermis had anisotricytic, isotricytic, tetracytic and anisocytic stomata (Figure 1C) with a stomatal index of 40.00. The lower epidermis had anisotricytic, isotricytic, tetracytic, anisocytic and anomocytic (Figure 1D) and a stomatal index of 76.47.

Table 1. Leaf epidermal characteristics of the studied *Physalis* species.

Plant part	*P. angulata*	*P. micrantha*
Lower epidermis	Irregular in shape, anticlinal wall undulating, stomata (anisotricytic, isotricytic, tetracytic, anisocytic and anomocytic) with glandular trichomes and a stomatal index of 76.47.	Irregular in shape, anticlinal wall undulating, stomata (isotricytic, tetracytic, tricytic and polar contiguous) with glandular trichomes and a stomatal index of 88.23
Upper epidermis	Irregular in shape, anticlinal wall undulating, stomata (anisotricytic, isotricytic, tetracytic, anisocytic) with glandular trichomes and a stomatal index of 40.0.	Polygonal in shape, anticlinal wall undulating, stomata (isotricytic, tetracytic, anisocytic but rarely anomocytic) with macrosclereid and a stomatal index of 38.09.

3.2. Anatomy of Petiole, Midrib, Lamina and Stem

3.2.1. Physalis micarantha

Petioles are hairy. The epidermis has two-layers. The upper surface has four-six layers of a parenchymatous cell with three separate arced vascular bundles (Figure 2A). The midrib is hairy. The upper cuticle protruded or projected with a relatively flat surface. The vascular bundle is small forming a semi-arc with parenchymatous cells of three-two layers on the lower surface and six-nine layers on the upper surface (Figure 3A). Lamina has one-layered palisade mesophyll (Figure 4A). The stem is oval with six protruded ends. Pith is small and hollow; the epidermis has one-layer and a hollow pith of about 245 µm wide (Figure 5A).

3.2.2. Physalis angulata

Petioles are hairy on both upper and lower surfaces. The epidermis has layers and one layer of hypodermis and vascular arced (Figure 2B). The midrib is hairy, with arced vascular bundles, parenchymatous cells of three-four layers on the lower surface and three-eight layers on the upper surface. The lower epidermis has one layer and one layer of hypodermis (Figure 3B). Lamina has one layer of palisade mesophyll and the vascular bundles are embedded in the spongy mesophyll or between the palisade and spongy mesophyll (Figure 4B). The stem is fairly rectangular in shape with five protruded ends; the epidermis has one layer and a hollow pith of about 375 µm wide (Figure 5B).

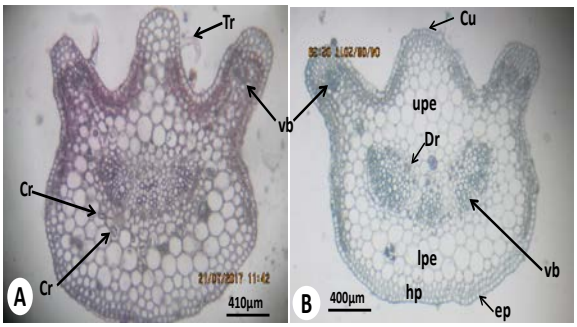

Figure 2. Petiole anatomy of *Physalis* species: (A) - *P. micrantha* and (B) - *P. angulata* (Cr-crystal, vb-vascular bundle, Tr-trichome, Cu-cuticle, upe-upper parenchymatous cells, lpe-lower parenchymatous cells, hp-hypodermis, ep-epidermis, Dr-druses).

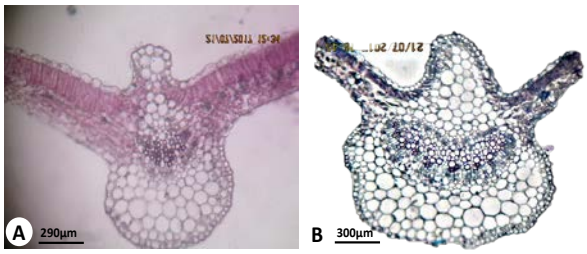

Figure 3. Midrib anatomy of *Physalis* species: (A) - *P. micrantha* and (B) - *P. angulata*.

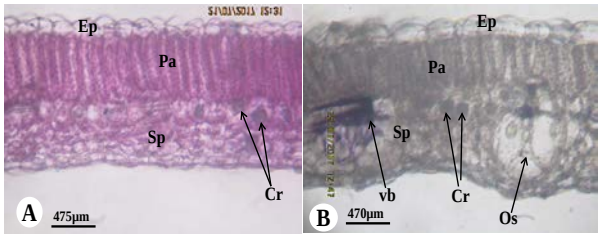

Figure 4. Anatomy of leaf lamina of *Physalis* species: (A) - *P. micrantha* and (B) - *P. angulata* (Ep-epidermis, Pa-palisade mesophyll, Sp-spongy mesophyll, Cr-crystal, Os-osteosclereide).

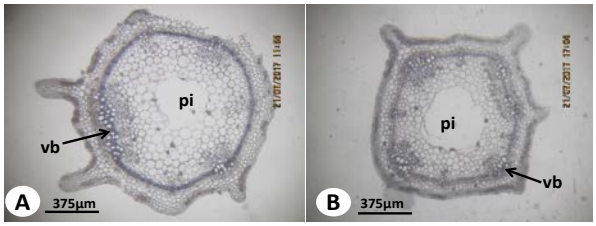

Figure 5. Stem anatomy of *Physalis* species: (A) - *P. micrantha* and (B) - *P. angulata* (pi-pith, vb-vascular bundle).

Table 2: Anatomy of petiole, midrib, lamina and stem of the *Physalis* species.

Plant part	*P. angulata*	*P. micrantha*
Petiole	Hairy on both surfaces, epidermis two-layered or having one layer of hypodermis	Winged with vascular bundles, the upper epidermis has two layers of collenchyma, 4-6 layers of parenchyma, one layer of collenchyma.
Lamina	Mesophyll one-layered, vascular bundles embedded in the spongy mesophyll or between the palisade and spongy mesophyll.	One layer of palisade mesophyll and osteosclereide embedded in the spongy mesophyll but extending to the lower epidermis.
Midrib	Hairy with arced vascular bundles, parenchymatous cells 3-4 layers on the lower surface and 3-8 layers on the upper surface, the lower epidermis has one layer and one layer of hypodermis	Upper cuticle protruded/projected with a relatively flat surface having 6-9 layers of parenchymatous cells. Lower parenchyma 3-5 cells with non-glandular sereiated hairs.
Stem	Rectangular in shape with 5-protruded ends, the epidermis is one- layered.	Oval in shape with six-protruded ends, pith hollow, with a continuous layer of sclerenchymatous cells.

3.3. Distribution of Calcium Oxalate, Secretory Cells, and Sclereides

Among the *Physalis* species studied here, the researchers observed calcium oxalate crystals and sclereids of different forms in the stem, petiole, midrib, and lamina (Figures 4 B and 6, and Table 3). The different forms of calcium oxalate include: pyramidal (Figure 6 B), rod (Figure 6 D), druses or star-shaped (Figures 6 C and 6 F) and cylindrical (Figure 6 E) while the sclereids are macrosclereides (Figures 6 G–6 I) and osteosclereide (Figure 4 B).

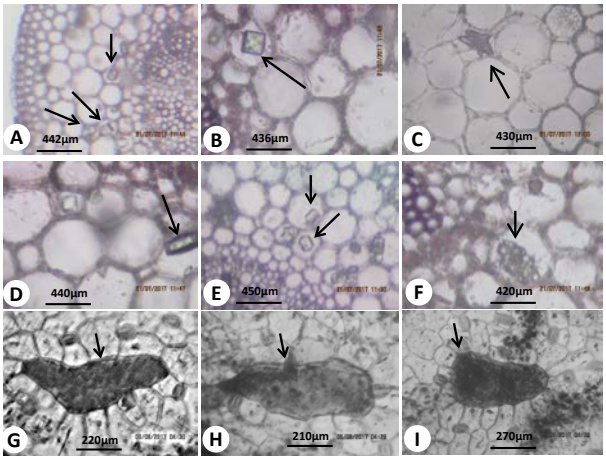

Figure 6. (A – E) *Physalis micrantha* Petiole, (F) *P. angulata* (G-I) - Macroscleried on Upper epidermis of *P. micrantha* (A-prismatic crystals; B-pyramidal; C and F- druses or star-shaped; D - rod and E – cylindrical).

3.3.1. Physalis micrantha

Druses were found in the spongy and palisade mesophylls in the lamina (Figure 4A), in the parenchymatous cell towards the lower epidermis, in and around the vascular bundles in the midrib, and predominantly in the cortex in the stem, while druses and prismatic crystals (cylindrical, pyramidal or rod shape) were found in the petiole (Figures 2A and 6A-E) and macrosclereides in the upper epidermis (Figures 6G – 6I).

3.3.2. Physalis angulata

Calcium oxalate crystals (druses) and secretory cells were observed mainly in and around the vascular bundles in the petiole (Figure 2B) and the midrib. Also, crystal sand was in the upper and lower parenchymatous cells in the midrib. In the lamina druses were found in the spongy and palisade mesophylls, osteoscereide embedded in the spongy mesophyll, but extending to the lower epidermis (Figure 4B) and druses predominantly in the cortex and the parenchymatous cells in the stem.

Table 3. Distribution of calcium oxalate, secretory cells and sclereids in the studied plants.

Plant part	*P. angulata*	*P. micrantha*
Petiole	Calcium oxalate crystals (druses) and secretory cells found in and around the vascular bundles.	Calcium oxalate crystals (druses, and prismatic crystals-cylindrical or rod shape).
Lamina	Druses found in the spongy and palisade mesophylls, osteoscereide embedded in the spongy mesophyll but extending to the lower epidermis.	Druses found in the spongy and palisade mesophylls.
Midrib	Mainly druses and crystal sand in the upper and lower parenchymatous cells, vascular bundles surrounded by secretory cells.	Druses found in the parenchymatous cell towards the lower epidermis and in and around the vascular bundles.
Stem	Druses predominantly found in the cortex and the parenchymatous cells.	Druses predominantly found in the cortex, spherical in shape.

4. Discussion

The importance of epidermal, anatomical, morphological and cytological characteristics in taxonomy of vascular plants have been investigated and recognized by several authors (Hutchinson and Dalziel, 1954; Metcalfe and Chalk, 1979; Olorode *et al.,* 2013; Wahua and Sam, 2013; Ekeke and Mensah, 2015; Ekeke and Agogbua, 2017). The anatomical, epidermal and morphological characteristics of the members of Solanaceeae including *Physalis* have been reported (Hutchinson and Dalziel, 1954; Metcalfe and Chalk, 1979; Olorode *et al.,* 2013; Wahua and Sam, 2013; Chockpisit and Aree, 2013). Chockpisit and Aree (2013) recognized that the epidermal cells of *Physalis* species are irregular in shape, with undulating anticlinal walls. Also, they reported that the spongy mesophyll has three-four layers and the palisade mesophyll has one layer. This is consistent with the observation in the current study.

The current findings state that the leaves of both *P. angulata* and *P. micrantha* are amphistomatic and dorsiventral, which is similar to the report of Sethi and Kannabiran (1975) with isotricytic, tetracytic, anisocytic, anomocytic, tricytic, anisotricytic and polar contiguous stomata. Sethi and Kannabiran (1975) further noted that the stomata type in *Physalis* was anomocytic, while Sandhya, *et al.* (2010) reported that the stomatal apparatus observed in *P. angulata* was of the anisocytic type. Zhang and Lu (1999) reported that anomocytic stomata were restricted only to the abaxial surface of the leaf in *P. angulata.* This observation is different from the observation regarding these species in this study. Chockpisit and Aree (2013) observed stomatal indices of 3.57 and 4.00 on the adaxial and abaxial surfaces of *P. angulata*, while Wahua and Sam (2013) observed stomatal indices of 20.0 and 13.64 on the adaxial and abaxial surfaces of the same species. The observation from this study is different because other stomata types along with the anomocytic and anisocytic types were observed. The stomatal index found in this study also differed from the previous reports. Wahua and Sam (2013) further reported uniseriate non-glandular and glandular trichome in both *P. angulata* and *P. micrantha* which corresponds with the current observation.

5. Conclusion

The difference in morphology and occurrence of calcium oxalate crystals and sclereid among these species is worthy of note. Druses and prismatic crystals (cylindrical, pyramidal or rod-shaped) and macrosclereides were found in *P. micarantha*, but only druses and osteosclereide were found in *P. angulata*. The variation confirms that these species are distinct as reported by Hutchinson and Dalziel (1954) and Olorode *et al*. (2013). The similarities in the anatomical and epidermal characteristics among the species suggest an interspecific relationship between the species, while the differences confirm the species to be distinct.

References

Burkill H M. 2000. **The Useful Plants of West Tropical Africa**. Vol.5 (Edition 2). Royal Botanic Gardens, Kew.

Chockpisit T, Aree T. 2013. Comparative Micro-Morphology, Anatomy and Architecture of Leaf of *Physalis. Inter J Biol, Biomol, Agricultural, Food and Biotechnol Engin.,* **7(8):** 806 – 810.

Ekeke C, Agogbua J U. 2017. Anatomical Study on *Commelina diffusa* Burn. f. and *Commelina erecta* L. (Commelinaceae). *J Appl Sci Environ Management* , **22 (1)**: 7-11.

Ekeke C, Mensah S I. 2015. Comparative Anatomy of Midrib and Its Significance in the Taxonomy of the Family Asteraceae from Nigeria. *J Plant Sci.,* **10(5)**: 200-205.

Hutchinson, J., Dalziel, J.M., 1954. **Flora of West Tropical Africa**. Crown Agents, London UK.

Kelly K., Quinn L, Steve C, Kirsten B, Hillary L, Mark C, Barbara N T. 2012. The Ethnobotany and Ethnopharmacology of Wild Tomatillos, *Physalis longifolia* Nutt., and Related *Physalis* Species: A Review1. *Economic Bot.,* **20 (10):** 1-13

Malvey P. 2004. Structure, nomenclature and classification of stomata. *Acta Bot. Sin*. **44(2):** 242-252.

Metcalfe C R, Chalk L. 1979. **Anatomy of the Dicotyledon: Systematic anatomy of the Leaf and Stem**. vol. 1 Oxford University Press, New York.

OkolI B E, Ndukwu, B C. 1992. Studies on Nigerian *Curcurbita moschata. Nig J Bot*., **5**: 18-26.

Olorode, O., Olayanju, S., Garba, A., 2013. *Physalis* (Solanaceae) in Nigeria. *Ife J Sci*., **15 (1)**: 101-109.

Sandhya S, Jaffery S A H, Vinod K R. 2010. "Pharmacognostical studies on the leaf and root of *Physalis angulata* L.," IJPRD, **2 (1)**: 1-8.

Sethi P D, Kannabiran B. 1975. "Phamacognostic study on four Indian *Physalis*." *J Res Indian Med*. **10(4):** 152.

Wahua C, Sam S M. 2013. Comparative Chemotaxonomic Investigations on *Physalis angulata* Linn. and *Physalis micrantha* Linn. (Solanaceae). *Asian J ApplSci.,* **1 (5)**: 220-228.

Whitson M, Manos P S. 2005. Untangling *Physalis* (Solanaceae) from the Physaloids: A Two-Gene Phylogeny of the Physalinae. *Systematic Bot.,* **30 (1)**: 216-230.

Zhang Z Y, Lu A M. 1999. A Comparative study of *Physalis, Capsicum* and *Tubocapsicum*; Three Genera of Solanaceae. In: M. Nee, D.E. Symon, R.N. Lester, and J.P. Jessop, Eds. **Solanaceae IV**, Kent, WhitsableLitho Ltd., pp. 81-96.

JJBS

Volume 12, Number 1,March 2019
ISSN 1995-6673
Pages 5 - 16

Jordan Journal of Biological Sciences

The Effects of the Aqueous Extracts of *Elaeis guineensis* Fruits on the Lipid Profile and Kidney Function Indices of Male Wistar Albino Rats

Robert I. Uroko[1*], Oluomachi N. Uchenna[1], Ngozi K. Achi[1], Amarachi Agbafor[1], Simeon I. Egba[1] and Chidiogo A. Orjiakor[2]

[1]*Department of Biochemistry, College of Natural Sciences, Michael Okpara University of Agriculture, Umudike, Abia-State,* [2]*Department of Biochemistry, Faculty of Biological Sciences, University of Nigeria, Nsukka, Enugu State – Nigeria*

Received May 18, 2018; Revised June 19, 2018; Accepted June 27, 2018

Abstract

Increasing the intake rate of aqueous extracts of palm fruits by local consumers for their nutraceutical benefits has necessitated the scientific investigations of the properties of these extracts to ascertain their safety levels. This study investigates the effects of fresh and fermented aqueous extracts of palm fruits (*Elaeis guineensis*) on lipid profile and kidney function indices of male Wistar albino rats. In this study, forty-five male Wistar albino rats were randomly divided into five groups, with group one having five rats while groups 2 – 5 had ten rats each. Group 1 received normal saline 2 mL/kg body weight (b.wt) orally for twenty-eight days. Five rats each in groups 2 – 5 received 100, 200, 400, and 600 mg/kg b. wt. of fresh and fermented aqueous extracts of palm fruits respectively for twenty-eight days. Blood samples were collected on the 29th day, rats were sacrificed and kidneys removed for histopathological examinations. Data collected were statistically analysed using one analysis of variance. Total cholesterol and low density lipoprotein cholesterol concentrations in the palm fruit aqueous extract-treated groups were significantly ($p < 0.05$) higher than those of normal rats in a dose-dependent manner. Triacylglycerol and high density lipoprotein cholesterol concentrations in the rats treated with the palm fruit aqueous extract were not significantly higher ($p > 0.05$) when compared with the normal control except for group 5 of the rats treated with a high dose of fermented palm fruit aqueous extracts. Serum urea, creatinine and uric acid concentrations of rats treated with aqueous extracts of palm fruits showed a significant increase ($p < 0.05$) when compared with the normal control rats. The aqueous extracts treated rats also showed a significant increase ($p < 0.05$) in the serum electrolytes (Na^+, K^+, Cl^-, and HCO_3^-) concentrations relative to the normal control rats. Histopathological studies showed tubular degeneration and regeneration, tubular necrosis and mild multifocal vacuolar degeneration of renal tubular epithelial cells of the rats treated with the aqueous extracts when compared with the normal control rats. Results of the present study suggest that the aqueous extracts of palm fruits could adversely affect the lipid profile, damage and impair renal functions as depicted by the kidney histomorphologies and serum electrolytes concentrations.

Keywords: Elaeis guineensis; Kidney histomorphology; Serum electrolytes; Lipid profile; Urea; Creatinine.

1. Introduction

There is increasing number of kidney diseases and cardiovascular disorders including heart attacks and strokes which result not only from genetic factors but also from unhealthy lifestyles, drug toxicity, and unhealthy diets (Santoshkumar *et al*., 2013). Prevention remains the best option for surviving kidney and cardiovascular disorders till date, as they have limited treatment options coupled with huge emotional and financial burdens (Helin and Winberg, 2008). Lipid profile gives the breakdown of one's fats in the blood which includes total cholesterol, high density lipoprotein-cholesterol, low density lipo-protein-cholesterol, and triacylglycerol. In a situation where there are high serum levels of total cholesterol, low density lipoprotein-cholesterol, triacylglycerol, and low serum levels of high density lipoprotein-cholesterol, it is generally referred to as negative lipid profile or abnormal lipid profile (Jain *et al*., 2010; Luqman *et al*., 2012; Sivaiah Reddy, 2012). These have increased the rate of lipid profile associated disorders such as hyperlipidaemia, diabetes mellitus, atherosclerosis and chronic kidney disease (Santoshkumar *et al*., 2013). Consumption of high fat diets could lead to elevated serum levels of one or more of total cholesterol, low-density lipoprotein cholesterol, triacylglycerol, or both total cholesterol and triacylglycerol as in case of combined hyperlipidaemia (Luqman *et al*., 2012; Sivaiah Reddy, 2012).

Kidneys are the major excretory organs in humans which play vital roles in the formation and excretion of urine, formation and secretion of erythropoietin that controls the rate of red blood cell formation, and rennin that regulates blood pressure (Mona *et al*., 2013). In addition, kidneys are highly involved in the removal of waste products of cell metabolism, excess water, and salts

* Corresponding author. e-mail: greaturoko@gmail.com; ir.uroko@mouau.edu.ng.

from the blood keeping blood pH within physiological range (Santoshkumar *et al*., 2013; Ubon *et al*., 2017). It has been observed that failure in kidney functions is the main reason behind the increasing cases of chronic kidney diseases globally, which has independently increased the risk factor for cardiovascular diseases (Anawat *et al*., 2017). There is an increasing number of death resulting from cardiovascular diseases worldwide, although cardiovascular diseases are preventable largely by managing or controlling modifiable risk factors (Zemdegs *et al*., 2011). Cardiovascular risk factors such as smoking, inactive lifestyle, poor dietary habits, hypertension, abnormal lipid profile and obesity can be effectively managed while other risk factors such as genetic makeup of an individual, sex, and age are difficult to control (Zemdegs *et al*., 2011). The fact that many cardiovascular risk factors are controllable makes it necessary to identify manageable risk factors that could aid in the prevention and reduction of cardiovascular diseases. It has been reported that improved dietary habits, physical activity, and lifestyle or behavioural changes could significantly lead to the reduction of cardiovascular diseases (Hunter *et al*., 2010).

The aqueous extracts of palm fruits (*Elaeis guineensis*) are rich in antioxidant components and possess a significant antioxidant activity capable of ameliorating oxidative stress associated with the activities of reactive oxygen species (Uroko *et al*., 2017). High fatty acids, low proteins and carbohydrates found in the aqueous extracts of palm fruits could negatively alter the lipid profile especially if the aqueous extracts are richer in saturated fats and low density lipoprotein than the high density lipoprotein and unsaturated fats (Akinsorotan, 2013; Uroko *et al*., 2017). It has been shown that the aqueous extracts of palm fruits contain high mineral contents such as sodium, potassium, magnesium and calcium, which could adversely affect the serum electrolyte balance thereby impairing consumers' health (Ohimain *et al*., 2012). The increase in the rate of consumption of "ofe akwu" and use of aqueous extracts from palm fruits to substitute water in the production of palm oil have increased the rate of consumption of the aqueous extracts of palm fruits by humans. There has been no comprehensive study of the effects of the consumption of aqueous extracts from palm fruits on human health. The extracts may be rich in constituents that could negatively alter lipid profile thereby increasing the risk of cardiovascular diseases and other associated health consequences. In addition, the extracts of palm fruits may be nephrotoxic, adversely impair renal functions, and compromise the health of innocent consumers. Thus, this study is designed to investigate the effects of aqueous extracts of palm fruits on lipid profile and kidney function indices of male Wistar albino rats.

2. Materials and Methods

2.1. Preparation of Aqueous Extract of Palm Fruits

Palm fruit bunches were collected from the Obeakpu palm oil milling site in Njaba, Imo State and were threshed manually using axe to remove the fruits from the bunches. Loose fruits were handpicked, washed, and boiled in high temperature wet-heat treatment (120-140°C) for two hours, and crushed with the aid of a mortar and pestle. Palm oil was extracted with water and the kernels including other solid wastes were removed, leaving behind the aqueous portion. A volume of twenty litres of freshly prepared aqueous extract of palm fruit was obtained, and first filtered with a mesh cloth to remove suspended solids, and then filtered with Whatman No. 1 filter paper. The filtrate was divided into two equal volumes, one portion was stored in a refrigerator, and the other portion was kept out of the refrigerator to ferment for twenty-one days. This was done to mimic the situations where people consume the aqueous extracts freshly through "ofe akwu or banga soup" and the second situation where it is used as water substitute to produce palm oil irrespective of its age. The two extracts were concentrated to dryness in a water bath at 50 °C and were used for the study.

2.2. Collection of Animals for the Study

Animals used in this study were obtained from the Animal House of the Department of Zoology, University of Nigeria, Nsukka. The animals were acclimatized at the Animal House of the Department of Biochemistry, College of Natural Sciences, Michael Okpara University of Agriculture, Umudike for seven days under a twelve-hour cycle of light and dark with free access to standard animal feed and water.

2.3. Experimental Design

Forty five male Wistar albino rats were used for this study. The rats were divided into five groups with group one having five rats and serving as the normal control. Groups two – five had ten rats each with five rats in each group receiving fresh and fermented aqueous extracts respectively for twenty-eight days, after which the rats were sacrificed on the 29th day and blood samples were collected for lipid profile and kidney function indices analyses. Kidney was collected from the normal control group, and groups two – five treated with the fresh and fermented aqueous extract respectively for the histo-pathological examination. The acute toxicity testing of the extracts in earlier studies had shown that the extracts are not acutely toxic at the highest dose tested. Thus, the acute toxicity testing of the extracts were not carried out again in this study.

Group 1: Orally administered normal saline 2 mL/kg b. wt. for 28 days.

Group 2: Five rats each were administered 100 mg/kg b. wt. of the fresh and fermented aqueous extracts of *E. guineensis* fruits for 28 days respectively.

Group 3: Five rats each were administered 200 mg/kg b. wt. of the fresh and fermented aqueous extracts of *E. guineensis* fruits for 28 days respectively.

Group 4: Five rats each were administered 400 mg/kg b. wt. of the fresh and fermented aqueous extracts of *E. guineensis* fruits for 28 days respectively.

Group 5: Five rats each were administered 600 mg/kg b. wt. of the fresh and fermented aqueous extract of *E. guineensis* fruits for 28 days respectively.

2.4. Determination of Total Cholesterol (T. chol)

The total cholesterol concentration was determined according to the method described by Allain *et al.*, 1974. Cholesterol is determined by the enzymatic hydrolysis of

cholesterol ester by cholesterol esterase that generates cholesterol which, reacts with oxygen in the presence of cholesterol oxidase to liberate hydrogen peroxide. The hydrogen peroxide liberated reacts with phenol and 4-amino antipyrine in the presence of peroxidase to give quinonemine. Cholesterol is quantified by measuring the absorbance of the quinonemine formed at 546 nm which is proportional to the cholesterol concentration.

2.5. Determination of High Density Lipoprotein

The high density lipoprotein (HDL) concentration was determined according to the method described by Albers *et al*. 1978. The principle of this method is based on the removal of low density lipoproteins (LDL and VLDL) and chylomicron fractions by quantitative lipoprotein precipitation by the addition of phosphotungstic acid in the presence of magnesium ions. The high density lipoprotein (HDL) fraction which remains in the supernatant is determined.

2.6. Determination of Low Density Lipoprotein (LDL)

The low density lipoprotein concentration was determined by the method of Assmann *et al*., 1984. Low density lipoprotein-cholesterol (LDL-Cholesterol) is determined as the difference between the total cholesterol and cholesterol content of the supernatant after precipitation of the LDL fraction by polyvinyl sulphate (PVS) in the presence of polyethylene glycol monomethyl ether.

2.7. Determination of Triacylglycerol Concentration (TAG)

Triacylglycerol (TAG) concentration was determined according to the method described by Tietz, 1990. The triacylglycerol concentration is determined by the enzymatic hydrolysis of triacylglycerol and a couple of reactions that generate quinoneimine as an indicator. The absorbance of the quinoneimine generated at 546 nm is directly proportional to the triacylglycerol concentration.

2.8. Determination of Serum Urea Concentration

Serum urea concentration was determined according to the method of Varley and Alan, 1984. Urea in serum is hydrolyzed to ammonia in the presence of urease which can be measured photometrically by Berthelot's reaction.

2.9. Determination of Creatinine Concentration

Determination of serum creatinine concentration was carried out as described by Peters, 1942. Creatinine in alkaline solution reacts with picric acid to form a coloured complex. The amount of the complex formed is directly proportional to the creatinine concentration.

2.10. Determination of Sodium Ion (Na+) Concentration

The sodium ion concentration in serum was determined using the method of Terri and Sesin, 1958. Sodium is precipitated as the triple salt of sodium-magnesium uranyl acetate with the excess uranium, which reacts with ferrocyanide, producing a chromophore whose absorbance varies inversely as the concentration of sodium in the test specimen.

2.11. Determination of Chloride Ion (Cl-) Concentration

Chloride ion concentration in the serum was determined according to the method of Skeggs and Hochstrasser, 1964. Chloride ions form a soluble non-ionized compound with mercuric ions and displace thiocyanate ions from non-ionized mercuric thiocyanate. The released thiocyanate ions react with ferric ions to form a colour complex that absorbs light at 480 nm. The intensity of the colour produced is directly proportional to the chloride concentration.

2.12. Determination of Potassium Ion (K+) Concentration

The potassium ion concentration in the serum was determined according to the method of Terri and Sesin, 1958. The potassium ion concentration in the serum is determined by using sodium tetraphenylboron in a specifically prepared mixture to produce a colloidal suspension, the turbidity of which is proportional to the potassium ion concentration in the range of 2 – 7 mEq/L.

2.13. Determination of Bicarbonate Ion Concentrations

The serum bicarbonate ion was determined using the enzyme spectrophotometric procedures as described by Forrester *et al*., 1976. Phosphoenolpyruvate carboxylase (PEPC) catalyzes the reaction between phosphoenol-pyruvate and bicarbonate to form oxaloacetate and phosphate ion. Oxaloacetate is reduced to malate with simultaneous oxidation of an equimolar amount of reduced nicotinamide adenine dinucleotide (NADH) to NAD; the reaction is catalysed by malate dehydrogenase. This results in a decrease in absorbance at 380 nm that is directly proportional to the bicarbonate concentration in the serum.

2.14. Determination of Uric Acid Concentration

Uric acid concentration was determined according to the method of Trinder as contained in Biotrust assay kit, 1969. Uric acid is oxidized to allantoin and hydrogen peroxide in the presence of uricase. The liberated hydrogen peroxide is detected by a chromogenic oxygen acceptor in the presence of peroxidase. The red quinine formed is proportional to the amount of uric acid present in the sample.

2.15. Tissue Preparation for Histopathological Analysis

The experimental animals were humanely sacrificed at the end of the study. Gross lesions were recorded as observed during the post mortem examination. Sections of the kidney were collected for histopathological examination. The collected samples were fixed in 10 % phosphate buffered formalin for a minimum of forty-eight hours. The tissues were subsequently trimmed, dehydrated in four grades of alcohol (70 %, 80 %, 90 % and absolute alcohol), cleared in three grades of xylene and embedded in molten wax. On solidifying, the blocks were sectioned, 5µm thick with a rotary microtome, floated in a water bathe and incubated at 60˚C for thirty minutes. The 5µm thick-sectioned tissues were subsequently cleared in three grades of xylene and rehydrated in three grades of alcohol (90 %, 80 % and 70 %). The sections were then stained with Hematoxylin for fifteen minutes. Blueing was done with ammonium chloride. Differentiation was done with 1 % acid alcohol before counterstaining with Eosin. Permanent mounts were made on degreased glass slides using a mountant; DPX.

2.16. Slide Examination

The prepared slides were examined with a Motic™ compound light microscope using x4, x10 and x40

objective lenses. The photomicrographs were taken using a Motic™ 9.0 mega pixels microscope camera at x100 and x400 magnifications'

2.17. Statistical Analysis

The data obtained from the experiment were analysed statistically using one-way analysis of variance (ANOVA) to get the grouped mean which was used to determine the significant difference between the group means at 95 % confidence level (P <0.05). Statistical Products and Service solutions (SPSS) software was used for this analysis (IBM Corporation, 2011).

3. Results

The data in the figure 1 show the total cholesterol concentration in the male Wistar albino rats which were administered graded doses of the fresh and fermented aqueous extracts of palm fruits respectively. The rats in groups two – three that were administered the fresh aqueous extract showed no significant increase ($P > 0.05$) in the total cholesterol concentrations when compared with the normal control. Similarly, the rats in group five which were administered the fermented aqueous extract showed no significant increase ($P > 0.05$) in the total cholesterol concentration when compared with the normal control. However, rats in groups four – five that were administered the fresh aqueous extract and rats of groups two – four that were administered the fermented aqueous extract of palm fruits showed a significant increase ($P < 0.05$) in the total cholesterol concentrations when compared with the normal control.

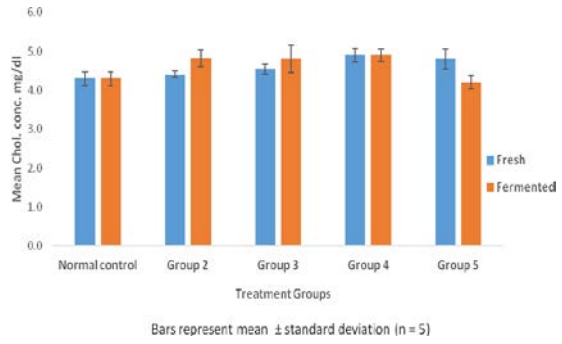

Figure 1. Effect of the aqueous extracts of palm fruits on serum total cholesterol concentrations of male Wistar albino rats

The data in figure 2 show the high density lipoprotein (HDL) concentrations of the normal rats and the rats administered graded doses of fresh and fermented aqueous extracts of palm fruits respectively. All the groups of rats administered fresh and fermented aqueous extracts respectively showed no significant increase ($P < 0.05$) in HDL concentration except the rats of group 4 that were administered fresh aqueous extract and rats of group 5 that were administered fermented aqueous extract that showed no significant decrease ($P < 0.05$) in HDL concentration when compared with HDL concentration of the normal control rats.

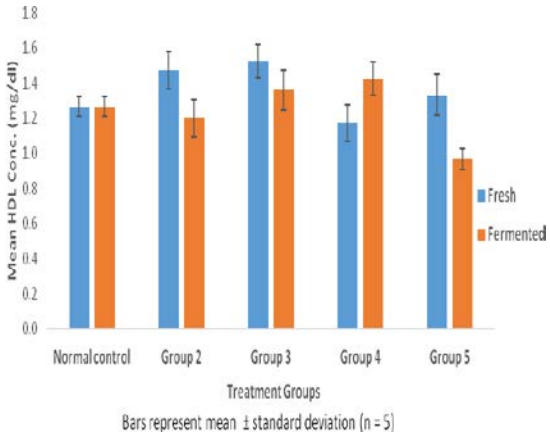

Figure 2. Effect of the aqueous extracts of palm fruits on serum high density lipoprotein concentrations of male Wistar albino rats

Figure 3 show the low density lipoprotein (LDL) concentration of normal rats and the rats administered graded doses of fresh and fermented aqueous extracts of palm fruits respectively. The rats of groups 2 and 3 that were administered fresh aqueous extract of palm fruits showed no significant ($P > 0.05$) decrease in LDL concentrations when compared with the LDL concentration of the normal control rats. Groups 4 and 5 rats that were administered the same fresh aqueous extract at higher concentrations showed no significant increase ($P > 0.05$) in LDL concentrations relative to the LDL concentrations of the normal control rats. However, groups 2 and 4 that were administered the fermented aqueous extract of palm fruits showed a significant increase ($P < 0.05$) in the LDL concentrations relative to the normal control rats. In addition, groups 2 and 5 rats administered the fermented aqueous extract showed no significant increase ($P > 0.05$) in LDL concentrations when compared with the LDL concentrations of the normal control rats.

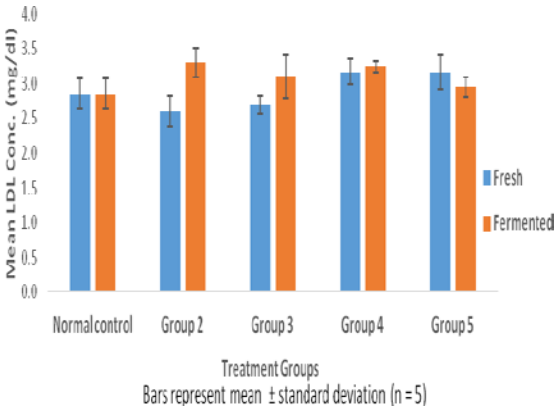

Figure 3. Effect of the aqueous extracts of palm fruits on serum low density lipoprotein concentrations of male Wistar albino rats

The data in figure 4 show the triacylglycerol (TAG) concentration of normal control rats administered distilled water and the rats administered graded doses of fresh and fermented aqueous extracts of palm fruits respectively. There were no significant ($P > 0.05$) increase in triacylglycerol concentrations observed in the rats of groups 2 and 3 that were administered the fresh aqueous extract of palm fruits when compared with the normal control. In addition, groups 2 and 3 rats administered

equivalent doses of fermented aqueous extract of palm fruits showed no significant ($P > 0.05$) increase in the TAG concentrations when compared with normal control. However, group's 4 – 5 rats administered equivalent doses of fresh and fermented aqueous extracts of palm fruits respectively showed no significant ($P > 0.05$) decrease in the TAG concentrations when compared with the TAG concentration of the normal control rats.

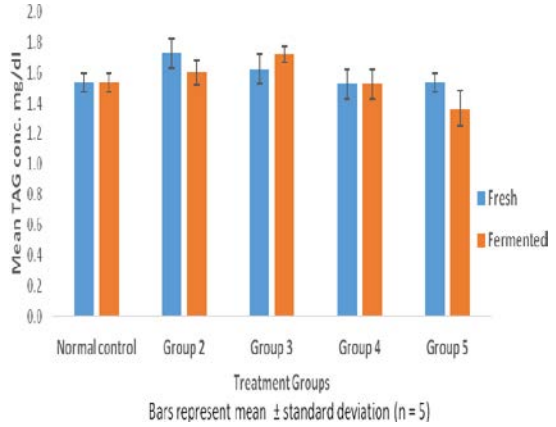

Figure 4. Effect of the aqueous extracts of palm fruits on the triacylglycerol concentrations of male Wistar albino rats

The data in figure 5 show the urea concentration of normal rats and the rats administered graded doses of fresh and fermented aqueous extracts of palm fruits respectively. Group 2 rats that were administered a low dose of the fresh aqueous extract showed no significant decrease ($P > 0.05$) in urea concentration when compared with the normal control. However, the rats in groups 3 – 5 administered the fresh aqueous extract of palm fruits and those in groups 2 – 5 administered the fermented aqueous extract of palm fruits showed a significant increase ($P < 0.05$) in the urea concentrations when compared with the urea concentrations of the normal control rats.

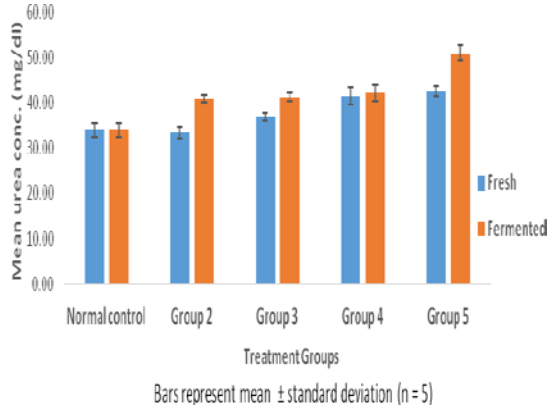

Figure 5. Effect of the aqueous extracts of palm fruits on serum urea concentrations of male Wistar albino rats

The data in figure 6 show the creatinine concentration of the normal control rats and the rats administered graded doses of fresh and fermented aqueous extracts of palm fruits respectively. All the rats administered the fresh and fermented aqueous extracts respectively showed a significant increase ($P < 0.05$) in the creatinine concentration respectively when compared with the creatinine concentration of the normal control rats.

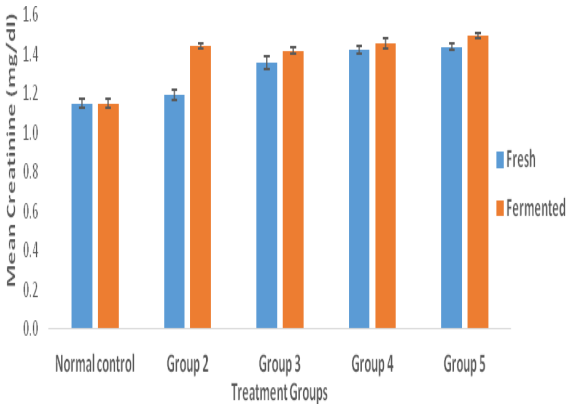

Figure 6. Effect of aqueous extracts of palm fruits on serum creatinine concentrations of male Wistar albino rats

Figure 7 shows the sodium electrolyte concentrations of the normal control rats and the rats administered fresh and fermented aqueous extracts of palm fruits respectively. All the groups of rats that were administered equivalent doses of the fresh and fermented aqueous extracts of palm fruits respectively showed a significant increase ($P < 0.05$) in the sodium electrolyte concentrations when compared with the sodium electrolyte concentrations of the normal control rats.

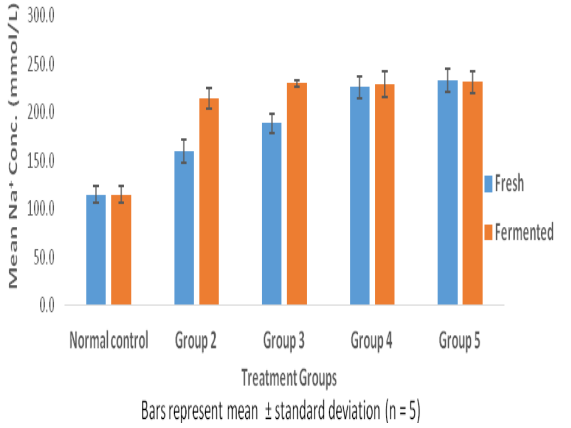

Figure 7. Effect of the aqueous extracts of palm fruits on serum sodium ion concentrations of male Wistar albino rats

Figure 8 shows the chloride ion concentration in the serum of normal control rats and the rats administered graded doses of fresh and fermented aqueous extracts of palm fruits respectively. Rats in groups 2 – 4 and rats in groups 6 – 5 that were administered fresh and fermented aqueous extracts of palm fruits respectively showed no significant increase ($P > 0.05$) in chloride ion concentrations when compared with the chloride ion concentrations of the normal control rats. In addition, group 5 rats that were administered the fresh aqueous extract of palm fruits and group's 2 – 3 rats that were administered the fermented aqueous extract showed no significant decrease ($P > 0.05$) in the chloride ion concentrations relative to the chloride ion concentration of the normal control rats.

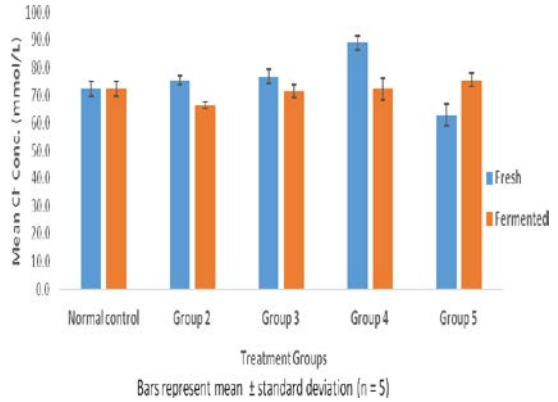

Figure 8. Effect of the aqueous extracts of palm fruits on serum Chloride ion concentrations of male Wistar albino rats

The data in figure 9 represents the serum potassium ion concentration of the normal control rats and the rats administered fresh and fermented aqueous extracts of palm fruits respectively. Group's 2 – 5 rats that were administered graded doses of the fresh extract of palm fruits showed a significant increase ($P < 0.05$) in the potassium ion concentration when compared with the potassium ion concentrations of normal control rats. Groups 2 and 4 that were administered the fermented aqueous extract showed no significant decrease ($P > 0.05$) in the potassium ion concentration when compared with the potassium concentration of the normal control rats. However, rats of group's 3 and 5 that were administered the same fermented aqueous extract of palm fruit showed an increase in the potassium ion concentrations, which is significantly high ($P > 0.05$) when compared with the normal control rats.

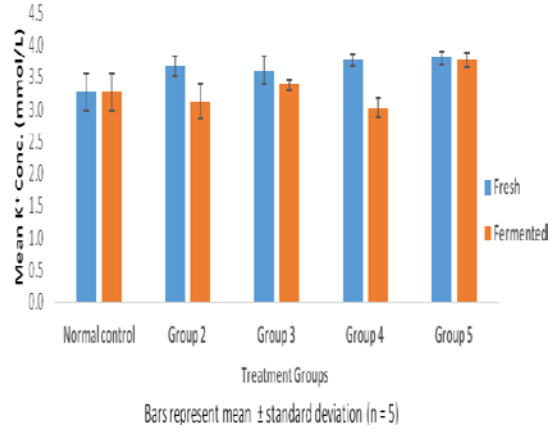

Figure 9. Effect of the aqueous extracts of palm fruits on serum potassium ion concentrations of male Wistar albino rats

The data in figure 10 show the hydrogen trioxocarbonate ion (HCO_3^-) concentrations of the normal control rats and the rats administered fresh and fermented aqueous extracts of palm fruits respectively. Rats of groups 2 and 3 that were administered the fresh aqueous extract of palm fruits showed a significant decrease ($P < 0.05$) in HCO_3^- concentrations when compared with the HCO_3^- concentrations of the normal control rats. Group-five rats that were administered equal doses of the fresh and fermented aqueous extracts of palm fruits respectively, showed a significant increase ($P < 0.05$) in the HCO_3^- concentrations relative to the HCO_3^- concentrations of the normal control rats. The group -three rats administered fresh extract showed no significant decrease ($P > 0.05$) in the HCO_3^- concentrations when compared with the HCO_3^- concentrations of the normal control rats. In addition, group-four rats administered the fresh aqueous extract and the rats of groups 3– 4 administered the fermented aqueous extract showed no significant increase ($P > 0.05$) in HCO_3^- concentrations when compared with the HCO_3^- concentrations of the normal control rats.

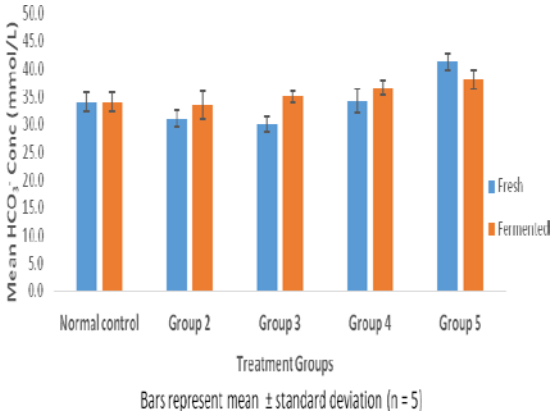

Figure 10. Effect of the aqueous extracts of palm fruits on serum bicarbonate ion concentrations of male Wistar albino rats

The data in figure 11 represent the uric acid concentrations of the normal control rats and the rats administered the aqueous extracts of palm fruits. Groups 2 – 4 that were administered the fresh aqueous extract of palm fruits showed a significant increase ($P < 0.05$) in the uric acid concentration when compared with the oral control rats. Group-six rats administered a high dose of the fresh aqueous extract showed no significant decrease ($P > 0.05$) in the uric acid concentration compared to the normal control. In addition, all the groups that were administered graded doses of the fermented aqueous extract of palm fruits showed no significant increase ($P > 0.05$) in uric acid concentration when compared with the uric acid concentration of the normal control rats.

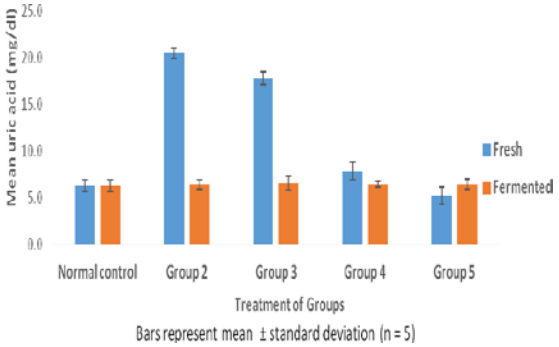

Figure 11. Effect of the aqueous extracts of palm fruits on serum uric acid concentrations of male Wistar albino rats

3.1. Histomorphological Features of Kidneys of Rats Administered Fresh and Fermented Aqueous Extracts of Palm Fruits Respectively

3.1.1. Group 1 (Normal Control Administered Normal Saline)

Sections of the kidney collected from the animals in this group showed the normal renal histo-architecture of laboratory rats. Normal Glomeruli (G) in normal Bowman's capsules (white arrow) was observed. The

Glomeruli were surrounded by a sea of normal renal tubules (proximal convoluted tubules, Pars recta, distal convoluted tubules and collecting ducts) both in the cortex and in the medulla. The renal interstitium were normal consisting of thin connective tissues and blood vessels (B). Renal tubules (arrow). H&Ex100; 400.

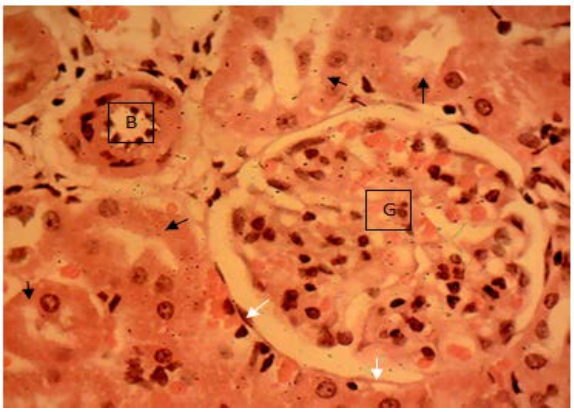

Figure 12. Kidney histomorphology of a normal control rat administered normal saline (2ml/kg b. wt.)

3.1.2. Group 2a (Administered Fresh Aqueous Extract)

Sections of the kidney collected from the animals in this group showed multifocal areas of tubular degeneration (black arrow) and regeneration (white arrow). The degenerating tubules showed tubular lining epithelial cells with cloudy, vacuolated cytoplasm and relatively normal to hyperchromatic nuclear, while the regenerating cells showed thin (barely visible) pale eosinophillic cytoplasm with large hypochromatic nuclei. Glomeruli (G). H&Ex100; 400.

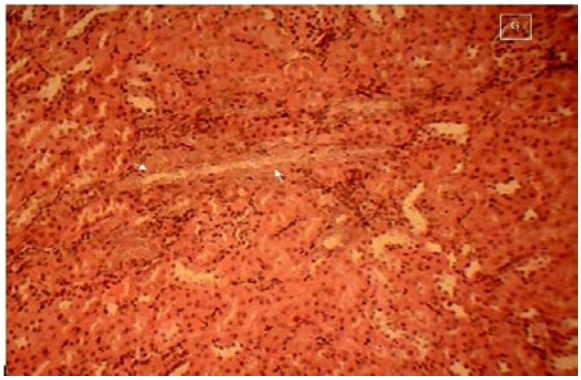

Figure 13. Kidney histomorphology of a rat administered fresh aqueous extract of palm fruits (100 mg/kg b. wt.)

3.1.3. Group 2b (Administered Fermented Aqueous Extract)

Sections of the kidney collected from the animals in this group showed the normal renal histo-architecture of laboratory rats. Normal Glomeruli (G) in normal Bowman's capsules (white arrow) was observed. The Glomeruli were surrounded by a sea of normal renal tubules (proximal convoluted tubules, Pars recta, distal convoluted tubules and collecting ducts) both in the cortex and in the medulla. The renal interstitium were normal consisting of thin connective tissues and blood vessels (B). Renal tubules (arrow). H&Ex100; 400

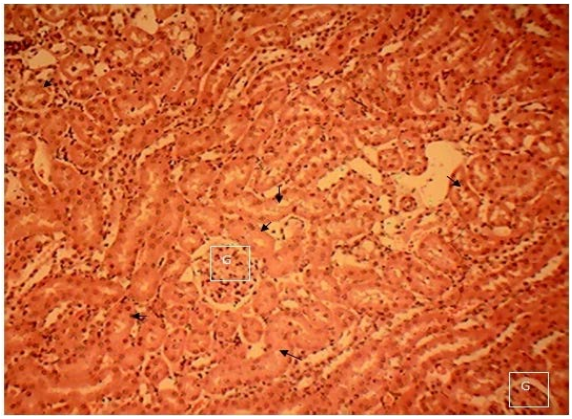

Figure 14. Kidney histomorphology of a rat administered fermented aqueous extract of palm fruits (100 mg/kg b. wt.)

3.1.4. Group 3a (Administered Fresh Aqueous Extract)

Sections of the kidney collected from the animals in this group showed a mild multifocal vacuolar degeneration of the renal tubular epithelial cells (arrow). The affected tubules showed epithelial lining cells with numerous minute clear cytoplasmic vacuoles and normal or pyknotic nuclei (blue arrow). Glomerulus (G). H&Ex400

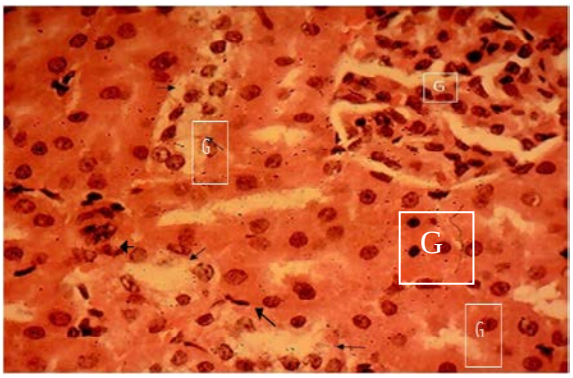

Figure 15. Kidney histomorphology of a rat administered the fresh aqueous extract of palm fruits (200 mg/kg b. wt.)

3.1.5. Group 3b (Administered Fermented Aqueous Extract)

Sections of the kidney collected from the animals in this group showed a mild multifocal vacuolar degeneration of the renal tubular epithelial cells (arrow). The affected tubules showed epithelial lining cells with numerous minute clear cytoplasmic vacuoles and normal nuclei. H&Ex400

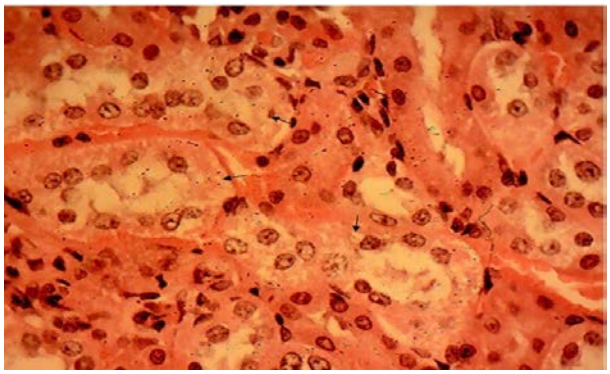

Figure 16. Kidney histomorphology of a rat administered the fermented aqueous extract of palm fruits (200 mg/kg b. wt.)

3.1.6. Group 4a (Administered Fresh Aqueous Extract)

Sections of the kidney collected from the animals in this group showed the normal renal histo-architecture of laboratory rats. Normal Glomeruli (G) in normal Bowman's capsules (white arrow) was observed. The Glomeruli were surrounded by a sea of normal renal tubules (proximal convoluted tubules, Pars recta, distal convoluted tubules and collecting ducts) both in the cortex and in the medulla. The renal interstitium were normal consisting of thin connective tissues and blood vessels (B). Renal tubules (arrow). H&Ex400.

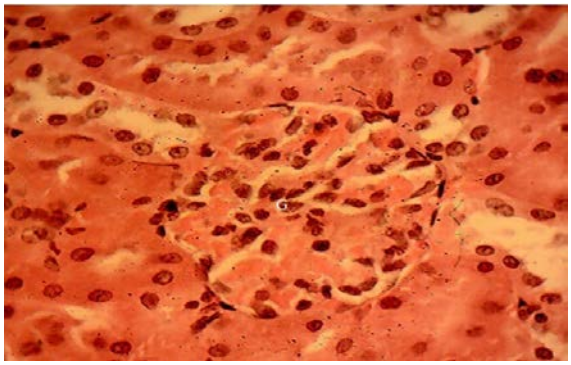

Figure 17. Kidney histomorphology of a rat administered the fresh aqueous extract of palm fruits (400 mg/kg b. wt.)

3.1.7. GROUP 4b (Administered Fermented Aqueous Extract)

Section of the kidney collected from this group showed focal area of tubular necrosis (black arrow) with mild to moderate inflammatory cellular infiltration (white arrow) of the renal interstitium. H&Ex100; 400.

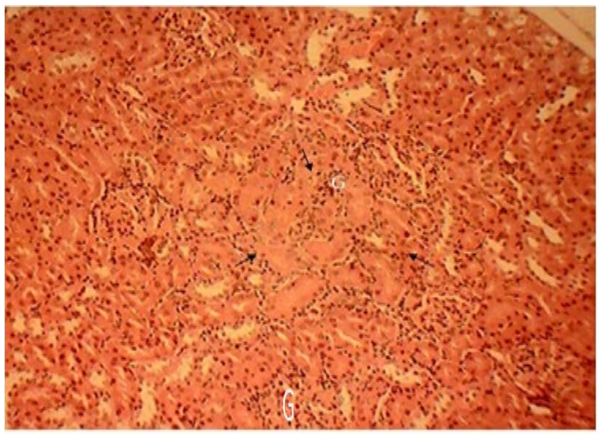

Figure 18. Kidney histomorphology of a rat administered the fermented aqueous extract of palm fruits (400 mg/kg b. wt.)

3.1.8. Group 5a (Administered Fresh Aqueous Extract)

Sections of the kidney collected from the animals in this group showed the normal renal histo-architecture of laboratory rats. Normal Glomeruli (G) in normal Bowman's capsules (white arrow) was observed. The Glomeruli were surrounded by a sea of normal renal tubules (proximal convoluted tubules, Pars recta, distal convoluted tubules and collecting ducts) both in the cortex and in the medulla. The renal interstitium were normal consisting of thin connective tissues and blood vessels (B). Renal tubules (arrow). H&Ex400.

Figure 19. Kidney histomorphology of a rat administered the fresh aqueous extract of palm fruits (600 mg/kg b. wt.)

3.1.9. Group 5b (Administered Fermented Aqueous Extract)

Sections of the kidney collected from the animals in this group showed a mild multifocal vacuolar degeneration of the renal tubular epithelial cells (arrow). The affected tubules showed epithelial lining cells with numerous minute clear cytoplasmic vacuoles and relatively normal to pyknotic (blue arrow) nuclei. Compare with normal renal tubule (white arrow). Glomerulus (G). H&Ex400

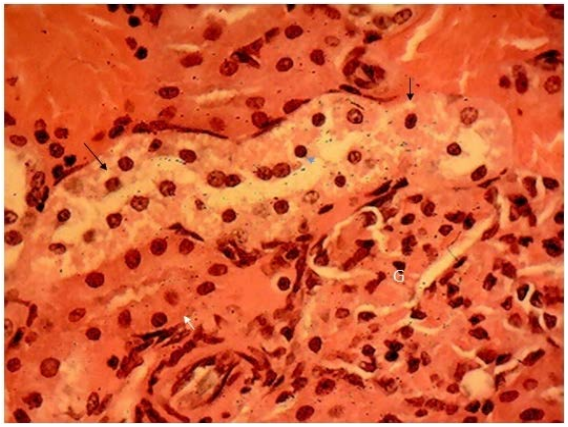

Figure 20. Kidney histomorphology of a rat administered the fermented aqueous extract of palm fruits (600 mg/kg b. wt.)

4. Discussion

This study investigates the effects of fresh and fermented aqueous extracts of *Elaeis guineensis* (palm fruits) on lipid profile and kidney function indices of male Wistar albino rats. The main objective is to understand any possible health implications of the consumption of fresh and fermented aqueous extracts of palm fruits on the consumers. Lipid profile is the breakdown of the components of fats found in one's blood at any given time. Such fats include triacylglycerol, total cholesterol, LDL - cholesterol and HDL – cholesterol which when present in an abnormal proportion increases the risk for cardiovascular diseases. Abnormal lipid profile has been greatly associated with heart attacks and strokes due to atheroma (atherosclerosis) caused by the deposition of cholesterol along the walls of arteries (Morris and Ferdinand, 2009).

The no significant increase ($P > 0.05$) in the total cholesterol concentration observed in the rats that were administered lower doses of fresh aqueous extracts of palm fruits showed that the increase in cholesterol concentrations observed in this study are likely a product of chance and may not be attributed to any effects by the aqueous extracts. Total cholesterol concentrations in blood are not constant but fluctuate based on the prevailing physiological conditions. However, higher cholesterol concentrations observed in groups 4 and 5 of the rats administered the fresh aqueous extract could be attributed to the ability of the fresh aqueous extract of palm fruits to increase cholesterol concentrations at higher doses. The significant increase observed in the total cholesterol concentrations in groups 2, 3 and 4 of the rats administered graded doses of the fermented aqueous extract of palm fruits could be attributed to the cholesterol promoting constituents (such as palmitic acid, lauric acid, stearic acid and glycidyl fatty ester) that may be present in the fermented aqueous extract (Kromhout *et al*., 1995; Sambanthamurthi *et al*., 2000). The constituents of the aqueous extract which could not promote an increase in the total cholesterol concentrations when equivalent doses of the fresh aqueous extract were administered may have been fermented or metabolised into more potent cholesterogenic metabolites that effectively promoted the increase in the total cholesterol concentrations in the rats. Additionally, the significant decrease observed in the total cholesterol concentration in the group-five rats that were administered the highest dose of the fermented aqueous extract of palm fruits suggests that the extract contains low concentration of anti-cholesterogenic constituents. The increased dose of the extract administered to group 5 of the rats may contain enough anti-cholesterogenic agents that drastically caused a decrease in the total cholesterol levels in the rats. The ability of the fermented aqueous extract to increase the total cholesterol concentration at low doses makes it bad for consumption as it could easily lead to an abnormal lipid profile, and aggressively endanger the lives of its consumers. Although, cholesterol plays vital roles in the body such as being an insulator, in addition to the maintenance of the membrane stability, the formation of steroid hormones among others, high concentrations of cholesterol in the blood increases the risk of heart diseases. Sparling *et al*. (1999) have reported that high concentration of serum cholesterol is one of the main controllable risk factors for cardiovascular diseases. Thus, care should be taken to avoid endangering one's health due to the unhealthy eating.

High density lipoprotein (HDL) cholesterol is a component of lipid profile generally considered as good cholesterol. HDL – cholesterol when present in higher concentrations regulates the amount of LDL – cholesterol in the blood. It achieves this maintenance of LDL – cholesterol level in the blood by transporting it from the arteries to the liver where it will be eliminated from the body (Hunter *et al*., 2010). The no significant increase in the HDL – cholesterol concentrations observed in this study could be ascribed to the normal changes in the physiological conditions rather than to the effects of the aqueous extracts, as its concentrations are not static, but fluctuates within a range of values. Similarly, the no significant decrease in the HDL – cholesterol concentrations observed in the rats of group 5 which were administered a higher dose of the fermented aqueous extract suggests by increasing the dose of the fermented extract administered, a significant decrease in the HDL – cholesterol concentration may result. This could negatively affect the health of an individual especially when there is a high concentration of LDL – cholesterol in the blood circulation. The abnormal lipid profile has been largely attributed to the increasing cases of cardiovascular diseases, which in turn is very relevant to the high mortality indices (Lewington *et al*., 2007; McQueen *et al*., 2008). Food items that significantly increase the HDL – cholesterol level at the expense of LDL – cholesterol is nutritionally preferred to those that decrease the HDL – cholesterol concentration and increase the LDL – cholesterol concentration. This is attributed to the health-promoting benefits associated with HDL – cholesterol as it helps remove LDL – cholesterol from the body (Morris and Ferdinand, 2009).

A healthy heart is maintained when there is low concentrations of LDL-cholesterol and high concentrations of HDL – cholesterol in the blood. This ratio reduces the risk of atherosclerosis and heart diseases. Higher concentrations of LDL–cholesterol and low concentrations of HDL – cholesterol in the blood lead to the narrowing of the arteries due to the deposition of LDL–cholesterol on the arterial walls, hindering the transport of blood to the brain and other vital organs (Nazawi and El-Bahr, 2012). The no significant differences observed in the HDL – cholesterol concentrations in the rats administered graded doses of fresh aqueous extract of palm fruits maybe attributed to the fresh extract having low saturated fats and a substantial amount of unsaturated fats that lower the LDL – cholesterol concentrations and promote a healthy heart. On the other hand, there were significant increases in the HDL – cholesterol levels of the rats in groups 2 and 4 that were administered the fermented aqueous extract of palm fruits which indicates that the extract may be rich in saturated fats and other cholesterogenic constituents that promote the HDL – cholesterol formation. Thus, the fermented aqueous extract of palm fruits could have deleterious effects on individuals who consume it regularly. The use of these aqueous extracts in the production of palm oil as a water substitute and in the preparation of local soup "ofe akwu" should be

discouraged. Although, the abnormal lipid profile is promoted by a genetic factor, the lack of physical activity and other related diseases, adhering to the principles of healthy eating remains the best way to maintaining a balanced lipid profile and reducing risk of strokes and heart diseases (Zemdegs *et al*., 2011).

Triacylglycerol is a major energy store in the body and its concentrations are greatly influenced by genetic factors, physical activities and the food intake. Low serum triacylglycerol concentrations promote a good health and heart functions while high triacylglycerol concentrations increases the risk of heart diseases. The no significant increases and decreases observed in the rats administered graded doses of the fresh and fermented aqueous extracts of palm fruits respectively relative to the normal control suggest that the extracts lack potentials to increase the blood triacylglycerol levels to the extent that will make their consumers vulnerable to heart diseases (Zemdegs *et al*., 2011). The observed change in the triacylglycerol concentrations might be attributed to the extracts. The fluctuations in triacylglycerol levels may be a result of some changes in the normal physiological conditions.

The dose-dependent significant increase observed in the creatinine concentrations of the rats administered fresh and fermented aqueous extracts of palm fruits respectively relative to the normal control could be attributed to some adverse effects of the aqueous extracts of palm fruits on kidney functions which led to the impairment of glomeruli filtration rate and increased the creatinine concentrations in the blood. Creatinine, which is a product of creatine phosphate breakdown released from skeletal muscles at a steady rate, serves as a more sensitive and specific test for renal functions because the changes in its concentration give a better assessment of the renal status. An increased serum creatinine level signifies impaired renal function in most cases (Nwodo *et al*., 2015). However, the high intake of dietary protein, oral creatine intake, crush injury and some drugs such as cimetidine and trimethoprim have been shown to raise the serum creatinine level even in the absence of any renal damage or renal malfunctioning. The significant creatinine concentrations observed in this study signify a renal impairment in rats. The serum concentrations together with the changes observed in the histomorphology of the kidney agree with the findings of Spanaus *et al*., (2010) and Dalton, (2010) who had independently reported that the serum creatinine concentration is a very reliable indicator of the glomerular filtration rate which is largely the most sensitive serum biomarker for detecting any little or early changes in the glomerular filtration rate in individuals. It is also in line with the earlier findings by Anjaneyulu *et al*., (2004) which state that increase in urea and the serum creatinine concentrations in rats indicates a progressive renal damage. The observed renal impairment in rats calls for a critical investigation of the effects of the aqueous extracts on the renal function indices of humans to prevent any associated adverse health effects.

Urea is a metabolic product of ammonia resulting from the breakdown of proteins and other amino group containing compounds in the liver. It is relatively non-toxic and serves as one of the markers of renal function though less specific. Increase in the blood urea concentration is associated with an impaired renal function. The dose-dependent increase in the serum blood urea concentrations observed in this study are probably due to the toxic effects of these extracts on the kidney that impaired the ability of renal glomeruli to filter urea from the blood (Nwodo *et al*., 2015). Measuring blood urea concentration is a less specific and sensitive method for ascertaining the renal function of an individual as its blood concentration can be increased by stress, high protein diets, and upper gastrointestinal (GI) bleeding (Wijeysundera *et al*., 2007). It has been shown that an increase in the urea concentration commonly occurs when there is impairment of the renal function and in combination with the observed increase in the serum creatinine concentration which indicates a progressive renal damage as observed in this study (Anjaneyulu *et al*., 2004, Shrestha *et al*., 2008)

Serum electrolytes concentrations affect the body functions including the regulation of blood acidity, water balance, muscle functions, nerve conduction, blood clotting and body fluids for the sustenance of life (Chernecky and Berger, 2013). Electrolyte imbalance frequently occurs due to the kidney failure, dehydration, fever and vomiting, thereby disturbing normal cellular functions (Husain *et al*., 2009). The high serum electrolytes concentrations observed in this study could be attributed to the effect of the extracts on kidney functions and partly to the richness of the extracts in micronutrients such as potassium, sodium, calcium and magnesium (Uroko and Njoku, 2014). Coupled with creatinine and urea, serum electrolyte concentrations give a better measure of kidney functions and a guide for choosing the treatment option. The excessive serum potassium concentration as seen in this study commonly occurs because of renal malfunction associated with the inability of the kidney to excrete potassium ions and the increased amount of potassium released from the damaged cells. An abnormal high potassium level could trigger a cardiac arrest, and may be effectively treated with insulin and glucose administration to get potassium into cells before addressing the main cause of the increase in the serum potassium concentrations (National Institute for Health and Care Excellence, 2013).

Uric acid is a metabolite of purine catabolism that is filtered by the glomeruli and both reabsorbed and secreted by the renal tubules (Rodwell, 2003). Blood uric acid concentration usually increases with renal damage or renal impairment and has been used as an indicator of renal functions. However, the increase in the blood uric acid concentration is not specific to renal impairment because many conditions can lead to increase in the blood uric acid concentration under normal renal functions. Severe haemolytic anaemia, lead poisoning, burns, a crush injury, tumour lysis and diuretic drugs are the most established causes of an increased blood uric acid concentration apart from renal impairment. The increased blood uric acid concentration observed in the rats administered low doses of the fresh aqueous extract show that the extract possesses chemical constituents capable of impairing renal functions possibly by causing severe haemolytic anaemia, or interfering with the glomeruli filtration rate, reabsorption, and secretion of uric acid by the renal tubules. Although many researchers have suggested that hyperuricemia only indicates renal dysfunction rather than a risk factor for its

progression, it is generally considered as an independent risk factor for the development and progression of coronary artery diseases (Madsen *et al*., 2005; Roncal *et al*., 2007). Thus, the consumption of fresh aqueous extract of palm fruits is of great health concern. None of the rats administered the fermented aqueous extract showed an increase in blood uric acid concentration suggesting that fermentation might have detoxified nephrotoxic constituents responsible for the observed increase in the blood uric acid concentration of the rats administered the fresh aqueous extract into non-toxic metabolites. Thus, the fermented aqueous extract of palm fruits may be said to lack the potential of impairing renal functions.

5. Conclusion

The findings of this study suggest that the fermented aqueous extracts of palm fruits have a high potential of negatively altering the lipid profile and increasing the health risks associated with a poor lipid profile. In addition, both the fresh and fermented aqueous extracts of palm fruits possess potentials that can impair renal functions if consumed in excess or for a long period as demonstrated in this study. At present, there is no scientific data on the effects of these aqueous extracts on humans, thus, the consumption of aqueous extracts of palm fruits through local dishes such as "ofe akwu" should be minimized, and their use as a water substitute for the production of palm oils in various palm oil mills should be discouraged.

Ethical Approval

A written ethical approval has been collected and preserved by the author(s) concerning the international standards or university standards.

Competing Interests

The authors declare that no competing interests exist.

References

Akinsorotan AM. 2013. Histopathological effects of acutely toxic levels of palm oil mill effluent on gill and liver of Nile tilapia fingerlings. *Inter J Sci Engin Res*., **4(3)**: 22-29

Albers JJ, Warmick GR and Cheng MC. 1978. Determination of high density lipoprotein (HDL)-cholesterol. *Lipids*, **13**: 926-932.

Allain CC, Poon LS, Chan CSG, Richmond W and Fu PC. 1974. Enzymatic determination of total serum cholesterol. *Clin Chem.*, **20**: 470-475.

Anawat T, Kanokporn S and Supap S. 2017. Hypoglycemic and hypolipidemic properties of herbal tea on Wistar rat. *Chiang Mai Vet J*., **15(1)**: 25-35

Anjaneyulu M. Chopra K. 2004. Quercetin, an antioxidant bioflavonoid, attenuates diabetic nephropathy in rats. *Clin Exper Pharmacol Physiol*., **31**:244-248.

Assmann G, Jabs HU, Kohnert U, Nolte W and Schriewer H. 1984. LDL-cholesterol determination in blood serum following precipitation of LDL with polyvinylsulfate. *Clin Chim Acta*, **140**: 77-83.

Chernecky CC and Berger BJ. 2013. Electrolytes Panel - Blood. In: Chernecky CC, Berger BJ, Eds. **Laboratory Tests and Diagnostic Procedures**, 6th ed. St. Louis, MO: Elsevier Saunders, pp. 464-467.

Dalton RN. 2010. Serum creatinine and glomerular filtration rate: Perception and reality. *Clin Chem.*, **56(5)**: 687–689

Forrester RL, Wataji LJ, Silverman DA and Pierre KJ. 1976. Enzymatic method for determination of CO_2 in serum. *Clin Chem.*, **22**:243–245.

Helin I and Winberg J. 2008. Insulin-dependent and non-insulin-dependent diabetes mellitus. *Acta Pædiatrica*, **69**: 607–611.

Hunter JE, Zhang J, Kris-Etherton PM. 2010. Cardiovascular disease risk of dietary stearic acid compared with trans, other saturated, and unsaturated fatty acids: a systematic review. *Amer J Clin Nutri.*, **91(1)**: 46-63.

Husain F, Arif-Maan M, Sheikh MA, Nawaz H and Jamil A. 2009. Trace elements status in type 2 diabetes. *Bangladesh J Med Sci.*, **8**: 52–56.

IBM Corporation. 2011. **IBM SPSS Statistics for Windows**, Version 20.0. Armonk, NY: IBM Corp.

Jain P, Patil S, Haswani N, Girase M and Suran S. 2010. Hypolipidemic activity of Moringa oleifera Lam., Moringaceae, on high fat diet induced hyperlipidemia in albino rats. *Brazilian J Pharmacognosy*, **20(6)**: 969-973.

Kromhout D, Menotti A, Bloemberg B, Aravanis C, Blackburn H, Buzina R, Dontas AS, Fidanza F, Giampaoli S, Jansen A. 1995. Dietary saturated and trans fatty acids and cholesterol and 25-year mortality from coronary heart disease: The Seven Countries Study. *Preventive Med*., **24**: 308–315.

Lewington S, Whitlock G, Clarke R. 2007. Blood cholesterol and vascular mortality by age, sex, and blood pressure: A metaanalysis of individual data from 61 prospective studies with 55 000 vascular deaths. *Lancet***, 370**: 1829-1839.

Luqman S, Srivastava S, Kumar R, Maurya AK and Chanda D. 2012. Experimental assessment of *Moringa oleifera* leaf and fruit for its antistress, antioxidant, and scavenging potential using in vitro and in vivo assays. *Evidence-Based Complement Alternative Med*., **2012**: 1-12.

Madsen TE, Muhlestein JB, Carlquist JF, Horne BD, Bair TL, Jackson JD. 2005. Uric acid independently predicts mortality in patients with significant, angiographically defined coronary disease. *Amer J Nephrol*., **25(1)**:45-59.

Mona SH, Eman ME and Aya AAO. 2013. Effect of *Moringa oleifera* on serum lipids and kidney function of hyperlipidemic rats. *J Appl Sci Res*., **9(8)**: 5189-5198

Morris A and Ferdinand K. 2009. Hyperlipidemia in Racial/Ethnic Minorities: Differences in lipid profiles and the impact of statin therapy. *Clin Lipidol*., **4(6)**: 741-754.

National Institute for Health and Care Excellence (NICE). 2013. **Acute Kidney Injury**. London.

Nazawi MH and El-Bahr SM. 2012. Hypolipidemic and hypocholesterolemic effect of medicinal plant combination in diet of rats: Black cumin seed (Nigella sativa) Turmeric (curcumin). *J Animal Vet Advances*, **11(12)**: 2013-2019

Nwodo OFC, Joshua PE, Ugwuoke MC and Uroko RI. 2015. Anti-malarial and some biochemical indices of the ethanol extract of *Zapoteca portoricensis* root on malaria-infected mice. *Asian J Biochem.*, **10(6)**: 281-289,

Ohimain EI, Enetimi IS, Izah SI, Oghenegueke EV and Perewarebo TG. 2012. Some selected physicochemical and heavy metal properties of palm oil mill effluents. *Greener J Phys Sci.*, **2(4)**:131-137

Peters JH. 1942. The determination of creatinine and creatinine in blood and urine with the photoelectric colorimeter. *J Biol Chem.*, **146**: 179-186

Rodwell VW. 2003. Metabolism of Purine and Pyrimidine Nucleotides. In: **Harper's Illustrated Biochemistry**, 26th Ed. USA: McGraw Hill Company, p. 299–300.

Roncal CA, Mu W, Croker B, Reungjui S, Ouyang X and TabahFisch I. 2007. Effect of elevated serum uric acid on cisplatin induced acute renal failure. *Amer J Physiol-Renal Physiol.*, **292**:116-122.

Sambanthamurthi R and Sundram K, Tan Y. 2000. Chemistry and biochemistry of palm oil. *Progress Lipid Res.*, **39**: 507–558.

Santoshkumar J, Manjunath S and Pranavkumar S. 2013. A Study of antihyperlipidemia, hypeolipedimic and anti-atherogenic activity of fruit of emblica officinalis (AMLA) in high fat fed Albino rats. *Inter J Med Res and Health Sci.*, **2(1)**: 70-77.

Shrestha S, Gyawali P, Shrestha R, Poudel , Sigdel M, Regmi P et al. (2008). Serum urea and creatinine in diabetic and non-diabetic subjects. *J Nepal Asso Med Lab Sci.*, **9**:11-2.

Sivaiah G and Reddy A. 2012. Evaluation of anti-hyper lipidemic activity of hydro alcoholic extract of *Moringa oleifera* seeds in high fat diet induced rat model. *K. Sivaiah*, **2(2)**: 72-76

Skeggs LT and Hochstrasser HC. 1964. Colorimetric determination of chloride. *Clin Chem.*, **10**: 918-936

Spanaus KS, Kollerits B, Ritz E, Hersberger M, Kronenberg F and von Eckardstein A. 2010. Mild and moderate kidney disease (MMKD) study group. *Clin Chem.*, **56**:740-749

Sparling PB, Snow TK and Beavers BD. 1999. Serum cholesterol levels in college students: opportunities for education and intervention. *J Am Coll Health*, **48**: 123-7.

Terri AE and Sesin PG. 1958. Colorimetric determination of sodium. *Amer J Clin Pathol.*, **29**:86-90

Tietz NW. 1990. **Clinical Guide to Laboratory Tests,** second Ed., W.B. Saunders Company, Philadelphia, PA., USA. pp: 554-556.

Trinder P. 1969. Determination of glucose in blood using glucose oxidase with an alternative oxygen acceptor. *Annual Clin Biochem.*, **6**: 24-25.

Ubon JA, Akpanabiabtu MI, Akanyung EO and Ufot UF. 2017. Effects of ethanolic extracts of *Cola millenii* K. Schum seed on biochemical and toxicological indices of male wistar albino rats. *J Pharmacog and Phytochem.*, **6(1)**: 160-166

Uroko RI and Njoku OU. 2014. Study on fresh and fermented palm oil mill effluents as an alternative source of improving soil fertility. *Nigerian J Biochem Mol Biol.*, **29(2)**: 58-67

Uroko RI, Agbafor A, Uchenna ON, Achi NK, Egba SI, Nweje-Anyalowu PC and Ngwu OR. 2017. Evaluation of antioxidant activity of aqueous extracts of palm fruits (*Elaeis guineensis).* *Asian J Biochem.*, **12**: 49 - 58

Varley H and Alan HG. 1984. Tests in Renal Disease. In: **Practical Clinical Biochemistry**, Vol. 1123. William Heinmann Medical Book Ltd; London. p.10

Wijeysundera DN, Karkouti K, Dupuis, JY, Rao V, Chan CT, Granton JT and Beattie WS. 2007. Derivation and validation of a simplified predictive index for renal replacement therapy after cardiac surgery. *J Amer Med Assoc.*, **297**: 1801-1809.

Zemdegs JCS, Corsi1 LB, Coelho1 LD, Pimentel GD, Hirai AT and Sachs A. 2011. Lipid profile and cardiovascular risk factors among first-year Brazilian university students in São Paulo. *Nutricion Hospitalaria*, **26(3)**:553-559.

JJBS

Volume 12, Number 1,March 2019
ISSN 1995-6673
Pages 17 - 21

Jordan Journal of Biological Sciences

Phenolic Compounds, Antioxidant and Antibacterial Activities of *Rhus flexicaulis* Baker

Mohamed Abdel-Mawgoud[1*], Fawzy G. Khedr[2] and Enas I. Mohammed[1]

[1]*Department of Medicinal and Aromatic Plants, Desert Research Center, Cairo;* [2]*Department of Botany, Faculty of Science, Zagazig University,Egypt*

Received June 3, 2018; Revised June 22, 2018; Accepted July 2, 2018

Abstract

The genus *Rhus* (sumac), belonging to the family *Anacardiaceae*, is one of the most widespread and recognizable genera in North America and Africa. It is known to be rich in biflavonoids, urushiols and bichalcones. This study describes the identification and quantification of many phenolic compounds, for the first time, in *Rhus flexicaulis*, including seven flavonoids and seventeen phenols, using liquid chromatography-mass spectrometry (LC-MS). The total phenolic content was (30.31 mg/g), the total flavonoid content was (20.93 mg/g) and the total antioxidant capacity was (2005.17 µmol/g) in *Rhus flexicaulis*. The results showed that the plant extract has an antibacterial activity against *Streptococcus pyogenes* and *Escherichia coli*.

Keywords: Phytochemical, Phenolic compounds, Antibacterial, Antioxidants, *Rhus flexicaulis*.

1. Introduction

The genus *Rhus* (sumac), belongs to the family *Anacardiaceae*, including about 250 species, which occur mainly in the tropics, subtropics and temperate areas of the world, especially in North America and Africa (Gallant *et al*. 1998). The sumac name is derived from "sumaga", meaning red in Syriac (Wetherilt and Pala, 1994). In general, *Rhus* species can grow in non-agricultural regions and various species have been used by indigenous people for medicinal and other purposes, suggesting a potential for commercializing the bioactivity of these plants without competing for food production land uses (Van Wyk and Wink 2004). For example, *R. glabra* (smooth sumac) is traditionally used by native people of North America in the treatment of bacterial diseases such as syphilis, gonorrhea, dysentery, and gangrene (Erichsen 1989). *R. coriaria* is commonly used as a spice by grinding the dried fruits with salt, and is also widely used as a medicinal herb in the Mediterranean and Middle East, particularly for wound healing (Sezik *et al*. 1991). The genus *Rhus* is known to be rich in biflavonoids, urushiols and bichalcones (Masesane *et al*. 2000). Sumac extracts have been shown to exhibit a wide range of biological activities, namely antimalarial, antiviral, antimicrobial and antitumorigenic activities (Ahmed *et al*. 2001 and Choi *et al*. 2012).

Rhus flexicaulis is a densely pilose-tomentose, perennial shrub that reaches up to 2-3 m long. Leaves are compound with three suborbicular to ovate-elliptic, sessile leaflets with an apex of entirely rounded margins; the terminal leaflet is larger than the two lateral leaflets. Flowers are arranged in lax terminal panicles. The fruit is a brownish, glossy drupe. The plant is growing in South-east Egypt, Sudan and Arabia regions (Bolous, 2000).

Recently, the essential oil of *Rhus flexicaulis* was analyzed by Gas Chromatography Mass Spectrometry (GC-MS). It was found that the major constituents of essential oil are β-bisabolene, β-farnesene, β-curcumene and caryophyllene oxide. Four classes of compounds have been detected in the *R. flexicaulis* oil including monoterpene hydrocarbons, oxygenated monoterpenes, sesquiterpene hydrocarbons and oxygenated sesquiterpenes. The phytochemical screening showed that *R. flexicaulis* contains moderate amounts of carbohydrates and / or glycosides, sterols, terpenes, flavonoids and tannins, while alkaloids, saponins, coumarines and anthraquinones were absent (Ibrahim *et al*. 2017).

This study is aimed at investigating the chemical constituents of this plant material collected from the field and its antibacterial activity in order to evaluate its potential uses and medicinal properties.

2. Material and Methods

2.1. Plant Collection and Preparation

The fresh aerial parts and of *Rhus flexicaulis* Baker were collected in March 2016 from Gebal Elba (Wadi Ma'arafai; south east of Egypt at about 600 m height, geographic position coordinates N: 27.5°22′12″; E: 20.2°36′20″) and were identified by the experts in Desert Research Center, Cairo, Egypt. A voucher specimen of the plant has been deposited at the Herbarium of Desert Research Center. The plants were stored in plastic bags under dark, chilled conditions during transportation to the

* Corresponding author. e-mail: mohamed_drc@yahoo.com.

laboratory. The plant samples were collected as leaves and stems (shoot system), then washed under tap water, and were air-dried at lab-temperature till constant weight. The plant samples were ground to fine powder to be used for chemical analyses. The plant material was brought to the Institute of Botany, Leibniz University Hannover, Germany.

2.2. Extraction of Phenolic Compounds

Fifty mg of the dried plant material was used. Extraction was performed three times with 2 mL 80 % Methanol (MeOH) using an overhead shaker and ultrasonic bath. After each extraction step, the samples were centrifuged for twenty minutes at 13,000 rpm, 10000 g and the supernatant was saved. The resulting supernatants were combined and centrifuged again for thirty minutes at 13.000 rpm to remove any suspended particles. The clear supernatant was used for further analysis (Dewanto *et al.* 2002).

2.3. Determination of Total Phenolic Content

Analysis of the total phenol content is based on a colorimetric measurement at 765 nm (Dudonné *et al.* 2009). A standard series of gallic acid (GA) was used for quantification. Each sample was measured as technical triplicate. Results were given as GA equivalents (GAE)/g dry weight. Twenty-five µL of extracted sample (1:10 diluted with H_2O) was incubated with 125 µL of "Folin-Ciocalteau" phenol reagent (1:10 diluted with water) for eight minutes at room temperature (RT). Exactly 125 µL of sodium carbonate (7.5 %) was added to the well and mixed by pipetting. The mixture was incubated for two hours in the dark. Absorbance was measured at 765 nm with a microplate reader (BioTek, Winooski, USA). The total phenol content was calculated by the factor estimated with the GA standard series.

2.4. Determination of Total Flavonoid Content

The extraction follows the procedure as described for the determination of total phenol content (Dewanto *et al.* 2002). Into each well 150 µL of deionized water was filled and 25 µL of a sample or one of the catechin hydrate standard solutions were added. Next 10 µL of a 3.75 % $NaNO_2$ solution was added, and the plate was gently shaken and afterwards incubated at room temperature for six minutes in darkness. After incubation, 10 µL of $AlCl_3$ (10 %) was added, and the plate is again gently shaken and incubated for five minutes at room temperature in the dark. After this step 50 µL of 1 M NaOH were added and the absorbance at 510 nm was measured using a microplate reader (BioTek).

2.5. Determination of Total Antioxidant Capacity (Oxygen Radical Absorbance Capacity) (ORAC)

The measuring system relies on the decrease of fluorescence over time. Fluorescein di-sodium salt was used as fluorophor, being slowly oxidized by 2,2'-azobis (2-methylpropionamidin) dihydrochloride (AAPH) (Huang *et al.* 2002, Gillespie *et al.* 2007). Depending on the amount of anti-oxidants in the sample, this process is decelerated. For quantification a calibration series with 6-hydroxy- 2, 5, 7, 8- tetramethylchroman-2-carbonic acid (Trolox™) was used. Results are given in Trolox™ equivalent (TE) pertaining to 1 g of dry weight.

The extraction follows the following procedure. In each well of a black, pre-cooled microtiter plate 120 µL of 112 nM fluorescein solved in 75 mM phosphate buffer (pH 7.4) was pipetted. Then 20 µL of trolox-standard solution, 20 µL of phosphate buffer (75 mM, pH 7.4) as blank were repeated three times on the plate, and then 20 µL of the samples have been added each in three replicates. The samples had to be diluted 1:50 with phosphate buffer. The plate was then placed into the pre-heated (37°C) microplate reader (BioTek) and incubated for fifteen minutes before fluorescence was measured at 485/520 nm. After the first measurement 80 µL of a 62 mM AAPH-solution in phosphate buffer was added to each well. Then the fluorescence at 485/520 nm was measured over the course of eighty minutes once every minute. The difference between each measurement was calculated and quantified using the standard row.

2.6. Identification of Phenolic Compounds by LC-MS

Liquid chromatography-mass spectrometry (LC-MS) analysis was performed using the HPLC system (Shimadzu; Darmstadt, Germany) consisting of a controller (CBM-20A), two pumps (LC-20AD), a column oven (CTO-20AC) and a photo diode array detector (SPD-M20A). A Vertex Plus column (250 x 4 mm, 55 µm particle size, packing material ProntoSIL 120-5 C18-H) with pre-column (Knauer, Berlin, Germany) was used for sample separation.

Prior to analysis the samples were diluted 1:2 in 80 % methanol (LC-MS grade) and 10 µL was used. The temperature of the column oven was set to 30ºC. Ammonium acetate (2 mM) was added to eluents of water (A) and methanol (B). Both eluents had a flow rate of 0.8 mL min^{-1}. The gradient was applied in the following manner: starting with 10 % B, then switching linearly to 90 % B in thirty-five minutes, two minutes of 90 %, switching to 10 % B in one minute and the subsequent equilibration at 10 % B for two minutes. UV/Vis spectra from 190-800 nm were recorded. Components were injected into an AB Sciex Triple TOF mass spectrometer (AB Sciex TripleTOF 4600, Canby, USA) following HPLC separation for identification. A temperature of 600°C was used for negative electrospray ionization. Mass spectra with the range of 100-800 Da were measured in the TOF range. MS/MS spectra from 50-800 Da at a collision energy of -30 were additionally recorded.

The phenolic acid and flavonoid standards for the identification and quantification were prepared in the same way. Peaks were compared by examining retention time and fragmentation pattern using the PeakView (SCIEX) software. Quantification of the identified compounds was done using a regression line generated by the software MultiQuant (SCIEX) that compares the area under the curve. Protochatechuic acid (PCS) was used as internal standard. For example, to quantify chlorogenic acid in *Rhus flexicaulis* extract, a quadratic regression line was formed using the following concentrations of the chlorogenic acid standards: 50 nM, 100 nM, 1 µM, 50 µM and 100 µM + 50 µM PCS. For vanillin and catechin, a linear regression line was formed using the following concentrations of the appropriate standard: 50 nM, 100 nM, 500 nM, 1 µM, 50 µM and 100 µM + 50 µM PCS and 10 nM, 100 nM, 1 µM and 10 µM + 50 µM PCS,

respectively. All standards were measured in the same way.

2.7. Antibacterial Assay

Disc diffusion method was used to determine the antibacterial activity of *Rhus flexicaulis* extract against *Streptococcus pyogenes* and *Escherichia coli* using 100 µL of suspension containing 10^8 CFU/mL of bacteria spread on Muller Hinton agar (Selim *et al*. 2013). The sterilized dried ethanol plant extract was loaded on filter paper discs to obtain a final concentration of 7.5 mg/disc. Loaded filter paper discs were placed on the top of Mueller-Hilton agar plates. Plated then incubated at 35°C for twenty-four hours to allow the diffusion of herbal plant extract. The presence of inhibition zones was measured by Vernier caliper, recorded and considered as indication for antibacterial activity. Negative controls were prepared using the same solvent employed to dissolve extract. After incubation for forty-eight hours at 37°C, the diameter of inhibition zones was recorded.

3. Results

3.1. Determination of Total Phenolic Content

Total phenolic content was examined with "Folin-Ciocalteau", a commonly used reagent for the estimation of the content of phenols in a sample. Results were expressed as gallic acid equivalents in (mg GAE g DW^{-1}). The results showed that the total phenolic content of *Rhus flexicaulis* was 30.31± 1.63 mg GAE g DW^{-1}.

3.2. Determination of Total Flavonoid Content

The total flavonoid content was determined following the same procedure described for the total phenol content. Results were expressed as catechine-hydrate equivalents in [mg g DW^{-1}]. The results showed that the total flavonoid content of *Rhus flexicaulis* was 20.93± 1.47 mg CE g DW^{-1}.

3.3. Determination of Total Antioxidant Capacity (ORAC)

The ORAC test is a standard test for total antioxidant capacity, standardized as Trolox™ equivalent (TE) in µmol/g. Data showed that the total antioxidant capacity of *Rhus flexicaulis* was 2005.17± 5.17 µmol TE g DW^{-1}.

3.4. Identification of Phenolic Compounds by LC MS

The LC-MS measurement resulted in data for the mass spectrum (ES^-), the retention time and the UV spectrum. These parameters have been compared to the standards and peaks found in the extract data. If both values accorded to each other, the compound was shown to be found in the plant extract (Table 1). The LC-MS analysis indicated that twenty-four compounds were present in the *Rhus flexicaulis* extract. These compounds include seven flavonoids namely kaempferol (1), quercetin (2), apigenin (3), catechin (4), epicatechin (5), isorhamnetin (6) and taxifolin (7), and seventeen phenolic acids namely cinnamic acid (8), gallic acid (9), ferulic acid (10), benzoic acid (11), gentisic acid (12), chlorogenic acid (13), p-coumaric acid (14), caffeic acid (15), P-Hydroxybenzoic acid (16), vanillic acid (17), vanillin (18), anisic acid (19), rosmarinic acid (20), pyrogallol (21), sinapic acid (22), syringaldehyde (23) and syringic acid (24) in *Rhus flexicaulis* for the first time. The total ion chromatogram is shown in figure 1.

The current results showed that phenolic acids were the major chemical constituents present in *Rhus flexicaulis*. Catechin was found to have the highest amount (34.99 µg/g), while Sinapic acid had the lowest amount (0.02 µg/g).

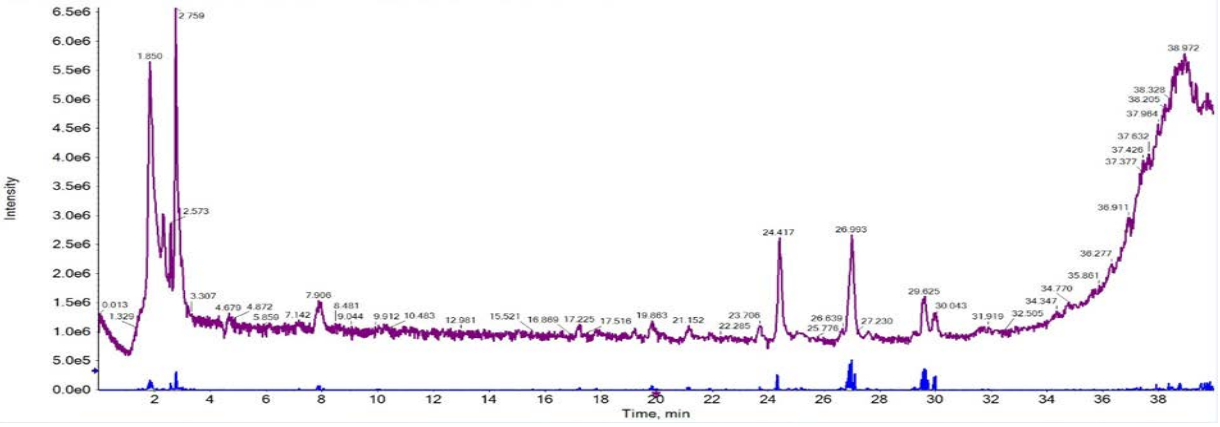

Figure 1. Total chromatogram of phenolic compounds of *Rhus flexicaulis*

Table 1: Phenolic acids and flavonoids detected in the Rhus flexicaulis extract. The identification was based on the m z -1 ratio and retention times compared to standards.

Peak No.	Compound	Mass	Retention Time (min)	$[MH]^-$	Chemical formula	Concentration(µg/g)
1	Catechin	290.27	12.3	289.2	$C_{15}H_{14}O_6$	34.99
2	Ferulic acid	194.1	16.5	193.1	$C_{10}H_{10}O_4$	0.30
3	Gallic acid	170.1	4.4	169.1	$C_7H_6O_5$	5.0
4	Apigenin	270.2	29.5	269.2	$C_{15}H_{10}O_5$	0.36
5	Gentisic acid	154.1	6.6	153.1	$C_7H_6O_4$	0.03
6	Chlorogenic acid	354.3	9.1	353.3	$C_{16}H_{18}O_9$	0.08
7	P-coumaric acid	164.1	15.7	163.1	$C_9H_8O_3$	0.25
8	Caffeic acid	180.1	12.2	179.1	$C_9H_8O_4$	0.33
9	Isorhamnetin	316.2	29.3	315.2	$C_{16}H_{12}O_7$	0.14
10	Quercetin	302.2	26.6	301.2	$C_{15}H_{10}O_7$	0.89
11	Cinnamic acid	148.1	22.2	147.1	$C_9H_8O_2$	0.03
12	Taxifolin	304.2	19.1	303.2	$C_{15}H_{12}O_7$	20.0
13	Epicatechin	290.2	15.4	289.2	$C_{15}H_{14}O_6$	0.50
14	Kaempferol	286.2	29.06	285.2	$C_{15}H_{10}O_6$	0.19
15	P-Hydroxybenzoic acid	138.1	10.08	137.1	$C_7H_6O_3$	0.09
16	Vanillic acid	168.1	11.1	167.1	$C_8H_8O_4$	2.54
17	Vanilin	152.1	16.9	151.1	$C_8H_8O_3$	1.90
18	Anisic acid	152	19.09	151	$C_8H_8O_3$	0.25
19	Rosmarinic acid	360.3	16.4	359.3	$C_{18}H_{16}O_8$	0.18
20	Pyrogallol	126.1	6.7	125.1	$C_6H_6O_3$	0.23
21	Sinapic acid	224.2	16.2	223.2	$C_{11}H_{12}O_5$	0.02
22	Syringaldehyde	182.1	17.4	181.1	$C_9H_{10}O_4$	1.82
23	Syringic acid	198.1	11.6	197.1	$C_9H_{10}O_5$	0.83
24	Benzoic acid	122.1	15.2	121.1	$C_7H_6O_2$	0.46

3.5. Antibacterial Activity

It was found that the average diameter of inhibition zones for the ethanolic extract was 19.51 and 37.3 mm on the growth of *Streptococcus pyogenes* and *Escherichia coli*, respectively.

4. Discussion

Data of this study showed that *R. flexicaulis* collected in Egypt contains appreciable amounts of total phenolic and total flavonoid contents, and a high total antioxidant capacity, suggesting the possibility to use this plant for medicinal purposes. The high antioxidant capacity might be attributed to the high amount of phenolics and flavonoids detected in this plant. Flavonoids are hydroxylated phenolic compounds that are synthesized by plants in response to microbial infections, and they have been found to be antimicrobial substances against a wide array of microorganisms *in vitro*. This activity may be ascribed to their ability to complex with extracellular and soluble proteins and to complex with bacterial cell walls (Marjorie, 1996). Flavonoids have enhanced great interest recently because of their potential beneficial effects on human health such as antiviral, anti-diabetic, anti-inflammatory, antitumor, anti-carcinogenic and anti-ageing properties (Cook and Samman, 1996; Ren *et al*. 2003 and Zhou *et al*. 2009). It was declared that these compounds contribute to all the former biological activities via their strong antioxidant potential and free radical scavenger ability (Sharififar *et al*. 2009).

Phenolic compounds give the plant an important value as they exhibit a wide range of anti-allergenic, anti-artherogenic, anti-inflammatory, anti-microbial, anti-oxidant, anti-thrombotic, cardioprotective and vasodilatory effects (Middleton *et al*. 2000; Puupponen-Pimia *et al*. 2001 and Manach *et al.* 2005). Also, phenolic compounds could be a major determinant of antioxidant potentials of foods and could, therefore, be a natural source of antioxidants. Some phenolic compounds recorded in the study plant have medical importance such as P-coumaric acid is believed to reduce the risk of stomach cancer (Ferguson *et al.* 2005).

The results of the present study indicate the existence of antimicrobial activity in the crude extracts of *R. flexicaulis*. This may be due to presence of the phytochemical groups as previously mentioned. Several studies indicated that many *Rhus* species have antimicrobial activity. For instance, *R. coriaria*, has been proven to have a broad range of antimicrobial activity by inhibiting the growth of *Bacillus cereus, Escherichia coli, Klebsiella pneumoniae, Proteus vulgaris, Pseudomonas aeruginosa, Shigella dysentariae, Staphylococcus aureus, S. epidermidis, Streptococcus pyogenes, Enterococcus faecalis*, and *Yersinia enterocolitica* (Nimri *et al.* 1999). It was also found that the *Rhus succedanea* leaf gall extracts have antibacterial activity against *Escherichia coli, Salmonella typhi, Micrococcus luteus*, and *Staphylococcus aureus* (Shrestha *et al.* 2013).

5. Conclusion

The results of the present study indicate that *Rhus flexicaulis* contains appreciable amounts of total phenolics and flavonoids, and a high total antioxidant and antibacterial activities, suggesting the possibility to use this plant for medicinal purposes This study provides valuable information for further phytochemical isolation and characterization studies of active compounds, necessary for the development of new drugs. The research efforts on *Rhus* extracts indicate a promising potential for the plant family to provide renewable bio-products with the following desirable bioactivities: antimicrobial, antifungal, antimalarial, antiviral, antifibrogenic, anti-inflammatory, antimutagenic, antioxidant, antithrombin, antitumorigenic, cytotoxic, hypoglycaemic, and leukopenic.

Acknowledgements

This work has been done at the Institute of Botany, Leibniz University of Hanover, Germany. The authors would like to thank Prof. Dr. Jutta Papenbrock for her kind support and suggestions to improve the manuscript.

References

Ahmed MS, Galal AM, Ross SA, Ferreira D, El Sohly MA, Ibrahim ARS and El-Feraly FS. 2001. A weakly antimalarial biflavanone from *Rhus retinorrhoea*. *Phytochem*, **58(4):** 599–602.

Boulos, L. 1988. A contribution to the flora of South Yemen (PDRY). *Candollea*, **43**: 549-585.

Boulos, L. 2000. Flora of Egypt, Al-Hadara Publishing, Cairo, Egypt, (2). 36-67.

Choi W, Jung H, Kim K, Lee S, Yoon S, Park J, et al. 2012. *Rhus verniciflora* stokes against advanced cancer. A perspective from the Korean integrative cancer center. *J Biomed Biotechnol*, **2012**:181–191.

Cook NC and Samman S. 1996. Flavonoids: chemistry, metabolism, cardioprotective effects and dietary sources. *Nutr Biochem*, **7**: 66-76.

Dewanto V, Wu X, Adom KK and Liu RH. 2002. Thermal processing enhances the nutritional value of tomatoes by increasing total antioxidant activity. *J Agric Food Chem*, **50**:3010–3014.

Dudonné S, Vitrac X, Coutière P, Woillez M and Mérillon JM. 2009. Comparative study of antioxidant properties and total phenolic content of 30 plant extracts of industrial interest using DPPH, ABTS, FRAP, SOD, and ORAC assays. *J Agric Food Chem*, **57**:1768–1774.

Erichsen-Brown C. 1989. Medicinal and Other Uses of North American Plants: A Historical Survey with Special Reference to the Eastern Indian Tribes. New York, NY, USA: Dover Publications.

Ferguson LR, Zhu S, and Harris PJ. 2005. Antioxidant and antigenotoxic effects of plant cell wall hydroxycinnamic acids in cultured HT-29. *Mol Nutr Food Res*. **49 (6):** 585–693.

Gallant JB, Kemp JR and Lacroix CR. 1998. Floral development of dioecious Staghorn Sumac, *Rhus hirta* (Anacardiaceae). *Int J Plant Sci*, **159(4):**539–549.

Gillespie KM, Chae JM and Ainsworth E. 2007. A Rapid measurement of total antioxidant capacity in plants. *Nat Protoc*, **2**:867–87.

Huang D, Ou B, Hampsch-Woodill M, Flanagan JA and Prior RL. 2002. High throughput assay of oxygen radical absorbance capacity (ORAC) using a multichannel liquid handling system coupled with a microplate fluorescence reader in 96-well format. *J Agric Food Chem*, **50**:4437–4444.

Ibrahim ME, Ahmed SS, Khalid AK and El-Sawi SA. 2017. Characterization of essential oil content isolated from *Rhus flexicaulis* (Baker). *Int Food Res J*, **24(2):** 897-899.

Kossah R, Nsabimana C, Zhao J, Chen H, Tian F, Zhang H and Chen W. 2009. Comparative Study on the Chemical Composition of Syrian Sumac (*Rhus coriaria* L.) and Chinese Sumac (*Rhus typhina* L.) Fruits. *Pakistan Journal of Nutrition*, **8(10):** 1570-1574.

Manach C, Williamson G, Morand C, Scalbert A and Remesy C. 2005. Bioavailability and bioefficacy of polyphenols in humans. I. Review of 97 bioavailability studies. *Am J Clin Nutr*, **81**: 230S–242S.

Marjorie C. 1996. Plant products as antimicrobial agents. *Clin Microbiol Rev*, **12**: 564-582.

Masesane IB, Yeboah SO, Liebscher J, Mügge C and Abegaz BM. 2000. A bichalcone from the twigs of *Rhus pyroides*. *Phytochem*, **53(8):** 1005–1008.

Middleton E, Kandaswami C and Theoharides TC. 2000. The effects of plant flavonoids on mammalian cells: implications for inflammation, heart disease and cancer. *Pharmacol. Rev*, **52**: 673-751.

Nimri LF, Meqdam MM and Alkofahi A. 1999. Antibacterial activity of Jordanian medicinal plants. *Pharm Biol.*, **37**: 196-201.

Puupponen-Pimia R, Nohynek L, Meier C, Kahkönen M, Heinonen M, Hopia A and Oksman-Caldentey KM. 2001. Antimicrobial properties of phenolic compounds from berries. *J Appl Microbiol.*, **90**: 494-507.

Ren W, Qiao Z, Wang H, Zhu L and Zhang L.2003. Flavonoids: promising anticancer agents. *Med Res Rev*., **23**: 519-534.

Selim SA, Aziz MHA, Mashait MS and Warrad MF. 2013. Antibacterial activities, chemical constitutes and acute toxicity of Egyptian *Origanum majorana* L., *Peganum harmala* L. and *Salvia officinalis* L. essential oils. *Afr J Pharm Pharmacol*., :**7(13)**:725–35.

Sezik E, Tabata M and Yesilada E. 1991. Traditional medicine in Turkey. 1. Folk medicine in northeast Anatolia. *J Ethnopharmacol*, **35**:191–196.

Sharififar F, Dehghn G and Mirtajaldini M. 2009. Major flavonoids with antioxidant activity from *Teucrium polium*. *Food Chem*, **112**: 885-888.

Shrestha S, Subaramaihha SR, Subbaiah SGP, Eshwarappa RSB and Lakkappa DB. 2013. Evaluating the Antimicrobial Activity of Methonolic Extract of *Rhus Succedanea* Leaf Gall. *BioImpacts*, **3(4):** 195-198.

Van Wyk BE and Wink M. 2004. Medicinal Plants of the World, Timber Press: Portland, USA.

Wetherilt H and Pala M. 1994. Herbs and Spices Indigenous to Turkey. In: Charalambous, G. (Ed.), Spices, Herbs and Edible Fungi: Developments in Food Science. Elsevier, Amsterdam, 285-307.

Zhou T, Luo D, Li X and Luo Y. 2009. Hypoglycaemic and hypolipidemic effects of flavonoids from lotus (*Nelum bonuficera*) leaf in diabetic mice. *J. Med. Plants Res*, **3**: 290-293.

JJBS

Volume 12, Number 1,March 2019
ISSN 1995-6673
Pages 23 - 30

Jordan Journal of Biological Sciences

Induced Morphological and Chromosomal Diversity in the Mutagenized Population of Black Cumin (*Nigella sativa* L.) Using Single and Combination Treatments of Gamma Rays and Ethyl Methane Sulfonate

Ruhul Amin[1], Mohammad Rafiq Wani[2*], Aamir Raina[1], Shahnawaz Khursheed[1] and Samiullah Khan[1]

[1]*Mutation Breeding Laboratory, Department of Botany, Aligarh Muslim University, Aligarh - 202 002, Uttar Pradesh, India;* [2]*Department of Botany, Abdul Ahad Azad Memorial Degree College Bemina- Cluster University, Srinagar-190 018, Jammu and Kashmir, India*

Received June 6, 2018; Revised June 30, 2018; Accepted July 2, 2018

Abstract

Induced mutagenesis has successfully been proven as the best viable approach for the genetic improvement of crop species. In the present scenario of high health vulnerability, the global demand for natural medicine derived from plant species has increased tremendously. Black cumin (*Nigella sativa* L.) – an important medicinal plant species of the family *Ranunculaceae* with immense therapeutic values, was selected for the present study in order to bring genetic improvement using the technique of induced mutagenesis. Dry and healthy seeds of two varieties of black cumin were exposed to different doses of gamma rays and EMS singly and in combination. The observations were recorded on morphological, cytological and physiological parameters in M_1 and M_2 generations to evaluate the mutagenic potency and to induce the desirable genetic variability in the crop. A broad spectrum of morphological variations with different frequencies affecting different plant parts and chromosomal aberrations were screened out in both the varieties in M_1 generation. Cytological abnormalities increased with increasing the doses/concentrations of the mutagen. The results reflect an increase in the mean values for chlorophyll and carotenoid contents at the 0.1 % EMS treatment in both varieties indicating an improved photosynthetic activity in this treatment. The rest of the treatments showed a decreasing trend in relation to the controls with increasing the mutagenic doses/concentrations vis-à-vis chlorophyll and carotenoid contents in both varieties. Observations on quantitative traits including plant height, number of fertile branches, number of capsules per plant, number of seeds per capsule and 1000 seed weight (g) showed significant inter-treatment variations at different mutagenic doses. A positive correlation among various yield attributing traits was recorded in M_2 generation. The findings of the present study are encouraging, and show that significant genetic variability had been induced by the mutagens, thus the rigorous selection of the desirable mutants may result in the development of improved and high yielding mutants of *Nigella sativa* in subsequent generations.

Keywords: Mutagens, Morphological variants, Chromosomal aberrations, Quantitative traits, *Nigella sativa*, Gamma radiation.

1. Introduction

Almost two third of the world's plant species have medicinal value in one way or another. Different plant parts such as stem, bark, leaves, seeds, and fruits are used for the treatment of a wide range of cardiovascular and inflammatory diseases. *Nigella sativa,* commonly known as black cumin, is an annual diploid (2n = 2x = 12) multi-branched herb with a great medicinal and therapeutic importance (Kirtikar and Basu, 1982; Chopra *et al.*, 1982). Most evidences show that black cumin is native of the Middle East and Western Asia (Iqbal *et al.,* 2010). In India, it is mostly grown in M.P., Bihar, Assam and Punjab. The other small scale cultivated states of India are U.P., Rajasthan, West Bengal and Tamil Nadu (Malhotra and Vashishtha, 2008).

Induced mutation has become increasingly popular in recent times as an effective tool for crop improvement. The mutant varieties developed in major crops have been cultivated by farmers in large areas and have boosted the food production, thus contributing to food security (Suprasanna *et al.*, 2016). Chemical mutagens have gained immense popularity, since they are easy to use, and can induce mutation at a very high rate (Raina *et al.*, 2016). Ethyl methane sulfonate (EMS) is an alkylating agent that donates alkyl group i.e., ethyl group (CH_3-CH_2) to the guanine producing O^6-ethyl guanine which pair with thymine to eventually produce point mutations. EMS induces miss pairing and base changes due to chemical modification of nucleotides (Greene *et al.*, 2003). Gamma rays, the highly energetic ionizing radiations constitute the most efficient and effective physical mutagen. Gamma rays are known to have a higher penetration power, and hence can induce various changes at the molecular level.

* Corresponding author. e-mail: botanyrafiq@gmail.com.

Mutation breeding, a much heralded shortcut breeding method mainly based on conventional breeding approaches, brings novel and high yielding genotypes through heritable changes (Singh *et al*., 2011; Laskar *et al.*, 2018; Ramachander *et al*., 2018; Verma *et al.*, 2018; Wani, 2018). It is generally employed to improve various agro-economically important traits such as seed yield, oil quantity and quality, etc. in different oil seed crops including *Nigella*. In the past, although different mutants in *N. sativa* have been created which include bushy and dwarf habit, feathery leaf, lax branching, early flowering and brown seed coat color (Datta *et al*., 1986), yet very limited work has been done vis-à-vis the induction of useful genetic variability which could lead to the genetic improvement of this crop. In this back drop, the present study was aimed at the generation of such micro- and macro-mutations in the agro-economic traits of *N. sativa* which could be propagated and exploited in subsequent generations for better profit. In addition, cytological abnormalities were estimated for establishing the sensitivity of the crop towards the mutagens applied.

2. Materials and Methods

2.1. Experimental Site

Aligarh, the site of present study, has a characteristic semi-arid and sub-tropical climate with hot dry summers and cold winters. The average rainfall in this district is 847.30 mm, while the average temperature is 35^{o}C and 15^{o}C during summer and winter, respectively. The soil of Aligarh is sandy loam and alkaline.

2.2. Biological Material

The experimental plant material selected for the present investigation is *N. sativa* L., commonly known as black cumin. Two varieties viz., NRCSSAN-1 and BHUVN-1 were used and the seeds were procured from National Botanical Research Institute (NBRI), Lucknow, Uttar Pradesh, India.

2.3. Experimental Procedure

Dry (moisture content 10-12%) and healthy seeds of black cumin (*N. sativa* L.) were used for the mutagenic treatments of EMS and gamma rays alone as well as in a combination. Seeds from each variety were distributed into thirteen sets of fifty seeds each for this experiment. One set of the seeds was taken as control, whereas the rest twelve sets were treated with different doses/ concentrations of mutagens i.e., four sets of seeds were irradiated with gamma rays (25Gy, 50Gy, 75Gy and 100Gy at a dose rate of 11.58 Gy/sec), four sets with different concentrations of EMS (0.1% EMS, 0.2% EMS, 0.3% EMS and 0.4% EMS) and four sets were treated with combination treatments (25Gy + 0.1% EMS, 50Gy + 0.2% EMS, 75Gy+ 0.3% EMS and 100Gy+0.4% EMS). As for the chemical treatment, pre-soaked seeds were subjected to a six-hour treatment with intermittent shaking at a room temperature of 25±2^{o}C. The gamma ray treatment was done with radioisotope ^{60}Co source at the National Botanical Research Institute, Lucknow, Uttar Pradesh, India. As for the combination treatments, the irradiated seeds were treated with EMS doses similarly as individual treatments. The treated seeds were then sown at University Agricultural Farm, Aligarh Muslim University, Aligarh in five replications of ten seeds per treatment to raise M_1 generation during the rabi season of 2015-2016.

For cytological studies, the flower buds of the treated and control plants were randomly collected from each replication separately, and the chromosome preparations were stained with 1 % acetocarmine solution and examined microscopically. Frequency of meiotic abnormalities was calculated according to Khursheed *et al.* (2015). The percentage of seed germination, pollen fertility and plant survival at maturity were calculated for each treated and control population according to Wani *et al.* (2011a). The seeds of normal-looking M_1 plants were harvested treatment wise individually and advanced for raising the M_2 generation in the plant progeny row during rabi season of 2016- 2017. Data on the morphological variations were taken throughout the season and tabulated according to the phenotypic category. Chlorophyll and carotenoid contents from fresh secondary emergent leaflets were extracted in 80 % acetone in mg.g^{-1} and estimated according to MacKinney (1941). In the M_2 generation, the breeding behavior was observed and different agronomic traits such as the number of fertile branches, the number of capsules per plant, the number of seeds per capsule and 1000 seed weight (g) were evaluated. Statistical analysis, namely mean, standard error, standard deviation, coefficient of variation (CV), analysis of variance (ANOVA), Duncan multiple range test (DMRT) and Pearson's correlation coefficient (*r*) were done using IBM SPSS 20 software to assess the induced intra- and inter population variations in these quantitative traits.

3. Results

3.1. Bio-physiological Parameters in M_1 Generation

Seed germination in the var. NRCSSAN-1 was recorded as 90.00 % in the control; however it decreased with increasing the concentrations of EMS, gamma rays and their combination. For var. NRCSSAN-1, germination was 80 % with 0.1 % EMS, while for gamma rays and combination treatments; it was 60 % with 100 Gy and 0.4 % EMS+100Gy. In the var. BHUVN-1, the seed germination was recorded as 80.00 % in the control and decreased to 50 % at 0.4 % EMS +100 Gy (Table 1). The pollen fertility decreased in a regular pattern with increasing the mutagenic concentrations. In the var. NRCSSAN-1, the pollen fertility decreased from 92.40 % in control to 77.00 % in 0.2 % EMS +50 Gy, whereas it decreased from 92.80 % in the control to 75.40 % with 0.2 % EMS +50 Gy in the var. BHUVN-1 (Table 1). The survival of plants at maturity decreased irregularly with respect to the controls of both the varieties when increasing the concentrations of the mutagens. The survival of untreated plants at maturity was 96 % and 95 % for the varieties NRCSSAN-1 and BHUVN-1 respectively, while it decreased from 92 % (0.1% EMS) to 75 % (0.4 % EMS +100 Gy) in NRCSSAN-1 and from 90 % (0.1% EMS) to 73 % (0.4 % EMS +100 Gy) in the var. BHUVN-1 (Table 1).

Table 1. Estimates of seed germination, pollen fertility, chlorophyll, and carotenoid contents in M_1 generation of *Nigella sativa*.

Treatment	Seed germination (%)		Pollen fertility (%)		Survival (%) at maturity		Chlorophyll content (mg/g)		Carotenoid content (mg/g)	
	NRCSS AN-1	BHUVN-1	NRCSS AN-1	BHUVN-1	NRCSS AN-1	BHUVN-1	NRCSS AN-1	BHUVN-1	NRCSS AN-1	BHUVN-1
Control	90	80	92.40	92.80	96	95	0.550	0.545	0.280	0.277
0.1%EMS	80	80	91.40	90.80	92	90	0.578	0.566	0.293	0.282
0.2%EMS	70	70	90.00	89.80	92	88	0.530	0.520	0.245	0.249
0.3%EMS	60	60	88.60	87.20	83	85	0.510	0.505	0.221	0.215
0.4%EMS	60	60	87.40	86.20	80	81	0.520	0.500	0.215	0.211
25 Gy	70	70	86.60	86.00	90	88	0.469	0.462	0.267	0.261
50 Gy	70	60	84.40	84.80	88	87	0.444	0.431	0.237	0.229
75 Gy	60	60	82.40	80.80	85	82	0.419	0.398	0.214	0.221
100 Gy	60	60	82.40	77.80	78	79	0.400	0.410	0.203	0.198
0.1%EMS + 25 Gy	70	70	78.60	77.00	89	85	0.433	0.351	0.219	0.208
0.2%EMS +50 Gy	60	60	77.00	75.40	86	83	0.367	0.303	0.214	0.199
0.3%EMS +75 Gy	60	60	80.60	81.40	79	75	0.315	0.287	0.192	0.186
0.4%EMS +100 Gy	60	50	77.20	76.20	75	73	0.258	0.243	0.187	0.183

3.2. Chlorophyll and Carotenoid Contents (mg/g Fresh Weight of Leaf)

The total chlorophyll and carotenoid contents in the M_1 generation decreased with increasing the concentrations of the mutagens except at 0.1 % EMS where it showed an increase over the controls in both varieties. The highest chlorophyll (0.578 mg/g and 0.566 mg/g) and carotenoid (0.293 mg.g-1 and 0.282 mg.g-1 FW) contents were noticed with the treatment of 0.1 % EMS in the varieties NRCSSAN-1 and BHUVN-1 respectively. The combination treatments showed more reduction with respect to chlorophyll and carotenoid contents as compared to the individual ones (Table 1).

3.3. Cytological Studies in M_1 Generation

The potency of mutagens is reliably estimated by cytological observations in M_1 generation. In this context, chromosomal abnormalities were studied in both varieties at different stages of meiotic division. The chromosomal variations include univalent, multivalent, laggards, bridges, stickiness, disturbed polarity, multinucleate condition and unequal separation of chromosomes at various stages. At the metaphase stage, the pollen mother cells (PMCs) with multivalent, precocious movement, stray chromosomes and chromosomal stickiness were observed in the treated population. The abnormalities increased at metaphase I/II with increasing the concentrations of the mutagens in both varieties. The induced anaphase abnormalities consisted of laggards, bridges and an unequal separation of chromosomes. The frequency of such abnormalities had increased significantly with increasing the mutagenic concentrations. The main chromosomal aberrations observed at telophase I/II were laggards, bridges, micronuclei, multinucleate condition and disturbed polarity (Plate I; Figures A-L). The maximum frequency of 22.46 % and 26.53 % chromosomal abnormalities was noticed with the treatment of 0.4 % EMS+100 Gy in the varieties NRCSSAN-1 and BHUVN-1 respectively (Tables 2 and 3).

Table 2. Frequency and spectrum of chromosomal abnormalities induced by EMS, gamma rays, and their combination in M_1 generation of *Nigella sativa* var. NRCSSAN-1.

Treatment	Total No. of PMCs observed	Metaphase-I/II					Anaphase-I/II				Telophase- I/II						
		Multivalent	Precocious movement	Stray chromosomes	Stickiness	Abnormalities (%)	Laggards	Bridges	Unequal separation	Abnormalities (%)	Laggards	Bridges	Micro nucleate	Multi nucleate	Disturbed Polarity	Abnormalities (%)	Total (%) of Abnormalities
Control	270	-	-	-	-	-	-	-	-	-	-	-	-	-	-	-	-
0.1% EMS	263	1	-	-	1	0.76	-	-	-	-	-	-	1	-	-	0.38	1.14
0.2%EMS	271	2	2	-	3	2.58	1	2	1	1.47	-	-	1	1	-	0.73	4.78
0.3%EMS	230	2	1	1	2	2.60	1	-	3	1.73	-	-	1	-	2	1.30	5.63
0.4%EMS	250	2	1	1	3	2.80	1	-	4	2.00	1	-	-	2	3	2.40	7.20
25 Gy	260	1	1	-	1	1.15	-	-	-	-	-	-	1	-	1	0.76	1.91
50 Gy	264	1	1	-	1	1.13	-	1	-	0.37	-	1	-	1	-	0.75	2.25
75 Gy	255	-	3	2	3	3.13	1	1	2	1.56	-	1	1	3	-	1.96	6.65
100 Gy	276	4	3	2	4	4.71	3	4	2	3.26	2	-	2	2	2	2.89	10.86
0.1%EMS + 25 Gy	267	3	3	3	4	4.86	4	2	3	3.37	1	1	1	2	3	3.03	11.26
0.2%EMS +50 Gy	284	4	6	4	4	6.33	5	3	3	3.87	2	1	2	3	3	3.87	14.07
0.3%EMS +75 Gy	232	4	5	3	4	6.89	4	6	3	5.60	2	1	2	2	3	4.31	16.80
0.4%EMS +100Gy	267	6	7	5	6	8.98	7	6	5	6.74	2	3	5	4	4	6.74	22.46

Table 3. Frequency and spectrum of chromosomal abnormalities induced by EMS, gamma rays, and their combination in M_1 generation of *Nigella sativa* var. BHUVAN-1.

Treatment	Total No. of PMCs observed	Metaphase-I/II					Anaphase-I/II				Telophase- I/II						
		Multivalent	Precocious movement	Stray chromosomes	Stickiness	Abnormalities (%)	Laggards	Bridges	Unequal separation	Abnormalities (%)	Laggards	Bridges	Micro nucleate	Multi nucleate	Polariy	Disturbed	Abnormalities (%)	Total (%) of Abnormalities
Control	264	-	-	-	-	-	-	-	-	-	-	-	-	-	-	-	-	-
0.1% EMS	253	1	-	1	1	1.18	-	-	-	-	-	-	1	-	-	0.39	1.57
0.2%EMS	238	2	1	-	2	2.10	1		1	0.84	-	-	1	1	-	0.84	3.78
0.3%EMS	219	2	1	1	2	2.73	1	-	3	1.82	-	-	1	-	2	1.36	5.91
0.4%EMS	217	2	2	1	2	3.22	-	2	4	2.76	1	-	-	2	3	2.76	8.74
25 Gy	260	1	-	1	1	1.15	-	1	-	0.38	-	-	-	1	1	0.76	2.29
50 Gy	255	1	1	-	1	1.17	-	1	1	0.78	-	-	1	1	1	1.17	3.12
75 Gy	245	2	2	1	2	2.85	1	1	2	1.63	-	-	1	2	2	2.04	6.52
100 Gy	227	3	2	2	3	4.40	3	3	2	3.52	2	-	1	1	2	2.64	10.56
0.1%EMS + 25 Gy	265	3	3	3	3	4.52	3	2	2	2.64	1	1	1	1	3	2.64	9.80
0.2%EMS +50 Gy	244	4	3	3	4	5.73	4	1	3	3.27	2	1	2	2	3	4.09	13.09
0.3%EMS +75 Gy	233	4	5	3	3	6.43	4	6	-	4.29	2	1	2	2	3	4.29	15.01
0.4%EMS +100Gy	211	5	4	5	7	9.95	6	7	5	8.53	2	3	3	5	4	8.05	26.53

3.4. Morphological Variations

Variations in cotyledonary and leaf morphology were observed after mutagenic treatments in both varieties. At the time of germination, a broad spectrum of cotyledonary leaf variants such as single (mono), three (tri) and four (tetra) cotyledonary leaves were observed in the treated population. Besides, variation in the number of cotyledonary leaves, change in cotyledonary leaf shape such as the needle-shaped and deformed leaves were also noticed (Plate II; Figures A-F). Other morphological variations include the increased number of leaflets (9-11) and a changed pattern of leaflets from alternate to opposite in some treatments (Plate II; Figures K-1-2).

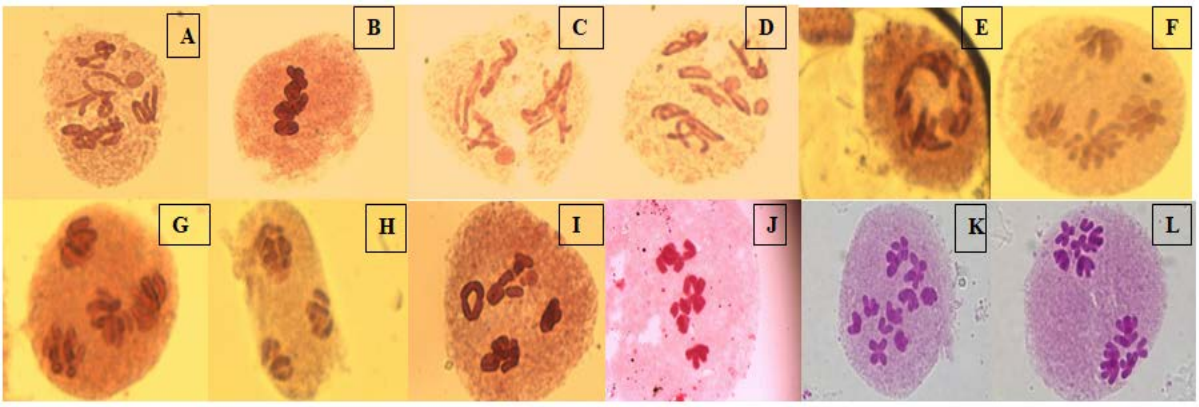

Plate I. Various chromosomal abnormalities observed in M_1 generation of *Nigella sativa* L.

A. Diakinesis showing bivalents and univalent with micronucleus; **B**. Chromosomal stickiness at metaphase- I; **C**. Disorientation of bivalents at diakinesis; **D.** Ring and rod-shaped bivalents ; **E**. Clumping of bivalents; **F**. Unequal separation at telophase- II with micronucleus; **G**. Unequal separation at anaphase- II; **H**. Tripolar telophase- II; **I**. Chromosomal stickiness at diakinesis; **J**. Chromosome clumping at diakinesis; **K**. Chromosomes moving towards poles at anaphase I (control); **L**,Telophase- I (control).

Three different types of chlorophyll variants, namley chlorina, xantha and albina were also recorded (Plate II; Figures G, I, J-2) in M_1 generation. The combined treatment of EMS and gamma rays showed a higher number of chlorophyll variants compared to the individual treatments in both varieties. The observation revealed that the leaf morphology was the most sensitive towards the applied doses of mutagens. The arrangement of petals in flowers and the number of petals varied from five in the control to six in the treated population. The other variation includes the flower which had leafy petals (Plate II; Figures L-N). Alteration in capsule size, i.e. small, bold, narrow and also the number of locules in capsule varied from five in the control to six, ten and thirteen in the treated population (Plate II; Figures O-1-4). On comparing different treatment doses, it was found that 0.4 % EMS+100 Gy generated the highest number of morphological variants followed by gamma rays and EMS in both varieties.

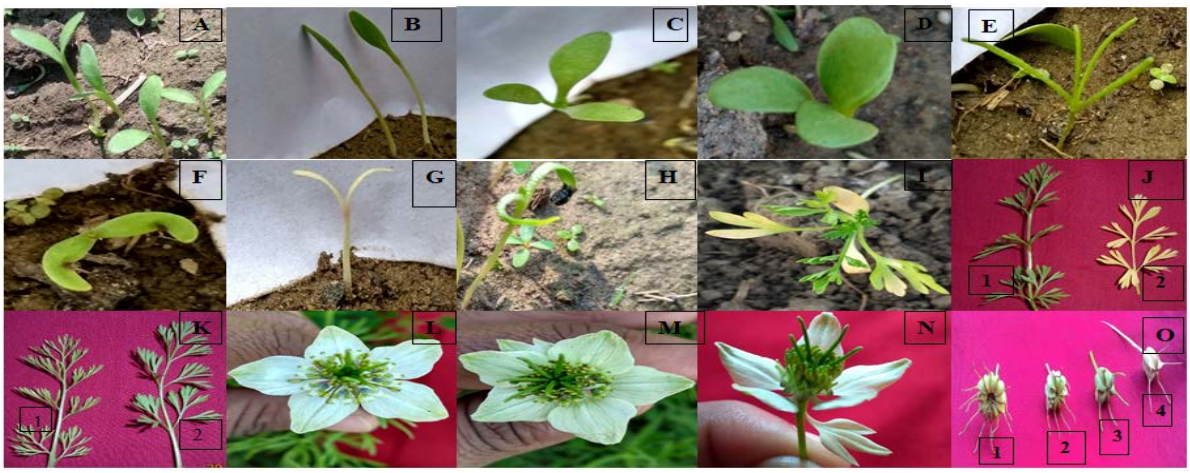

Plate II. Various morphological variants observed in M_1 generation of *Nigella sativa* L.

A. Bicotyledon plant (control); **B**. Monocotyledon ; **C**. Tricotyledon ; **D**. Tetracotyledon **; E**. Needle-shaped tetra cotyledon;**F**. Deformed cotyledon ; **G**. Albina cotyledon ; **H**. Horn-shaped cotyledon ; **I**. Xantha plant ; **J**. 1. Control plant 2. Chlorina plant; **K**. 1. Leaf with alternate leaflets (control) 2. Leaf with opposite leaflets; **L**. Flower with five petals (control); **M**. Flower with six petals; **N**. Flower with leafy petal ; **O**. Variation in locules number per capsule 1. Thirteen 2. Ten 3. Six 4. Five (control).

3.5. Quantitative Traits in M_2 Generation

The mean plant height of 60.14 cm and 59.58 cm was noticed in the controls of the varieties NRCSSAN-1 and BHUVN-1 respectively. The range of mean plant height was 56.96 cm (0.4 % EMS + 100 Gy) to 68.68 cm (25 Gy) in the var. NRCSSAN-1, while in the var. BHUVN-1 it was 54.76 cm with 0.4 % EMS + 100 Gy to 66.20 cm with 25 Gy (Table 4). The mean number of fertile branches decreased from 3.8 in control to 2.4 at 0.4 % EMS +100 Gy in the var. NRCSSAN-1, whereas in the var. BHUVN-1 it decreased from 5.80 in the control to 3.60 at 0.4 % EMS +100 Gy treatment (Table 4).

The number of capsules per plant increased from 7.8 (control) to 8.4 (0.1 % EMS) in the var. NRCSSAN-1 (Table 4), while in the rest of the treatments, it showed a decrease with respect to the control in both varieties. The number of seeds per capsule ranged from 72.40 to 78.60 in the var. NRCSSAN-1, whereas it ranged from 72.00 to 78.20 in the var. BHUVN-1 (Table 4). Mean 1000 seeds weight (g) in the control population was 2.02 g and 1.98 g in the varieties NRCSSAN-1 and BHUVN-1 respectively. In the var. NRCSSAN-1, the mean 1000 seed weight ranged from 1.62 g (0.4 % EMS+100Gy) to 2.02 g (0.1 % EMS) and in the var. BHUVN-1, the range was 1.56 g with 0.4 % EMS +100 Gy to 2.06 g with 0.1 % of EMS treatment (Table 4). Correlation studies among various pairs of yield attributing traits in M_2 generation are presented in Table 5. A positive correlation was seen among different yield contributing traits in both varieties.

4. Discussion

In the present investigation, seed germination, plant survival at maturity, and pollen fertility declined with increasing mutagenic concentrations. However, the extent of decrease was different with different mutagenic treatments as also reported earlier by different workers regarding various crop plants (Bhat *et al.*, 2006; Khan *et al.*, 2009; Jafri *et al.*, 2011; Amin *et al.*, 2015). The decrease in seed germination after mutagenic treatments has been ascribed to chromosomal aberrations, disturbed DNA and auxin synthesis and impaired cell metabolism (Kirtane and Dhumal, 2004). Progressive decrease in the rate of plant survival when increasing the doses of physical and chemical mutagens has been previously reported by Jayabalan and Rao (1987) in *Lycopersicon esculentum*, Kumar and Dubey (1998) in *Lathyrus sativus* and Amin *et al.* (2016) in *Nigella sativa*. Physiological imbalances and/or different types of chromosomal aberrations could be the main cause for the decreased plant survival (Khursheed *et al.*, 2015).

The magnitude of pollen sterility also increased with increasing the concentrations of mutagens. High pollen sterility was recorded with higher doses of individual and combination treatments. These results are in agreement with Kumar and Dubey (1998) and Jafri *et al.* (2011) who also reported a dose dependent increase in pollen sterility after mutagenic treatments. Estimation of chlorophyll content showed a wide variation in the mutagen-treated population. In this study, the total chlorophyll content decreased with increasing the mutagenic concentrations. Photosynthetic activity is greatly dependent upon chlorophyll content (Larcher, 1995). During the onset of the flowering phase, the greater content of chlorophyll which takes part in the process of organogenesis was observed (Simova-Stoilova *et al.*, 2001).

The frequency of morphological variants increased with increasing the mutagenic dose. The maximum frequency was observed with combination treatments of EMS and gamma rays. The variations in leaf morphology such as unequal notches, rudimentary and poor development of leaflets, stunted and poorly-branched plants were commonly observed in this study. Similar abnormalities have also been reported by various workers in *Lens culinaris* (Amin *et al.*, 2015), *Cicer arietinum* (Laskar *et al.*, 2015), *Choris gayana* (Krishna *et al.*, 1984), *Vicia faba* (Kumar *et al.*, 1993) and *Vigna radiata* (Wani *et al.*, 2011b). The leaf abnormalities have been mainly ascribed to chromosomal aberrations (Blixt, 1972; Grover and Virk, 1986.)

Table 4. Statistical analysis of various quantitative traits in M_2 generation of *Nigella sativa* L. varieties NRCSSAN-1 and BHUVN-1.

Treatment	Plant height Mean ± SE, CV%, shift in mean		No. of fertile branches Mean ± SE, CV%, shift in mean		No. of capsule per plant Mean ± SE, CV%, shift in mean		No. of seeds per capsule Mean ± SE, CV%, shift in mean		1000 seeds weight (gm) Mean ± SE, CV%, shift in mean	
	NRCSSAN-1	BHUVN-1	NRCSSAN-1	BHUVN-1	NRCSSAN-1	BHUVN-1	NRCSSAN-1	BHUVN-1	NRCSSAN-1	BHUVN-1
Control	60.14±1.09, 4.04, -	59.58^{bc}±1.50, 5.36, -	3.8^{a} ± 0.37, 22, -	5.8^{a}±0.48, 18.79, -	7.8^{ab} ± 0.2, 5.37,-	7.6^{a} ± 0.24, 7.19, -	78.20^{ab}±0.66, 1.89, -	76.8^{ab}±0.66 ,1.93,-	2.02^{a}± 0.03, 4.10, -	1.98^{a}± 0.03, 4.19, -
0.1% EMS	61.58^{b}±0.23, 0.83, 1.44	61.58^{ab}±0.22, 0.83, 2.0	3.6^{ab}±0.24, 15.19, -0.2	5.4^{ab}±0.24, 10.12, -0.4	8.4^{a} ± 0.24, 6.51, 0.6	7.6^{a} ± 0.24, 7.19, 0	78.60^{a}±0.24, 0.69, 0.40	78.2^{a}±0.48, 1.4, 1.4	2.02^{a} ± 0.03, 4.1, 0	2.06^{a}± 0.04, 4.32, 0.08
0.2%EMS	61.16^{b}±0.48, 1.75, 1.02	61.32^{ab}±0.68, 2.48, 1.74	3.2^{ab} ± 0.2, 13.96, -0.6	5.4^{ab}±0.24, 10.12, -0.4	7.4^{bc}± 0.24, 7.39, -0.4	7.2^{ab} ± 0.20, 6.2, -0.4,	76.20^{bcd}±0.37, 1.09,-2.0	76.4^{abc}±0.24, 0.71, -0.4	1.96^{ab}±0.04, 4.54, -0.06	1.94^{ab}±0.05, 5.87, -0.04
0.3%EMS	59.82^{b}±0.43, 1.61,-0.32	60.26^{bc}±0.47, 1.17, 0.68	3.8^{a}±0.58, 34.28, 0	5^{abc}±0.70, 31.60, -0.8	6.4^{def}±0.24, 8.54, -1.4	6.4^{cd}± 0.24, 8.54, -1.2	75.60^{cde}±0.50, 1.50,-2.6	75.2^{bcd}±0.37, 1.11, -1.6	1.82^{abc}±0.05 ,7.14, -0.2	1.8^{bc} ± 0.07, 8.77, -0.18
0.4%EMS	59.42^{ab}±0.49, 1.85,-0.72	59.20^{bc}±0.20, 0.77, -0.38	3.2^{ab}±0.37, 26.12, -0.6	4.2^{bcd}±0.37, 19.90, -1.6	6.4^{def}±0.24, 8.54, -1.4	6.6^{bcd}±0.24, 8.28, -1.0	74.80^{def}±0.37, 1.11,-3.4	74.8^{bcde}±0.2, 0.59, -2.0	1.80^{abc}±0.06, 7.83, -0.22	1.76^{cd}±0.04, 5.05, -0.22
25 Gy	68.68^{b} ± 6.46, 21.05, 8.54	66.20^{a} ± 5.44, 18.36, 6.62	3.8^{a} ± 0.37, 22, 0	5.4^{ab} ± 0.50, 21.11, -0.4	7.4^{bc} ± 0.24, 7.39, -0.4	7.2^{ab} ± 0.2, 6.2, -0.4,	77.20^{abc} ± 0.58, 1.68,-1.0	76.2^{abc} ± 0.96, 2.84, -0.6	1.86^{abc} ±0.11, 13.44, -0.16	1.78^{bc} ±0.08, 10.78, -0.20
50 Gy	59.18^{b} ± 1.73, 6.53, -0.96	58.18^{bc}± 1.71, 6.60,-1.4	3.4^{ab} ± 0.50, 33.52, -0.4	4.8^{abcd} ±0.58, 27.08, -1.0	6.6^{cde} ± 0.24, 8.28,-1.2	6.4^{cd} ± 0.24, 8.54, -1.2	74.40^{defg} ±0.40, 1.20,-3.8	74.6^{cde} ± 0.4, 1.19, -2.2	1.80^{abc} ±0.05, 6.77, -0.22	1.8^{bc}±0.07, 8.77, -0.18
75 Gy	59.44^{b}± 1.35, 5.09, -0.7	58.14^{bc} ± 1.32, 5.10,-1.44	3.6^{ab} ± 0.24, 15.19, -0.2	4.4^{bcd} ±0.24, 12.43, -1.4	6.2^{defg} ± 0.2, 7.29, -1.6	5.6^{e}± 0.24, 9.76, -2.0	75.00^{cde} ±0.54, 1.63,-3.2	74.8^{bcde} ± 0.37, 1.11, -2.0	1.76^{bc}±0.08, 10.28, -0.26	1.74^{cd} ± 0.05, 6.55,-0.24
100 Gy	59.04^{b} ± 1.30, 4.93, -1.1	57.64^{bc} ± 0.95, 3.69,-1.94	3.2^{ab} ± 0.37, 26.12, -0.6	4.2^{bcd} ± 0.37, 19.90, -1.6	5.6^{fg} ± 0.24, 9.76, -2.2	5.4^{e} ± 0.24, 10.12, -2.2	73.80^{efg} ± 1.28, 3.87,-4.4	74^{def} ± 0.77, 2.34, -2.8	1.80^{abc} ±0.05, 6.77, -0.22	1.76^{cd} ± 0.02, 3.06,-0.22
0.1%EMS + 25 Gy	58.92^{b}± 0.68, 2.59, -1.22	57.04^{bc} ± 0.84, 3.29,-2.54	3^{ab} ±0.31, 23.56, -0.8	4.4^{bcd} ±0.40, 20.31, -1.4	7^{bcd}± 0.44, 14.28, -0.8	6.8^{bc} ± 0.20, 6.57, -0.8	72.60^{fg} ± 1.02, 3.17,-5.6	73.6^{def} ± 0.87, 2.64, -3.2	1.76^{bc} ±0.08, 10.28, -0.26	1.74^{cd} ± 0.05, 6.55,-0.24
0.2%EMS +50 Gy	58.58^{b} ± 0.53, 2.02, -1.56	57.40^{bc} ±1.80, 7.02,-2.18	3.4^{ab} ± 0.24, 16.08, -0.4	4^{cd} ± 0.31, 17.67, -1.8	6.2^{defg}± 0.2, 7.2, -1.6	6^{e} ± 0.31, 11.78, -1.6	72.40^{g} ± 1.20, 3.73, -5.8	72^{f}± 1.18, 3.67,-4.8	1.72^{bc} ±0.10, 13.25, -0.3	1.66^{cde} ± 0.06, 9.09,-0.32
0.3%EMS +75 Gy	58.40^{b}± 0.88, 3.37, -1.74	56.18^{bc} ± 1.48, 5.89,-3.4	2.8^{ab} ± 0.37, 29.85, -1	3.8^{cd} ± 0.37, 22,-2.0	5.4^{g} ± 0.24, 10.12, -2.4	5.4^{e} ± 0.24, 10.12, -2.2	73.40^{efg} ± 0.50, 1.55,-4.8	73.4^{def} ± 0.24, 0.74, -3.4	1.68^{c} ±0.11, 14.76, -0.34	1.6^{de}± 0.03, 4.37, -0.38
0.4%EMS +100 Gy	56.96^{b}± 1.04, 4.11,-3.18	54.76^{c} ± 1.21, 4.94,-4.82	2.4^{b} ± 0.24, 22.86, -1.4	3.6^{d} ± 0.24, 15.19, -2.2	6^{efg} ± 0.31, 11.78, -1.8	5.6^{e} ± 0.24, 9.76, -2.0	73.40^{efg} ± 0.67, 2.06,-4.8	73^{ef} ± 0.70, 2.16, -3.8	1.62^{c} ±0.07, 10.12, -0.4	1.56^{e} ± 0.04, 5.7, -0.42

[#] Means within columns followed by the same letter is not different at the 5 % level of significance, based on the Duncan Multiple Range Test

Table 5. Correlation coefficients among various character pairs in M_2 generation of *Nigella sativa* varieties NRCSSAN-1 and BHUVN-1.

Character	NRCSSAN-1	BHUVN-1	NRCSSAN-1	BHUVN-1	NRCSSAN-1	BHUVN-1	NRCSSAN-1	BHUVN-1	NRCSSAN-1	BHUVN-1
	Plant height		No. of fertile branches		No. of capsules per plant		No. of seeds per capsule		1000 seed weight	
Plant height	1	1								
No. of fertile branches	0.157401	0.250644	1	1						
No. of capsules per plant	0.342627	0.383672	0.277462	0.569997	1	1				
No. of seeds per capsule	0.385105	0.447319	0.239124	0.467503	0.62645	0.453707	1	1		
1000 seed weight	0.301582	0.309606	0.102888	0.47832	0.609317	0.5803	0.515105	0.59463	1	1

Meiotic abnormalities have been considered to be one of the reliable indices for estimating the mutagenic sensitivity of the crop species. Structural rearrangement of chromosomes could be achieved through induced mutagenesis to create new combinations which otherwise are rarely obtained spontaneously or by conventional methods. In the present study, a broad spectrum of meiotic abnormalities including univalent, multivalent, laggards, bridges, stickiness, disturbed polarity, unequal separation of chromosomes etc. was induced by individual and simultaneous treatments of EMS and gamma rays in M_1 generation. The maximum chromosomal abnormalities were recorded with combination treatments compared to individual ones in both varieties. Similar mutagen-induced chromosomal abnormalities have been previously reported by many workers with different plant species including Kumar and Srivastava (2001) in *Plantago ovata*, Bhat *et al*. (2005) in *Vicia faba*, Jafri *et al.* (2011) and Khan *et al*. (2009) in *Cichorium intybus* and Goyal and Khan (2010) in *Vigna mungo*. The multivalent formation has been attributed to chromosomal pairing due to translocation and inversion. The occurrence of multivalent association is a common feature in the treated plants with the presence of more than two homologous chromosomes. Precocious separation occur by the effect of chemicals which break the protein moiety of the nucleoprotein backbone (Kumar and Rai, 2007; Amin *et al*., 2016). Laggards occur due to abnormal spindle formation and chromosomal breakage (Singh and Chaudhary, 2005; Khursheed *et al*., 2015).

Chromosomal bridges were observed at anaphase which seems to be the result of the non-separation of chiasma due to stickiness. According to Kumar and Singh (2003), the unequal separation of chromosomes occurs due to the random univalent movement to any one of the poles. The unequal separation, seen in the present investigation, may be due to the stickiness of chromosomes as was also reported in chickpea (Sharma and Kumar, 2004) and fenugreek (Srivastava and Kapoor, 2008). The formation of micronuclei due to lagging chromosomes has been reported by Kumar and Kumar (2000) and Ganai *et al.* (2005). During the anaphase and telophase stages, disturbed polarity occurred due to spindle disturbance. Stickiness of chromosomes was one of the most common abnormalities observed in the present investigation. Chromosomes were found clumped into one, two or many groups due to stickiness at metaphase causing a difficulty in the normal disjunction of chromosomes. These results are in agreement with those of Srivastava and Kapoor (2008) in fenugreek.

The nature and extent of genetic variability available within the species forms the basis for an effective selection for agro-economic traits under improvement. The mutagenic effectiveness of various doses of EMS and gamma rays alone and in combination was investigated concerning various quantitative traits, such as plant height (cm), number of fertile branches per plant, number of capsules per plant, number of seeds per capsules and 1000-seed weight (g) in M_2 generation. The assessment of mean, standard deviation (SD) and coefficient of variation (CV) in the control and treated population indicates that mutagenic treatments had induced a wider magnitude of variability for all these traits. Plant height had increased with the lower concentrations of EMS and gamma rays. Similar results were reported by Raina *et al.* (2017) in chickpea and Suprasanna *et al.* (2012) in vegetable crops. The increase in plant height at lower doses may be attributed to the induction of chromosomal abnormalities.

The characters like the number of capsules per plant, seeds per capsule and 1000-seed weight (g) showed a slight increase in the mean values at the lowest concentration of EMS (0.1 %), while higher concentrations of the single and combination treatments showed an inhibitory effect regarding these traits. The current results are consistent with the earlier reports of Tantray *et al.* (2017) and Khursheed *et al.* (2017). Positive correlations were observed among different character pairs controlling the yield. The possible cause of such positive associations could be ascribed to gene mutations.

5. Conclusion

It may be concluded from the present study that ample genetic variability had been induced by using lower doses of EMS and gamma rays alone or in combination. The mutagenic potency of such mutagens could be exploited further by carrying out extensive research in *N. sativa*- an economically important medicinal plant for a safer future.

References

Amin R, Laskar RA and Khan S. 2015. Assessment of genetic response and character association for yield and yield components in lentil (*Lens culinaris* L.) population developed through chemical mutagenesis. *Cogent Food and Agri.*, **1:** 1000715.

Amin R, Laskar RA, Khursheed S, Raina A and Khan S. 2016. Genetic sensitivity towards MMS mutagenesis assessed through *in vitro* growth and cytological test in *Nigella sativa* L. *Life Sci Inter Res J*., **3**: 1-9.

Bhat TA, Khan AH and Parveen S. 2005. Comparative analysis of meiotic abnormalities induced by gamma rays, EMS and MMS in *Vicia faba* L. *J. Indian Bot Soc*., **84:** 45-48.

Bhat TA, Khan AH and Parveen S. 2006. Effect of gamma rays on certain cyto-morphological parameters in two varieties of *Vicia faba* L. *Adv Plant Sci*., **19:** 227-232.

Blixt S. 1972. Mutation genetics in *Pisum*. *Agri Horticult Genet.*, **30:** 1–293.

Chopra RN, Chopra IC, Handa KL and Kapur LD. 1982. **Indigenous Drugs of India,** Academic Publishers, Calcutta, India.

Datta AK, Biswas AK and Sen S. 1986. Gamma radiation sensitivity in *Nigella sativa* L. *Cytologia*, **51**: 609-615.

Ganai FA, Khan AH, Bhat TA, Parveen S and Wani NA. 2005. Cytogenetic effects of methylmethane sulphonate (MMS) on two varieties of chickpea (*Cicer arietinum* L.). *J Cytol. Genet*., **6:** 97-102.

Goyal S and Khan S. 2010. Cytology of induced morphological mutants in *Vigna mungo* (L.) Hepper. *Egyptian J Biol*., **12:** 81-85.

Greene EA, Codomo CA, Taylor NE, Henikoff JG, Till BJ, Reynolds SH, Enns LC, Burtner C, Johnson JE, Odden AR, Comai L and Steven H. 2003. Spectrum of chemically induced mutations from a large scale reverse genetic screen in *Arabidopsis*. *Genet.*, **164:** 731–740.

Grover IS and Virk GS. 1986. A comparative study of gamma rays and some chemical mutagens on the induction of chromosomal aberrations in mung bean (*Vigna radiata* (L.) Wilczek). *Acta Botanica Indica*, **14:** 170–180.

Iqbal MS, Qureshi AS and Ghafoor A. 2010. Evaluation of *Nigella sativa* L. for genetic variation and *ex–situ* conservation. *Pak J Bot*., **42:** 2489-2495.

Jafri IF, Khan AH and Gulfishan M. 2011. Genotoxic effects of 5-bromouracil on cyto-morphological characters of *Cichorium intybus* L. *African J Biotechnol*., **10:** 10595-10599.

Jayabalan N and Rao GR. 1987. Effect of physical and chemical mutagens on seed germination and survival of seedling in *Lycopersicon esculentum* Mill. *J Indian Bot Soc*., **10:** 133-137.

Khan Z, Ansari MYK, Gupta H and Chaudhary S. 2009. Methylmethane sulphonate induced chromosomal variations in a medicinal plant *Cichorium intybus* L. during microsporogenesis. *Biol Med.*, **1:** 66-69.

Khursheed S, Laskar RA, Raina A, Amin R and Khan S. 2015. Comparative analysis of cytological abnormalities induced in *Vicia faba* L. genotypes using physical and chemical mutagenesis. *Chromosome Sci.*, **18:** 3-7.

Khursheed S, Raina A, Parveen K and Khan S. 2017. Induced phenotypic diversity in the mutagenized populations of faba bean using physical and chemical mutagenesis. *J Saudi Soc Agric Sci*., http://dx.doi.org/10.1016/j.jssas.2017.03.001

Kirtane S and Dhumal KN. 2004. Studies on induced mutations in onion: Biological and cytological effects of mutagens in M_2 generation. *Int J Mendel*., **21:** 11-13.

Kirtikar KR and Basu BD. 1982. **Indian Medicinal Plants.** volume I. In Singh B and Singh MP (Eds.), Dehradun, India.

Krishna G, Shivashankar G and Nath J. 1984. Mutagenic response of rhodes grass (*Choris gayana Kunth*.) to gamma rays. *Environ Exper Bot.*, **24:** 197–205.

Kumar G and Kumar R. 2000. Chromotoxic and mito-inhibitory effects of pesticides in *Trigonella foenum-graecum* L. *J Cytol Genet*., **1:** 11-15.

Kumar G and Rai P. 2007. Comparative genotoxic potential of mercury and cadmium in soybean. *Turkish J Biol.*, **31:** 13-18.

Kumar G and Singh V. 2003. Comparative analysis of meiotic abnormalities induced by gamma rays and EMS in barley. *J Indian Bot Soc*., **82:** 19-22.

Kumar G and Srivastava U. 2001. Cytomictic variations in isabgol (*Plantago ovate forsk*). *The Nucleus*, **44:** 180-182.

Kumar S and Dubey DK. 1998. Effect of separate and simultaneous application of gamma rays and EMS on germination, growth, fertility and yield in cultivars Nirmal and LSD-3 of khesari (*Lathyrus sativus* L.) Var. P-505. *J Phytol Res*., **11:** 165-170.

Kumar S, Vandana and Dubey DK. 1993. Studies on the effect of gamma rays and DES on germination, growth fertility and yield in faba bean. *FABIS Newsletter*, **32:** 15–18.

Larcher W. 1995. Gas exchange in plants. In: Larcher W (Eds.), **Physiological Plant Ecology,** 3rd Edition. Berlin, Springer, pp. 74-128.

Laskar RA, Khan S, Khursheed S, Raina A and Amin R. 2015. Quantitative analysis of induced phenotypic diversity in chickpea using physical and chemical mutagenesis. *J of Agronomy*, **14:** 102-111.

Laskar RA, Laskar AA, Raina A, Khan S and Younus H. 2018. Induced mutation analysis with biochemical and molecular characterization of high yielding lentil mutant lines. *Int. J. Biol Micromol*., **109:** 167-179.

MacKinney 1941. Absorption of light by chlorophyll solutions. University of California, Berkeley: Prom the Division of Fruit Products.

Malhotra SK and Vashishtha BB. 2008. Response of nigella (*Nigella sativa* L.) variety NRCSSAN-1 to different agro-techniques. *J. Spices Aromatic Crops*, **17:** 190-193.

Raina A, Laskar RA, Khursheed S, Amin R, Tantray YR, Parveen K and Khan S. 2016. Role of mutation breeding in crop improvement-past, present and future. *Asian Res J Agr*., **2:** 1-13.

Raina A, Laskar RA, Khursheed S, Khan S, Parveen K, Amin R and Khan S. 2017. Induced physical and chemical mutagenesis for improvement of yield attributing traits and their correlation analysis in chickpea. *Inter Lett Natural Sci.*, **61:** 14-22.

Ramachander L, Shunmugavalli N, Muthuswamy A and Rajesh S. 2018. Frequency of viable mutants in M_2 and M_3 generation of black gram (*Vigna mungo* (L.) Hepper) through induced mutation. *Inter J Curr Microbiol Appl Sci*., **7:** 1996-1999.

Sharma V and Kumar G. 2004. Meiotic studies in two cultivars of *Cicer arietinum* L. after EMS treatment. *Cytologia*, **69:** 243-248.

Simova-Stoilova LJ, Stoyanova Z and Demirevska-Kepova K. 2001. Ontogenic changes in leaf pigments, total soluble protein and Rubisco in two barley varieties in relation to yield. *Bulgarian J Plant Physiol.*, **27:** 15–24.

Singh AK and Chaudhary BR. 2005. γ-rays induced chromosome anomalies in two morphologically distinct varieties of *Capsicum annuum* L. *The Nucleus*, **48:** 80-84.

Singh AK, Gupta RK and Singh IP. 2011. Role of induced mutations for the improvement of pulse crops with special reference of mungbean. In Khan S, Kozgar MI (Eds.), **Breeding of Pulse Crops.** Kalyani Publishers, Ludhiana, India, pp. 104-125.

Srivastava A and Kapoor K. 2008. Seed yield is not impaired by chromosome stickiness in sodium azide treated *Trigonella foenum-graecum* L. *Cytologia*, **73:** 115-121.

Suprasanna P, Jain SM, Ochatt SJ, Kulkarni VM and Predieri S. 2012. Applications of *in vitro* techniques in mutation breeding of vegetatively propagated crops. **Plant Mutation Breeding and Biotechnology.** Wallingford, UK: CABI Publishing, pp. 371-385.

Suprasanna P, Mirajkar SJ and Bhagwat SG. 2016. Induced mutations and crop improvement. In: **Plant Biology and Biotechnology**. Springer: India, pp. 593-617.

Tantray AY, Raina A, Khursheed S, Amin R and Khan S. 2017. Chemical mutagen affects pollination and locule formation in capsules of black cumin (*Nigella sativa* L.). *Inter J Agri Sci*,, **8:** 108-117.

Verma AK, Dhanasekar P, Choudhary S, Meena RD and Lal G. 2018. Estimation of induced variability in M_2 generation of fennel (*Foeniculum vulgare* Mill.). *J Pharmaco Phytochem.*, **7:** 430-436.

Wani MR, Khan S and Kozgar MI 2011a. Induced chlorophyll mutations. I. Mutagenic effectiveness and efficiency of EMS, HZ and SA in mungbean. *Front Agri China*, **5:** 514–518.

Wani MR, Khan S, Kozgar MI and Goyal S. 2011b. Induction of morphological mutants in mungbean (*Vigna radiata* (L.) Wilczek) through chemical mutagens. *The Nucleus*, **48:** 243-247.

Wani MR. 2018. Early maturing mutants of chickpea (*Cicer arietinum*) induced by chemical mutagens. *Indian J Agri Sci.*, **88:** 635-640.

JJBS

Volume 12, Number 1,March 2019
ISSN 1995-6673
Pages 31 - 35

Jordan Journal of Biological Sciences

Pyocyanin and Biofilm Formation in *Pseudomonas aeruginosa* Isolated from Burn Infections in Baghdad, Iraq

Maha M . Khadim and Mohammed F. AL Marjani *

Department of Biology, College of Science, Mustansiriyah University, Baghdad- Iraq

Received May 26, 2018; Revised June 30, 2018; Accepted July 6, 2018

Abstract

Pseudomonas aeruginosa is emerging as important hospital pathogenic bacteria, which can persist in the environment for extended periods of time. Sixty-three isolates belonging to the *P. aeruginosa* were isolated from different clinical sources. The antimicrobial susceptibility test was performed by the disk diffusion method, and the biofilm formation was assayed by the micro titer plate. Pyocyanin was extracted from the culture supernatants, and the absorbance values were measured using a spectrophotometer. The percentage of resistance shown by the isolates were 87.3 % for cefotaxime, 52.38 % carbenicillin, 39.68 % imipenem, 11.11 % colistin, and 7.93 % Piperacillin-tazobactam. About 9.09 % exhibited positive results for the phenotypic production of extended spectrum β-lactamase, whereas 40 % of the imipenem-resistant isolates were Metallo-β lactamase (MBLs) producers. Among the burn isolates, 22.22 % formed moderate biofilms and 6.35 % formed strong biofilms. 34.92 % of the burn isolates were pyocyanin producers. All the pyocyanin-producer isolates carried phenazine biosynthetic operon *phzA-G* gene. The results of this study revealed a high prevalence of pyocyanin production and biofilm formation in the *P. aeruginosa* isolates from burn infections.

Keywords: *Pseudomonas aeruginosa*, Phenazine , Biofilm, Burn infections, Iraq.

1. Introduction

Pseudomonas aeruginosa is an important opportunistic pathogen primarily causing nosocomial infections in immunocompromised patients and is responsible for high mortality rates in burn centers (Samira and Fereshteh, 2015; Klrissa and Mohammad, 2016). However, it is capable of causing a wide range of infections with damaged epithelial barriers (Engel and Balachandran, 2008). *P. aeruginosa* synthesizes a characteristic blue redox-active secondary metabolite, that is chloroform-soluble and a member of the tricyclic compounds "phenazine" called pyocyanin (1-hydroxy-5-methyl-phenazine (Ran *et al*., 2003). One of the most important symptoms of critical infections generated by these bacteria is the production of blue pus. Pyocyanin has been shown to inhibit respiration in mammalian cells (Rada and Leto, 2013), and the beating of human respiratory cilia *in vitro* (Wilson *et al.,* 1987). *P. aeruginosa* strains that do not produce pyocyanin have a low pathogenicity and a higher susceptibility to the immune response (Lau *et al*., 2004). *P. aeruginosa* PAO1 consist of two homologous core loci (operon *phzA1B1C1D1E1F1G1* and *phzA2B-2C2D2E2F2G2*) to be coded of phenazine-1-carboxylic acid and two phenazine genes (*phzM* and *phzS*) responsible for converting the enzymes of phenazine-1-carboxylic acid to pyocyanin (Mavrodi *et al*., 2001). Another important factor contributing to the *P. aeruginosa* pathogenicity in causing fatal infections is its potential to form biofilms on abiotic and biotic surfaces (Karatuna and Yagci, 2010). The populations of bacteria in biofilms are usually more resistant to antibacterial agents and host-mediated clearance strategies compared to their planktonic counterparts, giving rise to chronic infections that are notoriously difficult to eradicate (Mah *et al*., 2003). Bacterial cells which grow in biofilms produce extracellular polymeric matrices which hold the cells of the biofilm community together. Polysaccharides are important components of the biofilm matrix, as they contribute to the overall biofilm structure and to the resistance of grown bacteria in biofilm to certain antibacterial agents (Wozniak *et al*., 2003). This study is aimed at investigating the ability of different isolates of *P. aeruginosa* to produce pyocyanin and biofilm formation.

2. Materials and Methods

2.1. Bacterial Isolates

A total of sixty-three clinical isolates of *P. aeruginosa* were collected from several hospitals in Baghdad between December 2016 and April 2017 and identified using vitek 2 system and 16SrRNA gene by PCR.

2.2. Antibiotic Susceptibility Testing

The susceptibility of isolates to different antibiotics was tested using the Kirby-Bauer disk diffusion method following the Clinical and Laboratory Standards Institute

* Corresponding author. e-mail: marjani20012001@gmail.com , dr.marjani@uomustansiriyah.edu.iq.

guidelines (CLSI, 2011). Using antibacterial agents included: gentamicin (GM), tobramycin (TN), amikacin (AK), ciprofloxacin (CIP), levofloxacin (LEV), colistin sulphate (CO), piperacillin tazobactam (PTZ), ceftazidime (CAZ), cefotaxime (CTX), aztreonam (ATM), carbenicillin (PY), and imipenem (IMP). On Mueller-Hinton agar plate (Himedia, India) using overnight culture at McFarland standard 0.5 followed by incubation at 35°C for eighteen hours.

2.3. Detection of Extended Spectrum β Lactamases Production

All isolates that showed resistance to the third generation of cephalosporin were tested to investigate the production of ESβLs by the disc approximation test, and the results were interpreted according to Collee *et al*. (1996) and Drieux *et al*. (2008). The tested isolates were inoculated according to Kirby-Bauer method onto the plate of Mueller-Hinton agar media. The Augmentin disc was placed in the center of the plate; cefotaxime and ceftazidime discs were placed at 3cm from center disc. The inhibition zones of the ceftazidime, cefotaxime and augmentin discs were compared after 16-18 hours of incubation at 35°C. The breadth of the zone of inhibition between ceftazidime, cefotaxime and augmentin disc was considered as isolates which produce extended spectrum β Lactamases.

2.4. Detection of Metallo-β Lactamase (MβLs)

The disc synergy test was used to detect the MβLs production according to Bashir *et al*., (2011) as follows: The tested *P. aeruginosa* isolates were inoculated according to the Kirby-Bauer method onto plates of Mueller-Hinton agar media. Two discs of imipenem antibiotic were placed on the plate; 5 µL of EDTA solution (final concentration is 0.5M) was added to one of them. The zones of inhibition of the imipenem disc and imipenem + EDTA disc were compared after incubation at 35°C for 16-18 hours. An increase in the inhibition zone size of at least 7 mm around the imipenem-EDTA disc more than the imipenem disc alone was considered as producers of MBLs.

2.5. Detection of Biofilm Formation

In the present study, *P. aeruginosa* isolates were screened for their ability to form biofilm by microtiter plate according to the method described by Mathur *et al*. (2006) and Lotfi *et al*. (2014). Twenty micro liter of bacterial suspension from an overnight culture was used to inoculate microtiter wells containing 180µL of Brain Heart Infusion (BHI) broth with 2 % sucrose. Control wells contained 200µL of BHI broth with 2 % sucrose. The covered microtiter plate was sealed with parafilm during incubation at 37°C for twenty-four hours. Unattached bacterial cells were removed by washing the wells three times with PBS (pH 7.2), they were dried at room temperature for fifteen minutes, and then 200µL of crystal violet (0.1%) was added to the wells for fifteen minutes. After removing the crystal violet solution, the wells were washed three times with PBS (pH 7.2) to remove the unbounded dye and, and were allowed to dry at room temperature, then they were extracted twice with 200µL of 95 % ethanol. The absorbance of each well was measured at 630nm using ELISA reader. The O.D value for control well was deducted from all the test O.D value.

2.6. Phenotypic Detection of Pyocyanin Production

Pyocyanin production was detected for all the sixty-three isolates on King's B medium (King *et al*., 1954) and Mueller-Hinton agar media by streaking the overnight culture followed by incubation at 30°C for twenty-four hours.

2.7. The Quantitative Pyocyanin Assay

The quantitative pyocyanin assay depends on the absorbance of pyocyanin at 520 nm in acidic solution. Five mL of culture grown in Tryptone broth (T-broth) for the production of pyocyanin was extracted with chloroform (3 mL) and then re-extracted into 1 mL of HCl (0.2-N) to give a pink to deep red solution. The absorbance of this solution was measured, and the concentrations expressed as µg/mL of pyocyanin produced by the culture supernatant were determined by multiplying the OD at 520 nm by 17.072 (Essar *et al*., 1990).

2.8. Molecular Detection of Pyocyanin Genes.

Detection of pyocyanin genes for producing isolates, using primers for phenazine biosynthetic operon *phzA-G*, and two phenazine modifying genes *phzM* and *phzS* genes as shown in Table 1 according to Jamileh *et al*.(2012).

Table 1. Primers for phenazine biosynthetic operon *phzA-G*, and two phenazine modifying genes *phzM*and *phzS* genes (AlphaDNA, Canada).

Genes	Primers	Primers Sequence(s)	PCR product
Phenazinebiosynthetic operon (*phzABCDEFG*)	PHZAF	5´-CCGTCGAGAAGTACATGAAT-3´	448 bp
	PHZAR	5´ -CATAGTTCACCCCTTCCAG-3´	
Phenazine-specific methyl- transferase (*phzM*)	PHZMF	5´-AACTCCTCGCCGTAGAAC-3´	313 bp
	PHZMR	5´-ATAATTCGAATCTTGCTGCT-3´	
Flavinecontaining Mono- oxygennase (***phzS***)	PHZSF	5´-TGCGCTACATCGACCAGAG-3´	664 bp
	PHZSR	5´-CGGGTACTGCAGGATCAACT-3´	

The typical colonies of *P. aeruginosa* were cultured on BHI agar (Himedia, India) for twenty-four hours at 37˚C. The total DNA was isolated from the colonies on BHI using microwave method according to Ahmed *et al*. (2014); cell pellets were washed with 1 mL of Tris- EDTA and were resuspended in 100 µL of TE. After the addition of 50 µL of 10 % Sodium dodecyl sulfate (SDS), the mixture was incubated for thirty minutes at 65°C. The lysates were centrifuged and the supernatants were removed. The microtubes were then placed in a microwave oven and heated. The pellets were dissolved in 200 µL of TE, and were extracted with an equal volume of

phenol/chloroform/ isoamyl alcohol (25:24:1) for fifteen minutes. The aqueous phase was recovered by centrifugation for twenty minutes and precipitated with ethanol. The total DNA was used as DNA template for PCR amplification. For PCR amplification, the reaction mixture (25 µL) contained: 1 µL (10 pmol/µL) of each forward and reverse oligo nucleotide primers as described in Table 1, 12.5µL of GoTaq®Green Master Mix2X (Promega, USA), 5µL of template, and 5.5µL of nuclease free water (Promega, USA). Amplifications were performed by a DNA Thermal Cycler (Gradient thermocycler Polymerase Chain reaction,TechNet-5000, USA). The cycling program included a five-minute initial denaturation step at 94˚C, followed by thirty cycles of denaturation for thirty seconds at 94˚C, annealing of primers for thirty seconds at 60 ˚C, and primer extension for thirty seconds at 72˚C with auto extension. After the last cycle, the PCR tubes were incubated for ten minutes at 72 ˚C. PCR products were detected by electrophoresis on 1 % agarose gel by staining with ethidium bromide.

3. Results and Discussion

3.1. Bacterial Isolates

P. aeruginosa infections are opportunistic bacteria in nature and ranged from those associated with catheter, ventilator, wound and burn to pulmonary infections in cystic fibrosis patients and keratitis in contact lens (Choy *et al*., 2008). In this study, 63 clinical isolates of *P. aeruginosa* obtained from patients with suspected infection were collected primarily from burn (n=37), wound swab (n=9), fluids (n=4), ear (n=4), keratitis (n=3), urine (n=3), catheters (n=2), and from blood (n=1).

3.2. Antimicrobial Susceptibility of P. aeruginosa isolates

The isolates showed high susceptibility for piperacillin + tazocin the resistance rate was 7.93% (n=5) in comparison to other antibiotics used in this study, and the high resistance was investigated to cefotaxime 87.3 % (n=55). The isolates were resistant to carbenicillin (52.38 %), and exhibited the same resistance for aztreonam and imipenem (39.68 %) (Table 2). Resistance to gentamicin, tobramycin, and amikacin was confirmed in 69.84 % (n=44), 74.6 % (n=47), and 61.9 % (n=39) of the isolates, respectively. Whereas 55.55 % (n=35) and 57.14 % (n=36) of the isolates exhibited resistance to ciprofloxacin and levofloxacin respectively.

Among the third generation cephalosporin resistant isolates, 9.09 % exhibited positive results for phenotypic production of extended spectrum β-lactamase (ESBLs), whereas 40 % of the imipenem resistant isolates were Metallo-β lactamase (MBLs) producers.

In the present study, a total of sixty-three MDR P. aeruginosa clinical isolates collected from several hospitals as a result of the emergence of MDR P. aeruginosa became difficult infections to treat. Clinically, antibiotics-resistant bacteria are responsible for the increased length of hospitalization, cost and mortality (Mansouri *et al*., 2013).

In the current study, isolates exhibited resistances for β-lactams in a varied levels especially for the third-generation cephalosporin, but at the same time several isolates were ESBLs producers.

Table 2. Antimicrobial susceptibility test results of *P. aeruginosa* isolates.

Antimicrobials Agents	Resistance %
Cefotaxime	87.3
Carbencillin	52.38
Aztreonam	39.68
Imipenem	39.68
Ceftazidime	30.15
Piperacillin-tazobactam	7.93
Tobramycin	74.6
Gentamicin	69.84
Amikacin	61.9
Levofloxacin	57.14
Ciprofloxacin	55.55
ColistinSulphate	11.11

Also, the isolates revealed resistance to gentamicin, tobramycin, ciprofloxacin, levofloxacin. These results are in agreement with those obtained by Al-Marjani and Khadam (2016). In fact, they isolated *P. aeruginosa* multi-drug resistant from different infection sites. This high multi resistance could be due to the production of hydrolytic enzymes and the acquisition of resistance mechanisms by *P. aeruginosa* strains. Nikokar *et al.* (2013) reported that 74.4 % of the isolates were resistant to carbenicillin, whereas Moazami-Goudarzi and Eftekhar (2013) showed that 94.7 % of isolates were imipenem resistant.

3.3. Biofilm Formation

All the isolates were divided into three categories according to biofilm analysis. 46.03 % (n=29) of isolates were categorized as weak biofilm producers, 39.68 % (n=25) produced moderate biofilm, and 14.28 % (n=9) formed strong biofilm. Isolates from burns and wounds had a greater ability to form strong and moderate biofilm compared with the isolates obtained from other sources (Table 3).

The results of the current study showed the ability of biofilm formation in clinical *P. aeruginosa* isolates. Biofilm formation is an important mechanism involved in resistance of bacteria.

Table 3. Type of specimen and biofilm formation in *P. aeruginosa* isolates

Biofilm Formation	Type of specimens								
	Burns No. (%)	Wounds No.(%)	Fluid No.(%)	Ear No. (%)	Keratitis No.(%)	Urine No.(%)	Catheters No.(%)	Blood No.(%)	Total No.(%)
Weak	19(30.16)	2(3.17)	2(3.17)	2(3.17)	2(3.17)	2(3.17)	0	0	29(46.03)
Moderate	14(22.22)	5(7.94)	1(1.59)	2(3.17)	0	0	2(3.17)	1(1.59)	25(39.68)
Strong	4(6.35)	2(3.17)	1(1.59)	0	1(1.59)	1(1.59)	0	0	9(14.2)
Total	37	9	4	4	3	3	2	1	63

In the current study 6.35% and 22.22% of burns isolates were strong and moderate biofilm producers respectively, and 3.17% and 7.94% of wounds isolates produced strongly and moderately biofilm respectively. Perez *et al*. (2011) showed the high potential of biofilm formation by clinical *P. aeruginos*a isolates regardless of the specimen source.

3.4. Phenotypic Detection of Pyocyanin Production

All fluids isolates 6.35 % (n=4) and keratitis 4.76 % (n=3) isolates produced pyocyanin on King's medium 12.7% (n=8) of wounds isolates and 34.92% (n=22) of burns isolates were pigment producers. Catheters isolates exhibited negative results (Table 4).

Table 4 . Type of specimen and pyocyanin production in *P.aeruginosa* isolates.

Pyocyanin production	Type of specimens								
	Burns No.(%)	Wounds No.(%)	Fluid No.(%)	Ear No.(%)	Keratitis No.(%)	Urine No.(%)	Catheters No.(%)	Blood No.(%)	Total No.(%)
Producer	22(34.92)	8(12.7)	4(6.35)	1(1.59)	3(4.76)	1(1.59)	0	1(1.59)	40(63.50)
Non	15(23.81)	1(1.59)	0	3(4.76)	0	2(3.17)	2(3.17)	0	23(36.50)
Total	37(58.73)	9(14.29)	4(6.35)	4(6.35)	3(4.76)	3(4.76)	2(3.17)	1(1.59)	63

3.5. The QuantitativePyocyanin Assay

The pyocyanin production was detected by quantitative assay for twenty-two isolates using spectrophotometer. *P. aeruginosa* isolated from burn infections were the highest pyocyanin producers. Pyocyanin production reached 10.85 µg/ml from the burn isolates, whereas the pyocyanin production in the rest of the *P. aeruginosa* isolates from wound infections ranged from 3.312 to 6.163 µg/ml, and from body fluids it ranged from 3.54 to 6.354 µg/ml. The variation in the production of pyocyanin among different *P. aeruginosa* isolates could be attributed to regulators. The overexpression of some genes in *P. aeruginosa* significantly reduced the homoserine lactone signals accumulation and affected the production of pyocyanin (El-Fouly *et al*., 2015).

3.6. Molecular Detection of Pyocyanin Genes.

All the pyocyanin-producer isolates carried phenazine biosynthetic operon *phzA-G* gene, and two phenazine modifying genes *phzS* and *phzM* genes.

phzM encodes a protein (36.4kDa) that most closely resembles O-methyl transferases of bacteria. *phzS* encodes a protein (43.6 kDa) similar to monooxygenases of bacteria. Among the pseudomonads, only *P. aeruginosa* has been found to contain two copies of the phenazine operon (Jamileh *et al*., 2012). *P. aeruginosa* isolates that do not produce pyocyanin have a low pathogenicity and a higher susceptibility to the immune response (Lau *et al*., 2004).

The EPS matrix of *P. aeruginosa* primarily consists of biomolecules, such as polysaccharides, proteins, extracellular DNA, metabolites (phenazines), siderophores and exotoxin. These molecules that are present in the matrix play an important role in the *P. aeruginosa* infections (Das *et al*., 2016).

Phenazines such as pyocyanin and the release of DNA from cells providing freely-available extracellular DNA by *P. aeruginosa*, are the major factors dictating the biofilm formation and the persistent infection within the host. Extracellular DNA is similarly a key factor in the biofilm formation of *P. aeruginosa* and in protecting the bacterial cells by inducing drug resistance. It is also a contributing factor to the high viscosity of cystic fibrosis sputum that blocks the respiratory airway passages (Das *et al*., 2016). Pyocyanin has been shown to intercalate with extracellular DNA to promote cell-to-cell interactions between the *P. aeruginosa* cells by influencing their physicochemical interactions and the cell surface properties. It has been suggested that pyocyanin may also contribute to the biofilm formation by the promotion of extracellular DNA (Das and Manefield, 2012).

4. Conclusion

In conclusion, this study determined the ability of MDR *P. aeruginosa* isolates for biofilm formation and pyocyanin production. Biofilm formation is associated with the increased resistance to the antibiotic and bacterial colonization within the burn infections. The resistant isolates achieve high levels of biofilm -specific resistance despite producing moderate or weak biofilms. Biofilm formation and pyocyanin can increase the toxicity and pathogenicity of this bacterium. All the *P. aeruginosa* even MDR and biofilm-forming isolates had low resistance to piperacillin-tazobactam.

Acknowledgments

This work was supported by the Department of Biology of the College of Science at Mustansiriyah University in Baghdad, Iraq.

References

Ahmed OB, Asghar AH and Elhassan MM. 2014. Comparison of three DNA extraction Methods for polymerase chain reaction (PCR) analysis of bacterial genomic DNA. *African J Microbiol Res.* , **8(6):**598-602.

AL-Marjani MF and Khadam ZA . 2016. Effect of Gamma Irradiation on Biofilm Formation of Some Gram- Negative Bacteria Isolated From Burn and Wound Infections . *Inter J of PharmTech Res.* , **9(12):***607-613.*

Bashir D, Thokar MA, Fomda BA, Bashir G ،Zahoor D, Ahmad S and Toboli AS. 2011. Detection of metallo-beta-lactamase (MBL) producing *Pseudomonas aeruginosa* at a tertiary care hospital in Kashmir. *African J Microbiol Res.*, **5(2):**164-172.

Choy MH, Stapleton F, Willcox MDP and Zhu H. 2008. Comparison of virulence factors in *Pseudomonas aeruginosa* strains isolated from contact lens- and non-contact lens-related keratitis. *J Med Microbiol.* , **57(12):**1539-1546.

CLSI. 2011. Performance standard for antimicrobial susceptibility testing; TwentyFirst informational supplement, **31(1),** 100-S21.

Collee JG, Fraser AG, Marmion BP and SimmonsA. 1996. **Mackie and McCarteny Practical Medical Microbiology**.14th ed. Churchill living stone, New York, USA 413-423.

Das T and Manefield M. 2012. Pyocyanin promotes extracellular DNA release in *Pseudomonas aeruginosa*. *PLoS ONE*, **7**: e46718.

Drieux L, Brossier F, Sougakoff W and Jarlier V. 2008. Phenotypic detection of extendedspectrum b-lactamase production in *Enterobacteriaceae:* review and bench guide. *J.Clin Microbiol Infect*, **14** (Suppl.1), 90–103.

Das T, Ibugo, AI, Klare W and Manefield M. 2016. Role of Pyocyanin and extracellular DNA in facilitating *Pseudomonas aeruginosa* biofilm formation. *J Immun Microbiol*.http://dx.doi.org/10.5772/63497

El-Fouly MZ , Sharaf AM , Shahin AAM , El-Bialy HA and Omara AMA.2015. Biosynthesis of pyocyanin pigment by *Pseudomonas aeruginosa*. *J of Rad Res Appl Sci.,* **8 (1):** 36-48

Engel J and Balachandran P. 2008. Role of *Pseudomonas aeruginosa* type III effectors in disease. *J Curr Opin Microbiol*., **12(1):**61-6.

Essar DW, Eberly L, Hadero A and Crawford IP. 1990. Identification and Characterization of Genes for a Second Anthranilate Synthase in *Pseudomonas aeruginosa*: Interchangeability of the Two Anthranilate Synthases and Evolutionary Implications. *J Bacteriol.*, **172(2):**884-900.

Høiby N, Bjarnsholt T, Givskov M, Molin S and Ciofu O. 2010. Antibiotic resistance of bacterial biofilms. *Inter J Antimicrb Agents*, **35(4):**322-332.

Jamileh N, Abbas AS and Afrooz R. 2012. Evaluation of pyocyanin biosynthetic genes in clinical and environmental isolates of *Pseudomonas aeruginosa* and detection of pyocyanin's antimicrobial effects with or without colloidal silver nanoparticles. *J Cell*, **14(1):** 7-18.

Karatuna O and Yagci A. 2010. Analysis of quorum sensing-dependent virulence factor production and its relationship with antimicrobial susceptibility in *Pseudomonas aeruginosa* respiratory isolates. *J Clin Microbiol Infect.*, **16(12):**1770–1775.

King EO, Ward MK and Raney DE. 1954. Two simple media for the demonstratoin of pyocyanin and fluorescein. *J Lab Clin Med*, **44**:301-307.

Klrissa S and Mohammad K. 2016. *Pseudomonas aeruginosa:* A review of their pathogenesis and prevalence in clinical settings and the environment. *J Infect Epidemiol Med*., **2(1):** 25-32.

Lau GW, Ran H, Kong F, Hassett DJ and Mavrodi D. 2004. *Pseudomonas aeruginosa* pyocyanin is critical for lung infection in mice. *J Infect Immun*., **72(7):** 4275-4278.

Lotfi GH, Hafida HA, Nihel KL, Abdelmonaim KH, Nadia AI, Fatima NAS and Walter ZI. 2014. Detection of biofilm formation of a collection of fifty strains of *Staphylococcus aureus* isolated in Algeria at the University Hospital of Tlemcen. *African J Bacteriol Res*., **6(1):**1-6.

Mah TF, Pitts B, Pellock B, Walker GC, Stewart PS and O'Toole GA. 2003. A genetic basis for *Pseudomonas aeruginosa* biofilm antibiotic resistance. *J Nature*, **426**(6964):306–10.

Mansouri S, Safa A, Najar SG and Najar AG. 2013. Inhibitory activity of Iranian plant extracts on growth and biofilm formation by *Pseudomonas aeruginosa*. *Malaysian J Microbiol*., **9(2):**176-183.

Mathur T, Singhal S, Khan S, Upadhyay DJ, Fatma T and Rattan A. 2006. Detection of biofilm formation among the clinical isolates of Staphylococci: an evaluation of three different screening methods. *Indian J Med Microbiol.*, **24(1):**25-29.

Mavrodi DV, Bonsall RF, Delaney SM, Soule MJ, Phillips G and Thomashow LS. 2001. Functional analysis of genes for biosynthesis of pyocyanin and phenazine-1-carboxamide from *Pseudomonas aeruginosa* PAO1. *J Bacteriol*., **183(21):** 6454-6465.

Moazami-Goudarzi S and Eftekhar F. 2013. Assessment of carbapenem susceptibility and multidrug-resistance in *Pseudomonas aeruginosa* burn isolates in Tehran. *Jundishapur J Microbiol.*, **6(2):**162-165.

Nikokar I, Tishayar A, Flakiyan Z, Alijani K, Rehana-Banisaeed S, Hossinpour M, Alvaei SA and Araghian A. 2013. Antibiotic resistance and frequency of class 1 integrons among *Pseudomonas aeruginosa*, isolated from burn patients in Guilan, Iran. *Iranian J Microbiol.*, **5(1):** 36-41.

Perez LR, Costa MC, Freitas AL and Barth AL. 2011. Evaluation of biofilm production by *Pseudomonas aeruginosa* isolates recovered from cystic fibrosis and non-cystic fibrosis patients. *Braz J Microbiol*., **42(2):**476–9.

Rada B and Leto TL. 2013. Pyocyanin effects on respiratory epithelium: relevance in *Pseudomonas aeruginosa* airway infections. *Trends Microbiol.*, **21(2):** 73–81.

Ran H, Hassett DJ and Lau GW. 2003. Human targets of *Pseudomonas aeruginosa* pyocyanin. *Proc Natl Acad Sci* , **100(24):** 14315-14320.

Samira H and Fereshteh E. 2015. Biofilm Formation and β-Lactamase Production in Burn Isolates of *Pseudomonas aeruginosa. J Jundishapur Microbiol.*, **8(3):**1-5.

Wilson R, Pitt T, Taylor G, Watson D, MacDermot J, Sykes D, *et al.* 1987. Pyocyanin and 1-hydroxy phenazine produced by *Pseudomonas aeruginosa* inhibit the beating of human respiratory cilia *in vitro*. *J Clin Invest.*, **79(1):** 221-229.

Wozniak DJ, Wyckoff TJ, Starkey M, Keyser R, Azadi P, O'Toole GA, *et al*. 2003. Alginate is not a significant component of the extracellular polysaccharide matrix of PA14 and PAO1 *Pseudomonas aeruginosa* biofilms. *Proc Natl Acad Sci.,* **100 (13)**:7907–7912.

Zahraa AK. 2016. The Effect of Gamma Rays on Multidrug Resistant Bacteria Isolated from Hospitals. AL- Mustansiriya University, Baghdad, Iraq. Msc.Thesis.

JJBS

Volume 12, Number 1,March 2019
ISSN 1995-6673
Pages 37 - 41

Jordan Journal of Biological Sciences

In- vitro Phytotoxic Effects of Cadmium on Morphological Parameters of *Allium cepa*

Nidhi Didwania*, Swati Jain and Deepti Sadana

Department of Biotechnology, Faculty of Engineering and Technology, Manav Rachna International Institute of Research and Studies, Haryana, -121004- India

Received February 23, 2018; Revised June 14, 2018; Accepted July 7, 2018

Abstract

The aim of this study is to investigate the phytotoxic effects of Cadmium (Cd) on germination and the early seedling growth of *Allium cepa* in the Faridabad district, India. The cadmium poses a major threat to agriculture and human health. Seeds of three different onion cultivars were exposed to five different Cd concentrations (20; 40; 60; 80 and 100 ppm). The germination percentage, germination index and growth parameters such as plumule and radical growth were compared to the untreated seeds. The inhibitory effects on the germination of onion seedlings and the inhibition was observed at 80 ppm and 100 ppm. The increased concentration of cadmium is directly proportional to the inhibitory effects on the seedling germination, and the root and shoot length of *Allium.* Pusa Ridhi performed better under Cd stress, while Pusa Madhavi had poor performance. Later, there had been a maximum decrease in seedling length (3.97 %), germination percentage (53.33 %) and the germination index (1.353%) at 100 ppm. Tolerance index varied among the onion cultivars; maximum tolerance index was observed in Pusa Ridhi followed by Pusa Red and Pusa Madhavi. From these results, it is evident that Pusa Ridhi could germinate effectively in soils contaminated with Cd, however, further studies are needed to signify its effects on the growth and yield of onions.

Keywords: Onion, Agriculture, Germination index, Tolerance index, Germination percentage.

1. Introduction

Onions are of great importance among the staple food, and are consumed worldwide as part of daily diets. Common red onion (*Allium cepa L.*) is a vegetable crop of great economic importance cultivated globally (Mogren *et al.,* 2007). Heavy metals, such as cadmium, are the most significant threat to plant organisms. Cadmium is an unessential heavy metal, but it poses threats and can have a series of harmful effects when taken in excess by a plant (Guo *et al.,* 2016). Also, the quick absorption of cadmium via roots can lead to a high rate of accumulation of cadmium in the plant tissues (Shah *et al.,* 2017). Cadmium present in soil can inhibit plants metabolism, and cause significant retardation in their growth **(**Luo *et al.,* 1998). The earth's biosphere is distinctly affected by heavy metal contamination. Depending upon the origin of the soil, metal concentration in the soil can be less than 1mg/kg or as high as 100,000 mg/kg (Aydinalp, 2009). Rare or noticeable concentration of some heavy metals such as Cadmium (Cd), Chromium (Cr), Copper (Cu), Mercury (Hg), Nickel (Ni) and Zinc (Zn), in the soil has caused harms to the natural and terrestrial ecosystems to a disruptive level. The extent of metal toxicity and sensitivity depends on factors such as the amount or concentration of metal pollution and the period of exposure (Kabir *et al.,* 2008). Heavy metal can pose stress, which causes physiological and biochemical constraints thereby decreasing the plant vigor and inhibiting the plant growth (Subin *et al.,* 2013). As the metal ion accumulates in the roots before the shoots, the roots of a plant are likely to be affected more compared to the shoots of that plant. Thus, Cd toxicity inhibits the plant roots growth (Liu *et al.,* 2003) and affects the root morphology (Daud *et al.,* 2009). It has been reported that cadmium suppress the biosynthesis of chlorophyll, and also targets the function of the photochemical reaction centers (Chugh *et al.,* 1999). Hence, it markedly reduces the chlorophyll content and inhibits leaf photosynthesis. Cadmium can naturally enter air, water, soil and foodstuffs through the weathering of rocks, volcanic eruptions and forest fires. In water, Cd can be found in ionic form or in inorganic complexes. It is obvious that Cd concentrations will be higher in soils being directly treated with Cd -containing fertilizers, sewage sludge, and city waste (Williams *et al.,* 1973). Rapid industrialization has played a major role in exceeding the natural Cd limit to a toxic level. Cd is strongly absorbed by clay materials and organic substances. In this form it accumulates in the upper layers of the soil, while in acid soils this element is transported into the deeper layers due to their weaker absorption. The aim of this study is to determine the influence of Cd at different concentrations on seed germination, germination index and various other physical parameters including root, shoot and seedling length of *Allium cepa*.

* Corresponding author. e-mail: nidhididwania.fet@mriu.edu.in.

2. Materials and Methods

2.1. Plant Material

Healthy seeds of three onion cultivars, namely Pusa Madahvi, Pusa Red and Pusa Ridhi were procured from the Indian Agriculture Research Institute, Pusa, New-Delhi.

2.2. Cadmium Treatment

Cadmium nitrate [$Cd(NO_{3)2.}H_2O$] (98 %) was procured from HiMedia Laborataties Chemicals, India and was used to prepare five cadmium concentrations viz. 20 , 40 , 60 , 80 and 100 ppm along with a control without Cadmium.

2.3. Seed Germination

Seeds of all the three onion cultivars were surface sterilized with 0.1 N $HgCl_2$ solutions for two minutes to prevent fungal infections (Ramasubramanian *et al.,* 1993). The treated Seeds were washed under running water and then with double distilled water for ten minutes. Ten seeds of the selected onion cultivars were placed at an equal distance on a Whatman paper bed with an equal volume (30 mL) of the prepared concentrations of Cd solutions in sterilized petripates. All the petriplates were then covered with Whatman filter paper and to keep them wet with the Cd solution; they were sprinkled with respective Cd solutions. Control was prepared with distilled water sprinkled on Watman filter both at the base and at top of seeds. (Subin *et al.,* 2013).

The seeds were allowed to germinate under a photoperiod of twelve hours at 25 ºC / 18 ºC temperature in an incubator. The research experiments were arranged in CRD-factorial and replicated five times. The seedlings were harvested after two weeks and the germination percentage, germination index, radical length and plumule length were recorded.

2.4. Determination of Plant Parameters

After a two-week exposure, the number of germinated seeds were counted and the seed germination was evaluated to estimate the viability of seeds. (Subin *et al.,* 2013; Stephen, 2009).

The germination percentage (GP) was determined by the method proposed by Stephen (2009) with the formula given below:

GP = Number of germinated seeds/Total number of seeds*100

The data in regard to root and shoot length was measured with the aid of meter rod (Khan *et al.,* 2006).

Seedling height = Mean of root length + Mean of shoot length

Germination index was determined according to the method described by Zhang (2012).

GI = Σ (Gt / Tt), where Gt is estimated as the no. of germinated seeds on Day (t) and Tt is the corresponding time to Gt in days.

Tolerance indices was estimated with the formula (Iqbal *et al.,* 1992):

$$\text{Tolerance indices (T.I)} = \frac{\text{Mean root length in metal solution}}{\text{Mean root length in control}} \times 100$$

2.5. Statistical Analysis

The data were analyzed by one-way analysis of variance (ANOVA) using SPSS (SPSS Inc., USA, version 13.0) to determine the statistical significance of differences among means of treatments (Peralta *et al.,* 2001). Significant differences among the treatments were evaluated at $P < 0.05$.

3. Results

3.1. Effect of Cadmium on Germination of Seeds

Cadmium has inhibitory effects among onion cultivars and drastic effects on the germination of seeds. The suppression of seed germination and germination index was observed above 40 ppm (Table 1). Among the three cultivars, the maximum reduction in the germination percentage and germination index was observed in Pusa Madhavi compared to Pusa Ridhi and Pusa Red. Inhibitory effect was maximum at the highest concentration (Cd-100 ppm). The germination index of Pusa Ridhi was remarkably affected by increasing the Cd concentration.

Table 1. Effect of different concentrations (20 ppm-100 ppm) of Cd on germination percentage (%) and germination index in three onion cultivarsGermination percent (%) Germination index.

Treatment (ppm)	Pusa Madhavi	Pusa Ridhi	Pusa Red	Pusa Madhavi	Pusa Ridhi	Pusa Red
Control	93.33±3.33	96.66±3.33	93.33±3.33	3.060±0.11	3.007±0.16	3.040±0.15
Cd -20	90.00±5.77	90.00±5.77	93.33±3.33	2.877±0.11	2.800±0.15	2.887±0.14
Cd -40	83.33±3.33	90.00±5.77	86.66±6.66	2.487±0.08	2.663±0.06	2.710±0.11
Cd -60	80.00±5.77	86.66±3.33	76.66±3.33	1.677±0.27	2.563±0.06	2.497±0.1
Cd -80	66.66±3.33	73.33±6.66	66.66±3.33	1.933±0.35	2.373±0.1	2.240±0.09
Cd -100	53.33±3.33	60.00±0.00	56.66±3.33	1.353±0.13	1.953±0.12	1.867±0.03

Significant difference at $p<0.05$. Data are mean ± SD. Replicate (n) = 5

3.2. Effect of Cadmium on Root Length, Shoot Length and Seedling Size

The root length, shoot length and seedling size revealed that the cultivars and the Cd concentration were statistically significant (0.05). The data presented indicates that the root length (RL), shoot length (SL) and seedling size (SS) are inversely proportional to the increase in the Cd concentrations.

3.2.1. Root Length

The data presented (Figure 1), indicates a decrease in root length with the increase in the cadmium concentration. The decline in root length ranged from 35 mm (with 20 ppm Cd) to 2.36 mm (with 100 ppm Cd). The root length of Pusa Madhavi was observed to be the least compared to the other onion cultivars. Pusa Ridhi and Pusa Red showed almost equal growth rates in the control, but at a higher concentration of cadmium, Pusa Red was more negatively affected and found to be as sensitive as Pusa Madhavi.

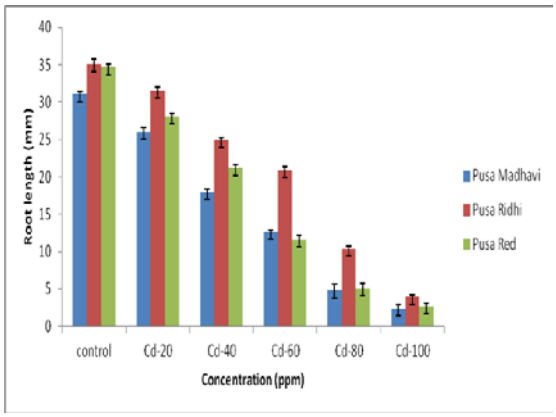

Figure 1. Effect of various Cd concentrations (ppm) on mean root length (mm) of three onion cultivars. Data are mean ± SD. Replicate (n) =5. Vertical bars show Standard error in root lengths.

3.2.2. Shoot Length

The data presented in (Figure 2) indicates the significant effect of cadmium toxicity to the shoot growth of onion seed cultivars. Similar to the case of root growth, Pusa Madhavi had the least growth rate among the three and is most affected by increasing the cadmium concentration. Significant decrease in the shoot growth was observed in all the three cultivars of onion. Shoot length of Pusa Ridhi was observed to be the highest at the concentration of 100 ppm when compared to the control.

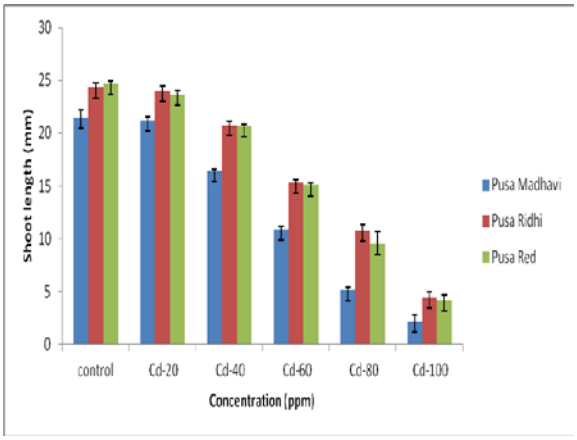

Figure 2. Effect of various Cd concentrations on mean shoot length (mm) of three different onion cultivars. Data are mean ± SD. Replicate (n) = 5. Bars show standard error in shoot length.

3.2.3. Seedling Length

There was an augmented effect of Cd stress on the seedling length as its inhibition was statistically significant compared to control. The seedling height of Pusa Ridhi was observed to be maximum in control and with a further addition of Cd from 20 to 100 ppm, but maximum inhibition occurred at 100 ppm (Figure 3). The seedling length for Pusa Madhavi and Pusa Red was almost the same at a higher concentration.

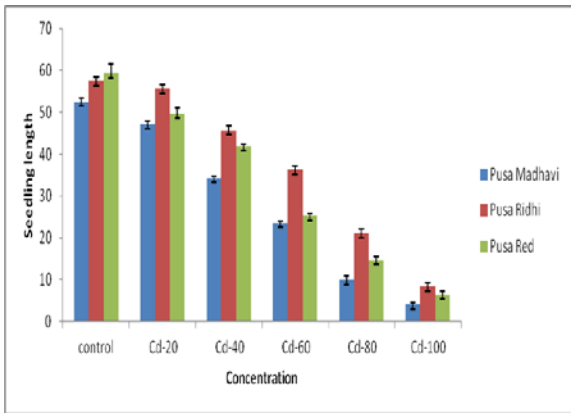

Figure 3. Effect of various Cd concentrations on seedling length (mm) of three different onion cultivars. Data are mean ± SD. Replicate (n) = 5. Bars show standard error in seedling length.

3.2.4. Effect of Cadmium on Tolerance Indices

All three cultivars showed different results in response to varied Cd concentration. Pusa Ridhi is found to be the most tolerant onion cultivar among the three tested. Tolerance of the three onion cultivars decreases in this order, Pusa Ridhi > Pusa Red > Pusa Madhavi (Figure 4).

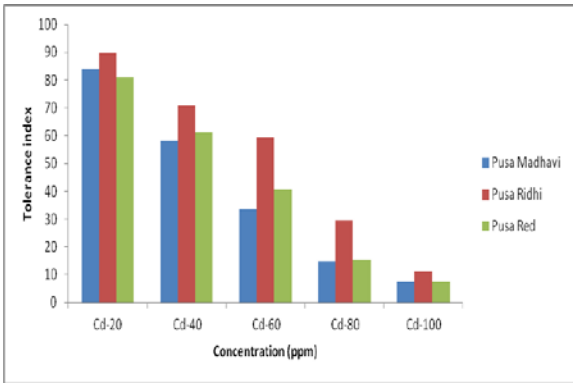

Figure 4. Tolerance indices of different onion cultivars to Cd stress

4. Discussion

The primary objective of this study is to assess the sensitivity of different cultivars of onion towards different cadmium concentrations. Cadmium along with lead and mercury are categorized as non-essential heavy metals as these are potentially toxic to humans. Also, the relative mobility of cadmium into the soil is high. The root system of onions is capable of absorbing cadmium easily from the soil or solution (Heidari *et al.*, 2011).

The growth performance of *Allium cepa* cultivars may have decreased as a result of meristematic cell reduction or hindrance to the functions of hydrolytic enzymes contained in the cotyledon and endosperms due to the toxicity of cadmium (Subin *et al.*, 2013). The mobilization of stored food materials to the plumule and radicle is a function of hydrolytic enzymes. The breakdown of stored food materials in seeds by the application of cadmium can also be one of the reasons for the retarded or inhibited growth (Katarzyna *et al.*, 2015).

Cadmium is detrimental to vegetables, cereals and fruit crops (Ahmad, 2012), and it induces innumerable health hazards in humans (Anon., 2004). Consequently there is an urgent need to determine the toxic level of Cadmium for onion growth. In the present investigation the increased Cadmium concentration resulted in highly significant inhibition of onion seed germination. Adverse effects of cadmium on seed germination determined its phytotoxicity to different rice cultivars due to the genetic diversity of cultivars (Zhang *et al*., 2005).

Similar studies were earlier reported by Raziuddin *et al.*, 2011 on the seedlings of wheat. Cd showed a strong inhibitory effect on the root elongation and coleoptile growth of the evaluated onion cultivars, especially at high cadmium concentrations. The ranges of Cd toxicity to root and shoot length were as follows: 2.36 mm, 2.16 mm for Pusa Madhavi and 3.91 mm, 4.39 mm for Pusa Ridhi respectively, while for Pusa Red the ranges were 2.59 mm and 4.15 mm at 100 ppm. The results are in conformity with Ahmad *et al*., 2011 who stated that the seedling length, root and shoot are effected in *Brassica juncea* due to the presence of high Cd content. This study along with the research of Guo *et al.*, done on three different *Miscanthus* species, reflect the fact that cadmium toxicity varies among genotypes of the same species (Guo *et al*., 2016).

Metal contamination disorganizes the metabolism of plants due to the enzyme interactions which leads to biochemical reactions which effects the seedling length (Ashraf *et al*., 2011). Several Researchers (Unyayar *et al*., 2006 and Shafi *et al*., 2010) reported the sensitivity of plant growth to Cd toxicity. Changes in the physiological mechanism as well the growth phases during germination might have contributed to the low tolerance indices of the different onion cultivars.

5. Conclusions

The current study concludes that root, shoot, seedling elongation and germination index of all the evaluated onion cultivars were observed to be positive indicators of Cd toxicity to onion. Different cultivars showed different adverse effect levels on onion growth indices at low concentrations of Cd, but the maximum inhibition occured at 100 ppm. Tolerance indices for Pusa Madhavi, Pusa Ridhi and Pusa Red were 7.47, 11.4 and 7.61 respectively. Pusa Madhavi is the most sensitive to Cd compared to other evaluated onion cultivars. In contrast, Pusa Ridhi could be well grown on cadmium-contaminated soils compared to others. The accumulation of heavy metals such as Cd in the soil and into the food chains is a worldwide concern. It can have damaging effects on human life and animal life as well.

References

Ahmad I, Akhtar MJ, Zahir ZA and Jamil A. 2012. Effect of cadmium on seed germination of four wheat (*Triticum aestivum* L.) cultivars. *Pak J Bot.*, **44 (5):** 1569-1574.

Ahmad P, Nabi G and Ashraf M. 2011. Cadmium-induced oxidative damage in mustard [*Brassica juncea* (L.) Czern. & Coss.] plants can be alleviated by salicylic acid. *South African J Bot.*, **77(1):** 36-44.

Anon YJ. 2004. Soil ecotoxicity assessment using cadmium sensitive plants. *Environ Pollut*, **127:** 21-26.

Ashraf MY, Sadiq R, Hussain M, Ashraf M and Ahmad MSA. 2011. Toxic effect of nickel (Ni) on growth and metabolism in germinating seeds of sunflower (*Helianthus annuus L.*)- *Biol Trace Elem Res*., **143**: 1695- 1703.

Aydinalp C. 2009. Concentration and speciation of Cu, Ni, Pb and Zn in cultivated and uncultivated soils. *Bulgarian J Agri Sci.*, **15 (2)** : 129-134.

Chugh LK and Sawhney SK. 1999. Photosynthetic activities of *Pisum sativum* seedlings grown in presence of cadmium. *Plant Physiol Biochem*, **37**: 297-303.

Daud MK, Sun YQ, Dawood M, Hayat Y, Variath MT, Wu YX, Raziuddin, Mishkat U, Salahuddin Najeeb U and Zhu SJ. 2009. Cadmium-induced functional and ultrastructural alterations in roots of two transgenic cotton cultivars. *J Hazard Mater*, **168**: 614-625.

Guo H, Hong C, Chen X, Xu Y, Liu Y, Dean J and Zheng B. 2016. Different growth and physiological responses to Cadmium of the three *Miscanthus* species, *PLoS ONE*. **11(4):** e0153475

Heidari M and Sarani S. 2011. Effects of lead and cadmium on seed germination, seedling growth and antioxidant enzymes activities of Mustard (*Sinapis arvensis L.*) ARPN. *J Agri Biol Sci.*, **6(1):** 44-47.

Iqbal MZ and Rahmati K. 1992. Tolerance of *Albizia lebbeck* to Cu and Fe application. *Ekologia (CSFR)*, **11**: 427-430.

Kabir M, Iqbal MZ, Shafiq M and Farooqi ZR. 2008. Reduction in germination and seedling growth of *Thespesia populnea l.*, caused by lead and cadmium treatments. *Pak J Bot.*, **40**: 2419-2426.

Katarzyna S, Klaudia K, Jakub W and Urszula P. 2017.Evaluation of cadmium, lead, zinc and copper levels in selected ecological cereal food products and their non-ecological counterparts. *Current Issues in Pharm Medical Sci*., **30** (3); 147-150.

Khan NA, Ahmad I, Singh S and Nazar R. 2006. Variation in growth, photosynthesis and yield of five wheat cultivars exposed to cadmium stress. *World J Agri Sci.*, **2:** 223-226.

Liu J, Li K, Xu J, Liang J, Lu X, Yang J and Zhu Q. 2003. Interaction of Cd and five mineral nutrients for uptake and accumulation in different rice cultivars and genotype. *Field Crops Res*, **83**: 271-281.

Luo LX, Sun TH and Jin YH. 1998. Accumulation of superoxide radical in wheat leaves under cadmium stress. *Acta Sci Circum.*, **18**: 495–499.

Mogren LM, Olsson ME and Gertsson UE. 2007. Effects of cultivar, lifting time and nitrogen fertiliser level on quercetin content in onion (*Allium cepa L.*) at lifting. *J Sci Food Agri.*, **87**: 470-476.

Peralta JR, Torresdey JLG, Tiemann KJ, Gómez E, Arteaga S, Rascon E and Parsons JG. 2001. Study of the effects of heavy metals on seed germination and plant growth on Alfalfa plant (*Medicago sativa*) grown in solid media. *Bull Environ Contam Toxicol*, **66**:727.

Ramasubramanian V, Kannan N and Ravichandran V. 1993. Communications in soil science and plant analysis. *J Comm Soil Sci Plant Analysis*, **24**: 2241-2249.

Raziuddin, Farhatullah, Hassan G, Akmal M, Shah SS, Mohammad F, Shafi M, Bakht J and Zhou W. 2011. Effects of cadmium and salinity on growth and photosynthesis parameters of brassica species. *Pak J Bot*, **43(1):** 333-340.

Shafi M, Zhang GP, Bakht J, Khan MA, Islam E, Dawood MK and Raziuddin. 2010. Effect of cadmium and salinity stresses on root morphology of wheat. *Pak J Bot.*, **42(4):** 2747-2754.

Shah K, Mankad AU and Reddy MN. 2017. Cadmium accumulation and its effects on growth and biochemical parameters in *Tagetes erecta L, J Pharmacog Phytochem*., **6(3):** 111-115

Stephen, G S. 2009 Primer on Seed Germination, https://employees.csbsju.edu/ssaupe/biol327/Lab/Seeds/ germination _percentage.htm, (01/07/2009).

Subin MP and Francis S. 2013. Phytotoxic effects of cadmium on seed germination, early seedling growth and antioxidant enzyme activities in *Cucurbita maxima* Duchesne. *Inter Res J Biol Sci*., **2(9)**: 40-47.

Unyayar S, Celik A, Cekic FO and Gozel A. 2006. Cadmium-induced genotoxicity, cytotoxicity and lipid peroxidation in *Allium sativum* and *Vicia faba*. *Mutagenesis*, **21**: 77–81.

Williams CH, David DJ and Aust J. 1973. The effect of superphosphate on cadmium content of soils and plants. *Soil Res.*, **11**: 43-56.

Zhang H 2012. Seed germination and early seedling growth of *Cynanchum bungei* Decne (*Asclepiadaceae*) in response to photoperiod, temperature and seed size. *Hortsci.*, **47(9):** 1338–1341.

Zhang S, Hu J, Chen ZH, Chen JF, Zheng YY and Song WJ. 2005. Effects of Pb pollution on seed vigor of three rice cultivars. *Rice Sci*., **12**: 197-202.

JJBS

Volume 12, Number 1,March 2019
ISSN 1995-6673
Pages 43 - 48

Jordan Journal of Biological Sciences

Investigating the Antimicrobial Potential of *in- vitro* Grown Microshoots and Callus Cultures of *Ammi visnaga* (L.) Lam.

Majd M. Al-Saleh[1], Rida A. Shibli[1*], Hamzah M. Al-Qadiri[2], Reham W. Tahtamouni[3], Maysaa M. Darwish[4] and Tamara S. Al- Qudah[1]

[1] *Hamdi Mango Center for Scientific Research (HMCSR),*[2]*Department of Nutrition and Food Technology, School of Agriculture, University of Jordan,* [3]*Department of Applied and Social Sciences, Princess Alia University College, Al-Balqa Applied University,* [4]*National Center for Agriculture Research and Extension, Amman, Jordan*.

Received May 9, 2018; Revised July 1, 2018; Accepted July 10, 2018

Abstract

Ammi visnaga (L.) Lam is a valuable herbal plant that is frequently collected for medicinal purposes. This study is conducted to evaluate the antimicrobial potential of the *in-vitro* grown microshoots and callus cultures of this plant against selected strains of bacteria and fungi. Shoot multiplication was obtained in MS medium containing 0.5 mg/L BA + 0.1 mg/L NAA, while callus multiplication was performed on MS medium containing 1.0 mg/L BA + 2.0 mg/L 2,4-D under light conditions. The aqueous and methanolic extracts were prepared from both culture types in addition to *in-vivo* grown plant material to experiment their antimicrobial activities. Generally, the *in-vitro* extracts of the microshoots and the callus cultures acted best against bacteria compared to the field plant extract. Moreover, the methanolic extracts were generally found to exhibit far better results and resistance against the tested microbes than the aqueous extracts. *C. albicans* was the most sensitive species to the microshoots extracts followed by gram-positive bacteria at MIC values of (3.125, 6.25) mg/mL. Meanwhile, *E. coli* bacteria were most sensitive to the microshoot extracts as they were completely inhibited at MIC value of (0.78 mg/mL). Moreover, the results of the callus extracts showed that *C. albicans* was the most sensitive at MIC values of (1.56 and 3.125) mg/mL, followed by gram-positive bacteria. On the other hand, gram-negative bacteria were the most resistant microbes to all experimented extract types in this study.

Keywords: *Ammi visnaga* , Antimicrobial activities, Callus, Microshoots

1. Introduction

Ammi visnaga (L.) Lam is a herbaceous medicinal plant which belongs to the family *Apiaceae*. It is found mainly in the Mediterranean regions, and is also distributed abundantly throughout the world as an introduced species. *A. visnaga* (L.) Lam is used frequently in many countries as a herbal medicine for different purposes. Ancient records revealed various medicinal properties of this plant as a popular source to cure a variety of different ailments (Hashim, *et al*., 2014).

Phytochemical studies on *Ammi visnaga* revealed the diversity of its chemical constituents, as they comprise several groups each with several compounds. The most important one includes Khellin (0.3-1.2 %) from the furanochromones group (2-4 %) (Hammouda *et al.*, 2005; WHO, 2007; Sellami *et al*., 2013; Hashim *et al.*, 2014; Talaat, *et al*., 2014). It is worth mentioning that, furanochromones particularly visnagin, khellin, and khellol-glucoside are exclusively extracted from two species only, which are *A. visnaga* (L.) Lam (*Umbelliferae*) and *Eranthis hyemalis* L. (*Ranunculaceae*) (Kaul and Staba, 1967; El-Fiky *et al*., 1989).

Habitat destruction as a result of population growth, urbanization and uncontrolled collection caused overexploitation of wild plants particularly medicinal plants (Al-Quran, 2011). Moreover, about 90 % of the natural resources used by industries are collected from wild plants. This is due to the difference in price between the wild and cultivated plants, which could explain the lack of favorable plant materials, or to the high demands for the wild materials, which resulted, in turn, in the destruction of medicinal plants. Therefore, it has become an urgent matter to take legal measures and establish a compact program for the sake of saving all medicinal plants (Craker, 2007; Sharma *et al.*, 2010; Tahtamouni, *et al*., 2015).

The recent development in biotechnology particularly in the techniques of plant tissue culture have come as a boon to cope up with this alarming situation and to overcome these problems through the rapid micropropagation method in order to save the natural herbal wealth (Sridhar and Aswath, 2014).

Initially, plant tissue culture was exploited as a research tool and was focused on attempts to culture and study the development of small, isolated segments of plant tissues or isolated cells. Plant tissue culture is now a well-established

* Corresponding author. e-mail: r.shibli@ju.edu.jo.

technology. Like many other technologies, it has gone through different stages of evolution; scientific curiosity, research tool, novel applications and mass exploitation (Idowu *et al.*, 2009).

Although the discovery of antibiotics was a turning point that revolutionized medicine in human history (Davies and Davies, 2010), the uncontrolled use of antibiotics in addition to the their side effects on human health led to an imperative necessity to find therapeutic alternates such as semisynthetic antibiotics (Be´rdy, 2012), or plant-derived antimicrobials (Upadhyay *et al.*, 2014). More than a quarter of the modern medicines are derived from medicinal plants either directly or indirectly through the new technology applications of folk knowledge. This percentage can reach 60 % in the case of antitumoral and antimicrobial pharmaceuticals (WHO, 2011).

Several researches have been conducted recently for the extraction of vital substances and secondary metabolites from *A. visnaga* (L.) Lam which reveals the importance of this valuable plant (Al-Snafi, 2013; Hashim *et al.*, 2014). In addition to its traditional importance in preventing or decreasing kidney stone formation in human patients, and its recent scientific importance against bronchial asthma and coronary diseases which are attributed to its essential oils (Rose and Hulburd, 1992; Satrani *et. al.*, 2004), *Ammi visnaga* can be used as antitumoral (Beltagy and Beltagy, 2015) and is considered as a good antifungal and antimicrobial agent against both gram-positive and gram-negative bacteria (Rasooli *et al.*, 2007; Dababneh, 2008; Ghareeb, *et al*., 2011; Khalfallah *et al*., 2011; Mahmood, 2014; Sabry *et al*., 2014; Jaradat *et al*., 2015).

Accordingly, this study is conducted to investigate the antimicrobial potential of the *in- vitro* grown microshoots and callus cultures of *Ammi visnaga* as they contain a wide array of chemical constitutes reported to be active against some strains of bacteria and fungi

2. Material and Methods

2.1. Khellin Test

As mentioned earlier, khellin is a furanochromone and is exclusively extracted from two species which are *Ammi visnaga* (L.) Lam (*Apiaceae*) and *Eranthis hyemalis* L. (*Ranunculaceae*) (Kaul and Staba, 1967; El-Fiky, *et al*., 1989). Due to the high similarity between *Ammi visnaga* (L.) Lam and *Ammi majus* L seeds, the plant material was identified by the taxonomist, Professor Ahmad Aloqla from the Biology Department at Yarmouk University, Irbid, Jordan, using the Khellin test. This was very essential for the current research, as the tissue cultured plant material (microshoots and callus) used in our experiments were started initially *in-vitro* from the seeds and by applying the Khellin test this would make sure that the starting plant material (seeds) is true to its name.

The *Ammi visnaga* (L.) Lam seeds were bought from the market while the *Ammi majus* seeds were brought from the National Center for Agricultural Research and Extension (NCARE) in Amman, Jordan.

The seeds were dried, powdered, sieved and 2.0 g was weighed for extraction and added to a 20 ml of ethanol solvent for two days in an incubator under continuous shaking, where the shaker was adjusted to room temperature with 200 rpm. Then the alcoholic extract was filtered using vacuum buchner funnels, and was concentrated in a rotary thin-film evaporator and stored in a refrigerator in a stand manner to precipitate for a few days until the formation of three layers: an upper oily layer removed by filtration with a gentle suction and a middle cream, a fatty layer removed by the help of petroleum ether and a lower green crystalline layer from where pure khellin was obtained. The extracted khellin was checked based on the fact that mixing 5-8 mg of khellin with a small piece of solid NaOH will produce a distinct rose-red color (Barakat, And Badran, 1951; Hassan and Zubair, 1980; Kar, 2003).

2.2. In-Vitro Multiplication

2.2.1. In-vitro Multiplication of Microshoot and Callus Cultures

Preliminary experiments were conducted for the *in-vitro* establishment and multiplication of microshoots and callus cultures. The best multiplication rate for the microshoots was obtained in MS medium (Murashige and Skoog, 1962) containing 0.5 mg/L BA in combination with 0.1 mg/L NAA, while the callus multiplication was best in MS medium containing 1.0 mg/L BA in combination with 2.0 mg/L 2,4-D under light condition. To obtain the recommended mother stock for the present experiment, the microshoots (microshoot about 2.0 cm long and each flask contained four microshoots) and callus clumps (clump weight=0.5 g, with four clumps in each Petri dish) underwent five subculturing intervals (four weeks/interval).

2.3. Antimicrobial Effect

2.3.1. Crude Extraction

An aqueous extract of field and *in-vitro* grown plant material was prepared by stirring 4 g of previously dried plant powder with 40 ml of sterilized distilled water, while 1 g of the dried plant powder was added to 10 mL 100 % of a methanol solvent for the methanolic extract preparation. Both types of the extracts were left two days at 25°C with continuous shaking at the incubator shaker adjusted at 200 rpm. This was followed by centrifugation at 2000 g for ten minutes and the resulted supernatant was concentrated by complete solvent evaporation under vacuum using a rotary evaporator device, and was finally stored in sterile falcon tubes in a refrigerator at 4°C after being dissolved with dimethyl sulphoxide (DMSO) to reach the 100 mg/ml stock for each extract and was sterilized by a syringe filter with 0.45 µm pore size (Jaradat *et al*., 2015).

2.3.2. Antibacterial and Antifungal Activity of the Extracts.

Selected microbial strains were obtained from the Hamdi Mango Center for Scientific Researches (HMCSR). In this study, gram-negative bacteria *Escherichia coli* (American Type Culture Collection) ATCC 10536, *Klebsiella pneumonia* ATCC (31488) and gram-positive bacteria *Staphylococcus aureus* ATCC 6538, *Bacillus subtilis* ATCC (6633), and a species of fungi called *Candida albicans* ATCC (10231) were used to study the antimicrobial activity of these extracts.

Bacterial strains were cultured by streaking onto a solid nutrient agar (NA), while the fungi strain was cultured on a potato dextrose agar. The cultured Petri dishes were, then, kept in an incubator overnight at 37˚ C for twenty-four hours. For the antimicrobial microdilution assay, the Muller Hinton broth and potato dextrose broth were used for the bacteria and yeast respectively .

2.3.3. Microdilution Assay

The plant extract solutions were serially diluted (2-fold) ten times with Muller Hinton, potato dextrose broth. Well number eleven was considered negative control of bacterial growth, while well number twelve contained nutrient broth only and was used for positive control of bacterial growth. The achieved ten concentrations of the methanolic and aqueous plant extracts were from (50) to (0.098) mg/mL. A serial two-fold dilution of DMSO with Muller Hinton or potato dextrose broth was prepared to ensure that the antimicrobial activity was not from DMSO. Moreover, the blank or the back ground were two-fold dilution for each extract with broth. The final bacterial concentration in each well (except positive control) was adjusted to 0.75×10^6 CFU/mL. After the inoculation of bacteria, the plates were covered and incubated overnight at 37˚C for twenty-four hours. The plates were then scanned with an enzyme-linked immunosorbent assay (ELISA) reader at 600 Nano mole (nm) to examine the bacterial density (Karaman *et al*., 2003) and at 405 nm to examine the yeast density (Scorzoni *et al*., 2007). The lowest concentration of the plant extract that did not allow any visible microbial growth in the test broth was considered the minimal inhibitory concentration (MIC) (Jorgensen and Ferraro, 2009; Jaradat *et al*., 2015).

3. Results

3.1. Khellin Test

A red-rose color was obtained through the interaction between khellin and NaOH which revealed a positive result from the *A. visnaga* (L.) Lam seeds ethanolic extract, while negative results were obtained from the *A. majus* extracts as no changes in the NaOH color occurred (Figure 1). Hence, this proves that this species is *Ammi visnaga* (L.) Lam.

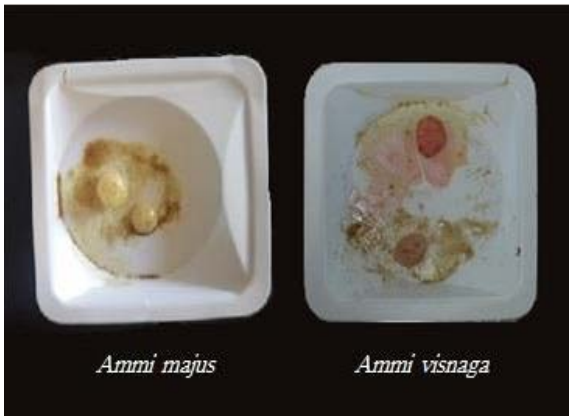

Figure 1. Khellin test experimented on *A. visnaga* (L.) Lam and *A. majus* seeds ethanolic extracts.

3.2. Antimicrobial Activity

3.2.1. Microshoots Extract

The results showed that both *A. visnaga* (L.) Lam *(in-vitro* microshoots and the field- collected plants) extracts possessed an antimicrobial activity against the tested bacterial and yeast strains; both types of the plant extract either aqueous or methanolic had a negative impact on the antimicrobial activities.

The aqueous extract of *A. visnaga* (L.) Lam at the level of 6.25 mg/mL was most effective against *E. coli*, while a concentration of 3.125 mg/mL was predominantly effective using the methanolic extracts (Figures 2 and 3). However the lowest MIC against *E. coli* were (0.78, 1.56 mg/mL) in the microshoots of methanolic and aqueous extracts respectively, while higher concentrations (12.50, 6.25 mg/mL) were needed to cause the inhibition of the microbes by the aqueous and methanolic extractions respectively in the field-collected shoot as shown in (Figures 2 and 3).

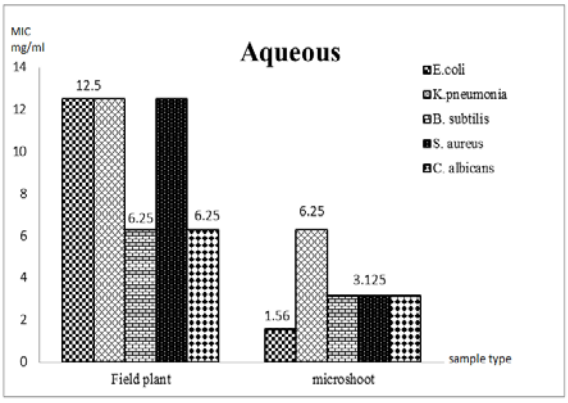

Figure 2. MIC values in mg/mL of aqueous *Ammi visnaga* extracts.

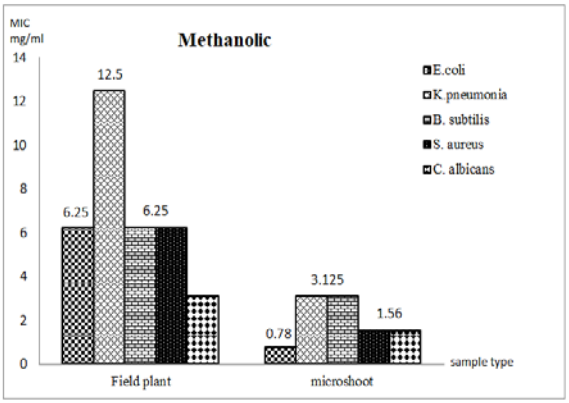

Figure 3. MIC values in mg/mL of methanolic *Ammi visnaga* microshoots extracts.

Similar finding were observed regarding the effect of different extracts against *K. pneumonia*, in which the predominantly effective concentrations of methanolic and aqueous extracts were 3.125, 6.25 mg/mL respectively, while the higher MIC (12.50 mg/mL) was obtained by both the methanolic and aqueous extracts of the *in-vivo* plant as shown in (Figures 2 and 3).

On the other hand, both methanolic and aqueous extracts have MIC of (3.125 mg/mL) against *B. subtilis*, and the *in- vivo* extract had the lowest efficacy (6.25

mg/mL) against this microbe as shown in (Figures 2 and 3). Interestingly, *S. aureus* was sensitive to the methanolic extracts even at low concentrations, in which the lowest activity was obtained by the field plant material extraction at a 6.25 mg/mL concentration, while *S. aureus* was less sensitive against the aqueous extracts in which the predominant effective concentration was (3.125 mg/mL) (Figures 2 and 3).

Regarding *C. albicans*, this could be the most sensitive microbial strain in this study because almost all inhibition concentrations ranged between 1.56 and 3.125 mg/mL, and only the aqueous field plant extract extract had 6.25 mg/mL MIC as shown in (Figures 2 and 3).

3.2.2. Callus Extracts

The current results showed that all *A. visnaga* (L.) Lam extracts regardless of their sources (*in vitro* calli and field-collected plants) whether (aqueous or methanolic) had an antimicrobial impact against the tested bacterial and yeast strains (Figures 4 and 5). As observed from the *A. visnaga* (L.) Lam aqueous extracts, a concentration of 6.25 mg/mL was the predominant effective concentration against *E. coli*, while a concentration of 3.125 mg/mL was the predominant effective using methanolic extracts (Figures 4 and 5). However, the lowest MIC against *E. coli* was (1.56 mg/mL) when using the methanolic control callus extract grown under light conditions, while higher concentrations (12.50, 6.25 mg/mL) were needed to cause inhibition by the aqueous and methanolic extractions respectively of the field-collected shoot as shown in (Figures 4 and 5). Similar findings were observed regarding the effect of different extracts against *K. pneumonia* in the current study, in which the predominant effective concentrations of methanolic and aqueous extracts were 3.125, 6.25 mg/mL respectively, Meanwhile, the higher MIC (12.50 mg/mL) obtained by both the methanolic and aqueous extracts of *in-vivo* plant as shown in (Figures 4 and 5).

Interestingly, *B. subtilis* was sensitive to the methanolic extracts even at low concentrations, in which the lowest activity was obtained by *in-vivo* plant material extraction at a 6.25 mg/mL concentration, while *B. subtilis* was less sensitive against the aqueous extracts in which the predominant effective concentration was (3.125 mg/mL) (Figures 4 and 5). On the other hand, both the methanolic and aqueous extracts have an MIC of (3.125, 6.25 mg/mL) respectively against *S. aureus*; only the *in-vivo* aqueous extract showed the lowest efficacy (12.5 mg/mL) against this microbe as shown in (Figures 4 and 5).

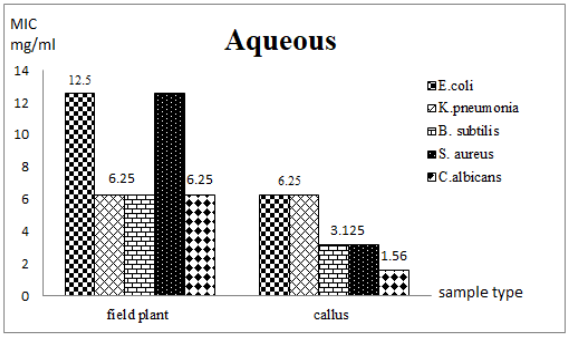

Figure 4. MIC values in mg/mL of *Ammi visnaga* (L.) Lam aqueous callus extracts.

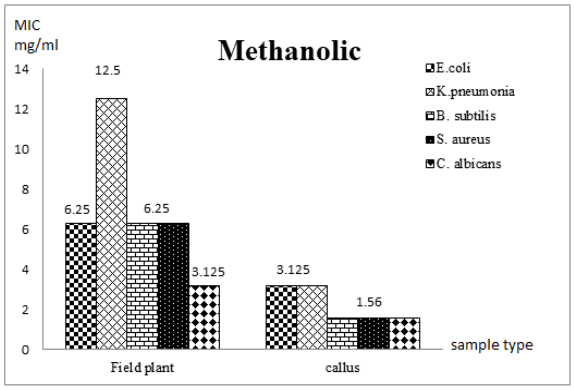

Figure 5. MIC values in mg/mL of *Ammi visnaga* (L.) Lam methanolic callus extracts

Regarding *C. albicans*, this could be the most sensitive microbial strain in this study where almost all inhibition concentrations ranged between 1.56 and 3.125 mg/mL; only the aqueous *in-vivo* extract had a 6.25 mg/mL MIC as shown in (Figures 4 and 5).

4. Discussion

It is evident from the aforementioned results that, the *in-vitro* extract concentrations of *A. visnaga* (L.) Lam exhibited far better results and resistance against both bacteria and fungi, hence it can be said that the *in-vitro* extracts possess greater antimicrobial activity compared to the field plant extracts. According to the Gobbo-Neto and Lopes (2007), the reason behind this may be that the plant secondary metabolites produced *in-vitro* are highly affected by the surrounding conditions including type and levels of growth regulators added to the media. Such findings were reported concerning many medicinally-important plants by several authors. For example, Barboza *et al.*, (2015) worked on *Anonna mucosa* (Jacq.), and Rasool *et al*., (2010) worked on *Prunella vulgaris* L., and both studies found out that biotechnological plant materials have the antibacterial properties similar to the *in-vivo* grown plants. Meanwhile, Kinyamasyo *et al*., 2014 and ElNour *et al*., (2015) revealed following a phytochemical screening of the seeds and callus extracts of *Nigella sativa* L and the plant material of *Aloe secundiflora* that the presence of secondary metabolites in such tested extracts may be responsible for their antimicrobial activity. Moreover, ElNour *et al*. (2015) results showed that the antimicrobial activities of the callus extracts of *Nigella sativa* L against *E. coli* were stronger than those of gentamicin and penicillin.

Moreover, the current study revealed that both the methanolic and aqueous extracts showed an antimicrobial activity against gram-positive and gram-negative bacteria as well as the studied fungi *C. albicans*. The methanolic extracts were as strong as or even more effective than the aqueous extracts, which may be related to the solubility of *A. visnaga* (L.) Lam active ingredients in organic solvents. This is similar to recent researches on *A. visnaga* (L.) Lam extracts conducted by (Ghareeb *et al*., 2011; Al-Snafi, 2015; Jaradat *et al*., 2015) who proved the antimicrobial efficacy of this valuable plant against the studied microbes, and showed an increase in the antimicrobial activity in the methanolic extracts .

Also, it can be noted that gram-positive bacteria were affected by the *A. visnaga's* extracts more than gram-negative ones; this susceptibility differences may be due to cell membrane structural differences between these classes of bacteria. Particularly speaking, the outer membrane permeability barrier protects the gram-negative bacteria (Rasool *et al*., 2010).

5. Conclusion

The results of the current study show that both extracts of the cultured tissue and the field grown *Ammi visnaga* (L.) Lam plant material could be useful in the development of new, alternative, and cheap antimicrobial drugs, particularly, against infections caused by these tested microbes. However, the obtained data revealed that the *in-vitro* extracts of the microshoots and the callus cultures gave the best antimicrobial results compared to those obtained by the field plant extract based on MIC values. Also, the present work clearly shows that the methanolic extracts exhibited far better results and resistance against the tested microbes. This finding may be attributed to the solubility of the active components of this plant in organic solvents.

References

Al-Quran S. 2011. Conservation of medicinal plants in Ajlun woodland -Jordan. *J Med Plants Res.*, **5 (24):** 5857-5862.

Al-Snafi A. 2013. Chemical constitute and pharmacological activities of *Ammi majus* and *Ammi visnaga*. A review. *IJPIR*, **3 (3):** 257-265.

Al-Snafi A.E. 2015. Therapeutic properties of medicinal plants: a review of their antibacterial activity (part 1). *IJPT*, **6 (3):** 137-158.

Barakat MZ and Badran N. 1951. New tests for the identification of khellin, visnagin and khellol-glucoside. *J Pharm Pharmacol*, **3 (1):** 576–580.

Barboza T J S, Ferreira A F, Ignacio ACPR and Albarello N. 2015. Antimicrobial activity of *Anonna mucosa* (Jacq.) grown *in vivo* and obtained by *in vitro* culture. *Braz J Microbiol*, **46 (3):** 785-789.

Be´rdy J. 2012. Thoughts and facts about antibiotics: Where we are now and where we are heading. *J Antibiot*, **65**: 385-395.

Beltagy A and Beltagy D. 2015. Chemical composition of *Ammi visnaga* l. and new cytotoxic activity of its constituents khellin and visnagin. *Int J Pharm Sci Res.*, **7 (6):** 285-291.

Craker L E. 2007. **Medicinal and Aromatic Plants—Future Opportunities**, *Issues in New Crops and New Uses*, 248-257.

Davies J and Davies D. 2010. Origins and evolution of antibiotic resistance. *Microbiol Mol Biol Rev.*, **74 (3):** 417-433.

Debnath M. 2008. Clonal propagation and antimicrobial activity of an endemic medicinal plant *Stevia rebaudiana. J. Med. Plants Res.*, **2 (2):** 045-051.

El-Fiky F K, Remmel R P and Staba E J. 1989. *Ammi visnaga*: Somatic embryo induction and furanochromone production in embryos, seedlings, and plants. *Planta Med.*, **55 (5)**: 446-451.

ElNour MEM, Ali AMA and Saeed BAT. 2015. Effect of different concentrations of auxins and combination with kinetin on callus initiation of *Trigonella foenum- graecum*.L. *Int J Eng Res Appl.*, **3 (2):** 117-122.

Ghareeb A, Zedan T and Gharb L. 2011. Antibacterial and antifungal activities of *Ammi visnaga* extracts against pathogenic microorganisms. *Iraqi J Sci.*, **52 (1):** 30-36.

Gobbo-Neto L and Lopes NP. 2007. Medicinal plants: factors of influence on the content of secondary metabolites. *Química Nova*, **30 (2):** 374-381.

Hammouda F M, Ismail S I, Abdel-Azim N S and Shams K A. 2005. *Ammi visnaga* (L.). In: Batanouny K H.(Ed), **A Guide to Medicinal Plants in North Africa, Malaga** : IUCN Center for Mediterranean Cooperation.

Hashim S, Jan A, Marwat K and Khan M. 2014. Phytochemistry and medicinal properties of *Ammi visnaga* (*apiacae*). *Pak J Bot*., **46 (3):** 861-867.

Hassan MA and Zubair MU. 1980. **Analytical Profiles of Drug Substances**. (9th volume), United Kingdome, London: Academic press. 371-374.

Idowu A,Ibitoye D and Ademoyegun O. 2009. Tissue culture as a plant production technique for horticultural crops. *Afr. J. Biotechnol.*, **8 (16):** 3782-3788.

Jaradat N, Abualhasan M, Al-Masri M, Speih R, Johari M and Awad M. 2015. phytochemical screening and *in-vitro* evaluation of antioxidant and antimicrobial activities of the entire khella plant (*Ammi visnaga* L.) a member of Palestinian flora. *J Pharmacogn Phytochem.*, **7 (1):** 137-143.

Jorgensen J and Ferraro M. 2009. Antimicrobial susceptibility testing: a review of general principles and contemporary practices. *J Med Microbiol.*, **49:** 1749-55.

Kar A. 2003. **Pharmacognosy and Pharmacobiotechnology,** New Delhi: New age international**.** 637-640.

Karamana I, Sahin F, Güllüce M, Ögütçü H, Sengül M and Adıgüzel A. 2003. Antimicrobial activity of aqueous and methanol extracts of *Juniperus oxycedrus* L. *J Ethnopharmacol.*, **85:** 231-235.

Kau1 B and Staba E. J. 1967. *Ammi visnaga* (L) Lam. tissue cultures multi-liter suspension growth and examination for furanochromones. *Plant Tissue Cult.*, **15 (2):** 145-156.

Khalfallah A, Labed A, Semra Z, Kaki B, Kabouche A, Touzani R and Kabouche R. 2011. Antibacterial activity and chemical composition of the essential oil of *Ammi visnaga* (L.) (*Apiacae*). From Constantine, Algeria. *IJMAP*, **1 (3):** 302-305.

Kinyamasyo E M, Mwagandi CL, Kaingu FB and Gicharu GK. 2014. *In vitro* analysis of antibacterial and antifungal potency of tissue cultured and indigenous *Aloe secundiflora* plant extracts. *JAES*, **3 (2):** 53-64.

Kunduat S, Haque SK M and Ghosh B. 2015. Comparative analysis of bioactive compounds in different habitat of *Centella asiatica* (L.) Urban: Application for *in vitro* clonal propagation of elite ecotype. *J Appl Pharm Sci.*, **5 (2):** 030-036.

Mahmood N. 2014. Study the effect of the alcoholic and water extracts of *Ammi visnaga* (L.) and *Matrica chamomila* on different bacteria which isolates from diarrhea. *Int J Adv Res.*, **2 (2):** 139-142.

Murashige T and Skoog T. 1962. A revised medium for rapid growth and bioassays with tobacco tissue cultures**.** *Plant Physiol.*, **15**: 473-497.

Rasool R, Ganai BA, Kamili A N, Akbar S and Masood A. 2010. Antioxidant and antibacterial activities of extracts from wild and *in vitro*- raised culture of *Prunella vulgaris* L. *Med Aromat Plant Sci Biotechnol.*, **4 (1):** 20-27.

Rasooli I, Taghizadeh M, Astaneh S, Rezaei M and Jaimand K. 2007. Phytobiological properties of *Ammi visnaga* L. and

Lavandula angustifolia Mill. Essential oils. *Int. J. Essen. Oil Ther.*, **1**: 1-7.

Rose J and Hulburd J. 1992. **The Aromatherapy Book Applications and Inhalations**. North Atlantic Books, Berkeley, California, 94712.

Sabry A, El-Said A, El-Zayat S, Abdel-Motaal F and Magraby T. 2014. Fungal contamination of *Ammi visnaga* seeds, antimicrobial activity of the plant seeds secondary metabolites and detection of alkaloids and non-alkaloids compounds. *Curr Microbiol.,* **3 (2):** 901-914.

Satrani B, Farah A, Fechtal M, Talbi M and Boumari, M.L. 2004. Chemical composition and antimicrobial and antifungal activities of the essential oil of *Ammi visnaga* (L.) Lam. *Acta Botanica Gallica*, **151:** 65-71.

Scorzoni L, Benaducci T, Almeida AMF, Silva DHS, Bolzani VDS and Gianinni MJSM. 2007. The use of standard methodology for determination of antifungal activity of natural products against medical yeasts *Candida* sp and *Cryptococcus* sp. *Braz J Microbiol*.**, 38:** 391-397.

Sellami HK, Napolitano A, Masullo M, Smiti S, Piacente S and Pizza C. 2013. Influence of growing conditions on metabolite profile of *Ammi visnaga* umbels with special reference to bioactive furanochromones and pyranocoumarins. *Phytochem J.*, **95**: 197-206.

Sharma S, Rathi N, Kamal B, Pundir D, Kaur B and Arya S. 2010. Conservation of biodiversity of highly important medicinal plants of India through tissue culture technology- A review. *Agri Biol J North Amer.*, **1 (5):** 827-833.

Sridhar TM and Aswath CR. 2014. Review on medicinal plants propagation: A comprehensive study on role of natural organic extracts in tissue culture medium. *Am J Plant Sci.*, **5:** 3073-3088.

Tahtamouni RW, Shibli RA, Al- Abdallat AM, Al- Qudah TS, Younis L, Al-Baba H and Al- Ruwaiei H. 2015. *In vitro* conservation and cryopreservation of medicinal and aromatic plants: a review. *Jordan J Biol Sci.*, **11(1):** 147-167.

Talaat I M, Khattab H I and Ahmed A M. 2014. Changes in growth, hormones levels and essential oil content of *Ammi visnaga* L. plants treated with some bioregulators. *Saudi J Biol Sci.*, **21**: 355-365.

Upadhyay A, Upadhyaya I, Kollanoor-Johny A and Venkitanarayanan K. 2014. Combating pathogenic microorganisms using plant-derived antimicrobials: A mini review of the mechanistic basis. *Biomed Res Inter.*, 1-18.

World Health Organization, (2007), **WHO Monographs on Selected Medicinal Plants**. WHO, Geneva, Switzerland, p. 23.

World Health Organization, (2011), **Traditional Medicines: Global Situation**, **Issues and Challenges**. WHO, Geneva, Switzerland, p. 1.

JJBS

Jordan Journal of Biological Sciences

Volume 12, Number 1,March 2019
ISSN 1995-6673
Pages 49 - 53

Contact and Fumigant Toxicity of *Uvaria afzelli* (Scott) against *Plodia interpunctella* (Hubner) Infesting Maize Grains in Nigeria

Folasade K. Olufemi-Salami*, Joseph O. Akinneye and Olufemi S. Salami

Department of Biology, Federal University of Technology, Akure. P.M.B. 704, Akure Ondo State, Nigeria.

Received May 26, 2018; Revised June 30, 2018; Accepted July 10, 2018

Abstract

In this study, the insecticidal efficacy of the powder and extract of *Uvaria afzelli* seed is evaluated against different life stages of *Plodia interpunctella* at the ambient temperature of 28 ± 2 ^{o}C and 75 ± 5 % relative humidity. The powder of the plant was tested at the rate of 0.1, 0.2, 0.3 and 0.4g dosages, while the extract was tested at 1, 2, 3 and 4 % concentrations per 20g of maize. The contact and fumigant toxicity of the plant was observed on the mortality and emergence of the adult moth. All the dosages and concentrations of the plant used as treatment through contact toxicity completely inhibited the emergence of the adult moth. Also, all the dosages of plant powder used as treatment achieved 100 % of insect mortality within ninety-six hours of application except the 0.1g dosage which recorded 98.17 % mortality. Within seventy-two hours of exposure, the powder of the plant used as fumigant recorded 100 % mortality of the moth at 0.4g dosage while the extract achieved 100% mortality within twenty-four hours regardless of the concentration used. Also, at 0.1g and above, for both extract and powder, 100 % inhibition of egg hatchability and adult emergence was recorded. The powder and extract of *U. afzelli* are highly toxic against different life stages of *P. interpunctella* when used as contact toxin and fumigant.

Keywords: Hatchability, Emergence, Mortality, *Uvaria afzeli*, Toxicity, Fumigant.

1. Introduction

Maize (*Zea mays* L.) is the third most important crop in the world in terms of growing area and production and grain yield (Shiri *et al*., 2010). It adjusts easily to a wide range of environmental and climatic conditions. Therefore, it is grown both in the tropic and temperate regions of the world. Its availability in stores and on the field has made it a choice of many infesting insects especially the coleopterans and lepidopterans (Gerpacio and Pingali, 2007).

Indian meal moth, *Plodia interpunctella* (Hubner) lepidopterans is one of the primary insect pests infecting maize in the tropics. It has caused an appreciable damage to maize grains both on the field and in stores. Moreover, infestation in the store is more pronounced. The infestation of maize grains by *P. interpunctella* has caused diminution in the quality and market value of the grains (Philips *et al*., 2000; Salami *et al*., 2017). Therefore, the control of this important insect pest of maize has become of major interest among the entomologists and store managers around the world.

For years, the control of this insect pest and other notorious storage pests has relied overwhelmingly on the use of synthetic chemical insecticides that are associated with many dents thwarting their widespread use nowadays. In fact, the governments of many advanced countries including the UK and USA have banned the use of some synthetic chemical insecticides because of their effects on both human and environmental health (Isman, 2006; Oni *et al*., 2016). Therefore, researches have been shifted toward the use of botanical-based insecticides since they were found to have little or no effect on the non-target organisms and the environment (Zibaee, 2011 and Olufemi -Salami *et al*, 2017).

Pepper fruit *Uvaria afzelli* (Scott), known as "*Gbongbose"* among the Yorubas in Nigeria is a medicinal plant which has been used for the treatment of various diseases such as stomach ache, coughing, amenorrhoea, neuralgia etc. (Okepekon, 2004, Odugbemi, 2006). It belongs to the family of *Annonaceae*. The fresh stem and root bark have been shown to be effective in the control of adult moths (*Cleistopholis patens*) reared on paddy rice (Akinneye and Oyeniyi 2016). However, further research has not been done on the entomocidal properties of *U. afzelli* seeds to explore its contact toxicity and fumigant action of its aroma on insects. Hence, the powder and oil of the seeds of *U. afzelli* in the control of insect pests of stored products might be as effective as the bark and the roots. This research, therefore, sought to investigate the contact and fumigant toxicity of the powder and ethanol oil extract of the seeds of *U. afzelli* against *P. interpunctella* infesting maize grains.

* Corresponding author. e-mail: kemisade@yahoo.com..

2. Materials and Methods

2.1. Insect Culture

The *P. interpunctella* used to establish the culture was obtained from naturally-infested maize grains from the Research Laboratory in the Department of Biology at the Federal University of Technology Akure, Ondo state, Nigeria. The moths larvae were reared in twenty-one plastic containers containing 300g of uninfested maize grains. The culture was maintained by continually replacing the devoured powder and sieving out frass and fragment. The plastic containers were covered with muslin cloth, fastened with rubber band, and placed inside a wire mesh cage of the dimensions 75cm ×50cm ×60cm (L×W×H) with its four strands dipped in water-kerosene mixture contained in a plastic container to prevent the entry of predatory ants into the cage. The culture was maintained at a temperature of 28 ± 2°C and a relative humidity of 75 ± 5% . The whole set up was left inside the breeding cage in the laboratory. The maize variety TZESR-20 obtained from the Agricultural Development Program, Akure, Nigeria was disinfested in the freezer at −2 °C for seventy-two hours. Following that, it was allowed to equilibrate in the laboratory.

2.2. Collection and Preparation of the Plant Materials

The seeds of *U. afzelli* were obtained from a farm at Modebiayo camp, in Ondo East Local Government Area of Ondo State, Nigeria. The seeds were air-dried, pulverized into fine powder using a Binatone Electric Blender (Model 373). The pulverized seeds were sieved with a mesh with a size of $1mm^2$ before being stored in plastic containers with airtight lids for subsequent use.

2.3. Preparation of the Ethanol Oil Extract

Eighty grams of the pulverized seeds were weighed into a muslin cloth and transferred into the thimble and were extracted with ethanol in a Soxhlet apparatus. The extraction was carried out for three hours. The extraction was terminated when the solvent in the thimble became clear. Then, the thimble was removed from the unit, and the solvent was recovered by redistilling using a rotary evaporator. The resulting extract contained both the solvent and the oil. After that, the oil was exposed to air so that the traces of the volatile solvent evaporate, leaving the oil extract. The resulting oil was kept in a plastic container to be used for the subsequent experiment.

2.4. Hatchability Inhibition by Pulverized Seed Powder

Thirty freshly-laid eggs (0-24h old) were placed on 20g of maize grains treated with 0.1, 0.2, 0.3 and 0.4g of the powder of *U. afzelli* seeds inside separate plastic containers (8 cm diameter and 4 cm depth) covered with muslin cloths. A control experiment (20g of maize grain-infested eggs of *P. interpunctella* without any seed powder) was setup under the same environmental conditions with the treatments. All treatments and control experiment were replicated three times. Daily observations were made with a dissecting microscope to determine the number of eggs that hatched. After forty days, the number of adults emerged was determined and the percentage was calculated using the formula:

$$\%\ \text{hatchability} = \frac{\text{number of eggs hatched}}{\text{Total number of eggs introduced}} \times \frac{100}{1}$$

2.5. Contact Toxicity of the U. afzelli Seeds Powder on the 3rd Larvae Instar and Adult P. interpunctella Emergence

The same procedures for the preparation of treatments in the hatchability inhibition of eggs of *P. interpunctella* were repeated for the 3rd instar larvae and 0-24h adults of *P. interpunctella*. Ten 3rd instar larvae and ten adult insects were introduced separately into each of the treatments and control experiment. The numbers of dead larvae and adult insects were counted after 24, 48, 72, and 96 hours following the treatment.

2.6. Contact Toxicity of the U. afzelli Powder on the Mortality of Adult P. interpunctella

Twenty grams of disinfected maize grains were treated with 0.1, 0.2, 0.3 and 0.4g of the *U. afzelli* powder in separate plastic containers (8 diameter and 4 cm depth). The mixtures were agitated gently to homogenize the distribution of powder. Ten pairs of freshly-emerged 0-24 hour old males and females (the sexes were differentiated using size; males are smaller, while females are bigger with a protruding abdomen) were introduced into the treated grains. The container was covered with a perforated lid covered with muslin cloth to provide aeration. The entire sets were kept in the breeding cages, and mortality was recorded every six hours for the duration of twenty-four hours.

2.7. Effects of the U. afzelli Extracts on adult mortality of P. interpunctella

Different concentrations of 1, 2, 3, 4 and 5 % of the oil extract were prepared by adding 0.1, 0.2, 0.3, 0.4 and 0.5 mL of the of seeds (powder) extract into 9.9, 9.8, 9.7, 9.6 and 9.5 mL, of ethanol (solvent) respectively. Twenty grams (20g) of disinfested maize grains were treated with different concentrations of the oil extract of *U. afzelli* seed in a plastic container. The mixtures were agitated gently to homogenize the distribution of the oil extract. Ten pairs of freshly emerged 0-24 hour old male and female of the *P. interpunctella* adults from the stock culture were introduced into the 20g treated maize. The containers were covered with perforated lids to provide aeration. The entire set up was kept in the laboratory, and mortality was recorded every six hours for the duration of twenty-four hours.

2.8. Fumigant Effect of the U. afzelli Seeds' Extracts on the Mortality of Adult P. interpunctella

Different concentrations of 1, 2, 3, 4 and 5 % oil extract were prepared. Whatman 1 filter paper was cut into four equal parts. One part of the paper was dipped into 1 % concentration and then packed in muslin cloth, and suspended using thread. The treated paper strips were introduced by suspension into the plastic containers containing 20g of maize grain and ten pairs of male and female freshly-emerged 0-24 hour-old *P. interpunctella* adults from the stock culture. The lids of the containers were punched and covered with muslin cloth. The same procedures were repeated for 2, 3, 4, and 5 % concentrations. Untreated paper strips dipped in ethanol were used as the control experiment. The set up was

replicated three times. Adult mortality was counted at 24, 48, 72 and 96 hours after application.

The fumigant effect of the plant was also examined on the eggs of Indian meal moth.

2.9. Data analysis

All data on mortality were corrected using Abbott (1925) Formula. Complete randomized bloc design was used for the experiment and data obtained were subjected to analysis of variance (ANOVA), and significantly different treatment means were separated using Tukey's Simultaneous Test ($P < 0.05$). SPSS 16.0 software package was used for all the statistical analysis.

3. Results

3.1. *Contact Toxicity of the U. afzelli Powder and Extract on Egg Hatchability and Adult Emergence of P. interpunctella*

The effect of *U. afzelli* powder and extract of *U. afzelli* on egg hatchability and adult emergence of *P. interpunctella* are shown in Table 1. At all dosages of the *U. afzelli* powder (treatments), hatchability and adult emergence were completely inhibited. The result of the control experiment was completely different from the treatments insomuch that, more than 50 % hatchability and adult emergence were obtained from the control experiment.

The *U. afzelli* ethanol oil extract completely inhibited egg hatchability and the adult emergence of *P. interpunctella* at all concentrations including the control experiment.

Table 1. Effect of *U. afzelli* powder and ethanolic extract on egg hatchability and adult emergence of *P. interpunctella*.

Rate (g/20 maize grain)	Mean % (±S.E) Egg hatch	Mean % (±S.E) Adult emergence
	Powder	
0.0	60.00±0.00^{b}	54.00±2.3^{b}
0.1	0.00±0.00^{a}	0.00±0.00^{a}
0.2	0.00±0.00^{a}	0.00±0.00^{a}
0.3	0.00±0.00^{a}	0.00±0.00^{a}
0.4	0.00±0.00^{a}	0.00±0.00^{a}
	Oil extract	
0.0	72.00±3.2^{b}	58.00±1.5^{b}
0.1	0.00±0.00^{a}	0.00±0.00^{a}
0.2	0.00±0.00^{a}	0.00±0.00^{a}
0.3	0.00±0.00^{a}	0.00±0.00^{a}
0.4	0.00±0.00^{a}	0.00±0.00^{a}

Means followed by the same letter in the same column are not significantly different at P≤0.05

3.2. Contact Toxicity of the U. afzelli Powder on Adult P. interpunctella

The toxicity effect of the *U. afzelli* powder on the adult *P. interpunctella* showed in Table 2 reveals that the toxicity of the seed powder on the adult moth is dosage and time-dependent. It also reveals that a minimum of twelve hours is needed at any dosage greater than 0.1g/20g to achieve a lethal effect on the moth. Moreover, a consistent progressive increase in mortality rate was obtained at 0.2g/20g dosage. Likewise, eighteen hours following treatment, 50 % mortality was achieved in all the dosages above 0.1g/20g. Nonetheless, the 54.17 % mortality recorded in 0.2g/20g dosage eighteen hours following treatment was not significantly different from the 41.67 % mortality recorded at 0.1g/20g dosage at the same post treatment time ($P \leq 0.05$). No significant difference was observed in all the dosages twenty-four hours following treatments. Nevertheless, a complete mortality was obtained in all treatments except in 0.1g/20g where 98.17% mortality was recorded at 24h post treatment

Table 2. Contact toxicity of *U. afzelli* seeds powder on the mortality of adult *P. interpunctella*.

Rate (g/20g maize grain)	Mean% mortality after			
	6h	12h	18h	24h
0.0	0.00±0.00^{a}	0.00±0.00^{a}	0.00±0.00^{a}	0.00±0.00^{a}
0.1	0.00±0.00^{a}	0.00±0.00^{a}	41.67±2.64^{b}	98.17±0.7^{b}
0.2	0.00±0.00^{a}	23.33±2.01^{b}	54.17±3.33^{b}	100±0.00^{b}
0.3	0.00±0.00^{a}	26.67±2.1^{b}	70.80±3.00^{c}	100±0.00^{b}
0.4	0.00±0.00^{a}	76.70±2.11^{c}	95.83±2.00^{d}	100±0.00^{b}

Means followed by the same letter in the same column are not significantly different at $P \leq 0.05$

3.3. Contact Toxicity of the U. afzelli Extract on Adult P. interpunctella

The effect of the extract of *U. afzelli* on the mortality of adult *P. interpunctella reported* in Table 3 reveals that the effectiveness of the extract is concentration and time-dependent. Twenty-four hours following treatment, the mortality rate increases with concentration; this explains why the highest mortality of 53.00 % after twenty-four hours of treatment was recorded at the 4 % concentration treatment. Moreover, forty-eight hours following treatment, all the concentrations used achieved over 50 % mortality of the moth except the 1 % concentration which achieved 33.33 % mortality ($P \leq 0.05$).

Table 3. Effect of extract of *U. afzelli* on adult mortality of *P. interpunctella*.

Rate (%)	Mean % mortality after			
	24h	48h	72h	96h
1	0.00±0.00^{a}	33.30±3.33^{b}	77.00±3.0^{b}	83.01±3.3^{b}
2	0.00±0.00^{a}	80.00±0.00^{c}	83.33±3.3^{b}	100±0.00^{c}
3	33.33±3.33^{b}	86.70±6.67^{c}	96.67±3.0^{c}	100±0.00^{c}
4	53.00±3.33^{c}	96.67±3.30^{c}	100±0.00^{c}	100±0.00^{c}
**Control 1	0.00±0.00^{a}	0.00±0.00^{a}	0.00±0.00^{a}	0.00±0.00^{a}
**Control 2	0.00±0.00^{a}	0.00±0.00^{a}	0.00±0.00^{a}	0.00±0.00^{a}

Means followed by the same letter in the same column are not significantly different at $P \leq 0.05$

**Control 1 is the maize grains treated with 2ml of ethanol

**Control 2 is the maize grains treated with neither extract nor solvent

3.4. Fumigant Toxicity of the U. afzelli Seeds' Powder on Adult Mortality of P. interpunctella

More than 50 % mortality of adult *P. interpunctella* was recorded at the 0.4g/20g dosage twenty-four hours

after treatment through fumigant action. The fumigant action proved to be dosage-dependent as shown in Table 4. The fumigant effect of 0.1g/20g dosage is very consistent. All the dosages at seventy-two hours following treatment produced adult mortality greater than 50 % through fumigant action. Complete mortality of adult *P. interpunctella* through fumigant action was achieved at all dosages greater than 0.1g/20g over a post-treatment period of seventy-two hours (Table 4).

Table 4. Fumigant toxicity of *U. afzelli* seeds powder on adult mortality of *P. interpunctella.*

Rate (g/20 maize grains)	Mean % mortality after			
	24h	48h	72h	96h
0.0	0.00±0.00^{a}	0.00±0.00^{a}	0.00±0.00^{a}	0.00±0.00^{a}
0.1	0.00±0.00^{a}	33.30±3.33^{b}	77.00±3.0^{b}	83.01±3.3^{b}
0.2	0.00±0.00^{a}	80.00±0.00^{c}	83.33±3.3^{b}	100±0.00^{c}
0.3	33.33±3.33^{b}	86.70±6.67^{c}	96.67±3.0^{c}	100±0.00^{c}
0.4	53.00±3.33^{c}	96.67±3.30^{c}	100±0.00^{c}	100±0.00^{c}

Means followed by the same letter in the same column are not significantly different at $P \leq 0.05$

3.5. Fumigant Toxicity of the Ethanol Oil Extract of U. afzelli on Adult Mortality of P. interpunctella

The fumigant effect of the *U. afzelli* ethanol oil extract on the mortality of adult *P. interpunctella* shown in Table 5 shows that the fumigant action of the oil extract irrespective of the concentration elicited more than 50 % and 100 % *P. interpunctella* mortality at eighteen and twenty-four hours post treatments.

Table 5. Fumigant toxicity of extract of *U. afzelli* on adult mortality of *P. interpunctella.*

Concentration (%)	Mean% mortality after			
	6h	12h	18h	24h
0	0.00±0.00^{a}	0.00±0.00^{a}	0.00±0.00^{a}	0.00±0.00^{a}
1	16.67±3.3^{b}	25.00±2.9^{b}	72.00±4.4^{b}	100±0.00^{b}
2	20.00±0.0^{b}	26.67±3.3^{b}	85.00±2.9^{b}	100±0.00^{b}
3	20.00±0.0^{b}	37.00±6.7^{b}	88.00±3.0^{b}	100±0.00^{b}
4	25.00±0.56^{c}	60.00±5.8^{c}	93.00±3.2^{c}	100±0.00^{b}

Means followed by the same letter in the same column are not significantly different at $P \leq 0.05$

4. Discussion

The insecticidal activity of the *U. afzelli* seeds extract against eggs hatchability and 3rd larva instar development to adult investigated in this study shows that the seeds' extract is very efficient in inhibiting the development of eggs to larvae and 3rd larva instar to adult. At all rates of application, the powder completely inhibited the egg hatching and the development to adult. The systematic toxicity of the seed powder might be traced to the ingestion of the powder into the alimentary system of the insect thereby causing some unpleasant situation in the feeding and digestion of the insects.

The powder of the seeds of *U. afzelli* inhibited hatchability. This may be attributed to the suffocation caused by the powder to the developing embryos. The air surrounding the eggs may also be polluted because of the sharp aromatic nature of the seeds. Concurrently, the extract inhibited egg hatching and development to adult stage from the 3rd larva instar. This result can be better explained since the ethanol oil extract used for the treatment of the maize grains has a better penetrating ability because of the size of the solutes. Similar extracts from the *Annona senegallensis* root and bark were effective against the egg hatching of *Callosobruchus maculatus* (Aku *et al*., 1998). *Cleisthopholis patens* oil extract has also been reported to have inhibited the egg hatch and development of *E. cautella.* Moreover, a significantly low number of adult's *C. maculatus* were reported to have emerged from the seeds treated with the extracts of African nutmeg seeds [*Monodora myristica* (Gaertn.) Dunal] (Akinneye, 2003; Okosun and Adedire, 2010).

The toxic effect of the powder and rate of application of *U. afzelli* on the mortality of adult *P. interpunctella* depend on the mass of the powder and exposure periods. The injuriousness of the powder was pronounced within a short range of time on adult *P. interpunctella*. The adaptation of the adult moth to survive with the toxicity posed by the powder proved useless. The efficacy of this powder to control adult *P. interpunctella* at a very low concentration is time-dependent. The phytochemical property of the seeds powder might have resulted in the cytoplasmic coagulation of the insect (Bhaduri *et al.* 1990). The results agreed with the findings of Lajide *et al.* (2003) who reported that *U. afzelli, Eugenia aromatic* and *Aframomum melegueta* powder were toxic to *C. maculatus* at all level of treatment within twenty-four hours of application. Akinneye *et al.* (2009) also reported the efficacy of plant powder in the control of *Ephestia cautella* with *Cleisthopholis patens.* Additionally, Ashamo and Akinneye (2004) reported that a minute quantity of *Eugenia aromatica* powder caused greater than 43.3 % mortality of the yam moth *Euzopherodes vapidella*.

The protective ability of the *U. afzelli* seed powder to the grains might be a result of the systematic blockage of the spiracles and diffusion of the aromatic property of the plant into the insect respiratory system thereby causing suffocation. This can be interrelated with the sharp increase in mortality of the insects as the powder mass increased. Similar findings have been reported by Adedire *et al*., (2011); Ileke and Olotuah, (2012).

The ability of the extract to cause 100 % adult moth mortality in all the concentrations at a period twenty-four hours of exposure may be attributed to the fumigant effect of the plant oil on the adult moth since there was a strong correlation between the death rate of the contact toxicity and fumigant action of the oil. The fumigant action of the oil might have caused death through respiratory inhibition, inhibition of oxidative phosphorylation, and amide metabolism (Ashamo, 2000).

Based on the results obtained from this research, it can be deduced that the *U. afzelli* powder ethanol oil extract used directly or in the form of fumigant can protect maize grain from infestation by *P. interpunctella* during storage.

The powder and extract of *U. afzelli* were good candidates for the control of *P. interpunctella* on maize grains since they completely inhibited the development of

P. interpunctella from egg to adult. Also, the powder and the ethanol oil extract after twenty-four hours of treatment, resulted into an adult mortality of 100 %. Therefore, both the powder and the ethanol oil extract of *U. afzelli* seeds are recommended for use to protect stored maize grains, and can also be integrated with other pest management procedures, since the plant powder and oil were edible, locally available, and medicinal. It is also recommended that the *U. afzelli* seeds could be produced and packaged on a large scale as botanical insecticides.

Acknowledgement

I acknowledge Dr. Akinneye Joseph and Mrs. Olufemi-salami, Folasade K. for their conceptual efforts in designing the project, executing the designed project and gathering data for analysis. The effort of Mr. Salami Olufemi cannot be jettisoned, he painstakingly drafted the manuscript and effected corrections often after group discussions on the manuscript.

References

Abbott WS. 1925. A method of computing the effectiveness of an insecticide. *J Econ Entom.*, **18**: 265-267.

Adedire CO and Lajide L. 2003. Ability of extracts of ten tropical plant species to protect maize grains against infestation by the maize weevils *Sitophilus zeamais* during storage. *Nig J Exp Biol.* **4**:175-179.

Adedire CO and Lajide L. 2003. Ability of extracts of ten tropical plant species to protect maize grains against infestation by the maize weevil, *Sitophilus zeamais*, during storage. *Nig J Expl App. Biol.* **4**:175-179.

Adedire CO and Okosun OO. 2010. Potency to cowpea seed Bruchid, *Callosobruchus maculatus* (Coleoptera : Chysomelidae : Bruchidae), of African Nutmeg seed (*Monodora myristica* Gaertn.) Dunal) extracted with different solvents. *Nig J Entomol.*, **27**:89-95.

Adedire CO, Obembe OM, Akinkurolere RO and Oduleye SO. 2011. Response of *Callosobruchus maculatus* (Coleoptera: Chrysomelidae : Bruchidae) to extracts of cashew kernels. *JP Dis Prot.*, **118**(**2**), 75-77.

Akinkurolere OR. 2007. Assessment of the Insecticidal Properties of *Anchomanes difformis* (P. Beauv.) powder on five beetles of stored produce. *J Entomol*. **4** (**1**): 51–55.

Akinneye JO and Oyeniyi EA. 2016, Insecticidal efficacy of *Cleistopholis patens* (Benth) against *Sitotroga cereallella* Olivier (Lepidoptera: Gelechiidae) infesting rice grain in Nigeria. *J Crop Prot.*, **5**(1):1-10

Akinneye JO and Ashamo MO. 2009. Insecticidal activity of *Cleisthopholis patens* (Benth) Engl and Diels (Annonaceae) against the stored product moth, *Ephestia cautella* (Walker). (Lepidoptera:Pyralidae), in stored cocao(*Theobroma cacao*(L.)) Beans. *Nig J Entomol.*, **26**:63-66.

Akinneye JO. 2003, Biology and control of the yam moth, *Euzopheroides vapidella* (Mann) Lepidoptera: Pyralidae). Federal University of Technology, Akure, Nigeria M.Tech. Thesis pp 65.

Aku AA, Ogunwolu EO and Attah JH. 1998. *Annona Senegalensis* (L.). (Annonaceae). Performance as botanical insecticide for the control of Cowpea Bruchid *Callosobruchus maculatus* (F.) (Coleoptera: Bruchidae) in Nigeria. *J P DisProt.*, **105(5)**: 513.

Ashamo MO and Akinneye JO. 2004. Toxicity of powder of some tropical plants against yam moth, *Euzopheroides vapidella* (Mann) (Lepidoptera: Pyralidae). *Nig J Expl. Appl. Biol.*, **5**:63-68.

Ashamo MO. 2000. Bionomics and control of the yam moth, Dasyses rugosella (Stainton) (Lepidoptera: Tineidae). Federal University of Technology Akure, School of Postgraduate Studies, Akure, Ondo State, Nigeria. D. Phil Thesis pp 187.

Bhaduri N, Gupta DP and Ram S 1990 .Effects of vegetable oil on the ovipositional behavior of *Callosobruchus maculatus* (Fabricius) In: Fuji, K., Gatehouse, A.M, Johnson C.D., Mitchel, R. and Yoshida R. (Eds.). **Bruchids and Legumes: Economics, Ecology and Coevolution**,., pp. 81-84 Dordrecht. Springer Netherland. Netherland.

Derbalah AS and Ahned SI. 2011. Oil and powder of spearmint as an alternative to *Sitophilus oryzae* chemical control of wheat grains. *J P Pro Res.*, **51** (2): 145–150.

Gerpacio RV and Pingali, PL. 2007. *Tropical and subtropical maize in Asia: production systems, constraints, and research priorities. Mexico: CIMMYT.*

Ileke KD and Olotuah OF. 2012. Bioactivity of *Anacardium occidentale* (L) and *Allium sativum* (L) powder and oils extracts against Cowpea Bruchid, *Callosobruchus maculatus* (Fab.) (Coleoptera : Chysomelidae : Bruchidae). *Inter J Biol.*, **4(1):**96-103

Isman MB. 2006. Botanical insecticides, deterrents, and repellents in modern agriculture and an increasingly regulated. *World Ann Rev Entomol.*, **51**: 45-66.

Ivbijaro MF. 1990. Storage insect pests and Nigerian's food security. *A symposium paper presented at the 25th Anniversary Conference of the Entomological Society of Nigeria*, at AERLS, Ahmadu Bello University, Zaria, 7-11.

Khoshnoud H, Ghiyasi M, Amirnia R, Fard SS, Tajbakhsh M, Salehzadeh H and Alahyary P. 2008. The potential of using insecticidal properties of medicinal plants against insect pests. *Pak J Biol Sci.*, **11** (10): 1380–1384.

Odugbemi T. 2006. **Outlines and Pictures of Medicinal Plants from Nigeria**. Uni. of Lag. Press, Lagos, *pp* 114.

Okosun OO and Adedire CO. 2010. Potency of cowpea seed bruchid, *Callosobruchus maculatus* (Fabricius) [Coleoptera: Bruchidae], of African Nutmeg seed [*Monodora myristica* (Gaertn.) Dunal] extracted with different solvents. *Nig J Entomol.*, **27**: 89-95.

Okpekon T, Yolou S, Gleye C, Roblot F, Loiseau P, Bories C, Grellier P, Frappier F, Lauren A and Hocquemiller R. 2004. Antiparasitic activities of medicinal plants used in Ivory Coast. *J Ethnopharm.*, **90**:91–97.

Olufemi-Salami FK, Akinneye JO and Salami OS. 2017. Morphometric analysis of the developmental stages and insecticidal efficacy of three botanical oils against adult *Callosobruchus Analis*: *J of Hort. Res.* , **25(2):** 81-84.

Phillips TW, Berbert RC, and Cuperus GW 2000. Post-harvest integrated pest management. In: Francis, F.J. (Ed.), **Encyclopedia of Food Science and Technology**.2nd Ed. Wiley Inc., New York, pp. 2690–2701.

Salami OS, and Olufemi-Salami FK 2017. Lemon grass (*Cymbopogon citratus* Stapf) methanol and ethanol extracts, a repellant with less insecticidal effect on maize weevils (*Sitophilus zeamais* Motschulsky) infesting maize (*Zea mays*) grains. *Plant Gene and Trait,* **8(5):** 56-60.

Shiri R, Karppinen J, Leino-Arjas P, Solovieva S, Viikari-Juntura E 2010. The association between obesity and low back pain: A meta-analysis. *Am J Epidemol*., **171**:135-154.

Zibaee A 2011. Botanical Insecticides and Their Effects on Insect Biochemistry and Immunity, In: Stoytcheva M (Ed.), **Pesticides in the Modern World – Pests Control and Pesticides Exposure and Toxicity Assessment.** InTech Publisher, Chap. 4.

JJBS

Volume 12, Number 1,March 2019
ISSN 1995-6673
Pages 55 - 60

Jordan Journal of Biological Sciences

The Role of Homogenate Hepatic Tissue in Myogenesis

Raith A. S. Al-Saffar* and Mohammad K. M. Al-Wiswasy

Department of Basic Medical Science,, College of Medicine, The Hashemite University, P.O. Box 330127- Zarqa- 13115, Jordan.

Received June 10, 2018; Revised July 11, 2018; Accepted July 14, 2018

Abstract

Two groups of albino rats were exposed to identical tibialis anterior muscle crush injury. Small pieces of the liver were obtained from both groups. The animals of the first group were left without implantation with the liver tissue. Those of the second group received homogenized autogenous liver mince labeled with Indian ink. From the follow up, it was noticed that the muscle regenerative process was faster in the animals of the second group when compared with those of the first, and that the labeled liver cells participated in the formation of myotubes, which formed mature muscle fibers and possibly new satellite cells in the crushed skeletal muscles. This suggests that the labeled liver tissue homogenate implanted at the injured site has a positive regenerative effect on the skeletal muscles. The results of this experiment may eventually revolutionize therapeutic procedures for some forms of muscle diseases.

Keywords: Stem cells, Homogenized liver tissue, Muscle regeneration**.**

1. Introduction

Muscle injuries constitute one of the most challenging problems of sports traumatology, since although common, their treatment is still controversial and often inefficient (Jarvinen *et al*., 2005). Long periods of leave of absence are usually necessary for athletes, and a full recovery is sometimes difficult (Armfield *et al.*, 2006).

The muscle regenerative process has been demonstrated to reproduce myogenesis by the proliferation of myogenic stem cells, followed by their fusion to form multinucleated cells, and their further differentiations into mature muscle fibers (Carlson, 1973; Al- Hadithi *et al*., 2002; Al-Yawer *et al.*, 2004).

The origin of these stem cells was widely considered to arise within the damaged tissue from the quiescent satellite cells (Kang and Krauss, 2010). These cells are activated in response to injury, and are claimed to be the source of myoblasts (Alameddine *et al*., 1989). These myoblasts proliferated, fused and formed multinucleate myotubes that matured into myofibres which replaced the damaged and dead muscle fibers (Kuang and Rundnicki, 2008; Kang and Krauss, 2010).

Al-Azzawi, (1972) suggested that some muscle precursors are possibly of local origin, but may have moved into the site of muscle injury from elsewhere. Recently, few authors reported that some of these stem cells have been proposed to be phagocytic cells of blood origin (Weissman, 2002; Al-Yawer *et al.*, 2004); or from the bone marrow (Seal and Rudnicki, 2000). These undifferentiated cells show high phagocytic activity engulfing various types of foreign substances as trypan blue, various acridine dyes, and horse radish peroxidase (Al-Azzawi, 1972).

The muscle tissue healing process usually starts promptly as soon as the injury occurs; however, it can evolve slowly and irregularly, hindered by an extensive formation of connective scar tissue (Buckwalter and Cruess, 1993). This scar tissue inhibits the complete regeneration of the preexisting muscles, since it leads to the destruction, exhaustion and depletion of the local myogenic cells, which may necessitate the recruitment of additional myogenic cells from another source other than the injured muscle itself.

The limitations described earlier gave rise to surveys investigating the biological measures capable of stimulating the muscle regeneration process and of preventing fibrosis formation (Huard *et al*., 2002). Among these new techniques, two lines of implantation have been studied extensively. The first was through **t**he local application of the following promoting agent: i. White blood cells (Al-Yawer *et al*., 2004; Denapoli *et al.*, 2016); ii. Platelet-rich plasma (Utomo *et al*., 2018); iii. Bone-marrow centrifugate (Ferrari *et al*., 1988; Matziolis *et al*., 2006). These promoting agents are substances used in the tissue culture of skeletal muscles to enhance myogenesis due to their supposed healing properties, and attributed to the ability to recruit, proliferate and differentiate cells involved in tissue repair. On the other hand, therapies are based on the direct local addition of embryonic stem cell cultures, in the hope that the latter will differentiate in the cells of the target tissue (Al-Hadithi *et al*., 2002; Musaro *et al*., 2004). The aim of this study is to shed light on tissues, apart from blood or bone marrow, such as liver, because of its well-known power of regeneration, and since it contains growth factors especially those affecting division and further the differentiation of myogenic progenitors like transferring and hypoxanthine related compounds (De La Haba *et al.*, 1975; It *et al*., 1982 and 1985; Mac Sween and Whaley, 1992).

* Corresponding author. e-mail: Raith_alsaffar@yahoo.com.

2. Materials and Methods

2.1. Animals Used and the Obtaining of Tissue Specimen

A total number of eighty mature albino male rats that are eight weeks old and weighing 150–200 g were used in this study. The animals were lightly anesthetized by intraperitoneal injection of 0.1 mL (equal to 6 mg) pentobarbitone sodium. Right paramedian incision, 2 cm long, was done in the right hypochondrium of the anesthetized animals. A small piece of the liver (0.25 × 0.5 cm) was obtained using fine scissors. Then the injured site was covered with a layer of gel foam. Finally, closure of the abdominal wall was achieved by using 2/0 silk.

2.2. Preparing the Hepatic Tissues

Manual mincing of the hepatic tissue into very minute pieces using a scalpel's blade after placing the tissue in 3–4 ml of normal saline (Al-Hadithi *et al.*, 2002). The homogenate was centrifuged for fifteen minutes at 3000 rpm (Al-Yawer *et al*., 2004).

2.3. Incubation Procedures of the Homogenate

The homogenized tissues were incubated in an incubation media (1/3 Minimum Essential Medium, EAGLE-modified) with 2/3 normal saline. Fifteen drops of 25 % diluted Indian ink were added to the above mixture. The mixture was then incubated for ninety minutes in a water bath at 37°C (Al-Yawer *et al*., 2004). The incubating medium was then centrifuged for five minutes at a rate of 1500 rpm. The supernatant was discarded, and the precipitate was resuspended with 1 ml of 0.9 % normal saline and was centrifuged again at a rate of 1500 rpm for five minutes. The supernatant was again removed, and the precipitate was washed thrice with 1 mL of normal saline, until the supernatant was clear enough (Alwan, 2004). The remaining precipitate was suspended in 1 ml of normal saline. One drop of this suspension was put on a microscopic slide (two microscopic slides were prepared), and was dried and fixed in 95 % methanol. The first slide was stained with Harris's hematoxylin and eosin stain, and the other slide was stained with Mayer's carmalum solution. These slides were prepared to study the general morphology, and the type of cells that phagocytosed the label (Al-Yawer *et al*., 2004).

2.4. Induction of Injury and Implantation of Labeled Cells

While the animals were under anesthesia, the upper, middle and lower third of the tibialis anterior muscle were crushed and the already labeled liver cells suspension (each its own) was implanted in the tibialis anterior muscle by inserting the needle of a 1ml syringe along the longitudinal axis of the muscle. 0.33 mL of labeled cell suspension was injected to each third of the muscle. Animals were sacrificed in groups of seven animals, each, after 1, 2, 3, 5, 7, 14, 21 and 28 days from induction of injury. In the remaining animals (control animals) the same procedure was repeated (small piece of liver was obtained) but without implantation of liver tissue obtained to the injured tibialis anterior muscle. Three control animals were used with each experimental group. After sacrifice, serial frozen section 8 microns thickness was prepared to study muscle regeneration by a light microscope.

3. Results

The examination of the hepatic tissue homogenate revealed that the main cells involved in the uptake of the label were monocytes and macrophages, but the uptake of the label was not equal in these cells (Figure l and 2).

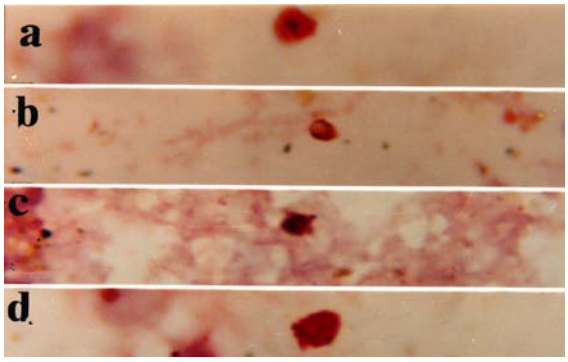

Figure 1. Hepatic tissue homogenate smear after labeling with Indian ink, showed different labeled cells: Macrophages engulfing fine-coarse carbon particles (a and d). Polymorphs showed poor uptake as only fine granules were present in their cytoplasm (b). Other cells, which were small with relatively large nucleus occupying almost all the cytoplasm, showed good uptake of carbon particles. These cells could be stem cells or mature lymphocytes (c). Mayer's carmalum stain (X1000).

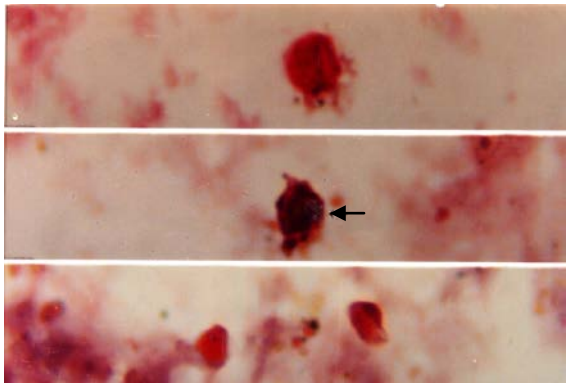

Figure 2. Photograph of hepatic tissue homogenate smear after labeling with Indian ink, showing large polyhedral cells (arrow), which could be heapatocyte or their precursors, engulfing coarse carbon particles; were as the cytoplasm of the others cells contains fine carbon particles. Mayer's carmalum stain (X 1000).

Large polyhedral cells, with centrally located nuclei, were also shown to engulf the Indian ink. Fine carbon particles were found distributed in their cytoplasm. These cells could be hepatocytes or their precursors.

Some cells, small in size with relatively large nuclei occupying almost all the cytoplasm revealed a good uptake of the label. These cells could be mature lymphocytes or undifferentiated stem cells. The polymorphs did not show any good uptake where only scarce granules were present.

On the first postoperative date, the injured area of the muscle tissue of the experimental group showed (Figure 3 and 4) necrotic fibers and inflammatory cell infiltration, mainly polymorphs, together with labeled cells of the implanted hepatic tissue. Some of the labeled cells were fusiform, others were rounded. Some of them showed fine carbon particles in their cytoplasm, while others showed coarse carbon particles indicative of the phagocytic activity of these cells.

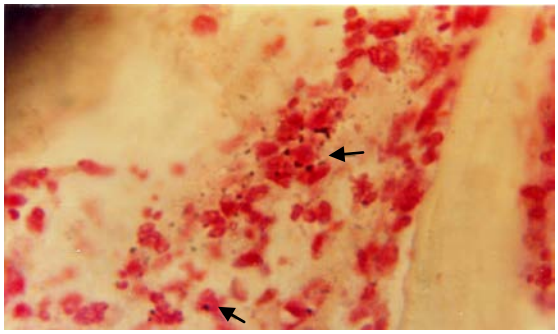

Figure 3. Injured tibialis anterior muscle implanted with hepatic tissue homogenate – Day one after injury. Labeled cells (arrows) were found among the inflammatory cells invading the injured area. Mayer's carmalum stain (X 1000).

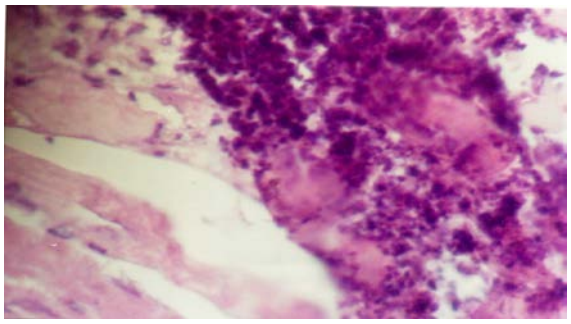

Figure 4. Injured tibialis anterior muscle implanted with hepatic tissue homogenate – Day one after injury. Huge amount of artificially administrated cells invaded the injured site of the muscle. H & E stain (X 400).

On the second postoperative date (Figure 5), numerous macrophages were profusely distributed throughout the injured area. Some of them were artificially introduced into the lesion since they contained carbon particles in their cytoplasm. Some of the labeled cells can be recognized as myoblasts, which are fusiform mononucleated cells with ovoid nuclei. Their cytoplasm was filled with relatively fine carbon particles. Other labeled cells appeared as elongated fusiform cells with elongated nuclei and sparse cytoplasm. These cells were in the process of transformation to either satellite cells or fibroblast.

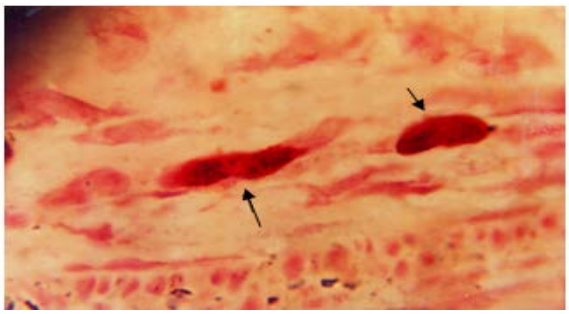

Figure 5. Injure tibialis anterior muscle implanted with hepatic tissue homogenate – Day two after injury. Labeled myoblast (arrows) participated in the formation of doublet. Mayer's carmalum stain (X 1000).

On day three after the injury (Figure 6), myoblasts populated the injured area. Some of them were artificially introduced into the lesion since they were labeled. All of them were just about to fuse to form multinucleated myotubes. Liver specific cells such as hepatocytes can also be recognized.

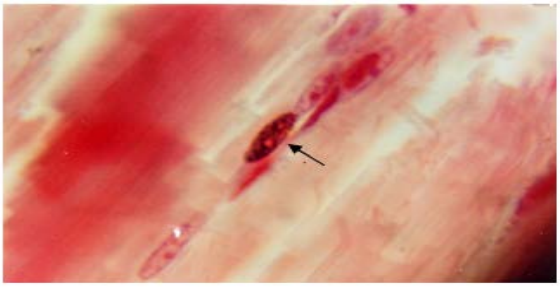

Figure 6. Injure tibialis anterior muscle implanted with hepatic tissue homogenate – Day three after injury. Myoblasts were just about to fuse or had begun to fuse into multinucleated myotubes. Many of them are labeled (arrow). Mayer's carmalum stain (X 1000).

On the fifth (Figure 7), seventh (Figure 8) and fourteenth (Figure 9) postoperative days, the necrotic area is diminished in size as a result of the progressive phagocytic activity of the macrophages. The infiltrating cells were decreased in number, and are mainly macrophages and fibroblasts. The labeled myoblasts in fortuitous area were seen attached to each other longitudinally forming strands termed the myotubes. These were parallel to the general alignment of muscle fibers. These myotubes containing the labeled cells have grown larger and larger at the end of day seven, and formed regenerating muscle fibers at day fourteen, since they appeared striated. However, they appeared smaller in diameter than mature fibers and their nuclei were mainly central.

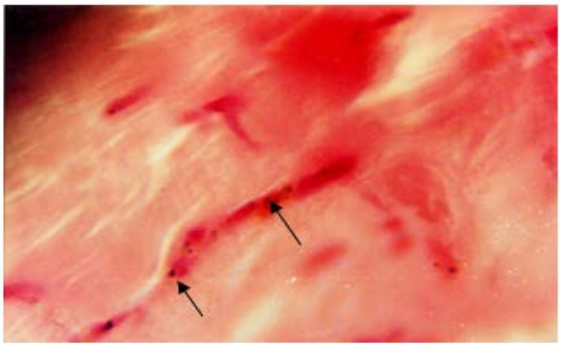

Figure 7. Injured tibialis anterior muscle implanted with hepatic tissue homogenate – Day five after injury. Early formation of myotubes can be recognized. Labeled myoblasts were found in some of these myotubes (arrows). Mayer's carmalum stain (X 1000).

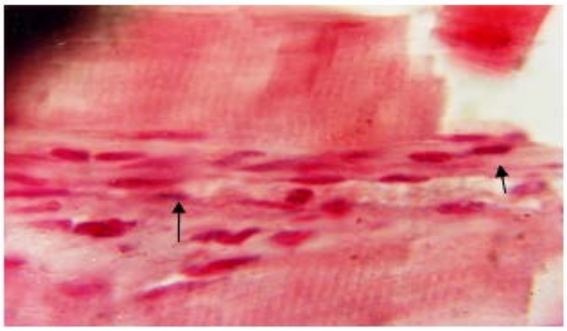

Figure 8. Injured tibialis anterior muscle implanted with hepatic tissue homogenate – Day seven after injury. Long myotubes were recognized parallel to the general alignment of the muscle fibers. Some of them contained labeled myoblasts (arrows). Mayer's carmalum stain (X 1000).

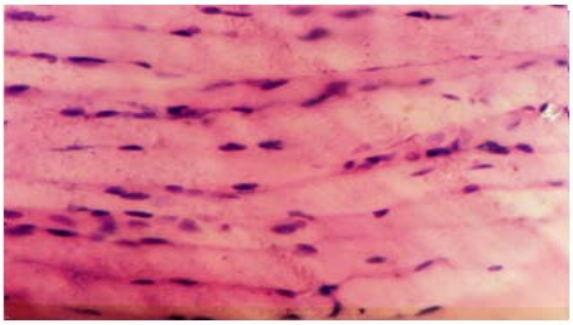

Figure 9. Injured tibialis anterior muscle implanted with hepatic tissue homogenate – Day fourteen after injury. Numerous regenerating muscle fibers were seen. They appeared smaller in diameter than mature fibers and their nuclei were central. H & E stain (X 400).

On day twenty one after injury (Figure 10), the fibers appeared more mature; their nuclei were either central or peripheral. Many of these regenerating fibers were labeled with carbon particles, indicating the engagement of labeled cells in the muscle regeneration. Some labeled cells were identified as satellite cells from their morphology.

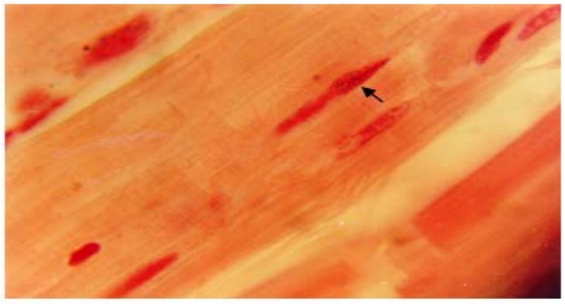

Figure 10. Injured tibialis anterior muscle implanted with hepatic tissue homogenate – Day twenty-one after injury. Regenerating muscle fibers with central or peripheral nuclei can be recognized. Some of them were labeled (arrow). Mayer's carmalum stain (X 1000).

On day twenty eight after injury (Figure 11 and 12), the labeled regenerating muscle fibers showed an increase in their diameter. The fiber diameter nearly equaled a normal one, and striations were clear. Their nuclei were peripherally located. However, some myonuclei were still centrally located.

The regenerative process in the muscles of the control animals, where no liver tissue has been implanted, shows a less formation of myoblasts and myotubes with delayed signs of maturity and excessive fibrosis.

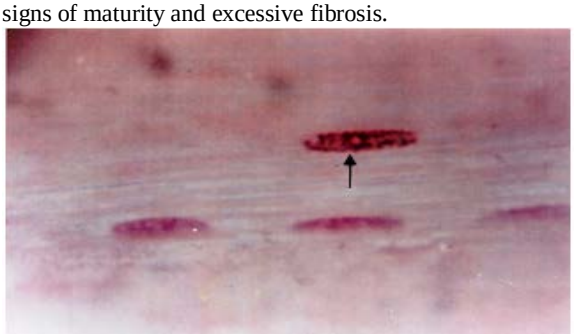

Figure 11. Injured tibialis anterior muscle implanted with hepatic tissue homogenate – Day twenty-eight after injury. Labeled regenerating fibers nearly equaled the normal one, with clear striations and peripheral location of their nuclei (arrow). Mayer's carmalum stain (X 1000).

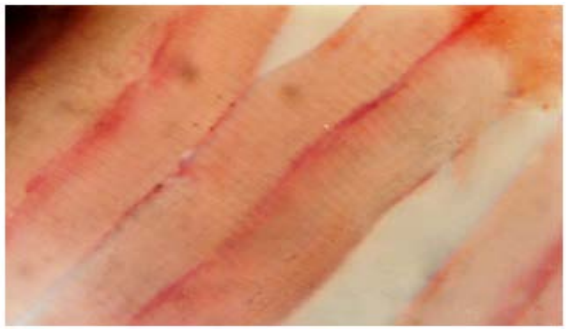

Figure 12. Injured tibialis anterior muscle implanted with hepatic tissue homogenate – Day twenty-eight after injury. Labeled regenerating fibers reached full maturity, showing clear striation with peripherally located nuclei. Mayer's carmalum stain (X 1000).

4. Discussion

Animals used in this study were mature young adult rats due to the presence of more satellite cells in the muscles at a younger age than at an older one (Allbrook, 1981); in addition, the viability of the tissue and its capacity to regenerate can be more in the young adult rats than in the older ones (Allbrook, 1981).

Indian ink was used for labeling the cells of the hepatic homogenate in this study, since cells labeled by Indian ink can be followed and traced for a long time (more than one month) when implanted at the site of the muscle injury. This is because the carbon particles are taken up by the cells (endocytosis) and endocytic vacuoles containing the undigested carbon particles fuse with the primary lysosomes to form secondary lysosomes. Eventually the residual undigested, insoluble contents remain within the cell as storage excretion (Al-Yawer *et al*., 2004). In addition to that, Indian ink was engulfed by the cells of the liver tissue homogenate.

The current results show that the monocytes and macrophages are the main types of cells involved in the phagocytosis of carbon particles in the hepatic homogenates. Monocytes are macrophages in the process of passing from the bone marrow, where they are formed, to peripheral tissues via the blood stream. These cells pass into extravascular sites through the walls of capillaries and venules (Bannister, 1995b). The author stated that macrophages were originally given different names according to their location. In the blood, they are represented by monocytes, whereas in the liver they are called littoral cells of the sinusoid (Von Kupffer cells).

Polymorphs showed poor uptake of the carbon particles, which is represented by the presence of scarce fine granules in their cytoplasm. This finding agreed with that obtained by Al-Yawer *et al*., 2004; Junqueira and Carnneiro, 2005. Polymorphs are active phagocytes of small particle like trypan blue (Al-Yawer *et al*., 2004). Carbon particles are relatively large, therefore, the uptake of this label by the polymorphs was relatively less than the uptake of trypan blue (Al-Yawer *et al*., 2004).

Some cells of a small size and with a relatively large nucleus occupying almost all the cytoplasm showed good uptake of the label in the hepatic homogenate. These cells could be mature lymphocytes or multipotent stem cells, since both of them have nearly the same size (Bannister,

1995b; Junqueri and Carnneiro, 2005). This finding was also reported by Vogelstein *et al*., 2001, who stated that the uptake of carbon particles by these cells can be attributed to their content of lysosomes, and in the case of stem cells, these cells may be differentiated into myoblast.

The tibialis anterior muscle was used for studying muscle regeneration in this project because this muscle is characterized by having a reasonable size with distal and superficial position which makes it easily accessible, and identifiable. Also it lacks interchangeability with other neighboring muscles, and there are no important structures related to it. Moreover, this muscle contains the three major fiber types, white, red and intermediate (Al-Azzawi, 1972). Crushing the muscle with a clamp is commonly used as a mean of studying the reaction of muscle to injury (Al-Hadithi *et al*., 2002; Al-Yawer *et al*., 2004).

After implantation of the hepatic tissue homogenate at the site of muscle injury in the experimental animals, the injured muscle retained its intrinsic capacity to undergo regeneration in response to injury. Therefore, liver enhances muscle regeneration. This may be due to the high concentration of growth factors that hepatic tissue contains. This finding agrees with the results obtained by De La Haba, *et al*., 1975; Bannister, 1995b who concluded that cells of the liver were themselves the manufacturer of growth factors.

In addition, this study shows that the labeled cells of the homogenate of the hepatic tissue participate in muscle regeneration, since the implanted labeled cells succeeded to form labeled myoblasts, labeled myotubes, and finally labeled regenerating muscle fibers. This finding was also reported by Al-Yawer *et al*., 2004, who concluded that the labeled cells of the buffy coat implanted at the site of muscle injury participate in the regeneration of muscle by forming labeled myoblasts, labeled myotubes, and finally labeled regenerating muscle fibers.

The hepatic tissue contains hepatocytes, Kupffer cells, multipotent stem cells, endothelial lining of sinusoids and arterioles, in addition to different types of white blood cells (Janqueira and Carnneiro, 2005). Most of these cells have the ability to ingest a foreign body (Al-hadithi *et al*., 2002). With the exception of multipotent stem cells, liver cells have no ability to be differentiated into other cell type. The role of hepatic homogenate in the regeneration of muscle tissue could be explained as:

(a) The liver is the main source of multipotent stem cells in addition to the bone marrow and the circulating mesenchymal cells. In the present study, labeled stem cells had participated in the process of muscle regeneration by the formation of labeled myoblasts. This finding is supported by other researchers (Vogelstein *et al*., 2001; Alwan, 2004) who pointed out that the multipotent stem cells have the ability to differentiate into multiple cell lineages, one of which is the myogenic pathway. In addition, Al-Azzawi, 1972; Bannister, 1995b; Malouf *et al*., 2001; Shafrtiz and Dabeva, 2002, reported that hepatic stem cells constitute a type of adult multipotent stem cells, which have the ability to be pluripotent stem cells, and differentiate into new cells, other than the cells of the organ from which it was obtained. On other hand, Al-Azzawi, 1972; Al-Taie *et al*., 1994; Caterson *et al*., 2001, concluded that mesenchymal stem cells are a rare population of undifferentiated cells isolated from adult tissue sources, and have the capacity to differentiate into mesodermal lineages, including muscle, bone, cartilage, tendon, fat and marrow stroma. This cell population may be expanded in culture, and subsequently permitted to differentiate into desired lineages.

(b) Other type of cells circulating in the blood and transferring to other tissue is the monocytes or macrophages (Jee and Nolan, 1963; Yarom *et al*., 1976; Turgon, 1988). i. Macrophages act as a scavenger engulfing dead cells and necrotic tissue and keep the field clear to regenerate (Leeson and Leeson, 1985); ii. Macrophages secreted a number of factors, which are chemo attractants for muscle precursor cells (Robertson *et al*., 1993); iii. Macrophages might stimulate the proliferation of muscle precursor cells (Junqueri and Carnneiro, 2005; Robertson *et al*., 1993).

(c) Some of the labeled cells appeared as elongated fusiform cells with elongated nuclei. These cells could be fibroblasts. This is in agreement with the finding of other researchers who found that undifferentiated mesenchymal cells are present in the circulating blood (Leeson and Leeson, 1985; Weissman, 2002; Caterson *et al*., 2001) or bone marrow (Ferrari *et al*., 1988; Al-Taie *et al*., 1994; Seale and Rudnicki, 2000). These cells give rise to fibroblasts when stimulated by injury (Leeson and Leeson, 1985; Caterson *et al*., 2001).

(d) The growth factor which is secreted by hepatic cells enhanced the regenerating process.

(e) Therefore, the only cells that could be differentiated into myotube are the multipotent hepatic stem cells, which can be detected easily by the presence of carbon particles in their cytoplasm.

Based on these observations, it can be said that when liver mince is added at the injured site can promote muscle regeneration. Similar results were reported after implantation of: i. Isolated white blood cells (Al-Yawer *et al*., 2004; Denapoli *et al*., 2016); ii. Platelet-rich plasma (Utomo *et al*., 2018); iii. Bone-marrow centrifugate (Ferrari *et al*., 1988; Matziolis *et al*., 2006).

The delayed appearance of maturity signs and the amount of fibrous cicatrix formed in the control animals indicate that the removal of liver tissue per se does not have any effects on the regeneration of crushed muscle unless the liver mince is added at the injured site.

5. Conclusion

It can be concluded from the present study that liver mince appears to promote the regeneration of crushed muscles by increasing the amount of regenerating tissue, which is recognized in the early days as increased myoblasts and myotubes, and by increasing the speed of regeneration, which is recognized in the late stages as the presence of more advanced signs of maturity. This effect of liver mince on the regeneration of injured skeletal muscles is explained by the effects of growth-promoting factors which are present in high levels in the liver tissue.

References

Alameddine HS, Dehaupas M, and Ferdeau M. 1989. Regeneration of skeletal muscle fibers from autologous satellite

cells multiplied in vitro. An experimental model for testing cultured cells myogenicity. *Muscle Nerve*, **12**: 544-555.

Al-Azzawi HT. 1972. Some histochemical studies on myopathies . Ph.D Thesis, University of Dundee: 105-108.

Al-Hadithi NK, Al-Saffar RAS, and Al-azzawi HT. 2002. A study on myogenesis using liver tissue homogenates. *J Fac Med. Bagdad*, **3**: 454-467.

Allbrook DB. 1981. Skeletal muscle regeneration. *Muscle & Nerve*, **4**:234-245.

Al-Tai TB, Al-Azawi HT, Al-Baghdadi HAG, and Neaory KAW. (1994). On the use of bone marrow in muscle regeneration. The seventh Scientific Congress, College of Medicine, University of Baghdad and Saddam Medical City.

Alwan BC. 2004. Stem cell implantation in spinal cord injury. Ph.D. thesis, College of Medicine, University of Baghdad.

Al-Yawer MA, Al-Saffar RAS, Al-Neamy KAW, and Al-Azzawi HT. 2004. The role of circulating phagocytic cells in muscle regeneration. *IPMJ*., **3 (1):** 28-32.

Armfield DR, Kim DH, Towers JD, Bradley JP, and Robertson DD. 2006. Sport-related muscle injury in the lower extremity. *Clin Sport Med*., **25(4)**: 803-842.

Bannister LH. 1995b. Haemolymphoid system. In: William, P.L., Bannister, L.H., Berry, M.M, Collins, P., Dyson, M., Dussek, J.H., and Ferguson, M.W.J. (Eds). **Gray's Anatomy**, 38th ed. Churchill Livingston, pp: 1374-1385.

Buckwalter JA, and Cruess RL. 1993. A cura does tecidos musculoesqueletion. In: Rockwood CA, Green DP, and Bucholz RW (Eds). **Fraturas em adultos** 3rd Ed, Sao Paulo: Melano, pp 179-219.

Carlson BM. 1973. The regeneration of skeletal muscle a review. *Am J Anat*., **137**: 119-150.

Caterson EJ, Nesti LJ, Albert T, Danielson K, and Tuan R. 2001. Aplication of mesenchymal stem cells in regeneration of musculoskeletal tissue. *Med Gen Med*., E1.

De La Haba G, Kamali HM, Tied DM. 1975. Myogenesis of avian striated muscle in vitro: Role of collagen in myofiber formation. *Proceeding of National Academy of Sci* (USA), **72**: 2729-2732.

Denapoli PMA.,Stilhano RS, Ingham SJ, Han SW, and Abdalla RJ. 2016. Platelet-rich plasma in murine model: Leukocytes, growth factors, FIT-1, and muscle healing. *Am J Sports Med*., **44(8):** 1962-1971.

Ferrari G, Cusella-De Angelis G, Coletta M, Paolucci E, Stornaiuolo A, and Cossu G. 1988. Muscle regeneration by bone marrow-derived myogenic progenitors. *Science*, **279**: 1528-1530.

Huard J, Li Y, and Fu FH. 2002. Muscle injuries and repair: current trends in research. *J Bone Joint Surg. Am*., **84(5):** 822-832.

It I, Kimura I, and Ozawa E. 1985. A myotrophic from chick embryo extract: its purification, identity to transferring and indispensability for avian myogenesis. *Dev Biol*., **94**:366-377.

Jarvinen T A, Jarvinen T L, Kaariainen M, Kalimo H, and Jarvinen M: 2005. Muscle injuries: biology and treatment. *Am J Sports Med*., **33(5):** 745-764.

Jee WSS, and Nolan PD. 1963. Origin of osteoclasts from fusion of phagocytes. *Nature*, **200**: 225-227.

Junqueira LC and Carnneiro J. 2005. Blood Cells and Hematopoiesis. In: Malley J, Lebowitz H and Peter J (Eds), **Histology Text & Atlas**, 11th ed.. McGraw-Hill Companies, New York: 223-253.

Kang JS, and Krauss RS. 2010. Muscle stem cells in developmental and regenerative myogenesis. *Curr Opin Clin Nutr Metab Care*, **13**: 243-248.

Kuang S, and Rundnicki MA. 2008. The emergining biology of satellite cells and their therapeutic potential. *Trend Mol Med*., **14**: 82-91.

Leeson CR and Leeson TS. 1985. Specialize connective tissue: blood. In: Leeson TS, Leeson CR and Paparo AA (Eds), **Textbook of Histology**., 5th Ed:105-171.

MacSween RNM and Whaley K. 1992. Liver, billiary tract and pancreas: Liver cell regeneration. In: MacSween RNM, and Whaley K (Eds) , **Muir's Textbook of Pathology**, 3rd Ed. UK: 746.

Malouf NN, Coleman WB, Grisham JW, Lininger RA, Madden VJ, Sproul M, and Anderson PAW. 2001. Adult-derived stem cells from the liver become myocytes in the heart in Vivo. *Am J Pathol*., **158**: 1929-1935.

Matziolis G, Winkeler T, Schaser K, Wiemann M, Krocker D, Tuischer J, Perka C, and Duda GN. 2006. Autologous bone marrow-derived cells inhance muscle strength following skeletal muscle crush injury in rats. *Tissue Eng*., **12(2):** 361-367.

Musaro A, Glacinti C, Borsellino G, Pelosi L and Cairns L. 2004. Stem cell-mediated muscle regeneration is enhanced by local isoform of insulin-like growth factor 1. *Proc Nati Academic Sci*. (USA), **101(5):** 1206-1210.

Robertson TA, Maley MA, Grounds MD, and Papadimitriou JM. 1993. The role of macrophages in skeletal muscle regeneration with particular reference to chematoxis. *Exp Cell Res*., **297(2):** 321-331.

Seale P, and Rudnicki MA. 2000. A new look at the origin, function, and "stem-cell" status of muscle satellite cells. *Dev-Biol*., **218**: 115-124.

Shafrtiz DA, and Dabeva MD. 2002. Liver stem cells and model systems for liver repopulation. *J of Hepatol*., **36 (4):** 552-564.

Sloper JC, Bateson RG, Hindle D, and Warren J. 1970. Muscle regeneration in man and the mouse. In: **Regeneration of Striated Muscle and Myogenesis**. Excerpta Medica, Amsterdam. The Netherlands: pp157-164.

Turegon ML. 1988. **Clinical Haematology: Theory and Procedures** 1st Ed., Lippincott Williams & Wilkins,pp 71-74.

Utomo DN, Mahyudin F, Hemugrahanto KD, Suroto H, Chilmi MZ, and Rantam FA. 2018. Implantation of platelet rich fibrin and allogenic mesenchymal stem cells facilitate the healing of muscle injury: An experimental study on animal. *Inter J Surgery Open*, **11**:4-6.

Vogelstein B, Bloom BR, Goodman CS, King PA, Mckhann GM, Weisfeldt ML, Merikangas KR, Sharples FE, Pellmar TC, Schoen R A, Joy JE, Avila B, Holliday L, Sweatt D, and Grossblatt N. 2002. The stem cell and the future of regenerative medicine. The Natural Academy Press.

Weissman IL. 2002. Translating stem and progenitor cell biology to the clinic: Barriers and opportunities. *Science*, **2000**; 287: 1442-1446.

Yarom R, Behar A J, Yanko L, Hall T, and Peters P. 1976. Gold tracer studies of muscle regeneration. *J Neuro Pathol Exp Neurol*, **35**: 445-457.

JJBS

Volume 12, Number 1,March 2019
ISSN 1995-6673
Pages 61 - 65

Jordan Journal of Biological Sciences

IgA Nephropathy in Northern Jordan: Evaluation Using the MEST-C Score of Oxford Classification System

Najla H. Aldaoud[1*], Bayan A. Alzumaili [1], Raya D. Marji[1], Muna M. Alhusban[2], Hadil Y. Zureigat[2], Ashraf O. Oweis [3] and Ismail I. Matalka[1]

[1]*Department of Pathology and Microbiology, King Abdullah University Hospital and Jordan University of Science and Technology, P.O. Box (3030) Irbid, 22110;* [2]*The University of Jordan , School of Medicine, Amman;* [3]*Division of Nephrology, Department of Medicine, Jordan University of Science and Technology, Irbid, Jordan,*

Received June 2, 2018; Revised July 7, 2018; Accepted July 18, 2018

Abstract

IgA nephropathy (IgAN) is the most common primary glomerular disease worldwide. However, predicting prognosis from the histopathological evaluation of a tissue biopsy has not been well-established until recently. The aim of this research is to evaluate IgAN patients in Northern Jordan by the MEST-C score of Oxford Classification System. Clinical data and histopathology reports of twenty-seven patients diagnosed with IgAN were retrospectively reviewed. These data were retrieved from the electronic health information system of King Abdullah University hospital. The results showed a male predominance (70 %) and a mean age of (24 ± 16) years at diagnosis. MEST-C Oxford classification was as follows: five (18.5 %) patients had mesangial hypercellularity (M1), six (22.2 %) patients had endo-capillary hypercellularity (E1), eight (29.6 %) patients had segmental glomerulosclerosis (S1), four (14.8 %) patients had interstitial fibrosis/tubular atrophy (IFTA) score of (T1) and (0 %) had a score of (T2). As for crescents, three (11.1 %) had (C1) and one (3.7 %) had (C2). A significant negative correlation was found between the final estimated glomerular filtration rate (eGFR) at follow-up and the total MEST-C score (Spearman's Rho = 0.460, $p<0.05$). Histopathological parameters represented by the MEST-C Score of Oxford Classification can predict outcome in the study's cohort, and is similar to previous published studies.

Keywords: IgA Nephropathy, MEST-C score, Oxford classification, Northern Jordan.

1. Introduction

IgA nephropathy (IgAN) is the most common primary glomerular disease worldwide (D'Amico, 1987). Its prevalence is notably high in South East Asia, where IgAN is the diagnosis in 30–50 % of renal biopsies (Schena, 1990). Clinical presentation of IgAN ranges from persistent microscopic hematuria to a rapidly progressive renal failure, but its progression is generally slow with up to a 30 % of the patients progressing to end-stage renal disease (ESRD) within twenty years (D'Amico *et al*., 1987; Moriyama *et al*., 2014).

Nephrologists use clinical information to identify major risk factors for the progression of IgAN to distinguish cases of IgAN that carry a good prognosis from those who exhibit a progressive course and eventually might need renal replacement therapy. These risk factors include age, the extent of proteinuria, low glomerular filtration rate at first presentation, and hypertension (D'Amico, 2004)

On the other hand, predicting prognosis from the histopathological evaluation of a tissue biopsy has not been well-established until recently. Oxford Classification of IgA nephropathy is the most accepted classification and the most utilized one by practicing nephropathologists. This system identifies the following key predictors in the biopsy that can serve as prognostic markers, (MEST-C score): M, mesangial hypercellularity; E, endocapillary proliferation; S, segmental glomerulosclerosis and/or adhesion; T, tubular atrophy and interstitial fibrosis; and C, cellular or fibrocellular crescents. Each of the previous histologic parameters was found to be independently associated with a clinical renal outcome (Cattran *et al*., 2009; Roberts *et al*., 2009; Trimarchi *et al*., 2017).

The aim of this study is to describe the histopathologic features of IgAN patients in Northern Jordan using MEST-C score of Oxford classification system of IgAN, and to report the correlation between the histopathological lesions and clinical presentation at the time of the renal biopsy and on follow-up.

2. Patients and Methods

Twenty-seven kidney biopsies for twenty-seven patients were reviewed. All cases were presented to King Abdullah University Hospital, Irbid, Jordan, and have been diagnosed with primary IgAN in the period between 2004 and 2017. The diagnosis of IgA nephropathy was confirmed by Hematoxylin and eosin stain (H&E) histological examination and by Immunofluorescence studies. Patients with a clinical history of Henoch Schonlein purpura and renal biopsies with fewer than six

* Corresponding author. e-mail: naglaadaoud@yahoo.com.

identifiable glomeruli were excluded from the study. All cases were reviewed and scored using the MEST-C score of the Oxford Classification of IgAN (Cattran *et al.*, 2009; Trimarchi *et al.*, 2017). Clinical and laboratory data were retrieved from King Abdullah University hospital medical records. Laboratory tests carried out at time of diagnosis included urine dipstick protein, serum creatinine and eGFR (estimated Glomerular Filtration Rate), calculated by Chronic Kidney Disease Epidemiology equation (CKD-EPI equation) and were recorded. Serum creatinine and eGFR were available for twenty-three patients only and the same tests were repeated on follow-up. Proteinuria was measured using the protein dipstick test and was available for twenty-two patients only at the time of the diagnosis and on follow- up. This study was approved by the Institutional Review Board of Deanship of Research at Jordan University of Science and Technology under research grant number 20180225.

2.1. Statistical Analysis:

The mean values and standard deviations were calculated, and the statistical significance of the differences between groups was calculated using independent t test and Chi-square. The Spearman's co-efficient of correlation was used to check the correlation between the total MEST-C score and the final e-GFR. SPSS IBM 23 was used for statistical analysis. $P < 0.05$ was considered statistically significant.

3. Results

3.1. Patients' Characteristics

Among the twenty-seven patients, nineteen (70.4 %) were males and eight (29.6 %) were females. The patients' age ranged from one year to sixty-six years with a mean of ± SD of 24.0 ± 16.7 (median = 21). The follow-up period ranged from 1.2 months to 13.3 years. The mean age of females was 22.9 (± 17.9), while the mean age of males was 24.4 (±16.6). Table 1 summarizes the baseline characteristics of the twenty-seven patients.

Table 1. Baseline characteristics of the study cohort of 27 patients with IgA nephropathy**.**

Variable	N (%)
Age, mean ±SD	24.0 ± 16.7
Sex: Male	19 (70.4%)
Female	8 (29.6%)
Follow up,(Years), mean ±SD	3.9 ± 3.7
eGFR ml/min/1.73m^2, mean ±SD	90 ± 47.4

eGFR: estimated glomerular filtration rate

3.2. Clinical Features and Laboratory Results at Presentation and During Follow –up.

In the study's small cohort, the patients' age (P=0.03), not their sex (P=0.62), had an effect on eGFR. The mean serum creatinine level for the twenty-three patients was 107.7µmol/L ± 97.7 with a median of 74 µmol/L. The mean ± S.D serum creatinine for the females was 136.3 µmol/L ± 158 (median 63), while that of males was 95.3 µmol/L ± 58.8 (median=76.5). The eGFR at diagnosis was 90 mL/min ± 47.4 (median=89). Proteinuria detected by dipstick urine analysis showed a significant effect on eGFR (P=0.046); one patient (4.5 %) showed trace, five (22.7 %) had a score of 1+, 3 (13.6 %) a score of 2+ and 8 (36.4 %) a score of 3+, while no protein was found in five patients (22.7 %).

The eGFR at follow-up had a mean value of 91.7 ml/min ± 44.5 (median=98). Serum creatinine at follow-up had a mean value of 132.4 µmol/L ± 163.1 (median=69). As for the twenty-two patients with a record of proteinuria, on follow-up, nine showed no proteinuria (40.9 %), one showed trace (4.5 %), five showed 1+ (22.7 %), six showed 2+ (27.3 %) and one showed 3+ (4.5 %).

Out of the twenty-three patients, five (21.7 %) patients had chronic kidney disease (CKD) stages 3-5 (eGFR<60 mL/min/1.73m^2) at presentation, three (60 %) were males and two were females (40 %). Their mean age was 27±14.2 (median=33).The clinical characteristics and MEST-C score classification for these five patients is summarized in Table 2. During follow-up, two (8.7 %) patients developed CKD (stages 3-5) (eGFR<60 mL/ min/ 1.73m^2) upon a follow-up period of four to five years; their mean age was 43.5±31.8 and both were males. Their mean serum creatinine at diagnosis was 115.5 µmol/L ±26.2, and the serum creatinine on follow-up had a mean of 322.5 µmol/L ± 238.3. Their MEST-C scores were (M0, E0, S1, T1, C0) and (M0, E1, S1, T0, C1), respectively.

Although the mean age of patients with C0 score was lower than the mean age of those with a C1 score (21 years for C0 VS 41 years for C1), the difference was not statistically significant (P=0.056). In an attempt to correlate the total MEST-C score to laboratory parameters, the score variables were added together, producing a total score for each patient, and this value was correlated with the laboratory findings. A significant negative correlation was found between the final eGFR at follow-up, and the total MEST-C score (Spearman's Rho =0.460, P<0.05). It seems that those who initially had extensive involvement of glomeruli on initial biopsy end up with a worse prognosis as reflected by their low eGFR at follow-up. Older patients were found to have lower eGFR (Spearman Rho=-0.475, P<0.05) and higher creatinine (Spearman Rho=0.576, P<0.05) levels at follow-up. The Chi Square test yielded a significant association between the degree of interstitial fibrosis and tubular atrophy (IFTA) and segmental glomerulosclerosis (P<0.05).

3.3. MEST-C Score

MEST-C Scoring System was performed on all the twenty-seven renal biopsies; the number of glomeruli ranged between six and fifty-five with a median of fourteen glomeruli per biopsy. Mesangial hypercellularity was found in all biopsies, twenty-two (81.5 %) in 50 % of glomeruli or less (M0) and five (18.5 %) patients had mesangial hypercellularity in greater than 50 % of the glomeruli (M1). Twenty-one (77.8 %) had E0 and six (22.2%) patients had endocapillary hypercellularity (E1). Nineteen (70.4 %) had a score of S0, while eight (29.6 %) had a score of S1. twenty-three (85.2 %) had a score of T0, four had T1 (14.8 %) and no cases had T2 (0 %). As for crescents, twenty-three (85.2 %) had a score of C0, three (11.1 %) had C1 and one had C2 (3.7 %). Table 3 summarizes the clinical and histological variables in the renal biopsies of the twenty-seven patients with comparison with other studies.

Table 2. Clinicopathologic characteristics of the 5 patients with CKD stage (3-5) at presentation.

Clinicopathologic variable	Value
Age at presentation mean ±SD	27±14.2
Male : Female	3:2
Mean serum creatinine at diagnosis	115.5 μmol/L±26.2
Mean serum creatinine at follow up	322.5 μmol/L±238.3
Mesangial hypercellularity score	
≤0.5 (M0)	4(80%)
>0.5 (M1)	1(20%)
Endocapillary hyercellularity score	
Absent (E0)	4(80%)
Present (E1)	1(20%)
Segmental glomerulosclerosis	
Absent (S0)	2(40%)
Present (S1)	3(60%)
Tubularatrophy/interstitial score	
≤25% (T0)	2(40%)
26-50% (T1)	3 (60%)
>50% (T2)	0(0%)
Crescents	
Absent (C0)	4(80%)
≤25% (C1)	1(20%)
>25% (C2)	0(0%)

CKD, chronic kidney disease

Table 3. A comparison of both the clinical and histopathological parameters in the current study and the largest cohorts for patients with IgA nephropathy.

Variables	Our study	Oxford cohort* (2009)	Zeng *et al** (2012)	Moriyama *et al* (2014)	VALIGA cohort (2014)
Age (mean ±SD, years)	24±16	30 (4–73)†	34 (18-73)†	33±12	36±16
Sex M:F	60:40	72:28	50:50	40:60	73:27
Follow-up (mean, years)	3.83±3.7	5 (1–22)†	4.4(0.6-14)†	7.9±7.1	4.7(2.4-7.9)†
eGFR initially (mL/min/1.73m2)	90±47	83±36	85 ±32	78.5±26	73±30
CKD (stage 3-5) at presentation	21.7 %	*	*	24%	37%
Progression to CKD or ESRD	8.7%	22%, 13%¥	15%, 8.8%¥	-	14%, 12%¥
MEST-C Score at diagnosis					
M1	18.5%	81%	43%	47.6%	28%
E1	22.2%	42%	11%	44.3%	11%
S1	29.6%	76%	83%	74.6%	70%
T1	14.8%	30%	24%	23.0%	17.4%
T2	0%	5%	3.3%	5.8%	3.6%
C1	11.1%	-	48%‡	6.7%‡	11%‡
C2	3.7%	-	2.4%	-	-
Total number of patients	27	256	1026	1012	1147

eGFR, estimated glomerular filtration date; CKD, chronic kidney disease; ESRD, end-stage renal disease, M, mesangial hypercellularity; E, endocapillary hypercellularity; S, segmental glomerulosclerosis; T, tubular atrophy and interstitial fibrosis; C, crescents

** Inclusion criteria were an initial (eGFR) >30 mL/min/1.73 m2 and an initial proteinuria with protein excretion >0.5 g/24 h.*

† Median.

¥ The two numbers represent 50% decrease in eGFR (%) and ESRD (<15ml/min per 1.73m2) (%) respectively;

‡ C1 or C2.

4. Discussion

IgAN is the most common type of glomerulonephritis worldwide (D'Amico, 1987). Although IgAN is slowly progressive, it is not a benign disease. There have been several classification systems suggested in the past in an attempt to improve the capability to predict the outcome of the patients and guide their therapy (Alamartine *et al*., 1990; Haas, 1997; Katafuchi *et al.*, 1998; H. Lee *et al*., 2012; Radford *et al.*, 1997; Wakai *et al*., 2006).

Since 2009, the Oxford classification of IgAN has been widely used and accepted by both pathologists and nephrologists. It has been proven in many studies that the pathological features: mesangial hypercellularity, endocapillary hypercellularity, segmental glomerulus-clerosis and the extent of tubular atrophy/interstitial fibrosis are independently predictive of the clinical outcome (Cattran *et al.*, 2009; Coppo *et al*., 2014; Roberts *et al.*, 2009).

Furthermore, Barbour *et al* (Barbour *et al*., 2016), using a large international cohort, examined whether combining the MEST score with cross-sectional clinical data at biopsy provides earlier risk prediction in IgAN than the current best methods that use two years of follow-up data. Their work showed that the combination of MEST score with readily available blood pressure, proteinuria, and eGFR at the time of biopsy predicted the composite renal outcome similar to using clinical data over two years of follow-up.

The patients' age in the present study had a mean of twenty-four years old at presentation with nearly 30 % of them being ten years of age or younger. Similar results have been shown by D'Amico *et al* (2004) who reviewed the largest IgAN studies in the literature; six of them from Europe, Asia and North America. The mean age in their study ranged between twenty-two and twenty-seven years old. On the other hand, in the present study, the mean age at presentation is slightly lower than that of the largest three cohorts of IgAN in the literature (Coppo *et al*., 2014; Moriyama *et al*., 2014; Zeng *et al.*, 2012) with the mean age ranging between thirty-three and thirty-six years.

In North American studies of IgAN, the male to female ratio was about 2:1 for children and adults (Wyatt *et al*., 1998). In addition, most studies on Caucasian population showed male predominance (Coppo *et al.*, 2014; Galla, 1995; Schena, 1990), whereas the ratio is nearly 1:1 in Asia (Le *et al.*, 2012; Lee *et al*., 2012; Moriyama *et al*., 2014; Zeng *et al*., 2012). The current study also found also male predominance as shown by North American and Caucasian series.

This study found that about 30 % of the patients with CKD of the stages three to five (eGFR<60 mL/min/1.73m^2) at the time of diagnosis were above thirty years old. But, if all age groups included; this percentage will go down to 21.7 %, with a male predominance and a mean age of twenty-seven years at the presentation. This percentage is lower than that of the large VALIGA cohort (n = 1147), including mostly Italian patients, where they found that 37 % of their patients presented with CKD at the stage three to five (Coppo *et al.*, 2014).

Older patients were found to have lower eGFR and higher serum creatinine levels at follow-up in this study. Having said that, it is known that a slight increase in the eGFR is expected at an advanced age due to anatomical,

functional and physiological changes in the aging kidneys (Douville *et al.*, 2009; Glassock and Rule, 2012). Moriyama *et al* (Moriyama *et al*., 2014) showed that old age at presentation using univariate analysis is associated with the risk of progression to an end-stage renal disease. But the multivariate Cox regression analysis showed that it was insignificant, and so was the factor of being male (Moriyama *et al.*, 2014). Moreover, it was shown that both the older age at presentation and being a male are weak predictors as clinical prognostic factors according to the most accurate studies in the literature analyzed by D'Amico (D'Amico, 2004).

During initial follow-up, clinical indicators as urine dipstick protein levels showed improvement with various treatments, where (36.4 %) of the patients had a score of 3+, and only (22.7 %) had no protein in their urine at presentation. During further follow-up only (4.5 %) showed 3+ urine protein level and about (41 %) showed no proteinuria. Cattran *et al* and the Oxford Group had an improvement in proteinuria on follow-up, with proteinuria of 1.7 (0.5–18.5) g/day at the time of biopsy and 1.1 (0.1–9.3) g/day levels on follow-up (Cattran *et al.,* 2009). So did the VALIGA cohort, with proteinuria of 1.3 (0.6–2.6) g/day at the time of biopsy and 0.8 (0.4–1.6) g/day levels on follow-up (Coppo *et al.,* 2014). Zeng *et al.,* (2012) found also similar values.

In any kind of injury (including immune-complexes as in IgA Nephropathy), an inflammatory response is initiated (as hypercellularity or crescent formation) as a healing process that may lead to renal recovery without significant damage, or to glomerular scars and / or interstitial fibrosis with clinical manifestation of worsening renal function(Lee and Kalluri, 2010)

Regarding the Oxford MEST-C classification, our renal biopsies showed the following percentages: five (18.5 %) patients had mesangial hypercellularity in greater than 50 % of the glomeruli (M1), six (22.2 %) patients had endocapillary hypercellularity (E1), eight (29.6 %) patients had segmental glomerulosclerosis (S1), four (14.8 %) patients had interstitial fibrosis/tubular atrophy score of (T1) and (0 %) had a score of (T2). As for crescents, three (11.1 %) had (C1) and one (3.7 %) had (C2). A comparison of the current results with the Oxford cohort (Cattran *et al.*, 2009; Roberts *et al.*, 2009) and the largest three cohorts reported in the literature for patients with IgAN(Coppo *et al*., 2014; Moriyama *et al.*, 2014; Zeng *et al*., 2012) is shown in Table 3, with both clinical and histopathological data included.

Although clinical data in this study, including initial eGFR, initial CKD (stages 3-5) patients and progression to CKD or ESRD upon follow-up showed lower percentages than those provided by the aforementioned cohorts, these relatively milder clinical presentations are consistent with a milder MEST-C Oxford classification scores than most of the scores provided by the same cohorts.

The present study showed that those who initially had extensive involvement of glomeruli on initial biopsy end up with worse prognosis as reflected by their low eGFR at follow-up. In fact, this is consistent with the Oxford group results (Cattran *et al*., 2009; Roberts *et al.*, 2009) that were validated in the much larger VALIGA cohort - that also came with less restricted inclusion criteria – where they showed that histological signs of chronic and irreversible damage had the strongest association with an unfavorable outcome (Coppo *et al.*, 2014).

The present study had the following limitations; first, it is a retrospective observational review. Second, though the selected center is a tertiary referral teaching hospital, the number of patients included is relatively small (only 27 patients) and larger numbers should be included in future studies.

5. Conclusion

This is the first–ever study of IgA nephropathy profile in a single tertiary referral teaching hospital in Northern Jordan. It showed that histopathological damage of the glomeruli using the MEST-C Score of Oxford Classification, age of the patients, and proteinuria are associated with a worse outcome. The selected patients showed milder MEST-C scores than most of the scores provided by the large cohorts.

Future studies with a larger number of patients and including different geographic areas in Jordan are recommended. These studies might highlight the possibility of familial clustering and geographic variations which can be further compared with profiles from the Levant region.

Acknowledgment

This study was approved by the Institutional Review Board of Deanship of Research; Jordan University of Science and Technology, under research grant number 20180225.

References

Alamartine E, Sabatier J Cand Berthoux F C. 1990. Comparison of pathological lesions on repeated renal biopsies in 73 patients with primary IgA glomerulonephritis: value of quantitative scoring and approach to final prognosis. *Clin Nephrol.*, **34(2)**: 45-51.

Barbour S J, Espino-Hernandez G, Reich H N, Coppo R. Roberts I S, Feehally J, Herzenberg A M and Cattran D C. 2016. The MEST score provides earlier risk prediction in lgA nephropathy. *Kidney Int.*, **89(1)**: 167-175.

Cattran D C, Coppo R, Cook H T, Feehally J, Roberts I S, Troyanov S, Alpers C E, Amore A, Barratt J, Berthoux F, Bonsib S, Bruijn J A, D'Agati V, D'Amico G, Emancipator S, Emma F, Ferrario F, Fervenza F C, Florquin S, Fogo A, Geddes C C, Groene H J, Haas M, Herzenberg A M, Hill P A, Hogg R J, Hsu S I, Jennette J C, Joh K, Julian B A, Kawamura T, Lai F M, Leung C B, Li L S, Li P K, Liu Z H, Mackinnon B, Mezzano S, Schena F P, Tomino Y, Walker P D, Wang H, Weening J J, Yoshikawa N and Zhang H. 2009. The Oxford classification of IgA nephropathy: rationale, clinicopathological correlations, and classification. *Kidney Int.*, **76(5)**: 534-545.

Coppo R, Troyanov S, Bellur S, Cattran D, Cook H T, Feehally J, Roberts I S, Morando L, Camilla R, Tesar V, Lunberg S, Gesualdo L, Emma F, Rollino C, Amore A, Praga M, Feriozzi S, Segoloni G, Pani A, Cancarini G, Durlik M, Moggia E, Mazzucco G, Giannakakis C, Honsova E, Sundelin B B, Di Palma A M, Ferrario F, Gutierrez E, Asunis A M, Barratt J, Tardanico Rand Perkowska-Ptasinska A. 2014. Validation of the Oxford classification of IgA nephropathy in cohorts with different presentations and treatments. *Kidney Int.*, ***86*(4)**: 828-836.

D'Amico G. 1987. The commonest glomerulonephritis in the world: IgA nephropathy. *Q J Med.*, **64(245)**: 709-727.

D'Amico G. 2004. Natural history of idiopathic IgA nephropathy and factors predictive of disease outcome. *Semin Nephrol.*, **24(3)**: 179-196.

D'Amico G, Colasanti G, Barbiano di Belgioioso G, Fellin G, Ragni A, Egidi F, Radaelli L, Fogazzi G, Ponticelli CandMinetti L. 1987. Long-term follow-up of IgA mesangial nephropathy: clinico-histological study in 374 patients. *Semin Nephrol.,* **7(4):** 355-358.

Douville P, Martel A R, Talbot J, Desmeules S, Langlois Sand Agharazii M. 2009. Impact of age on glomerular filtration estimates. *Nephrol Dial Trans.*, **24(1)**: 97-103.

Galla J H. 1995. IgA nephropathy. *Kidney Int.*, **47(2)**: 377-387.

[Glassock R Jand Rule A D. 2012. The implications of anatomical and functional changes of the aging kidney: with an emphasis on the glomeruli. *Kidney Int.,* **82(3)**: 270-277.

Haas M. 1997. Histologic subclassification of IgA nephropathy: a clinicopathologic study of 244 cases. *Am J Kidney Dis,* **29(6)**: 829-842.

Katafuchi R, Kiyoshi Y, Oh Y, Uesugi N, Ikeda K, Yanase Tand Fujimi S. 1998. Glomerular score as a prognosticator in IgA nephropathy: its usefulness and limitation. *Clin Nephrol.,* **49(1)**: 1-8.

Le W, Liang S, Hu Y, Deng K, Bao H, Zeng Cand Liu Z. 2012. Long-term renal survival and related risk factors in patients with IgA nephropathy: results from a cohort of 1155 cases in a Chinese adult population. *Nephrol Dial Trans.*, **27(4)**: 1479-1485.

Lee H, Kim D K, Oh K H, Joo K W, Kim Y S, Chae D W, Kim Sand Chin H J. 2012. Mortality of IgA nephropathy patients: a single center experience over 30 years. *PLoS One,* **7(12)**: e51225.

Lee S Band Kalluri R. 2010. Mechanistic connection between inflammation and fibrosis. *Kidney Int Suppl.*,**(119)**, S22-26.

Moriyama T, Tanaka K, Iwasaki C, Oshima Y, Ochi A, Kataoka H, Itabashi M, Takei T, Uchida Kand Nitta K. 2014. Prognosis in IgA nephropathy: 30-year analysis of 1,012 patients at a single center in Japan. *PLoS One,* **9(3):** e91756.

[Radford M G, Jr, Donadio J V, Jr, Bergstralh E Jand Grande J P. 1997. Predicting renal outcome in IgA nephropathy. *J Am Soc Nephrol.*, **8(2)**: 199-207.

Roberts I S, Cook H T, Troyanov S, Alpers C E, Amore A, Barratt J, Berthoux F, Bonsib S, Bruijn J A, Cattran D C, Coppo R, D'Agati V, D'Amico G, Emancipator S, Emma F, Feehally J, Ferrario F, Fervenza F C, Florquin S, Fogo A, Geddes C C, Groene H J, Haas M, Herzenberg A M, Hill P A, Hogg R J, Hsu S I, Jennette J C, Joh K, Julian B A, Kawamura T, Lai F M, Li L S, Li P K, Liu Z H, Mackinnon B, Mezzano S, Schena F P, Tomino Y, Walker P D, Wang H, Weening J J, Yoshikawa Nand Zhang H. 2009. The Oxford classification of IgA nephropathy: pathology definitions, correlations, and reproducibility. *Kidney Int.,* **76(5):** 546-556.

Schena F P. 1990. A retrospective analysis of the natural history of primary IgA nephropathy worldwide. *Am J Med.,* **89(2)**: 209-215.

Trimarchi H, Barratt J, Cattran D C, Cook H T, Coppo R, Haas M, Liu Z H, Roberts I S, Yuzawa Y, Zhang Hand Feehally J. 2017. Oxford Classification of IgA nephropathy 2016: an update from the IgA Nephropathy Classification Working Group. *Kidney Int.,* **91(5)**: 1014-1021.

Wakai K, Kawamura T, Endoh M, Kojima M, Tomino Y, Tamakoshi A, Ohno Y, Inaba Yand Sakai H. 2006. A scoring system to predict renal outcome in IgA nephropathy: from a nationwide prospective study. *Nephrol Dial Trans.,* **21(10):** 2800-2808**.**

Wyatt R J, Julian B A, Baehler R W, Stafford C C, McMorrow R G, Ferguson T, Jackson E, Woodford S Y, Miller P Mand Kritchevsky S. 1998. Epidemiology of IgA nephropathy in central and eastern Kentucky for the period 1975 through 1994. Central Kentucky Region of the Southeastern United States IgA Nephropathy DATABANK Project. *J Am Soc Nephrol.,* **9(5)**: 853-858.

Zeng C H, Le W, Ni Z, Zhang M, Miao L, Luo P, Wang R, Lv Z, Chen J, Tian J, Chen N, Pan X, Fu P, Hu Z, Wang L, Fan Q, Zheng H, Zhang D, Wang Y, Huo Y, Lin H, Chen S, Sun S, Wang Y, Liu Z, Liu D, Ma L, Pan T, Zhang A, Jiang X, Xing C, Sun B, Zhou Q, Tang W, Liu F, Liu Y, Liang S, Xu F, Huang Q, Shen H, Wang J, Shyr Y, Phillips S, Troyanov S, Fogo Aand Liu Z H. 2012. A multicenter application and evaluation of the oxford classification of IgA nephropathy in adult chinese patients. *Am J Kidney Dis.,* **60(5)**: 812-820.

JJBS

Volume 12, Number 1,March 2019
ISSN 1995-6673
Pages 67 - 75

Jordan Journal of Biological Sciences

The Importance of Foliar Anatomy in the Taxonomy of the Genus *Alocasia* (Schott) G. Don

Oluwabunmi O. Arogundade* and Olubukola Adedeji

Department of Botany, Obafemi Awolowo University, Ile-Ife, Nigeria.

Received June 13, 2018; Revised July 23, 2018; Accepted August 4, 2018

Abstract

The anatomy of the epidermis, transverse sections of the leaves and petioles of three species of *Alocasia* (Schott) G. Don in Nigeria were examined in this study in order to report any anatomical characters of taxonomic importance among them. The species are *Alocasia cucullata* (Lour.) Schott, *A. macrorrhiza* (L.) G. Don, and *A. plumbea* (Schott) G. Don. Standard procedures were followed in preparing the epidermal peels, transverse sections of the leaves, and the three regions of the petiole: proximal, median and distal regions. Generic characters among the species include polygonal to irregular epidermal cell shape, a straight anticlinal wall pattern, elliptic and circular-shaped stomata, brachyparacytic stomatal complex type, round abaxial petiole outline and the presence of druses, raphides, and starch grains in the petiole. The presence of peltate trichomes on the adaxial surface of *A. cucullata* as well as additional anomocytic stomata complex on both of its surfaces and mucilaginous cells in *A. plumbea* which are the diagnostic features were discussed. Other diagnostic features include the presence of druses on the abaxial surfaces of *A. macrorrhiza* and *A. plumbea*, highest stomata index in *A. macrorrhiza*, collenchyma type, tannins and adaxial petiole outline. The *Alocasia* species can be separated based on their leaf anatomical features.

Keywords: *Alocasia*, Leaf anatomy, Mesophyll, Mucilaginous cells, Petiole anatomy, Stomatal complex, Trichome.

1. Introduction

Alocasia (Schott) G. Don, tribe Colocasieae, is a genus of broad-leaved rhizomatous perennials in the Family *Araceae*. Their leaves are usually glossy, and they can be easily identified wherever they grow (Bown, 2000). The genus has been reported to be the largest in the family with about one-hundred species distributed in the tropical, subtropical and temperate regions of the world (Boyce, 2008).

Species of this genus are also found growing in different habitats and exhibiting diverse habits. An example is *Alocasia macrorrhiza* which grows as a weed or as a creeping plant with aerial roots to help support it. The same plant is wild in Malaysia and is naturalized in many areas of the tropics. Another *Alocasia* with the ability to climb and produce aerial roots is *A. amazonica*, which is available for cultivation under the name African Mask. Some other species of *Alocasia* including *A. cucullata*, *A. sanderiana* (also known as Kris Plant, a native of the Philippine Islands), and *A. plumbea* are being cultivated as houseplants and ornamentals, and are naturalized throughout the tropics (Bown, 2000; Ivancic *et al*., 2009).

The morphological attributes of the members of this genus have been variously described (Hussey and Keighery, 1997; Bown, 2000). The large cordate to hastate, occasionally peltate (especially in juveniles) leaves grow to a length of 20 - 90 cm on long petioles. The thick, glossy leaves often have marked margins or colourful midribs and veins. *Alocasia* species may flower at any time during the growing season. Flowers are spathe about 4½ inches long which grow at the end of a short stalk, but are not conspicuous; often hidden behind the leaf petioles (Hussey and Keighery, 1997). Suratman and Suranto, (2016) evaluated the morphological, anatomical and isozyme variation among twenty accessions of giant taro (*A. macrorrhiza* (L.) G. Don) from different collection sites in Central Java (Indonesia). Chromosome number 2n = 28, 42, 56, 70 and 84 has been reported for the genus *Alocasia* (Mayo *et al*., 1997); this affirms that polyploidy occurs in the genus.

This work is intended to fill the knowledge gap in the area of foliar and petiole anatomy of the genus *Alocasia*. Three species found growing in the South Western part of Nigeria were used for this research. They are *Alocasia cucullata* (Lour.) Schott, *Alocasia macrorrhiza* (L.) G. Don and *Alocasia plumbea* (Schott) G. Don.

2. Materials and Methods

2.1. Epidermal Studies

The scrape technique of Metcalfe (1960) adopted by Arogundade and Adedeji (2016) was used to obtain the epidermal peels of both the adaxial and abaxial surfaces of the leaves. The median portion of well-expanded leaves

* Corresponding author. e-mail: : oluwabunmiarogundade@gmail.com; okeesano@oauife.edu.ng.

were peeled by placing the desired epidermal surface face down on a glass slide and then all tissues above the required epidermis were scraped off with a sharp blade. The epidermal peels were then stained in 1 % aqueous Safranin O, and mounted in dilute glycerine for microscopic examination. Photomicrographs of the epidermis were taken for both the adaxial and the abaxial surfaces.

The epidermal cell shape, anticlinal cell wall pattern, and stomata type were studied. The epidermal cell area was calculated by multiplying the length and width of the epidermal cells. Also calculated was the Stomata Indices (S.I) for the two surfaces using the formula below according to Metcalfe and Chalk (1979):

$$S.I = \frac{S}{S + E} \times 100$$

Where S.I = Stomata Index

S = Number of stomata

E = Number of ordinary epidermal cells plus the subsidiary cells in the same unit area.

2.2. Transverse Sections of the Leaf and the Petiole

The transverse sections of the leaves and the three regions of the petiole - the proximal, median and distal regions of the tree species were cut with the aid of a Reichert sliding microtome at a thickness of 8 – 15 µm. The sections were stained with Safranin O, and counter-stained with Alcian blue. After that, they were made to pass through a series of ethanol (50, 70, 80, 90 % and absolute) for differentiation and dehydration. The sections were then mounted in 25 % dilute glycerin solution for examination under the microscope.

2.3. Microscopy

Observation and examination of the peels and sections were made using Olympus XSZ-107BN light microscope. Photomicrographs of the sections were made using photo micrographic apparatus- microscope with built-in-camera optics.

3. Results

3.1. Epidermal Studies

Tables 1 and 2 give the summary of the important qualitative and quantitative foliar epidermal features of the adaxial and abaxial surfaces of the species respectively. Figure 1 shows the photomicrographs of the two surfaces for all the species.

Table 1. Summary of important qualitative foliar epidermal features of the adaxial and abaxial surfaces of the studied species

Species	Surface	Epidermal cell shape	Anticlinal wall pattern	Stomata shape	Stomata type	Other features on surface
A. cucullata	Adaxial	Polygonal	Straight	Elliptic, Circular	Brachyparacytic Anomocytic	Scales
	Abaxial	Polygonal to Irregular	Straight	Elliptic, Circular	Brachyparacytic Anomocytic	Nil
A. macrorrhiza	Adaxial	Polygonal to Irregular	Straight	Elliptic, Circular	Brachyparacytic	Nil
	Abaxial	Polygonal to Irregular	Straight to wavy	Elliptic, Circular	Brachyparacytic Anomocytic	Druses
A. plumbea	Adaxial	Polygonal to Irregular	Straight	Elliptic, Circular	Brachyparacytic	Nil
	Abaxial	Polygonal to Irregular	Straight	Elliptic, Circular	Brachyparacytic Anomocytic	Mucilaginous cells and Druses

Table 2. Summary of important quantitative foliar epidermal features of the adaxial and abaxial surfaces of the studied species

Species	Surface	Epidermal area (µm^2)			Stomata area (µm^2)			Stomata index (%)		
		Minimum value	Maximum value	Mean value	Minimum value	Maximum value	Mean value	Minimum value	Maximum value	Mean value
A. cucullata	Adaxial	523.6	935.0	720.12	214.2	306.0	275.81	2.33	6.25	3.64
	Abaxial	510.0	1142.4	768.94	238.0	336.6	274.31	7.62	10.64	9.24
A. macrorrhiza	Adaxial	374.0	680.0	532.85	190.4	299.2	229.98	5.84	8.70	7.41
	Abaxial	224.4	816.0	489.74	183.6	272.0	244.53	8.98	12.36	10.34
A. plumbea	Adaxial	299.2	822.8	526.32	183.6	272.0	217.87	4.29	6.56	5.40
	Abaxial	336.6	856.8	565.22	238.0	336.6	282.61	8.21	12.59	10.82

3.1.1. A. cucullata

On the adaxial surface, epidermal cells are largely polygonal with a straight anticlinal wall. They vary in size, shape, and arrangement. The epidermal cell area ranges between 523.6 µm^2-935.0 µm^2; with a mean value of 720.12 µm^2. The leaf is amphistomatous and stomata are restricted to the non-venous regions; brachyparacytic occasionally anomocytic, elliptic in shape, occasionally circular. Stomata size ranges between 214.2 µm^2 -306.0 µm^2; with a mean value of 275.81 µm^{2,} and the stomata index ranges between 2.33 -

6.25 %; with a mean value of 3.64 %. Scales are present (Figure 1 A and B).

On the abaxial surface, epidermal cells are largely polygonal, occasionally irregular with a straight anticlinal wall. They vary in size, shape and arrangement. Epidermal cell area ranges between 510.0 μm^2- 1142.4 μm^2 with a mean value of 768.94 μm^2. Stomata are restricted to the non-venous regions; brachyparacytic occasionally anomocytic, and they are elliptic in shape, occasionally circular (Figure 1C). Stomata size ranges between 238.0 μm^2 -336.6 μm^2 with a mean value of 274.31 $\mu m^{2,}$ and the stomata index ranges between 7.62 - 10.64 % with a mean value of 9.24 %.

3.1.2. A. macrorrhiza

On the adaxial surface, epidermal cells are polygonal to occasionally irregular with a straight anticlinal wall. They vary in size, shape and arrangement. The epidermal cell area ranges between 374.0 μm^2-680.0 μm^2 with a mean value of 532.85 μm^2. Leaf is amphistomatous and stomata are restricted to the non-venous regions; brachy-paracytic, elliptic in shape, occasionally circular (Figure 1D). Stomata size ranges between 190.4 μm^2 - 299.2 μm^2 with a mean value of 229.98 $\mu m^{2,}$ and the stomata index ranges between 5.84 - 8.70% with mean value of 7.41%.

On the abaxial surface, epidermal cells are polygonal to occasionally irregular with a straight to wavy anticlinal wall. They vary in size, shape and arrangement. Epidermal cell area ranges between 224.4 μm^2-816.0 μm^2 with a mean value of 489.74 μm^2. Stomata are restricted to the non-venous regions; they are brachyparacytic, occasionally anomocytic, and are elliptic in shape, occasionally circular. Stomata size ranges between 183.6 μm^2 -272.0 $\mu m^{2,}$ with a mean value of 244.53 $\mu m^{2,}$ and stomata index ranges between 8.98 - 12.36 % with a mean value of 10.34 %. Druses are present (Figure 1E).

3.1.3. A. plumbea

On the adaxial surface, epidermal cells are polygonal to irregular with a straight anticlinal wall. They vary in size, shape and arrangement. Epidermal cell area ranges between 299.2 μm^2 - 822.8 μm^2 with a mean value of 526.32 μm^2. The leaf is amphistomatous, and stomata are restricted to the non-venous regions; they are brachyparacytic and elliptic in shape, occasionally circular (Figure 1F). Stomata size ranges between 183.6 μm^2 – 272.0 μm^2 with a mean value of 217.87 $\mu m^{2,}$ and stomata index ranges between 4.29 – 6.56 % with mean value of 5.40 %.

On the abaxial surface, epidermal cells are polygonal to irregular with a straight anticlinal wall. They vary in size, shape and arrangement. Epidermal cell area ranges between 336.8 μm^2 - 856.8 μm^2 with mean value of 565.22 μm^2. Stomata are restricted to the non-venous regions; they are brachyparacytic, occasionally anomocytic. Shape is elliptic, occasionally circular. Stomata size ranges between 238.0 μm^2 - 336.6 μm^2 with a mean value of 282.61 $\mu m^{2,}$ and stomata index ranges between 8.21 - 12.59 % with a mean value of 10.82 %. Mucilaginous cells and druses are present (Figure 1G).

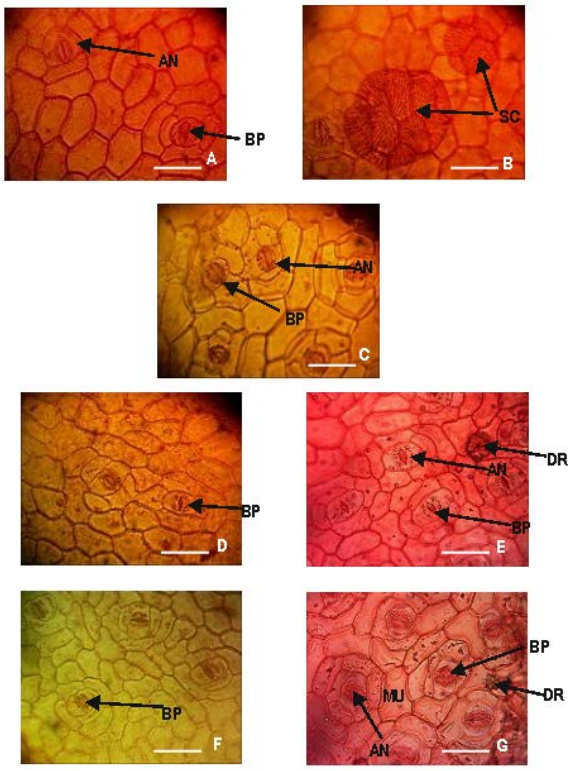

Figure 1. Genus *Alocasia* – Leaf epidermal surfaces

A and B. Adaxial epidermis of lamina of *A. cucullata;* C. Abaxial epidermis of lamina of *A. cucullata;* D. Adaxial epidermis of lamina of *A. macrorrhiza;* E. Abaxial epidermis of lamina of *A. macrorrhiza;* F. Adaxial epidermis of lamina of *A. plumbea;* G. Abaxial epidermis of lamina of *A. plumbea*

Legend: **BP**-Brachyparacytic stomata, **AN**-Anomocytic stomata

SC-Scales, **MU**-Mucilaginous cell Scale bar: A –G = 125 µm

3.2. Transverse Sections of the Leaf

A summary of the important features of the transverse sections of the leaf is shown in Table 3 while the photomicrographs are shown through Figures 2, 3 and 4.

3.2.1. A. cucullata

The Upper and lower epidermis are one-layered with uniseriate cells. Palisade and spongy layers are differentiated. The mesophyll thickness ranges from 134 µm to 268 µm. Palisade mesophyll cells are present only on the upper surface of the leaf and the mid-rib. They are cylindrical in shape, and packed together while the spongy mesophyll cells are oval to oblong or irregular in shape with air spaces in between them. Angular collenchyma cells are present in the mid-rib, and the vascular bundle type is Collateral. Few raphides and druses are present (Figure 2 A- H).

3.2.2. A. macrorrhiza

The upper and lower epidermis are both one-layered with uniseriate cells. Palisade and spongy layers are differentiated. The mesophyll thickness ranges from 174.2 µm to 294.8 µm. Palisade mesophyll cells are present only on the upper surface of the leaf, and the mid-rib. They are cylindrical in shape, and packed together. On the other hand, the spongy mesophyll cells are oval to oblong or irregular in shape with air spaces between them. Lacunar collenchyma cells are present in the mid-rib, and

the vascular bundle type is Collateral. Raphides, druses, tannins, and starch grains are present. (Figure 3 A - H).

3.2.3. A. plumbea

The upper and lower epidermis are both one-layered with uniseriate cells. The mesophyll thickness ranges from 187.6 µm to 348.4 µm. Palisade and spongy layers are differentiated. Palisade mesophyll cells are present only on the upper surface of the leaf and the mid-rib. They are cylindrical in shape and packed together, while the spongy mesophyll cells are oval to oblong or irregular in shape with air spaces between them. Lacunar collenchyma cells are present in the mid-rib, and the vascular bundle type is Collateral. Druses, an abundance of raphides and starch grains are present. (Figure 4 A - G).

Table 3. Summary of the Features on the Transverse Section of the Leaves of the *Alocasia* studied Species.

Characters / Species	No. of Cells of Upper & Lower Epidermis	Collenchyma Cell Type	No. of Layers of Palisade Mesophyll	Mesophyll Thickness			Raphides (+/-)	Druses (+/-)	Tannins (+/-)	Starch grains (+/-)
				Minimum (µm)	Maximum (µm)	Average (µm)				
A. cucullata	1	Angular	1-2	134.0	268.0	180.63	+	+	-	-
A. macrorrhiza	1	Lacunar	1-2	174.2	294.8	209.93	+	+	+	+
A. plumbea	1	Lacunar	1-2	187.6	348.4	248.70	+	+	-	+

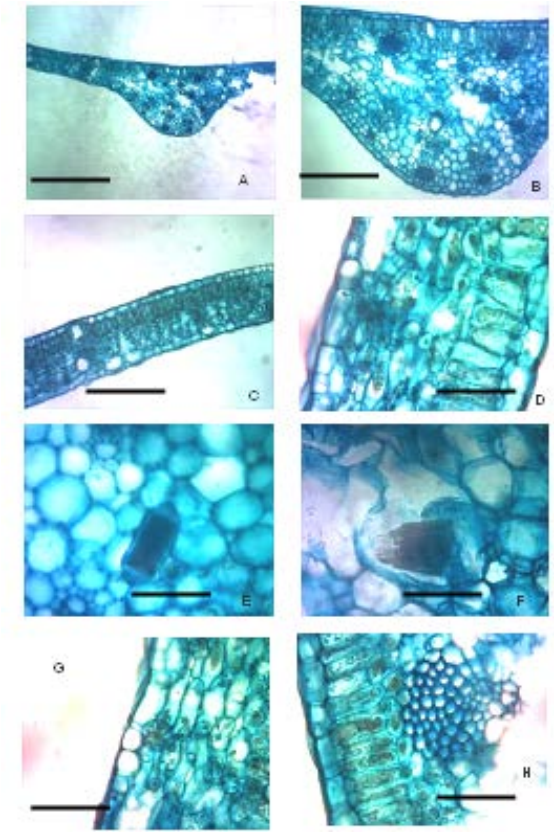

Figure 2.Transverse Section of the Leaf of *A. cucullata* A - Outline of transverse section. B - Mid-rib region. C - Leaf lamina. D - Leaf lamina. E & F - Raphides. G – Druses. H - Palisade layer and angular collenchyma cells.
Scale bars: A= 15 µm, B= 40 µm, C-F= 120 µm.

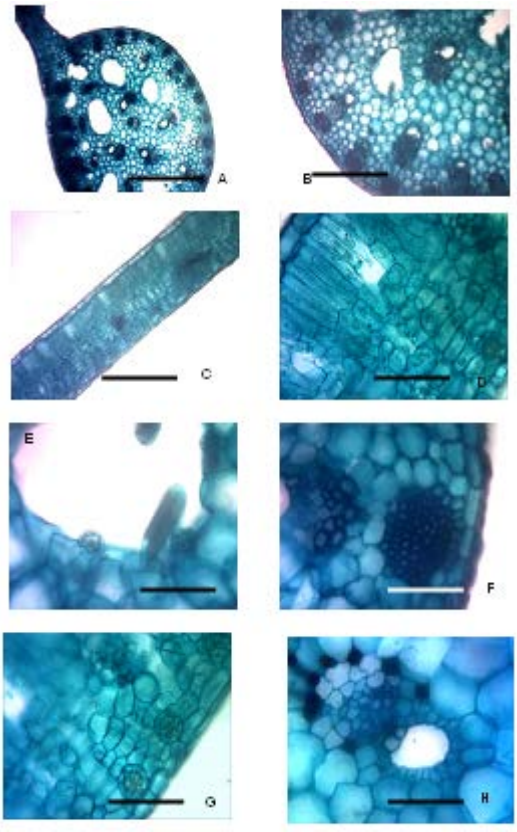

Figure 3. Transverse Section of the Leaf of *A. macrorrhiza* A - Outline of transverse section. B - Mid-rib region. C - Leaf lamina. D - Leaf lamina. E - Raphides and druses. F - Lacunar collenchyma cells. G – Druses. H - Vascular bundle and tannins
Scale bars: A= 15 µm, B= 40 µm, C-H= 120 µm.

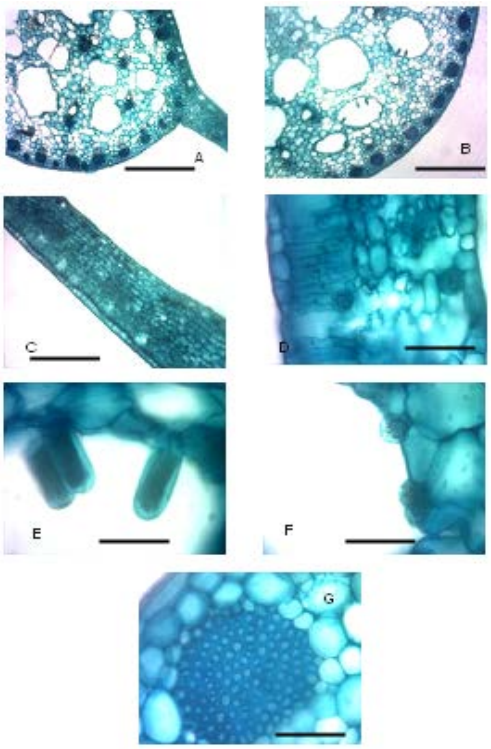

Figure 4. **Transverse Section of the Leaf of *A. plumbea*** A - Transect of the outline of transverse section. B - Transect of the mid-rib region. C - Leaf lamina. D - Leaf lamina. E - Raphides. F – Druses. G - Lacunar collenchyma cells. Scale bars: A= 15 µm, B= 40 µm, C-G= 120 µm

3.3. Transverse Sections of the Three Regions of the Petioles

3.3.1. A. cucullata

Proximal region: The petiole outline is circular. The epidermis is one-layered with uniseriate cells. The cortex is made up of one to five layers of parenchyma cells; the angular collenchyma cells occur as discontinuous bundles, and are separated by parenchyma cells. Collenchyma cells are present on both the adaxial and abaxial surfaces. Air spaces are present, and are surrounded by parenchyma cells. Vascular bundles are collateral, and are scattered throughout the ground tissue. The xylem is surrounded by xylem parenchyma. Cell inclusions include spindle-shaped raphides. Druses are absent **(**Figure 5 A - G).

Median region: The petiole outline is circular. The epidermis is one-layered with uniseriate cells. The cortex is composed of one to five layers of parenchyma cells; angular collenchyma cells occur as discontinuous bundles, and are separated by parenchyma cells. Collenchyma cells are present on both the adaxial and abaxial surfaces. Air spaces are present and are surrounded by parenchyma cells. Vascular bundles are collateral, and are scattered throughout the ground tissue. The xylem is surrounded by xylem parenchyma. Cell inclusions include spindle-shaped raphides, druses, and starch grains **(**Figure 6 A - G).

Distal region: The adaxial outline of the petiole is concave, while the abaxial outline is round. The epidermis is one-layered with uniseriate cells. The cortex is composed of one to five layers of parenchyma cells; angular collenchyma cells occur as discontinuous bundles on both the adaxial and abaxial surfaces. The collenchyma cells are separated by parenchyma cells. Air spaces are present, and are surrounded by parenchyma cells. Vascular bundles are collateral, and are scattered throughout the ground tissue. The xylem is surrounded by xylem parenchyma. Cell inclusions include Unmodified and spindle-shaped raphides, druses, and starch grains **(**Figure 7 A - H).

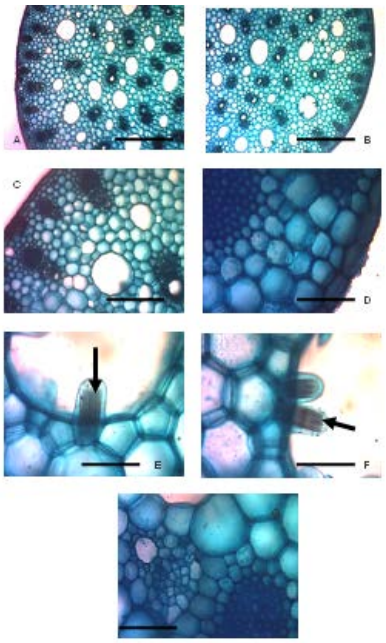

Figure 5. Proximal region of *A. cucullata*
A - Abaxial outline of petiole. B - Adaxial outline of petiole. C & D - Petiole transects. E &F - Spindle-shaped raphides (Arrowed). G - Vascular bundle. Scale bars: A & B= 10 µm, C = 30 µm, D–G=100 µm

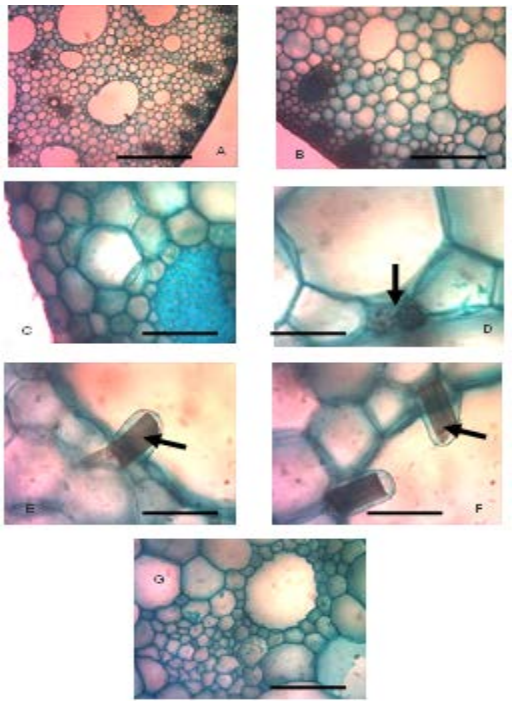

Figure 6. Median region of *A. cucullata* A - Outline of petiole. B & C - Petiole transects. D - Druses (Arrowed). E & F - Spindle-shaped raphides (Arrowed). G - Vascular bundle. Scale bars: A = 10 µm, B = 30 µm, C – G = 100 µm.

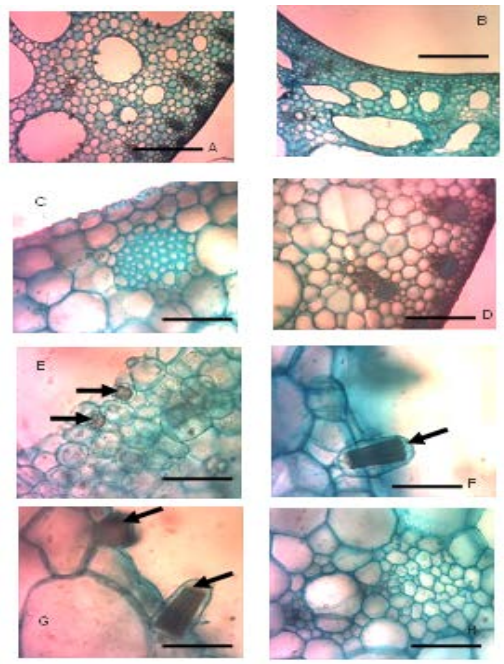

Figure 7. Distal region of A. cucullata

A - Abaxial outline of petiole. B - Adaxial outline of petiole. C & D - Petiole transects. E - Druses (Arrowed). F & G - Spindle-shaped and unmodified raphides (Arrowed). H - Vascular bundle. Scale bars: A & B= 10 µm, C = 30 µm, D–H=100 µm

3.3.2. A. macrorrhiza

Proximal region: The adaxial outline of the petiole is convex, while the abaxial outline is round. The epidermis is one-layered with uniseriate cells. The cortex is composed of one to six layers of parenchyma cells; lacunar collenchyma cells occur as discontinuous bundles and are separated by parenchyma cells. Collenchyma cells are present on both the adaxial and abaxial surfaces. Air spaces are present, and are surrounded by parenchyma cells. Vascular bundles are collateral, and are scattered throughout the ground tissue. The xylem is surrounded by xylem parenchyma. Cell inclusions include spindle-shaped raphides, druses, tannins, and starch grains **(**Figure 8 A - H).

Median region: The adaxial outline of the petiole is convex, while the abaxial outline is round. The epidermis is one-layered with uniseriate cells. The cortex is composed of one to six layers of parenchyma cells; lacunar collenchyma cells occur as discontinuous bundles and separated by parenchyma cells. Collenchyma cells are present on the abaxial surface only. Air spaces are present, and are surrounded by parenchyma cells. Vascular bundles are collateral and are scattered throughout the ground tissue. The xylem is surrounded by xylem parenchyma. Cell inclusions include spindle-shaped raphides, druses, tannins, and starch grains **(**Figure 9 A - G).

Distal region: The adaxial outline of the petiole is concave, while the abaxial outline is round. The epidermis is one-layered with uniseriate cells. The cortex is composed of one to five layers of parenchyma cell; lacunar collenchyma cells occur as discontinuous bundles, and separated by parenchyma cells. Collenchyma cells are present on the abaxial surface only. Air spaces are present, and are surrounded by parenchyma cells. Vascular bundles are collateral and are scattered throughout the ground tissue. The xylem is surrounded by xylem parenchyma. Cell inclusions include spindle-shaped raphides, druses, and starch grains **(**Figure 10 A - H).

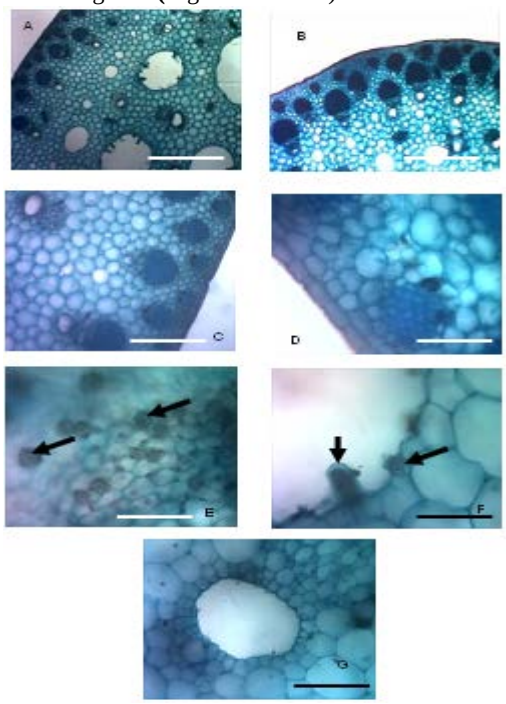

Figure 8. Proximal region of *A. macrorrhiza*

A - Abaxial outline of petiole. B - Adaxial outline of petiole. C & D- Petiole transects. E - Spindle-shaped raphides (Arrowed). F - Spindle-shaped raphide and druse (Arrowed). G - Druse (Arrowed). H - Vascular bundle. Scale bars: A & B= 10 µm, C = 30 µm, D–H=100 µm

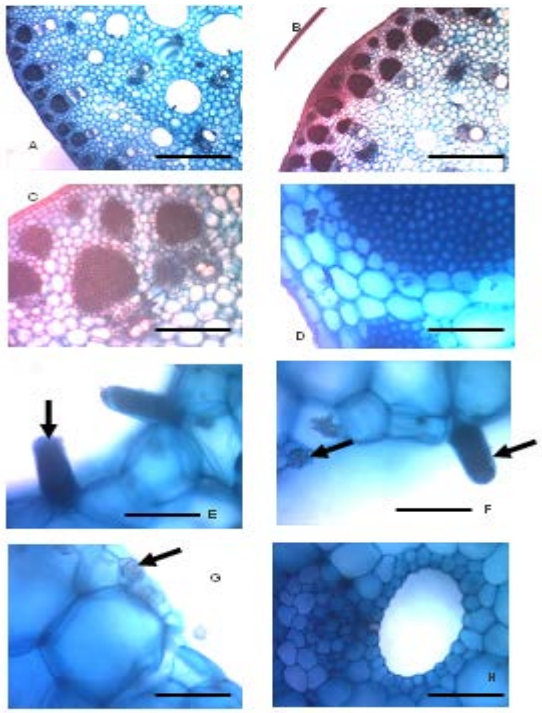

Figure 9. Median region of *A. macrorrhiza* A - Abaxial outline of petiole. B - Adaxial outline of petiole. C & D - Petiole transect. E - Druses (Arrowed). F - Spindle-shaped raphide and druse. G - Vascular bundle. Scale bars: A & B= 10 µm, C = 30 µm, D–G=100 µm

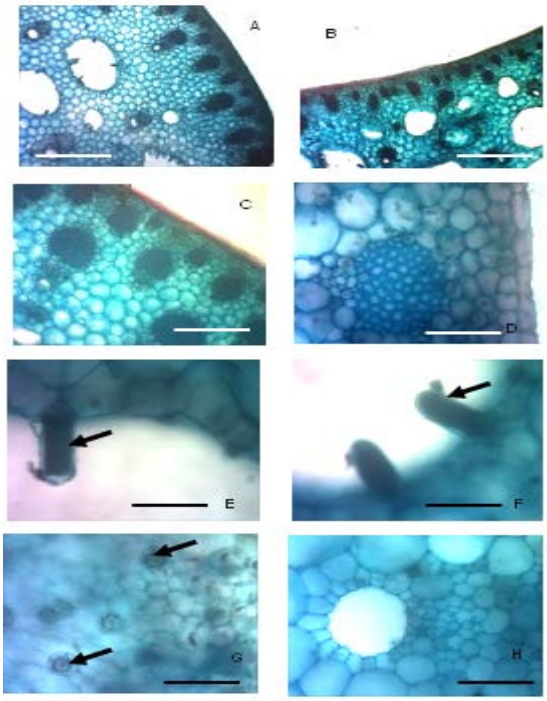

Figure 10 .Distal region of *A. macrorrhiza* A - Abaxial outline of petiole. B - Adaxial outline of petiole. C & D - Petiole transect. E & F - Spindle-shaped raphides (Arrowed). G - Druses in the region (Arrowed). H - Vascular bundle. Scale bars: A & B= 10 µm, C = 30 µm, D–H=100 µm.

3.3.3. A. plumbea

Proximal region: The adaxial outline of the petiole is flat, while the abaxial outline is round. The epidermis is one-layered with uniseriate cells. The cortex is composed of one to six layers of parenchyma cells; lacunar collenchyma cells occur as discontinuous bundles, and are separated by parenchyma cells. Collenchyma cells are present on both the adaxial and abaxial surfaces. Air spaces are present, and are surrounded by parenchyma cells. Vascular bundles are collateral, and are scattered throughout the ground tissue. The xylem is surrounded by xylem parenchyma. Cell inclusions include numerous spindle-shaped raphides, very few druses, and starch grains **(**Figure 11 A - H).

Median region: The adaxial outline of the petiole is concave, while the abaxial outline is round. The epidermis is one-layered with uniseriate cells. The cortex is composed of one to six layers of parenchyma cells; lacunar collenchyma cells occur as discontinuous bundles, and are separated by parenchyma cells. Collenchyma cells are present on the abaxial surface only. Air spaces are present, and are surrounded by parenchyma cells. Vascular bundles are collateral, and are scattered throughout the ground tissue. The xylem is surrounded by xylem parenchyma. Cell inclusions include numerous spindle-shaped raphides, very few druses, and starch grains **(**Figure 12 A - G).

Distal region: The adaxial outline of the petiole is concave, while the abaxial outline is round. The epidermis is one-layered with uniseriate cells. The cortex is composed of one to seven layers of parenchyma cells; lacunar collenchyma cells occur as discontinuous bundles, and are separated by parenchyma cells. Collenchyma cells are present on the abaxial surface only. Air spaces are present, and are surrounded by parenchyma cells. Vascular bundles are collateral, and are scattered throughout the ground tissue. The xylem is surrounded by xylem parenchyma. Cell inclusions include numerous spindle-shaped raphides, druses, and starch grains **(**Figure 13 A - H).

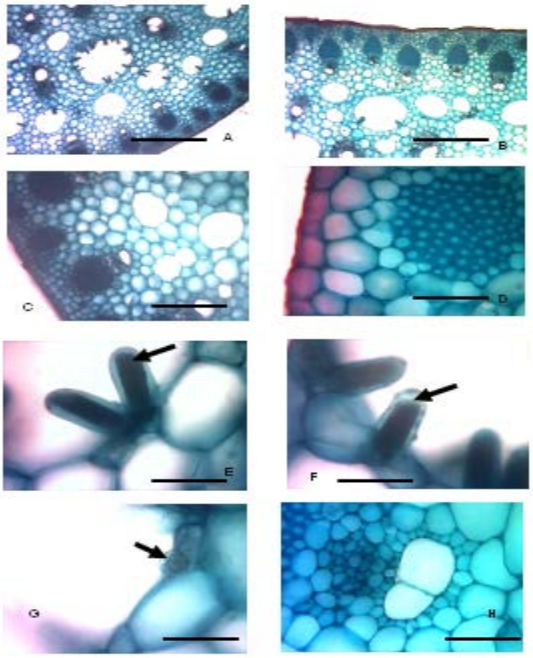

Figure 11. Proximal region of *A. plumbea* A - Abaxial outline of petiole. B - Adaxial outline of petiole. C & D - Petiole transects. E & F - Spindle-shaped raphides (Arrowed). G - Druse (Arrowed).H - Vascular bundle. Scale bars: A & B= 10 µm, C = 30 µm, D–H=100 µm.

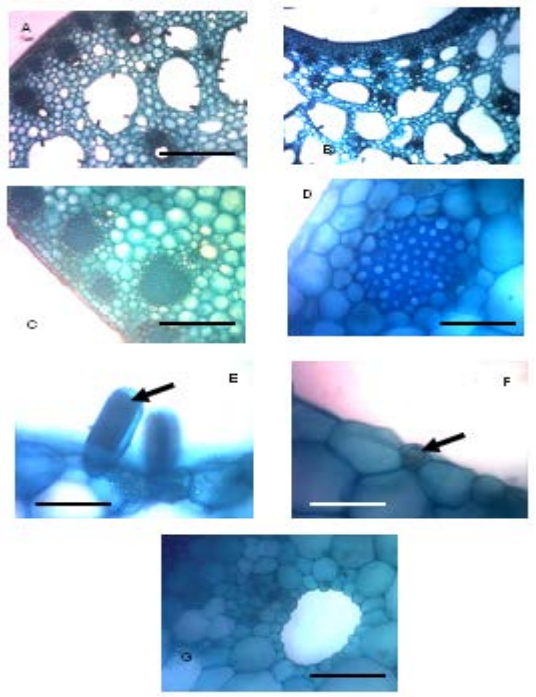

Figure 12. Median region of *A. plumbea* A - Abaxial outline of petiole. B - Adaxial outline of petiole. C & D - Petiole transects. E - Spindle-shaped raphides (Arrowed). F - Druses (Arrowed). G - Vascular bundle Scale bars: A & B= 10 µm, C = 30 µm, D–G=100µm.

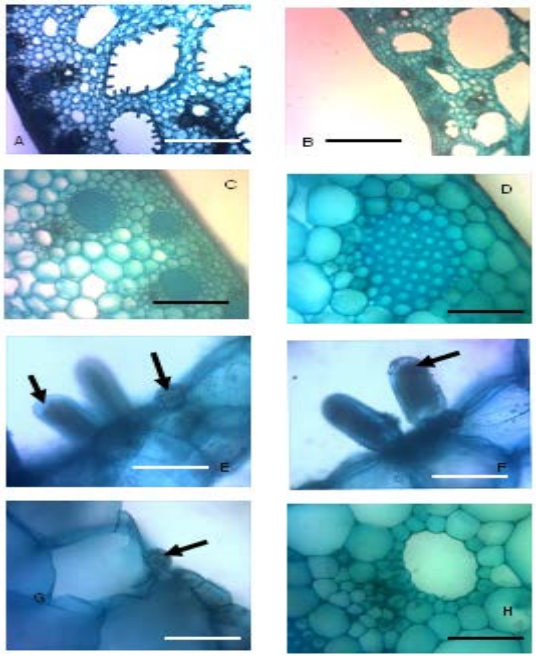

Figure 13. Distal region of *A. plumbea* A - Abaxial outline of petiole. B - Adaxial outline of petiole. C & D - Petiole transects. E - Spindle-shaped raphides and druse (Arrowed). F - Spindle-shaped raphides (Arrowed).G - Druse (Arrowed). H - Vascular bundle. Scale bars: A & B= 10 µm, C = 30 µm, D–H=100 µm.

4. Discussion

The epidermal characters of the three species of *Alocasia* show more similarities than differences. This is actually expected since the three species are of the same genus. They all have polygonal to irregular epidermal cell shape, a straight anticlinal wall pattern, elliptic and circular-shaped stomata as well as brachyparacytic stomatal complex types. The few exceptions to these include the polygonal epidermal cell shape found only on the adaxial surface of *A. cucullata*, additional wavy anticlinal wall patterns found on the abaxial surface of *A. macrorrhiza*, and additional anomocytic stomatal complex found on both surfaces of *A. cucullata* and the abaxial surfaces of the other two species, that is, *A. macrorrhiza* and *A. plumbea*. In as much as the frequency of stomata can be affected by the environment, the specific stomata types are only determined by genetic factors (Hetherington and Woodward, 2003). Therefore, the species of *Alocasia* in this study can be separated based on the stomatal complex type. *A. cucullata* is the only species with anomocytic stomatal type on both the adaxial and abaxial leaf epidermal surfaces.

Suratman and Suranto (2016) conducted an anatomical epidermal research on twenty accessions of *A. macrorrhiza* (Giant Taro) in Indonesia, and reported the absence of stomata on the adaxial surfaces. This is contrary to the findings of this research. Brachyparacytic stomata are present on the adaxial surface of *A. macrorrhiza* and, interestingly, the stomata index is the highest on this same surface when compared with the other two species in this study. One factor that could be responsible for this observation is the fact that all the *A. macrorrhiza* accessions used for this study were found growing in water-logged areas, so the higher stomata index is an indicator for higher transpiration rate. On the whole, there were more stomata on the abaxial surfaces than on the adaxial surfaces of all the species. Higher stomata frequency on abaxial surfaces in most plant species have been confirmed by several researchers (Muradoglu and Gundogdu, 2011; Suratman and Suranto, 2016). Mean epidermal cell area was higher on the abaxial surfaces of *A. cucullata* and *A. plumbea* which is a deviation from the usual adaxial epidermal cell area higher than the abaxial epidermal cell area.

Mucilaginous cells were found occurring on the abaxial surface of *Alocasia plumbea* as distinct cells from the other epidermal cells. This is most likely responsible for the slimy nature of the leaves on squeezing, and clearly separates *Alocasia plumbea* from the other two species of the studied *Alocasia*. According to Bredenkamp and VanWyk (1999), mucilage in plants plays a role in the storage of water and food, seed germination and membrane thickening. Druses of calcium oxalate crystals were found on the abaxial surfaces of *A. macrorrhiza* and *A. plumbea*, but not on any of the surfaces of *A. cucullata*. This is another important foliar epidermal delimiting feature among the species. Adedeji and Illoh (2004) also separated some species of *Hibiscus* based on the presence of druses in them.

Scales, a type of trichome, also known as peltate hair, were encountered on the adaxial surface of *A. cucullata* bringing a clear-cut demarcation between *Alocasia cucullata* and the other two species of the *Alocasia* in this study. Trichomes function in the reduction of the heating effect of sunlight, thereby controlling the rate of transpiration in plants where they occur (Pandey, 2007). Trichomes types have been used severally in the classification of genera and even species (Gravano *et al*., 1998; Adedeji and Illoh, 2004; Fróes *et al*., 2015). Ina and Eka (2013) also separated some species of *Alocasia* in Indonesia based on the presence of multicellular trichome in just one of the ten species studied.

An interesting aspect of this research is the observation of definitive ways by which each of the species of *Alocasia* maintain its water retaining capacity. Each of these species has a unique feature on its epidermis which enables it to adapt to its environment in terms of water conservation. *A. cucullata* possess scales on its adaxial surface in order to reduce transpiration rate; *A. macrorrhiza* found growing in water-logged areas have the highest stomata index so as to increase its transpiration rate and *A. plumbea* possess mucilaginous cells in order to conserve more water in its system. These distinctive features are very important in the taxonomy of the genus.

The transverse sections of the leaves of the *Alocasia* species studied are similar in the number of upper and lower epidermal layers, the presence of palisade mesophyll on the adaxial surface of the mid-rib, differentiated palisade and spongy mesophyll layers, the number of palisade mesophyll layers in the leaf lamina and the presence of calcium oxalate crystals - raphides and druses. Notwithstanding, there are qualitative and quantitative features that can be employed in the delimitation of the species. Angular collenchyma cells, found in the transverse sections of the leaf of *A. cucullata* only, delimit it from the other two species with lacunar collenchyma

type. Tannins were also observed on the lamina surface of *A. macrorrhiza* only. Tannins are non-nitrogenous complex compounds, and are the derivatives of phenols (Pandey, 2007). Their primary function is to serve as protection for plants against injury, decay termites, and pests (Simpson, 2010). The highest mesophyll thickness was encountered in *A. plumbea*, and the least was seen in *A. cucullata*.

The adaxial outline of the petioles presents a delimiting feature among the species studied as it ranges from concave to flat to round and then to a convex outline. Two different combinations of each of these outlines were found in each of the species. It is round in the proximal and median regions of *A. cucullata*, and concave in the distal region. It is convex in the proximal and median regions of *A. macrorrhiza*, and concave in the distal region. It was found to be flat in the proximal region of *A. plumbea* and concave in the median and distal regions. The abaxial petiole outline, on the other hand, is a unifying feature as it is round in all the species. The distribution of cells in the transverse section of the three regions of the petioles of the *Alocasia* species is similar to that of the leaf. A one-layered epidermis with uniseriate cells was found in all the species. Also the exact collenchyma cell types present in the leaves were found in the petioles, and tannins were encountered only in *A. macrorrhiza*. These can also be employed in separating the species. Collateral vascular bundles scattered in the ground tissues were found in the three regions of all the species studied, and all the xylem cells are surrounded by xylem parenchyma. This affirms the monocotyledonous status of the genus *Alocasia* (Fahn, 1974; Simpson, 2010).

5. Conclusion

This study concludes that the species of *Alocasia* can be classified using the foliar anatomical characters such as the presence of peltate trichomes, mucilaginous cells, anomocytic stomata type, angular collenchyma cells, tannins, and adaxial petiole outline. Each of the three studied species was observed to have developed some unique features in order to improve or maintain their water retaining capacity. All these features are quiet diagnostic in the taxonomy of the species.

Acknowledgements

The researchers appreciate the efforts of Dr. A.J. Akinloye and Mr. Abiodun Omole and their assistance in sectioning the plant samples.

References

Adedeji O and Illoh HC. 2004. Comparative foliar anatomy of ten species in the genus *Hibiscus* L. in Nigeria. *New Botanists* **31**:147-180.

Arogundade OO and Adedeji O. 2016. Foliar Epidermal Study of some Species of *Aglaonema* Schott (Araceae) in Nigeria. *Ife J Sci.*, **18(1)**:293–303.

Bown D. 2000. **Aroids: Plants of the Arum Family.** Timber Press, Portland, Oregon.

Boyce C. 2008. A review of *Alocasia* (Araceae: Colocasieae) for Thailand including a novel species and new species' records from S.W. Thailand. *Thai Forest Bull.*, **36**: 1-17.

Bredenkamp CL and VanWyk AE. 1999. Structure of mucilaginous epidermal cell walls in *Passerina* (Thymelaeaceae). *Botanical J Linnean Soc.*, **129**: 223-238.

Fahn A. 1974. **Plant Anatomy** (Second Revised Edition). Pergamon Press Ltd, Oxford, England. P. 7.

Fróes FFP, Gama TSS, Feio AC, Demarco D and Aguiar-dias ACA. 2015. Structure and distribution of glandular trichomes in three species of Bignoniaceae. *Acta Amazonica* **45(4)**: 347 – 354

Gravano E., Tani C., Bennici A. and Gucci R. 1998. The Ultrastructure of Glandular Trichomes of *Phillyrea latifolia* L. (Oleaceae) Leaves *Annals of Bot.*, **81**: 327 335.

Hetherington AM and Woodward FI. 2003. The role of stomata in sensing and driving environmental change. *Nature* **424**: 901-908.

Hussey BMJ and Keighery GJ. 1997. **Western weeds: a guide to the weeds of Western Australia.** Plant Protection Society of Western Australia. Victoria Park, Western Australia.

Ina E and Eka FT. 2013. Leaf surface comparison of three genera of Araceae in Indonesia. *Buletin Kebun Raya* **16 (2)**: 131-145.

Ivancic A, Roupsard O, Garcia JQ, Sisko M, Krajnc AU and Lebot V. 2009. Topology of thermogenic tissues of *Alocasia macrorrhizos* (Araceae) inflorescences. *Botany* **87**: 1232-1241.

Kay DE. 1987. **Root Crops**. Second Edition (Revised by E.G.B. Gooding). Tropical Development and Research Institute, London.

Kumoro AC, Budiyati CS and Retnowati DS. 2014. Calcium oxalate reduction during soaking of giant taro (*Alocasia macrorrhiza* (L.) Schott) corm chips in sodium bicarbonate solution. *Inter Food Res J.*, **21(4)**: 1583-1588.

Manner HI. 2011. Farm and Forestry Production and Marketing Profile for Giant Taro (*Alocasia macrorrhiza*). In: Elevitch CR (ed.). **Specialty Crops for Pacific Island Agroforestry**. Permanent Agriculture Resources (PAR), Holualoa, Hawai'i.

Mayo S, Bogner J and Boyce PC. 1997. **The Genera of *Araceae***. Royal Botanic Gardens, Kew, Surrey, UK.

Metcalfe CR and Chalk L. 1979. **Anatomy of Dicotyledons**. (2nd Ed.)Vol.1, Oxford University Press, New York.

Metcalfe CR. 1960. **Anatomy of Monocotyledons**. I. Gramineae. Clarendon Press, Oxford.

Muradoglu F and Gundogdu M. 2011. Stomata size and frequency in some walnut (*Juglans regia*) cultivars. *Inter J Agri Biol.*, **13**: 1011-1015.

Pandey BP. 2007. **Plant Anatomy**. S. Chand and Company Limited, Ram Nagar, New Delhi.

Simpson MG. 2010. **Plant Systematics**. Second Edition. Elsevier Academic Press, Amsterdam.

Suratman AP and Suranto SK. 2016. Morphological, anatomical and isozyme variation among giant taro (*Alocasia macrorrhizos*) accessions from Central Java, Indonesia. *Biodiversitas* **17(2)**: 422-429.

JJBS

Jordan Journal of Biological Sciences

Volume 12, Number 1,March 2019
ISSN 1995-6673
Pages 77 - 82

Investigation of rs121918356 and rs121918355 *LTBP2* Mutations and LTBP2 Serum Levels in Primary Congenital Glaucoma in a Sample of Iraqi Children

Salwa H. N. Al-Ruba'ei[1*], Suzanne Jubair[2], Ali N. M. Al-Sharifi[3] and Mohanned M. B. Al-Moosawi[4]

[1] Mustansiriyah University, College of Science, Chemistry Department, Baghdad; [2] University of Kerbala, College of Pharmacy, Kerbala; [3] Ibn Al-Haitham Teaching Eye Hospital; [4]Central Public Health Laboratory, Baghdad, Iraq

Received June 26, 2018; Revised July 17, 2018; Accepted July 25, 2018

Abstract

Primary congenital glaucoma (PCG) is a severe type of glaucoma which occurs early in life and is a leading cause of blindness in early childhood. Latent Transforming beta Binding Protein 2 (*LTBP2*) gene is reported to be a PCG-related gene. This study is designed to investigate the involvement of *LTBP2* mutations (rs121918356 and rs121918355) in the PCG incidence in a sample of Iraqi children, and determine the *LTBP2* protein both in the patients and the control groups. Venous blood was collected from one-hundred child patients diagnosed with PCG and one-hundred healthy children. Genomic DNA was extracted, and two DNA fragments concerning the two mutations were amplified. The mutations were followed up using the restriction fragment length polymorphism technique and direct sequencing. Serum LTBP2 protein was measured using ELISA technique. No mutation was detected in any of the examined samples. A highly significant (p=0.0001) elevated serum LTBP2 protein was observed in the patients' group compared to the control group. In conclusion, *LTBP2* mutations (rs121918356 and rs121918355) are not related to the PCG in the Iraqi population. The PCG patients have higher LTBP2 protein levels compared to the healthy controls.

Keywords: Primary congenital glaucoma (PCG), LTBP2 gene, LTBP2 protein, Iraqi children, Q111X mutation, R299X mutation.

1. Introduction

Glaucoma involves a group of ocular disorders including optic nerve disintegration (Fan *et al*., 2006) and when left untreated, irreversible and permanent loss of vision can occur (Ray *et al*., 2003; Zhou *et al*., 2017). The optic nerve disintegration includes damage of retinal ganglion cells. Destruction of the retinal ganglion cells results in loss of visual field (Sarfarazi, 1997). Affecting almost sixty-five million people, glaucoma is considered as the second major reason of blindness in the world (Quigley, 1996). It is classified into three major types according to etiology, age of onset, and the anatomy of the anterior chamber (Ray *et al*., 2003). These are: primary congenital glaucoma (PCG), closed angle glaucoma, and primary open-angle glaucoma (Mohanty *et al*., 2013; Faiq *et al*., 2013). PCG is a severe type of glaucoma which occurs early in life (seen up to 3 years) (Shohdy *et al*., 2017) and is a leading reason for blindness in early childhood. PCG is featured by a developing anomaly of the trabecular meshwork (TM) which lies in the anterior chamber angle of the eye causing an elevated intraocular pressure (IOP), which leads to optic nerve damage and irreversible vision loss (Achary *et al*.,2006; Sarfarazi and Stoilov, 2000). PCG is inherited in an autosomal recessive pattern, and it is more prevalent in communities with a high ratio of consanguinity. PCG pervasiveness varies from 1:10,000 for Western communities, 1:3,300 for Southern India, 1:2,500 for Saudi Arabia, and 1:1,250 for the Slovakia Gypsy population (Ali *et al*., 2009; Khan *et al*., 2011). It is apparent that PCG is essentially a heterogenetic disorder (with a multitude of gene defects) (Shohdy *et al*., 2017). To date, four loci have been categorized under the class of GLC3 (GLC3 refers to the nomenclature of the Human Genome Organization (HGO) for congenital glaucoma), and they are: GLC3A, GLC3B, GLC3C, and GLC3D. The letters A, B and C that follow the numbers refer to the chronology of the gene mapping (Cascella *et al*., 2015). The most reported PCG- related loci are GLC3A and GLC3D; GLC3A is located on 2p21 chromosomal region and is related to the *CYP1B1* gene (El Akil *et al*., 2014; Badeeb *et al*., 2014). *CYP1B1* gene mutations are associated with 33 % of the sporadic and 80 % of the familial PCG cases (Cascella *et al*., 2015; Plasilova *et al*., 1999). Regarding GLC3D (14q24) locus, several autosomal recessive null mutations were found in this position which belongs to the *LTBP2* gene. This gene encodes for Latent Transforming beta Binding Protein 2. Null mutations related to PCG were found in consanguineous families of European Gypsy population, Pakistani families and Iranian families (Narooie-Nejad *et*

[*] Corresponding author. e-mail: drsalwahnaser@uomustansiriyah.edu.iq, salwahnaser@gmail.com.

al., 2009; Azmanov *et al*., 2011) At the same time, *LTBP2* mutations that are not related to PCG were found in other populations (Mohanty *et al.*, 2013; Safari *et al*., 2015; Lima *et al*., 2013).

LTBP2 is a large gene with thirty-six exons which codes for 1821 amino acids of latent transforming growth factor (TGF)-β binding protein 2 (Safari *et al*., 2015). *LTBP2* mutations were found to be linked to severe PCG cases (Azmanov *et al*., 2011). Ali *et al*. selected *LTBP2* as a disease-related gene because of its elevated expression in the anterior chamber of the eye. Homozygous nonsense mutations (c.895 C/T; p.R299X; rs121918356 and c.331 C/T; p.Q111X; rs121918355) were identified in some consanguineous Pakistani and Slovak Gypsy families (Ali *et al*., 2009; Azmanov *et al*., 2011). These two mutations are considered as the most reported pathogenic mutations related to PCG. When occurring, these two mutations cause stop codons, thus producing truncated non-functional LTBP2 protein (Ali *et al*., 2009).

This study is the first genetic study which investigates the role of *LTBP2* mutations (rs121918356 and rs121918355) in the incidence of primary congenital glaucoma in a sample of Iraqi patients and compares the serum LTBP2 protein levels among patients and controls.

2. Materials and Methods

2.1. Study Subjects

This study adheres to the tenets of the Declaration of Helsinki and is approved by the Ethics Committee of the Department of Chemistry, College of Science at Mustansiriyah University in Baghdad, Iraq, it is also approved by the Iraqi Ministry of Health as well. All the samples were provided after obtaining informed consents of the children's parents prior to children's inclusion in the study.

One hundred unrelated PCG Iraqi child patients (58 males and 42 females) were included in this study and one-hundred unrelated healthy children (60 males and 40 females) from the same ethnicity without any systemic or ocular disease served as controls; the baseline characteristics of the PCG patients are illustrated in table 2. Five mL of venous blood was obtained from all the enrolled children by using plastic disposable syringes and were divided into two parts. The first part (2 mL) was put in EDTA tubes, and was stored at −20 °C until further use in the genetic analysis, while the second part (3 mL) was put into gel tubes and was left for fifteen minutes at a room temperature 25 °C, then the blood was centrifuged at 2000 ×g for ten minutes to collect sera. Aliquots were placed in Eppendorf tubes and stored at -40 ºC until use for the LTBP2 protein evaluation. The patients were recruited from Ibn Al-Haitham Teaching Eye Hospital in Baghdad, Iraq, while the healthy children were volunteers. All the patients were diagnosed by a glaucoma specialist (Ali N.M.Al-Sharifi, C.A.B.Opth). The standards adopted to diagnose PCG are as follows (Chen *et al*., 2016): Age of onset runs between one month and three years with a mean of twenty-four months, the elevated IOP (more than 21 mmHg), enlarged cornea so the parameter was bigger than 11 mm and increased cup to disk ratio. The exclusion criteria according to Chen and co-workers (Chen *et al*., 2016) included other ocular anomalies, such as the anterior segment dysgenesis, aniridia, neurofibromatosis, Sturge–Weber syndrome and congenital hereditary endothelial dystrophy.

2.2. Genotyping

Genomic DNA was extracted from whole blood using a genomic DNA extraction kit according to the manufacturer's instructions (Geneaid, Taiwan). The purity and concentration of the genomic DNA were assessed by a nanodrop (BioDrop μLITE, BioDrop co., UK), while the DNA integrity was confirmed using 0.8 % (w/v) agarose gel electrophoresis which is pre-stained with ethidium bromide (0.5 μg/mL) in Tris-Borate-Ethylene-diamine tetra-acetic acid (TBE) buffer. Two DNA fragments (850 and 247 bp), lying on exon 1 and exon 4 of the *LTBP2* gene respectively were amplified by polymerase chain reaction (PCR) using thermocycler (MyGenieTM 96/384 Thermal Block, Bioneer, Korea). PCR was worked in a total volume of 25 μL mixture containing 3μL;100-150ng of genomic DNA, 2μL; 20 p mol/μL of each primer (forward and reverse primers),13 μL of free DNAase distilled water and 5 μL AccuPower PCR premix (Bioneer, Korea), depending on the following protocol: initial denaturation at 95 °C for five minutes, thirty cycles of amplification (denaturation at 94 °C for forty-five seconds, annealing at primer specific annealing temperature for forty-five, seconds extension at 72 °C for one minute and final extension at 72 °C for five minutes). All the lyophilized primers were purchased from Bioneer (Bioneer, Korea) and they are listed in Table 1. The PCR products integrity was checked using 1.5 % (w/v) agarose gel electrophoresis (Figure 1A and B).

Restriction fragment length polymorphism- Polymerase chain reaction (RFLP-PCR) technique was used to identify the mutations in exon 1 and exon 4 (c.331 C/T; p.Q111X; rs121918356 and c.895 C/T; p.R299X; rs121918355) of *LTBP2* gene respectively. An 850 bp fragment encompassing c.331 C>T mutation position on exon 1 of *LTBP2* gene was amplified using specific primer sequences (Table 1).The detection of the mutation was done using AlwNI endonuclease (Biolabs, United Kingdom). In case of c.895C/T mutation on exon 4, a 247 bp fragment containing the whole exon was amplified using specific primers sequences (Table 1), AlwNI endonuclease enzyme was used to detect the mutation. The products of digestion (restricted fragments) were visualized using 3 % (w/v) agarose gel electrophoresis (Figure 2A and Figure 2B). Sanger sequencing was performed for all samples concerning the two exons as further screening using the standard methods (Figure 3A and B).

Table 1. PCR primers, restriction enzymes and digestion conditions used to genotype *LTBP2* gene.

Exon	Primers	Ta (^{0}C)	Product Size (bp)	Restriction enzyme	Digestion conditions	Sizes of restricted fragments
1	F-GGGCCTGGTGTGGATAAAAG R- TTCCCTCTCCCATGCTCAC	65	850	A1wNI	10 µl of PCR product, 0.5 (5 unit) µl of A1wNI enzyme, 5 µl of buffer and 4.5 µl of DDW in a total volume of 20 µl were incubated for 2 hrs. at 37 ^{0}C.	Two pieces of 527 bp and 323bp
4	F-GCGGTTGTCTCCACAGGA R- AGGCCCTGCTCTTCTAGGAC	64	247	A1wNI	10 µl of PCR product, 0.5 (5 unit) µl of A1wNI enzyme, 5 µl of buffer and 4.5 µl of DDW in a total volume of 20 µl were incubated for 2 hrs. at 37 ^{0}C.	One intact fragment of 247 bp.

Ta: annealing temperature. DDW: deionized sterile DNAase and RNAase free distilled water.

2.3. LTBP2 Protein Measurement

The level of LTBP2 protein was measured in the sera for all patients and control groups using the enzyme-linked immune sorbent assay (ELISA) kit according to the manufacturer's instructions (Cat # MBS760698, Mybiosource/ US).

2.4. Statistical Analysis

SPSS (statistical package for social sciences) version 19 was used for the statistical analysis of serum LTBP2 protein in both the patients and control groups. T- Test was used for the statistical comparison between means and $p<0.01$ was considered statistically significant.

3. Results

Two fragments for exon 1 and exon 4 of the *LTBP2* gene were amplified and *LTBP2* mutations (c.331 C/T; p.Q111X; rs121918356 and c.895 C/T; p.R299X; rs121918355) were tracked using RFLP-PCR technique. In case of c.331 C/T mutation, the product of the enzyme digestion for the wild-type is two pieces of the size 527 bp and 323bp (Figure 2A). Mutation is supposed to change the recognition site for AlwNI endonuclease and give an intact 850 bp fragment; all the DNA samples included in this study showed the wild type pattern. In case of c.895 C/T mutation, according to Ali (Ali *et al*, 2009) an AlwNI recognition site is formed in case the mutation is present, while in the wild type, the 247bp fragment would remain intact. All the DNA samples included in this study showed the wild type pattern (Figure 2B). Sequencing using Sanger protocol was done as further screening for all the samples concerning both the DNA fragments, and to discover if there were other nucleotide variations in these loci (Figure 3A and B). No variation was observed in any of the examined samples. Highly-significant elevation ($p=0.0001$) of the serum LTBP2 protein was noticed in the patients groups compared to the control groups (Table 3).

Table 2. Characteristics of child patients enrolled in the study.

Group description		Total patients=100
Sex	Male	58
	Female	42
Consanguinity	Yes	74
	No	26
Family history of glaucoma	Yes	8
	No	92

Table 3. Statistical analysis of Serum LTBP2 protein distributed among total patients and total control, male Patients and male control and female patients and female control.

Group	LTBP2 Protein ng/ml Mean ±SE	95 % C.I. for Mean L.b.	U.b.	*P*-Value
Total patients	1.955±0.137	0.506	1.064	
Total controls	1.169± 0.323	0.505	1.065	.0001**
Male patients	1.952± 0.172	0.449	1.143	
Male controls	1.156± 0.042	0.441	1.151	.0001**
Female Patients	1.957± 0.226	0.297	1.243	
Female controls	1.187± 0.049	0.302	1.238	.0001**

SE: Standard error, 95% C.I.: 95% Confidence interval, L.b.: Lower Bound, U.b.: Upper Bound. ** Significant at $p<0.01$

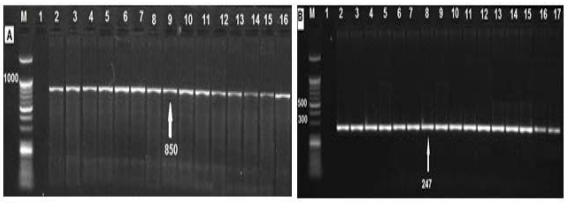

Figure 1. Electropherograms representing. A: Agarose gel electrophoresis photographs of an 850 bp PCR product of *LTBP2* gene on 1.5 % agarose gel. M: 25bp DNA marker. Lane 1 shows negative control and Lanes 2-16 show the PCR products. B: Agarose gel electrophoresis photographs of a 247 bp PCR product of *LTBP2* gene on 1.5% agarose gel. M: 25bp DNA marker. Lane 1 shows negative control and Lanes 2-17 show the PCR products.

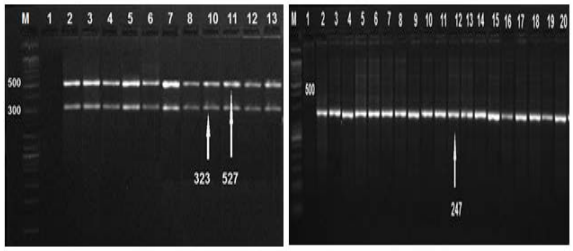

Figure 2. PCR-RFLP genotyping. A: PCR-RFLP genotyping of Q111X mutation using A1wNI endonuclease on 3 % agarose gel. M: 25bp DNA marker. Lane 1 shows negative control and lanes 2-13 represent wild type pattern of digestion producing two bands at 527bp and 323 bp. B: PCR-RFLP genotyping of R299X mutation using A1wNI endonuclease on 3 % agarose gel. M: 25bp DNA marker. Lane 1 shows negative control and lanes 2-20 represent wild type pattern producing intact 247 bp fragments.

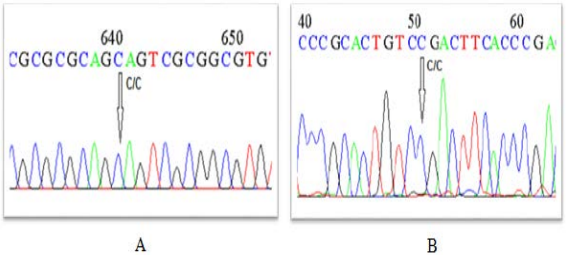

Figure 3. Sanger sequencing of PCR product. A: Regarding Q111X mutation, direct sequencing shows homozygous wild type pattern C/C. B: Regarding R299X mutation, direct sequencing shows homozygous wild type pattern C/C.

4. Discussion

Null mutations (c.331 C/T; p.Q111X; rs121918356 and c.895 C/T; p.R299X; rs121918355) of the *LTBP2* gene were primarily found to cause PCG in some individuals from Pakistani and Romani populations (Ali *et al*., 2009; Azmanov *et al*., 2011). PCG patients from several other populations, such as Slovakian Romani and Iranian populations were found to have mutations in *LTBP2* (Narooie-Nejad *et al*., 2009; Azmanov *et al*., 2011). However, other studies on British, American, and North Indian PCG patients did not discover deleterious mutations in *LTBP2* (Mohanty *et al*., 2013; Lima *et al*., 2013). In this study, DNA of one-hundred sporadic patients with PCG and one-hundred healthy Iraqi children (control) were screened for mutations in exon 1 and exon 4 of *LTBP2* gene. Mutations were not found in the population of this study, and this finding is consistent with the results of a previous study on a Saudi population (Abu-Amero *et al*., 2011) where no mutation was found in the LTBP2 gene in the Saudi PCG patients as illustrated in Table 4.

This study shows a little prevalence of PCG in males over females (Table 2). PCG is reported to be more prevalent in male subjects than females; males account for approximately 65 % of PCG cases (El Akil *et al*., 2014). The cases that have a family history in this study represent eight (8%) of the total cases (Table 2). It was reported that most of the PCG cases are sporadic, nonhereditary, and not familial (Sarfarazi, 1997). From 10 % to 12 % have a family tendency with variable penetrance (40-100 %) (Sarfarazi, 1997). Consanguinity is a factor in seventy-four (74%) of the cases in this study (Table 2). Regarding the autosomal recessive pattern of PCG inheritance, consanguinity is considered a risk factor for PCG in some populations such as Saudi, Iranian, Pakistani, and Slovak Gypsy populations, (Narooie-Nejad *et al*., 2009; Azmanov *et al*., 2011; Abu-Amero *et al*.2011). It can be said then that consanguinity plays an important role in the PCG incidence in the Iraqi population as a community with high consanguinity.

LTBP2 protein is the biggest member in the LTBPs family. It has a structure domain analogous to that of other LTBPs, particularly the form of LTBP1, but it also involves distinctive regions, which makes it related to fibrillin-1 (Hirani, 2007). LTBP2 co-localizes with fibrillin, and its aggregation largely associates with the fibers of fibrillin-1 (Robertson *et al*., 2015). Fibers are largely expressed in the eye especially in the TM. The interconnected circumferential network of the elastic fiber is much similar to the elastic fiber structure in blood vessels, and likely provides basic elastic properties to the aqueous humour (AH) outflow system, which is constantly accompanied with pulsatile force. Expression of fibrillin-1 in the TM confirms a distribution of microfibrils overlapped with TM elastic fibers (Kuchtey and Kuchtey, 2014). The flow of aqueous homour is concomitant with the ocular pulse. Microfibril defects could alter elasticity of the TM, collector channels, and episcleral veins, which could obstruct the pumping action of the TM and the pulsatile outflow of AH causing accumulation of the AH and increasing of the IOP in glaucoma. LTBP2 is the microfibril-associated protein, therefore, *LTBP2* mutations had been shown to cause PCG (Kuchtey, 2011; Johnstone, 2004). Microfibril defects could be involved in glaucoma through changing the biomechanical properties of the tissue and through affecting the signaling of transforming growth factor beta (TGFβ) (Kuchtey and Kuchtey, 2014). Microfibrils are the main reservoir of latent TGFβ and are essential for TGFβ signaling and localization. Abnormal microfibrils could be a reason for TGFβ elevation in the AH of glaucomatous eyes (Kuchtey and Kuchtey, 2014). LTBP2 co-localizes with fibrillin-1, and it is involved in the activation and secretion of TGFβ. In addition, some studies show that the assembly and secretion of TGFβ require the co-expression of LTBP (Miyazono *et al*., 1991; Rahmi and Hesketh, 2000). Other studies reported that the concentration of TGFβ2 in the AH of pseudoexfoliation syndrome patients was high compared to the controls, and that the LTBP2 protein is co-expressed with TGFβ2 in the eye; thus, it was found to be elevated as well in the pseudoexfoliation syndrome patients (Schlotzer-Schrehardt *et al*., 2001). This fact is consistent with the results obtained from the present study in which LTBP2 protein levels in patients' sera are significantly higher (p=0.0001) than those of the healthy control (Table 3). The increased expression of *LTBP2* is required for the increased secretion of TGFβ in PCG patients and that explains the cause (other than *LTBP2* mutations) underling the elevation of LTBP2 protein level in the PCG patients participating in this study. These findings indicate that the high LTBP2 protein levels can be detected in the PCG patients' sera as well as in the patients' AH. On the other hand, there is no observed differentiation in LTBP2 protein levels among the male and female patients, which indicates that the sex is not a controlling factor concerning the LTBP2 protein level. Limitation of this study include: the small size of the sample, only few mutations in LTBP2 gene were examined. The observed elevation in LTBP2 might not reflect the situation in the eyes.

Table 4. LTBP2 polymorphisms/ mutations reported in other populations for patients with primary congenital glaucoma.

No.	Nucleotide change	Exon / Intron location	Heterozygous/ Homozygous	Type of mutation	Amino acid change	Reference SNP number	Population	Reference
1	g.75070493 C>G	Intron 5	homozygous			rs3742793	North Indian	Mohanty *et al.*, 2013
2	c.331C>T	Exon 1	homozygous	Nonsense	p.Q111X	rs121918356	Pakistani	Ali *et al*., 2009
3	c.412delG	Exon 1	homozygous	Frame shift	p.A138PfsX278		Pakistani,	Ali *et al*., 2009
							Gypsy	Azmanov *et al*., 2011
4	c.1243_1256del14	Exon 6	homozygous	Frame shift	p.E415RfsX596	N A	Pakistani,	Ali *et al*., 2009
							Gypsy	Narooie-Nejad *et al*., 2009
5	c.895C>T	Exon 4	homozygous	Nonsense	p.R299X	rs121918355	Gypsy	Azmanov *et al*., 2011
6	c.5376delC	Exon 36	homozygous	Frame shift	p.W1793fsX55	NA	Iranian	Narooie-Nejad *et al*., 2009
7	c.1415delC	Exon 7	homozygous	Frame shift	p.S472fsX3	NA	Iranian	Narooie-Nejad *et al*., 2009
8	c.1287G>A	Exon 6		Silent	p.L429L	rs61738025	Iranian	Narooie-Nejad *et al*., 2009
	c.4808G>A	Exon 33		Missense	p.R1603H	rs75200417	Iranian	Narooie-Nejad *et al*., 2009
9	c.956C>A	Exon 4	heterozygous	Missense	p. P319Q	rs2304707	Chinese,	Chen *et al*., 2016
							Iranian,	Narooie-Nejad *et al*., 200920
							American,	
							British	Sharafieh et al., 2013
10	c.3611C>T	Exon 24	heterozygous	Missense	p. A1204V	rs45468895	Chinese	Chen *et al*., 2016
11	c.4286G>A	Exon 29	heterozygous	Missense	p. R1429Q	rs116914994	Chinese	Chen *et al*., 2016
12	c.5380G>A	Exon 36	heterozygous	Missense	p. E1794K	rs763035721	Chinese	Chen *et al*., 2016
13	No detected mutation						Saudi	Abu-Amero *et al*.2011
14	No detected mutation							Current study

NA: Not Available

5. Conclusion

The null mutations (c.331 C/T; p.Q111X; rs121918356 and c.895 C/T; p.R299X; rs121918355) which are considered as pathogenic mutations in some populations are not found in the current study's groups, which means that they have no relation to the PCG disease in the selected sample of Iraqi population. The PCG patients have higher LTBP2 protein levels when compared to controls. The elevated levels of LTBP2 protein in the patients may suggest the involvement of other loci of *LTBP2* gene in the incidence of the disease; at the same time, this elevation may not have other genetic reasons.

Acknowledgment

The authors would like to thank all the children's parents for their approval to participate in this study.

References

Abu-Amero KK, Osman EA, Mousa A, Wheeler J, Whigham B, Allingham RR, Hauser MA and Al-Obeidan SA. 2011. Screening of CYP1B1 and LTBP2 genes in Saudi families with primary congenital glaucoma: genotype-phenotype correlation. *Mol Vis*, **17**: 2911.

Achary MS, Reddy AB, Chakrabarti S, Panicker SG, Mandal AK, Ahmed N, Balasubramanian D, Hasnain SE and Nagarajaram HA. 2006. Disease-causing mutations in proteins: Structural analysis of the CYP1b1 mutations causing primary congenital glaucoma in humans. *Biophys J*, **91(12):**4329–4339.

Ali M, McKibbin M, Booth A, Parry DA, Jain P, Riazuddin SA, Hejtmancik JF, Khan SN, Firasat S, Shires M, Gilmour DF, Towns K, Murphy AL, Azmanov D, Tournev I, Cherninkova S, Jafri H, Raashid Y, Toomes C, Craig J, Mackey DA, Kalaydjieva L, Riazuddin S and Inglehearn CF. 2009. Null mutations in LTBP2 cause primary congenital glaucoma. *Am. J Hum Genet*, **84(5):**664–671.

Azmanov DN, Dimitrova S, Florez L, Cherninkova S, Draganov D, Morar B, Saat R, Juan M, Arostegui JI, Ganguly S, Soodyall H, Chakrabarti S, Padh H, López-Nevot MA, Chernodrinska V, Anguelov B, Majumder P, Angelova L, Kaneva R, Mackey DA, Tournev I and Kalaydjieva L, 2011. LTBP2 and CYP1B1 mutations and associated ocular phenotypes in the Roma/Gypsy founder population. *Eur J Hum Genet*, **19(3):** 326–333.

Badeeb OM, Michea S, Koenekoop RK, den Hollander AI and Hedrawi MT. 2014. CYP1B1 mutations in patients with primary congenital glaucoma from Saudi Arabia, *BMC Med Genet*, **15(1):**109.

Cascella R, Strafella C, Germani C, Novelli C, Ricci F, Zampatti S and Giardina E. 2015. The genetics and the genomics of primary congenital glaucoma. *BioMed Res Int*,**2015:** ID 321291.

Chen X, Chen Y, Fan BJ, Xia M, Wang L and Sun X. 2016. Screening of the LTBP2 gene in 214 Chinese sporadic CYP1B1-negative patients with primary congenital glaucoma. *Mol Vis*, **22**:528-535.

El Akil S, Melki R and Belmouden A. 2014. Genetic heterogeneity in Moroccan primary congenital glaucoma patients, *Life Sci J*, **11(11):** 890-898.

Faiq M, Sharma R, Dada R, Mohanty K, Saluja D and Dada T.2013. Genetic, biochemical and clinical insights into primary congenital glaucoma. *JOCGP*, **7(2):**66-84.

Fan BJ, Wang DY, Lam DSC and Pang CP. 2006. Gene mapping for primary open angle glaucoma. *Clinical Biochem*., **39(3):** 249-258.

Hirani R, Hanssen E and Gibson M. 2007. LTBP-2 specifically interacts with the amino-terminal region of fibrillin-1 and competes with LTBP-1 for binding to this microfibrillar protein. *Matrix Biol*, **26(4):** 213–223.

Johnstone MA. 2004. The Aqueous outflow system as a mechanical pump evidence from examination of tissue and aqueous movement in human and non-human primates. *J Glaucoma*, **13(5):**421-438.

Khan AO, Aldahmesh MA and Alkuraya FS. 2011. Congenital megalocornea with zonular weakness and childhood lens-related secondary glaucoma- a distinct phenotype caused by recessive LTBP2 mutations. *Mol Vis*, **17**:2570-2579.

Kuchtey J and Kuchtey RW. 2014. The Microfibril Hypothesis of Glaucoma: Implications for Treatment of Elevated Intraocular Pressure. *J Ocul Pharmacol Ther*., **30(2-3):**170-180.

Kuchtey J, Olson LM, Rinkoski T, MacKay EO, Iverson T and Gelatt K. 2011. Mapping of the disease locus and identification of ADAMTS10 as a candidate gene in a canine model of primary open angle glaucoma. *PLoS Genet*, **7(2):** e1001306.

Lima S, Tran-Viet K, Yanovitch TL, Freedman SF, Klemm T, Call W, Powell C, Ravichandran A, Metlapally R, Nading EB, Rozen S, Young TL. 2013. CYP1B1, MYOC, and LTBP2 Mutations in primary congenital glaucoma patients in the United States. *Am J Ophthalmol*., **155(3):** 508–517.

Miyazono K, Olofsson A, Colosetti P and Heldin C. 1991. A role of the latent TGF-3 1-binding protein in the assembly and secretion of TGF-B1. *EMBO J*, **10 (5):**1091-1101.

Mohanty K, Tanwar M, Dada R and Dada T. 2013. Screening of the LTBP2 gene in a north Indian population with primary congenital glaucoma. *Mol Vis.*, **19**:78-84.

Narooie-Nejad M, Paylakhi SH, Shojaee S, Fazlali Z, Rezaei Kanavi M, Nilforushan N, Yazdani S, Babrzadeh F, Suri F, Ronaghi M, Elahi E, Paisán-Ruiz C. 2009. Loss of function mutations in the gene encoding latent transforming growth factor beta binding protein 2, LTBP2, cause primary congenital glaucoma. *Hum Mol Genet*, **18 (20):** 3969–3977.

Plasilova M, Stoilov I, Sarfarazi M, Kádasi L, Feráková E and Ferák V. 1999. Identification of a single ancestral CYP1B1mutation in Slovak Gypsies (Roms) affected with primary congenital glaucoma. *J Med Genet*, **36(4):**290–294.

Quigley HA. 1996. Number of people with glaucoma worldwide. *Brit J Ophthalmol*. **80(5)**: 389-393.

Rahmi O and Hesketh R. 2000. The Latent transforming growth factor b binding protein (LTBP) family. *Biochem J*.; **352**: 601-610.

Ray K, Mukhopadhyay A and Acharya M. 2003. Recent advances in molecular genetics of glaucoma. *Mol Cell Biochem*, **253(1-2):** 223-231.

Robertson IB, Horiguchi M, Zilberberg L, Dabovic B, Hadjiolova K and Rifkin DB. 2015. Latent TGF-β-binding proteins. *Matrix Biol*, **47**: 44-53.

Safari I, Akbarian S, Yazdani S and Elahi E. 2015. A Possible role for LTBP2 in the etiology of primary angle closure glaucoma. *J Ophthalmic Vis Res*, **10 (2):** 123-129.

Sarfarazi M and Stoilov I. 2000. Molecular genetics of primary congenital glaucoma. *Eye*, **14:** 422-428.

Sarfarazi M. 1997. Recent advances in molecular genetics of glaucomas. *Hum Mol Genet*, **6(10):** 1667-1677.

Schlotzer- Schrehardt U, Zenkel M, Kuchle M, Sakai LY and Naumann GO. 2001. Transforming growth factor-β1 and its form binding protein in pseudoexfoliation syndrome. *Exp Eye Res*, **73**: 765-780.

Sharafieh R, Child AH, Khaw PT, Fleck B and Sarfarazi M. 2013. LTBP2 gene analysis in the GLC3C-linked family and 94 CYP1B1-negative cases with primary congenital glaucoma. *Ophthalmic Genet*, **34(1-2):** 14-20.

Shohdy KS, Rashad WA, Fargoun MK and Urban P. 2017. The morphogen behind primary congenital glaucoma and the dream of targeting. *Rom J Morphol Embryol*, **58(2):**351-361.

Zhou T, Souzeau E, Siggs OM, Landers J, Mills R, Goldberg I, Healey PR, Graham S, Hewitt AW, Mackey DA, Galanopoulos A, Casson RJ, Ruddle JB, Ellis J, Leo P, Brown MA, MacGregor S, Sharma S, Burdon KP and Craig JE. 2017. Contribution of mutations in known mendelian glaucoma genes to advanced early-onset primary open-angle glaucoma. *Invest Ophthalmol Vis Sci*, **58(3):**1537-1544.

JJBS

Volume 12, Number 1,March 2019
ISSN 1995-6673
Pages 83 - 87

Jordan Journal of Biological Sciences

Mathematical Prediction of Nucleic Acids 3-D Structures Using Inter-Spin Distances and Nonlinear Least Squares Analysis

Samer I. Awad*

The Hashemite University, Faculty of Engineering, Biomedical Engineering Department, Zarqa, Jordan, 13115

Received June 11, 2018; Revised July 27, 2018; Accepted August 4, 2018

Abstract

Nucleic acids consist of several double helical arms (three to eight of them). These arms are connected at a junction point, with or without several unpaired bases in one or more of the different strands. Current structural information on several nucleic acids is still limited. Electron paramagnetic resonance (EPR) can provide distance measurements of site-directed spin labels (SDSL) applied to the double helical arms. These distances can be used to generate several quadratic equations that characterize the three-dimensional (3-D) structure of the nucleic acid. In this work, a nonlinear least squares algorithm is used to solve these equations along with molecular constraints simultaneously. The solution that this algorithm calculates can be used to create the predicted 3-D structure. The algorithm was tested using twenty-five cases for known DNA structures. Root-mean-square deviation (RMSD) was used in this study to evaluate the accuracy of the predicted structures. The calculated RMSD values had an average of 2.56 and a standard deviation of 1.65.

Keywords. DNA; Nucleic Acid; Biological Macromolecule; Site-directed spin labels; Electron paramagnetic resonance; Least-squares; Levenberg-Marquardt.

1. Introduction

The biological function of nucleic acids molecules is highly dependent on their three-dimensional structures (Hvidsten *et al.*, 2009). Most of these structures are poorly understood which limits the understanding of the biological mechanisms of nucleic acids (Dawson and Bujnicki, 2016; Doudna, 2000). Calculating the 3-D structures of nucleic acids and thus having a better understanding of their function play an important role in therapeutic and diagnostic medical applications. Examples of these applications include drug design, ribosome structuring, and nanoengineering (Greer *et al.*, 1994; Maune *et al.*, 2010).

Structural analysis of biological macromolecules is mainly implemented using X-ray crystallography and high-resolution nuclear magnetic resonance (NMR) spectroscopy. Both methods can provide high resolution structural details; however, they have serious limitations (Banaszak, 2000). X-ray crystallography can be difficult to use with macromolecules that have high flexibility in their structures such as membrane proteins (Mchaourab *et al.*, 2011; Jeschke, 2012). Although NMR spectroscopy can provide some information on this flexibility, it has molecular mass limitations that exclude a large number of macromolecules (Mittermaier and Kay, 2009).

Site-directed spin labeling (SDSL) offers an alternative approach for the structure prediction of nucleic acids (Borbat *et al.*, 2002; Jeschke and Polyhach, 2007). In SDSL, nitroxide spin labels are introduced into specific sites of a macromolecule. Distances between pairs of labels can be measured from which valuable structural information can be obtained. Electron paramagnetic resonance (EPR) spectroscopy techniques have been successfully used for providing such information (Schweiger, 2001). Using conventional continuous wave (CW) EPR spectroscopy and SDSL, distances in the range of 8-20 Å can be measured (Hubbell *et al.*, 2000; Steinhoff and Suess, 2003). Pulsed Double Electron−Electron Resonance (DEER or PELDOR) can access longer distances in the range of 20-80 Å to characterize relatively large biological macromolecules (Jeschke, 2004; Sale *et al.*, 2005).

Several studies have employed different techniques for the prediction of 3-D structures of biological macromolecules. Tung *et al.* employed several computations based on deuterium labeling to determine the atomic model of the cAMP-dependent protein kinase (Tung *et al.*, 2002). Pulsed electron paramagnetic resonance (ESR) based on the detection of double quantum coherence (DQC) and nitroxide spin-labels were used by Borbat et al. to establish the structure of T4 Lysozyme (Borbat *et al.*, 2002). Jeschke and Polyhach studied the effects of varying several experimental parameters on the sensitivity of spin labels distance measurements using EPR and DEER coupled with Monte Carlo search algorithm (Jeschke and Polyhach, 2007). Hatmal employed spin label distance measurements using EPR and DEER coupled with the Quasi-Newton method implemented in Fortran and MATLAB to determine the structure of DNA and RNA junctions, and for the central region of endophilin

* Corresponding author. e-mail: samer.awad@gmail.com.

(Hatmal, 2011). Zhang *et al*. also employed Monte Carlo algorithm to detect the global structure of Phi29 packaging RNA based on site-directed spin labeling (Zhang *et al*., 2012). A neural network technique was used by Hamad *et al*. to predict the 3-D protein structure as a function of enzyme family types and amino acid sequences (Hamad *et al*., 2017).

In this work, a least squares algorithm was used to process the distance measurements acquired using SDSL for the prediction of biological macromolecule structure. The acquired distances were used to create a group of quadratic equations (distance equations). These equations were next solved simultaneously using the Levenberg-Marquardt algorithm limited by molecular constraints to provide the 3-D model of the nucleic acid using the internal geometries of the corresponding arms. This algorithm has been developed fully in MATLAB (Mathworks, Inc., Natick, MA, USA), and was successfully tested using twenty-five cases for known DNA structures. Root-mean-square deviation (RMSD) was calculated to evaluate the accuracy of the predicted structures against the true ones.

2. Methods

The following steps were used in the framework of nucleic acid structure prediction in this work (shown in figure 1).

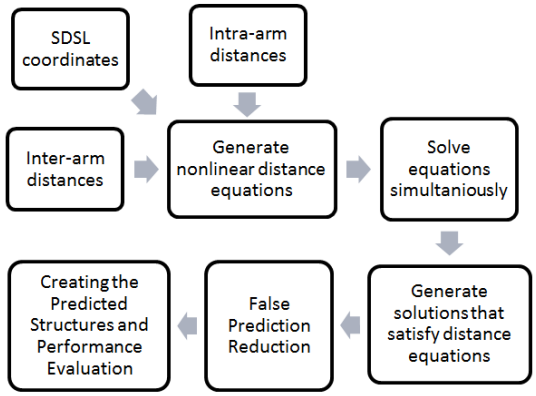

Figure 1. A flowchart of the proposed approach.

2.1. Acquiring Distance Measurements of SDSL Pairs

*Acquiring SDSL Coordinates***:** This process starts with obtaining the structure of each individual arm from a protein databank. In this work, "worldwide protein data bank" (www.wwpdb.org) and "RCSB protein data bank" (www.rcsb.org) were used (Heinz *et al*., 1993). Next, nitroxide spin labels were attached to several positions on each arm using a published algorithm (Beasley *et al*., 2015). The locations of several spin labels were then averaged resulting in one point. This reduces the structural information of each arm into the x, y, and z coordinates of such points. The resulting coordinates identify each arm independent of the nucleic acid and aligned with the positive z-direction.

*Acquiring Intra-Arm Distances***:** The distances between points belonging to the same arm (intra-arm distances) acquired in the previous process were then calculated.

*Acquiring Inter-Arm Distances***:** The distances between points in two different arms (inter-arm distances) can be obtained using the aforementioned EPR spectroscopy techniques. Alternatively, these distances can be obtained computationally for known structures of nucleic acids. The later method was implemented in this work using a published algorithm (Beasley *et al.*, 2015). In this context, the inter-arm distances serve as constraints in the mathematical analysis to reduce the number of degrees of freedom available to the arm with respect to the rest of the macromolecule structure (or with respect to a reference arm). Hence, more estimated distances can reduce the number of possible structures that satisfy the distance equations simultaneously.

2.2. Generating Non-linear Equations Using the Input Information

The inter-spin distances generated were next used to create distance equations of the form:

$$[X_j - X_k]^2 + [Y_j - Y_k]^2 + [Z_j - Z_k]^2 = d^2 \quad (1)$$

where $X_j, Y_j, and\ Z_j$ are the coordinates of the first point and $X_k, Y_k, and\ Z_k$ are the coordinates of the second point, and d is the distance between them. One of the arms in the macromolecule structure was used as a reference. For this arm, the coordinates of the points were kept unchanged with the arm aligned with the positive z-direction, while the coordinates of other arms were changed to account for inter-arm distances. The overall number of distance equations equals the number of the inter-distances plus the number of intra-distances. Three different types of distance equations were created (all having the form of eq. 1):

- Equations between points inside the same arm for arms other than the reference arm. The coordinates of both points are unknowns, since the arm will be reoriented considering the inter-arm distances.
- Equations between a point on the reference arm with known coordinates and a point on a non-reference arm with unknown coordinates.
- Equations between two points on two different non-reference arms where the coordinates of both points are unknowns.

2.3. Solving the Non-Linear Equations

The distance equations generated in the previous step must be solved simultaneously to reorient the arms using a non-linear curve-fitting method. Several least squares methods can be implemented for solving non-linear equations including: Gauss-Newton, trust-region methods, and Levenberg-Marquardt (Björck, 1996). Trust-region methods have the limitation that they can only be used to analyze determined systems of equations in which the number of unknowns equals the number of equations (Byrd *et al*., 1987; Moré and Sorensen, 1983). The Levenberg-Marquardt method can outperform the Gauss-Newton method as it can find a solution even if the initial conditions were far off the final minimum (Pujol, 2007). Since the number of distance equations can be less than the number of unknowns in DNA structure prediction, the Levenberg-Marquardt method was used in this work.

Similar to other minimization algorithms, Levenberg-Marquardt is an iterative procedure. This means that it needs an initial guess to start a minimization. The initial guess was chosen using a series of values through a for-

loop that has a start value, a step value, and an end value. These values were selected taking into consideration the typical dimensions of macromolecules. The final solutions came in the form of new x, y, and z coordinates of the different points on each non-reference arm revealing the structure of the macromolecule.

2.4. False Prediction Reduction

Inter-spin distances acquired using EPR spectroscopy can be difficult to obtain. In many cases, they are fewer than the number required to obtain a unique solution. In this work, an additional step was added to furthermore reduce the number of solutions. The glycosidic N-N distances between arms (the distance at the junctional area between arms) are known to be more than 4 Å and less than approximately 12 + 8n Å, where n is the number of unpaired bases between the ends of arms in the junction area (Banaszak, 2000). Solutions that violated this rule were discarded. Additionally, some solutions can have overlapping arms. Some overlap (or clash) between arms is physically possible and should be accepted if it came up as a structural prediction. Solutions with more than 10 clashes of more than 75% of the sum of the van der Waals radii of any two interacting atoms were also discarded (Banaszak, 2000).

2.5. Creating the Predicted Structures and Performance Evaluation

As previously mentioned, inter-arm distances were obtained computationally for known 3-D structures of DNA (real and hypothetical). This option was chosen to evaluate the accuracy of the calculated solutions generated by the proposed approach against known structures. The evaluation was done using root-mean-square deviation (RMSD):

$$RMSD = \sqrt{\frac{\sum_{n=1}^{N}(x_{1,n}-x_{2,n})^2+(y_{1,n}-y_{2,n})^2+(z_{1,n}-z_{2,n})^2}{N}} \quad (2)$$

where (x_1, y_1, z_1) are the coordinates of a point predicted by the proposed algorithm, (x_2, y_2, z_2) are the coordinates of the same point in the known nucleic acid structure, and N is the total number of points.

3. Results

To test the proposed algorithm, five different hypothetical DNA structures and one real DNA structure (PDB ID: 1EKW) with different number of inter-arm distances and spin label positions were used (total of 25 cases). For the hypothetical cases, the arms were built using standard B-DNA parameters creating planner and non-planner 3-way junction DNA structures. Table 1 lists the different cases used along with: number of inter-arm distances, number of resulting structures with and without false prediction reduction, and lowest RMSD.

The final output of the proposed algorithm was in the form of reoriented coordinates of points on each non-reference arm along with unchanged coordinates of points on the reference arm. To visualize the DNA structure prediction, all these points were plotted on a 3-D graph. Figure 2 shows the two structure predictions of a sample DNA molecule (the second sample in table 1). Points on the reference arm, second and third arms are colored blue, red, and green, respectively. The difference between the two predictions in figure 2 is the location and orientation of the third arm (colored green).

Table 1. Results of structure predictions for real and hypothetical DNA molecules using different inter-arm distances and label positions.

DNA sample	Number of inter-arm distances	Number of resulting structures without false prediction reduction	Number of resulting structures with false prediction reduction	Lowest RMSD
Planer 3-way DNA junction	9	3	1	0.66
	8	2	1	0.98
	7	4	2	1.68
	6	146	18	1.56
Non-Planer 3-way DNA junction	16	1	1	0.70
	9	4	1	0.96
	9	7	1	0.96
	9	8	1	0.92
	8	4	1	0.97
	7	17	2	1.21
	6	37	5	1.90
Non-Planer 3-way DNA junction (Modified distances)	9	4	1	3.69
	8	6	1	4.78
	7	11	1	4.04
	6	174	1	3.98
1EKW	9	6	1	2.33
	8	4	1	2.33
	7	16	2	2.32
	6	78	4	5.55
	5	428	17	6.52
Non-Planer 3-way distorted DNA junction	9	4	1	2.52
	8	6	1	2.57
	7	10	2	4.91
	6	43	4	3.42
Non-Planer 3-way distorted DNA junction (Modified distances)	9	4	1	2.60

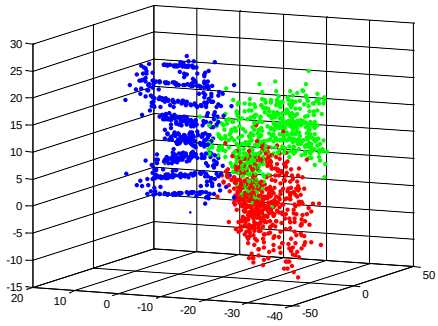

(a)

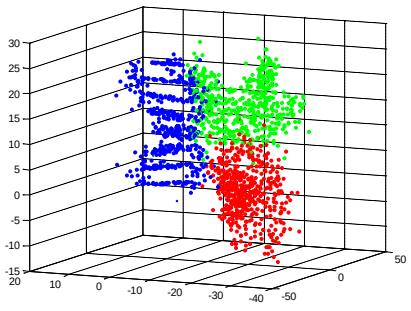

(b)

Figure 2. Two structure predictions of a sample DNA molecule (the second sample in table 1). Points on the reference arm, second and third arms are colored blue, red, and green, respectively.

4. Discussion and Conclusions

This paper describes structure prediction of biological macromolecules based on distance measurements of spin labels using a least squares algorithm. Inter-arm and intra-arm distances were acquired and used to create non-linear distance equations. These equations were solved simultaneously using the Levenberg-Marquardt algorithm to predict the orientations of macromolecule's arms revealing the 3-D structure. Several predictions were obtained when the number of inter-arm distances was less than the number required to obtain a unique solution (underdetermined cases). In these cases, molecular constraints were applied to reduce the number of predictions. Twenty-five DNA cases were used to test the algorithm. The average of lowest RMSD of the predictions was 2.56 with a standard deviation of 1.65 ranging from 0.66 to 6.52.

A strong correlation can be noticed between a higher number of inter-arm distances (hence more distance equations) and a lower number of predictions and lower RMSD values. This is due to the fact that more equations lead to less degrees of freedom for the non-reference arms orientations and a better chance to reach the true shape of the molecule. Additionally, changing the chosen SDSL pairs (while keeping the same number of distances) could affect the RMSD values (samples 2 and 3 in table 1). The reason for this is that the degrees of freedom of arms could be different which could lead to different predictions and hence different RMSD values.

Future work will include studying the effects of varying the number of distances on the number predictions and RMSD values. Additionally, the effects of varying the chosen spin label pairs will be studied. Future work will also include testing the algorithm using DNA structures with a larger number of arms and using experimental EPR data for other types of biological macromolecules.

References

Banaszak L. 2000. **Foundations of Structural Biology**, 1st Ed. Academic Press, San Diego.

Beasley K, Sutch B, Hatmal M, Langen R, Qin P and Haworth I. 2015. Computer Modeling of Spin Labels: NASNOX, PRONOX, and ALLNOX. *Methods Enzymol*, **563**: 569–593.

Björck A. 1996. **Numerical Methods for Least Squares Problems**, 1st Ed. SIAM, Philadelphia.

Borbat PP, Mchaourab HS and Freed JH. 2002. Protein structure determination using long-distance constraints from double-quantum coherence ESR: Study of T4 lysozyme. *J Am Chem Soc.*, **124**: 5304–5314.

Byrd R, Schnabel R and Shultz G. 1987. A Trust region algorithm for nonlinearly constrained optimization. *SIAM J Numer Anal.*, **24:** 1152–1170.

Dawson WK and Bujnicki JM. 2016. Computational modeling of RNA 3D structures and interactions. *Curr Opin Struct Biol.*, **37**: 22-28.

Doudna J. 2000. Structural genomics of RNA. *Nat Struct Mol Biol.*, **7:** 954 - 956.

Greer J, Erickson J, Baldwin J and Varney M. 1994. Application of the Three-Dimensional Structures of Protein Target Molecules in Structure-Based Drug Design. *J Med Chem.*, **37**: 1035-1054.

Hamad EM, Rawashdeh NA, Khanfar MF, Al-Qasem EN and Al-Gharabli SI. 2017. Neural network based prediction of 3D protein structure as a function of enzyme family type and amino acid sequences. *Jordan J Biol Sci.*, **10**: 73-78.

Hatmal M. 2011. Molecular and computational analysis of spin-labeled nucleic acids and proteins. PhD Thesis, University of Southern California, Los Angeles, USA.

Heinz D, Baase W, Dahlquist F and Matthews B. 1993. How amino-acid insertions are allowed in an alpha-helix of T4 lysozyme. *Nature*, **361**: 561–564.

Hubbell W, Cafiso S and Altenbach C. 2000. Identifying conformational changes with site-directed spin labeling. *Nat Struct Biol.*, **7**: 735-739.

Hvidsten T, Laegreid A, Kryshtafovych A, Andersson G, Fidelis K and Komorowski J. 2009. A comprehensive analysis of the structure-function relationship in proteins based on local structure similarity. *PLOS One*, **4**: e6266.

Jeschke G, Bender A, Paulsen H, Zimmermann H and Godt A. 2004. Sensitivity enhancement in pulse EPR distance measurements. *J Magn Reson.*, **169**: 1-12.

Jeschke G. 2012. DEER Distance measurements on proteins. *Annu Rev Phys Chem.*, **63**: 419–446.

Jeschke G and Polyhach Y. 2007. Distance measurements on spin-labelled biomacromolecules by pulsed electron paramagnetic resonance. *Phys Chem Chem Phys*, **9**: 1895–1910.

Maune H, Han S, Barish R, Bockrath M, Goddard W, Rothemund P and Winfree E. 2010. Self-assembly of carbon nanotubes into two-dimensional geometries using DNA origami templates. *Nat Nanotech.*, **5**: 61 - 66.

Mchaourab H, Steed P and Kazmier K. 2011. Toward the fourth dimension of membrane protein structure: Insight into dynamics from spin-labeling EPR spectroscopy. *Structure*, **19**: 1549–1561.

Mittermaier A and Kay L. 2009. Observing biological dynamics at atomic resolution using NMR. *Trends Biochem. Sci*, **34**: 601–611.

Moré J and Sorensen D. 1983. Computing a trust-region step. *SIAM J Sci Stat Comput.*, **4**: 553–572.

Pujol J. 2007. The solution of nonlinear inverse problems and the Levenberg-Marquardt method. *Geophysics*, **72**: W1-W16.

Sale K, Song LK, Liu YS, Perozo E and Fajer P. 2005. Explicit treatment of spin labels in modeling of distance constraints from dipolar EPR and DEER. *J Am Chem Soc.*, **127**: 9334-9335.

Schweiger A and Jeschke G. 2001. **Principles of Pulse Electron Paramagnetic Resonance**. Oxford University Press, Oxford, UK.

Seeman NC. 1982. Nucleic acid junctions and lattices. *J Theor Biol.*, **99**: 237-247.

Steinhoff H and Suess B. 2003. Molecular mechanisms of gene regulation studied by site-directed spin labeling. *Methods*, **29**: 188-195.

Tung CS, Walsh DA and Trewhella J. 2002. A structural model of the catalytic subunit-regulatory subunit dimeric complex of the cAMP-dependent protein kinase. *J Biol Chem.*, **277**: 12423–12431.

Zhang X, Tung C, Sowa G, Hatmal M, Haworth I and Qin P. 2012. Global structure of a three-way junction in a Phi29 packaging RNA dimer determined using site-directed spin labeling. *J Am Chem Soc.*, **134**: 2644-2652.

JJBS

Volume 12, Number 1,March 2019
ISSN 1995-6673
Pages 89 - 97

Jordan Journal of Biological Sciences

Association of Genetic Variants of Enzymes Involved in Folate / One-Carbon Metabolism with Female Breast Cancer in Jordan

May F. Sadiq[1,2*], Nadia M. Abu Issa[2], Montaser O. Alhakim[2], Almuthanna K. Alkaraki[1], Omar F. Khabour[2], Rami J. Yaghan[3] and Mohammed Y. Gharaibeh[2]

[1]*Department of Biological Sciences, Faculty of Science, Yarmouk University, Irbid 21163;* [2]*Department of Medical Laboratory Sciences, Faculty of Applied Medical Sciences;* [3]*Department of General and Pediatric Surgery, Faculty of Medicine, Jordan University of Science and Technology, Irbid 22110, Jordan.*

Received May 22, 2018; Revised August 5, 2018; Accepted August 8, 2018

Abstract

Folate/one-carbon metabolism plays key roles in gene expression, and in the synthesis and repair of DNA. Therefore, it differently influences the pathogenesis of different diseases including cancer in different populations. This case-control study examined the association between the risks of female breast cancer with five functional single-nucleotide polymorphisms (SNPs) in the folate/one-carbon metabolism. These were *MTR* A2756G (rs1805087), *MTHFR* C677T (rs1801133), *MTHFR* A1298C (rs1801131), *TYMS* 1494 ins/del 6 (rs151264360) and *MTRR A66G* (rs1801394). This study included two-hundred female breast cancer cases and two-hundred age-matched female controls. The DNA samples were extracted from peripheral blood and were genotyped by PCR-RFLP. Comparisons between frequencies of alleles and genotypes in the different groups were evaluated using Pearson chi square test (P= 0.05), while the associations between each SNP and the risk of breast cancer were estimated by logistic regression analysis and calculation of odds ratios (OR) with 95 % confidence intervals (CI). Results showed that *MTR* 2756GG genotype is directly associated with breast cancer (OR = 4.360; CI= 1.213-15.666; P = 0.011), while its heterozygous genotype *MTR* 2756AG had no such risk, indicating that *MTR* 2756G allele is recessive to the wild type allele *MTR* 2756A in the whole group of cases, but is dominant in the post-menopausal cases. Besides, significant differences appeared in the distributions of both *MTR* 2756G allele (P = 0.022) and its genotypes (P = 0.008) between the pre- and post-menopausal cases respectively, which indicated for the first time, that the post-menopausal status affects the dominance of the polymorphism *MTR* A2756G as a risk factor for breast cancer. The results also showed that *MTHFR* C677T, *TYMS* 1494 ins/del 6 and *MTRR A66G* are strongly associated with breast cancer only when present in double compound heterozygous states (odd ratios between 2.6 and 6.7). In conclusion, folate/one-carbon metabolism contributes to the risk of female breast cancer in Jordan, and this contribution can be modified by the menopausal status of the females.

Keywords: Single nucleotide Polymorphism, *MTR*, *MTHFR*, *TYMS*, *MTRR*, Breast cancer, Jordan.

1. Introduction

Breast cancer constitutes a major concern for public health because it is the most common cancer among women worldwide (Ferlay *et al.*, 2015). In Jordan, breast cancer accounted for 37.3 % of the top five common cancers among Jordanian women (Jordan Cancer Registry, 2016). Hereditary female breast cancer represents about 5 % to 9 % of all breast cancer cases worldwide, while most of the cases are due to sporadic mutations in housekeeping genes that result in abnormal genetic and epigenetic changes (Choi and Mason, 2000).

Folate/one-carbon metabolic pathway is the most essential cellular source of the methyl group that is required for the synthesis and repair of DNA, and is required for the modulation of gene expression (Choi and Mason, 2000; Duthie, 1999; Duthie *et al.*, 2002; Friso *et al.*, 2002; Balaghi and Wagner, 1993), which can influence the pathogenesis of various types of cancers including breast cancer (Gao *et al.*, 2009; Pardini *et al.*, 2011).

Methylene tetrahydrofolate reductase (MTHFR) is a key player enzyme in the folate / one-carbon metabolic pathway that is involved in catalyzing the irreversible reduction of 5,10-methylenetetrahydrofolate (methylene-THF) to 5-methyltetrahydrofolate (5-methyl THF), the major form of circulating folate in the plasma that is essential for the synthesis of purine nucleotides (Friso *et al.*, 2002; Balaghi and Wagner, 1993; Gao *et al.*, 2009). The reduction of 5, 10-methylene THF by MTHFR produces 5-methyltetrahydrofolate (5-methyl THF), the methyl donor for methionine synthesis from homocysteine. Methionine is the precursor of S-adenosylmethionine (SAM), which is the universal methyl group donor in several cellular reactions, especially those essential for DNA synthesis and repair as well as gene expression (Duthie *et al.*, 2002; Zhang *et al.*, 2007).

* Corresponding author. e-mail: may@yu.edu.jo or maysadiq333@yahoo.com.

A different essential enzyme in this pathway is methyltetrahydrofolate-homocysteine methyltransferase reductase (MTRR), which reactivates the enzyme methyltetrahydrofolate-homocysteine methyltransferase (MTR) that uses SAM in the presence of vitamin B12 as a cofactor to remethylate homocysteine to methionine. Both MTRR and MTR are directly involved in methylation of DNA and other cellular components and gene expression. (Choi and Mason, 2000). The same folate form 5, 10 methylene THF is also used as a substrate for the essential enzyme thymidylate synthase (TYMS) in both the regeneration of dihydrofolate and the synthesis of deoxythymidine monophosphate (dTMP) required for DNA synthesis and repair.

In Jordan, deficiencies in folate and Vitamin B12 are associated with colorectal cancer (Waly *et al*., 2012). In addition, MTHFR C677T was reported to be associated with different common disorders such as thalassemia major (Al-Sweedan *et al*., 2009), failure of in-vitro fertilized-embryo transfer implantation (Qublan *et al*., 2006), arterial thrombosis (Eid and Shubeilat, 2005), increased sensitivity to methotrexate (Al-Refai *et al*., 2009), maternal risk for Down syndrome (Sadiq *et al*., 2011), male infertility (Mfady *et al*., 2014) and the risk of breast cancer (Awwad *et al*., 2015).

This study explores the association between the risk of breast cancer in Jordanian females and each of the following functional folate/one-carbon-related single nucleotide polymorphisms (SNPs): MTR A2756G (rs1805087), *MTHFR* C677T (rs1801133), *MTHFR*A1298C (rs1801131), *TYMS* 1494 ins/del 6 (rs151264360), and *MTRR* A66G (rs1801394). These five functional variants were reported to alter the activity of their respective enzymes. Both *MTHFR* C677T (rs1801133) and *MTHFR* A1298C (rs1801131) are associated with the reduction in the MTHFR enzyme activity which is one of the factors responsible for DNA methylation (Weisberg *et al*., 1998; Frosst *et al*., 1995). *TYMS* 1494 ins/del 6 (rs151264360) is associated with the disruption of TYMS enzyme and reduction in its activity (Ulrich *et al*., 2000), leading to the depletion of dTMP and accumulation of dUMP, which consequently causes misincorporation of dUMP in place of dTMP leading to DNA single and double strand breaks as well as genomic instability (DeVos *et al*., 2008). Also, *MTRR* A66G (rs1801395) resulted in the reduction of the MTRR enzyme activity, and leads to reduction in the functional MTR enzyme and consequently the hypomethylation of DNA, and was proved to be associated with the risk of cancers (Wang *et al*., 2017).

In addition, the effect of the menopausal status of breast cancer cases on the risk of breast cancer associated with the studied SNPs was examined in this current study. Furthermore, the possible associations between the double compound genotypes of these SNPs with the risk of breast cancer in all the cases were investigated in this study in order to better understand the molecular bases of breast cancer, which may help in future management of the disease in Jordan.

2. Materials and Methods

2.1. Subjects

This study is a case-control study, which included two-hundred confirmed breast cancer cases and another two-hundred age-matched female Jordanian control women. The average mean ages (± SD) of the case and control female groups were 50.22 ± 10.8 and 49.03± 10.4 years respectively with no significant age difference between them (P= 0.919). All subjects were recruited during the period from March 2009 to January 2012 from two referral hospitals for cancer in the northern and middle regions of Jordan. All participants completed a questionnaire, which included their menopausal status when diagnosed with breast cancer and signed a separate informed consent. This study was approved by the ethics committee at Jordan University of Science and Technology and the Ministry of Health. Each participant signed an informed consent before her inclusion in the study. Respect for the anonymity and confidentiality of information were also strictly complied with the Declaration of Helsinki (World Medical, 2013).

2.2. Blood Samples and DNA Isolation

Peripheral blood samples were collected from each subject in EDTA tubes and genomic DNA was extracted using commercially available kits (Qiagen, Gentra Puregen, Germany) according to the manufacturer's instructions.

2.3. Genotyping

Genotyping was performed by polymerase chain reactions followed by restriction fragment length polymorphism (PCR-RFLP) according to earlier established methods as summarized in Table 1. Amplifications of each SNP was carried out in a total volume of 25µL containing the specific forward and reverse primers, master mix (GOTag® Green Master Mix, Promega, USA or Quick-load® Taq 2X master mix, BioLabs) and 50-100 ng of genomic DNA. Restriction digestions by the proper enzymes (Promega, USA or New England BioLabs) were performed according to the instructions of the manufacturer (Table 1). PCR products and their digestion products were separated on 3 % agarose gels. Results were validated by simultaneously running positive control DNA of known genotypes.

2.4. Statistical Analysis

Comparisons between frequencies of alleles and genotypes in the different groups were evaluated using Pearson Chi square test (P= 0.05). Comparisons between cases and female control groups) and identification of the risk factors associated with breast cancer were achieved using logistic regression analysis and calculation of odds ratios (OR) at 95 % confidence intervals (CI). All statistical analyses were applied using IBM SPSS Statistics software (version 23.0).

Table 1. Primers and conditions used for genotyping analysis of the examined polymorphisms.

SNP ID	Variant	[a]Primers sequence (5'→ 3')	PCR conditions	Restriction enzyme, and incubation conditions	Fragment length produced in base pairs	Primers reference
rs1801133	*MTHFR C677T*	F: TGAAGGAGAAGGTGTCTGCGGGA R: AGGACGGTGCGGTGAGAGTG	95°C for 8 min followed by 30 cycles: 94°C for 60s, 63°C for 60s, 72°C for 60s then extension at 72°C for 5 min.	Hinf I, 37°C, 16 hours	C allele: 198 T allele: 175 + 23	Yi *et al*, 2002
rs1801131	*MTHFR A1298C*	F: CAAGGAGGAGCTGCTGAAGA R: CCACTCCAGCATCACTCACT	95°C for 8 min followed by 30 cycles: 94°C for 60s, 63°C for 60s, 72°C for 60s then final extension at 72°C for 5 min.	*Mbo* II, 37°C, 16 hours	A allele: 72+28 C allele: 100	Yi *et al*, 2002
rs 1805087	*MTR* A2756G	F:CATGGAAGAATATGAAGATATTAGA C R: GAACTAGAAGACAGAAATTCTCTA	95°C for 5 min, followed by 35 cycles: 95°C for 45s, 55° C for 35s, 72°C for 72s, then final extension at 72°C for 5 min.	*Hae* III, 37°C, 2 hours.	A allele: 189 G allele: 159 bp + 30 bps	Leclerc *et al* 1996
rs1801394	*MTRR A66G*	F: GCAAAGGCCATCGCAGAAGACAT R: AAACGGTAAAATCCACTGTAACGGC	30 cycles: 94°C for 60s, 35s for 60°C for 60s, 72°C for 60s; then final extension at 72°C for 5 min.	*Nsp* I, 37°C, 16 hours	G allele: 94+24 A allele: 118	Feix *et al*.2004
rs151264360	*TYMS* 1494 ins/del6	F: CAAATCTGAGGGAGCTGAGT R: CAGATAAGTGGCAGTACAGA	95°C for 5 min. followed by 40 cycles: 95°C for 45 seconds, 72°C for 60s; then final extension at 72°C for 5 min.	*Dra* I, 37°C, 2 hours	+6 bp allele: 88 +70 - 6bp allele: 152 -/+ genotype: 158 + 152 + 88 + 70	Ulrich *et al*. 2000

[a] Primers were obtained from Alpha DNA, Canada.

3. Results

3.1. Distribution of the Different Alleles and Genotypes in All Jordanian Cases and Control Females

Genotyping of *MTHFR* C677T, *MTHFR* A1298C and *MTRR* A66G SNPs is presented in Figure 1, while the genotyping of TYMS (1494 ins/del 6) and *MTR* A2756G is presented in Figure 2. The distributions of the different genotypes of each of the five examined SNPs between the cases and the control females were in accordance with Hardy Weinberg equilibrium ($P > 0.05$). The numbers and frequencies of the different alleles and genotypes in the cases and the control female groups with their analyses were verified in odd ratios (ORs) and 95 % confidence intervals (CIs) in Table 2.

Genotypic analysis of all breast cancer cases as one group compared to the control females showed only significant statistical difference between the controls and the cases in the distribution of the homozygous mutant genotype *MTR* 2756GG (OR = 4.36; CI= 1.21-15.7; P = 0.011), while the heterozygous genotype *MTR* 2756 AG showed lack of association with the risk of breast cancer (OR = 0.88; CI=0.88-1-31; P =0.260).

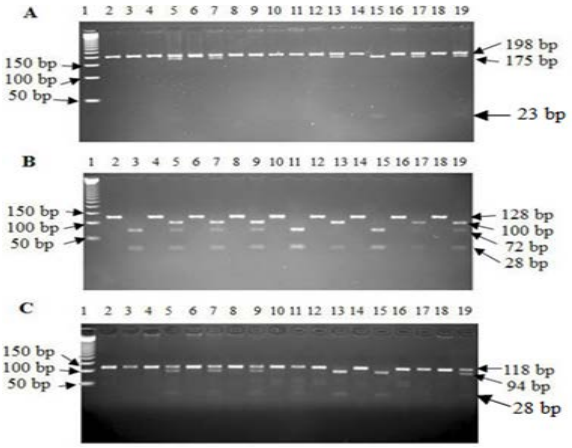

Figure 1. Representative results of PCR-RFLP genotyping of *MTHFR* C677T, MTHFR A1298C and *MTRR* A66G. Lane 1 In all three panels has DNA marker (50 bp ladder). The even numbered lanes of each pair have undigested PCR product, followed by its respective digestion products in the odd numbered lane. **Panel A:** Genotyping analysis of *MTHFR* C677T: lanes 2/3: positive control with previously known wild type genotype CC (single 198 bp band); lanes 4/5: heterozygous CT (198 bp and 175 bp bands). Tested Jordanian Samples: lanes 6/7, 12/13, 16/17 and 18/19: CT genotype; Lanes 8/9 and10/11: CC genotype; lane 14/15: TT genotype. **Panel B:** Genotyping analysis of *MTHFR* A1289C: lanes 2/3: positive control with previously known wild type AA genotype, (72 bp and 28 bp bands); Lanes 4/5: Positive control with previously known genotype: AC (100 bp, 72 bp and 28 bp bands). Tested Jordanian subjects: lanes 6/7, 8/9 and 18/19: AC genotypes; lanes 12/13 and 16/17: CC genotypes; lanes 10/11 and 14/15: AA genotype. **Panel C:** Genotyping analysis of *MTRR* A66G: lanes 2/3: positive control with previously known genotype: AA, wild type genotype (single 118 bp band); lanes 4/5 AG Positive control with previously known genotype: (118 bp and 94 bp). Tested Jordanian subjects: lanes 6/7, 8/9 and 18/19: AG; lanes 12/13 and 14/15: GG.

Table 2. Alleles and genotypes frequencies of *MTHFR* (C677T), *MTHFR* A1298C, *MTR* A2756G, *MTRR* A66G and *TYMS* (1494 ins/del6) polymorphisms in all breast cancer patients and the control females

Polymorphism Alleles and genotypes	Cases Number and (%)	Control females Number and (%)	OR (95% CI)	*P*-value
MTHFR C 77T				
C	268 (0.67)	264 (0.64)	1.00 (ref.)	
T	132 (0.33)	136 (0.36)	1.04 (0.778-1.391)	0.789
CC	94 (0.47)	92 (0.46)	1.00 (ref.)	
CT	80 (0.40)	82 (0.41)	1.05 (0.687-0.596)	0.830
TT	26 (0.13)	26 (0.13)	1.02 (0.522-1.890)	0.945
CT & TT	106 (0.53)	108 (0.54)	1.04 (0.703-1.542)	0.841
MTHFR A1298C				
A	364 (0.64)	255 (0.638)	1.00 (ref.)	
C	136 (0.36)	145 (0.362)	1.10 (0.826-1.476)	0.505
AA	90 (0.45)	87 (0.436)	1.00 (ref.)	
AC	84 (0.42)	81 (0.405)	0.99 (0.653-1.525)	0.991
CC	26 (0.13)	32 (0.16)	1.27 (0.702-2.310)	0.426
AC & CC	110 (0.55)	113 (0.565)	1.06 (0.716-1.577)	0.763
MTRR A66G				
A	263 (0.658)	239 (0.598)	1.00 (ref.)	
G	137 (0.343)	161 (0.403)	1.27 (0.949-1.685)	0.108
AA	87 (0.435)	72 (0.36)	1.00 (ref.)	
AG	87 (0.435)	95 (0.475)	1.312 (0.861-0.022)	0.203
GG	26 (0.13)	33 (0.165)	1.53 (0.841-2.798)	0.162
AG & GG	113 (0.565)	128 (0.64)	1.39 (0.916-2.046)	0.125
MTR A2756G				
A	335 (0.83)	325 (0.81)	1.00 (ref.)	
G	65 (0.16)	75 (0.18)	1.215	0.352
AA	138 (0.69)	138 (0.69)	1.00 (ref.)	
AG	49 (0.24)	59 (0.29)	0.875 (0.534-1.309)	0.260
GG	13 (0.06)	3 (0.01)	4.360 (1.213-15.66)	0.011
AG & GG	62 (0.31)	62 (0.31)	1.00 (0.655-1.528)	0.543
TYMS (1494 ins/del6)				
+	194 (0.48)	199 (0.49)	1.00 (ref.)	
-	206 (0.51)	201 (0.50)	0.923 (0.695-1.225)	0.724
+/+	48 (0.24)	44 (0.22)	1.00 (ref.)	
+/-	103 (0.51)	106 (0.53)	0.897 (0.546-1.474)	0.764
-/-	49 (0.24)	50 (0.25)	0.938 (0.529-1.665)	0.908
+/- & -/-	156 (0.78)	152 (0.76)	0.893 (0.560-1.423)	0.361

Ref: Reference category (wild type allele or genotype); +: (6bp ins) wild type allele; -: (6bp del) mutant allele; OR: Odds Ratio; CI: confidence interval according to multinomial logistic regression.

3.2. Distribution of the Different Genotypes in the Pre- and Post-Menopausal Breast Cancer Cases

The total number of cancer patients who answered the question related to their menopausal status at the time of diagnoses were 185 subjects. Of these, 113 cases were pre-menopausal cases, while 72 were postmenopausal cases. The analysis of the distributions of the different alleles and genotypes between these two groups showed significant difference only in the distribution of the *MTR* A2756G alleles (P =0.22) and genotypes (P=0.008), which indicates a significant association between the risk of breast cancer and the SNP *MTR* A2756G in the post-menopausal group (Table 3). Such differences indicates a positive dominant association between *MTR* 2756 G mutant allele and the risk of breast cancer in the post-menopausal breast cancer cases. No other significant statistical differences were observed in the distributions of the other studied SNPs between the pre-and post-menopausal cases.

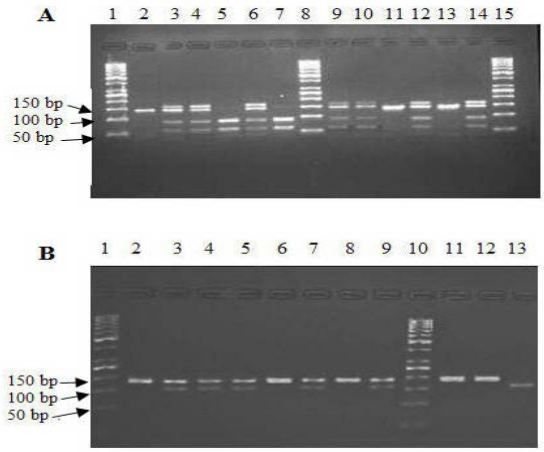

Figure 2. Representative results of PCR-RFLP genotyping of *TYMS* (1494 ins/del 6) and *MTR* A2756G.

Panel A: Genotyping analysis of *TYMS* (1494 ins/del 6) gel: lanes1, 8 and 15: DNA marker (50 bp ladder); lane 2: positive control of mutant homozygote -6bp/-6bp (152 bp band). Tested Jordanian samples: lanes 3, 4, 6, 9, 10, 12 and 14: heterozygotes +6bp/-6bp (158 bp, 152 bp, 88bp and 70 bp); lane 5: wild type homozygote +6bp/+6bp (88 bp and 70 bp bands); lanes 11 and 13: mutant homozygote -6bp/-6bp.

Panel B: Genotyping analysis of *MTR* A2756G: Lanes 1 and 10: DNA marker (50 bp ladder); lane: 2: positive control of wild type AA (189 bp band); lane 3: positive control of a heterozygote AG (189 bp and the 159 bp bands). Tested Jordanian samples: lanes 4, 5, 7 and 9 have AG heterozygotes; lane 13: mutant homozygote GG (159 bp band).

3.3. Frequencies of the Different Observed Compound Genotypes among Breast Cancer Cases and the Control Females.

No significant differences were found between the breast cancer cases and the control women in the observed compound genotypes between *MTR* A2756G with any of the other four studied SNPs (Table 4). However, significant differences were observed between the breast cancer cases and the control females in five out of the eight observed double compound genotypes between *TYMS* ins-del6bp and *MTRR* A66G (Table 5), in addition to four out of the seven observed compound double genotypes between *MTRR* A66G and *MTHFR* 677C as well as with a single double heterozygous genotype between *MTHFR*A1298A and A*MTRR* 66G out of nine observed double genotypes (Table 6).

Table 3. Distribution of the different genotypes in the pre-and postmenopausal breast cancer cases

Polymorphism	Menopausal Status[a]		*P*-value
	Pre-menopause No. (%)	Postmenopause No. (%)	
MTHFR C677T			
C (ref)	151 (40.8)	95 (25.7%)	0.477
T	75 (20.3)	49 (13.2%)	
CC (ref)	55 (29.7%)	31 (16.8%)	0.406
CT	41 (22.2%)	33 (17.8%)	
TT	17 (9.2%)	8 (4.3%)	
MTHFR A1298C			
A (ref)	154 (41.6%)	91 (24.6%)	0.192
C	72 (19.5%)	53 (14.3%)	
AA (ref)	54 (29.2%)	29 (16.8%)	0.599
AC	46 (24.9%)	33 (17.8%)	
CC	13 (7%)	10 (5.4%)	
MTRR A66G			
A (ref.)	145 (39.2%)	98 (26.5%)	0.256
G	81 (21.9%)	46 (12.4%)	
AA (ref)	49 (26.5%)	33 (17.8%)	0.576
AG	47 (25.4%)	32 (17.3%)	
GG	17 (9.2%)	7 (3.8%)	
MTR A2756G			
A (Ref.)	198 (53.5%)	114 (30.8%)	0.022
G	28 (7.6%)	30 (16.2%)	
AA (ref)	87 (47.0 %)	42 (22.7%)	0.008
AG	24 (13 %)	30 (16.2 %)	
GG	2 (1.1 %)	0 (0 %)	
TYMS (1494 ins/del6bp)			
+6bp (ref.)	103 (27.8%)	77 (20.8%)	0.085
-6bp	123 (33.2%)	67 (18.1%)	
(+6bp/+6bp) (ref.)	23 (12.4%)	17 (9.2%)	0.153
(-6bp/-6bp)	33 (17.8%)	12 (6.5%)	
(+6bp/-6bp)	57(30.8%)	43 (23.2%)	

[a]The total number of cases analyzed is185, which included only cases with known menopausal status at their diagnosis with breast cancer; Ref: Reference category, which is the wild type allele or genotype; No: number of subjects; +: (*TYMS* 6bp ins) wild type allele; (-6bp: *TYMS* del6bp) mutant allele; OR: Odds Ratio; CI: confidence interval according to multinomial logistic regression.

Table 4. Frequencies of the observed double compound genotypes of *MTR* A2756G with each of the other studied polymorphisms compared with their wild type double compound genotypes in all BC patients and controls**.**

Compound genotype	Cases number (%)	Controls number (%)	OR (95% CI)	*P*-value
MTR A2756G/*MTHFR*C677T				
AA/CC	(62) 31.0	(62) 31	1.00 (ref.)	
AG/CC	(30) 15.0	(25) 12.5	1.200 (0.635 - 2.269)	0.575
GG/CC	(2) 1.0	(5) 2.5	0.400 (0.75 - 2.140)	0.284
AA/CT	(55) 27.5	(55) 27.5	1.000 (0.598 - 1.671)	1.000
AG/CT	(24) 12.0	(20) 10	1.200 (0.602 - 2.392)	0.605
GG/CT	(1) 0.5	(7) 3.5	0.143 (0.017 - 1.196)	0.073
AA/TT	(21) 10.5	(21) 10.5	1.000 (0.497 - 2.013)	1.000
AG/TT	(5) 2.5	(4) 2	1.250 (0.320 - 4.876)	0.748
GG/TT	(0)	(1) 0.5		
MTR A2756G/ *MTHFR* A1298C				
AA/AA	(70) 35	(60) 30.0	1.00 (ref.)	
AG/AA	(20) 10.0	(24) 12.0	0.714(0.360 –1.419)	0.337
GG/AA	0 (0)	(3) 1.5	-	-
AA/AC	(53) 26.5	(58) 29.5	0.783 (0.471 - 1.301)	0.345
AG/AC	(29) 14.5	(14) 7.0	1.776 (0.860 - 3.666)	0.121
GG/AC	(2) 1	(9) 4.5	0.190 (0.040 - 0.916)	0.039
AA/CC	(15) 7.5	(20) 10.0	0.643(0.303 - 1.365)	0.250
AG/CC	(10) 5	11 (5.5)	0.779 (0.310 - 1.962)	0.596
GG/CC	(1) 0.5	(1) 0.5	0.857 (0.52 - 14.000)	0.914
MTR A2756G/*MTRR* A66G				
AA/AA	(61) 30.5	(47) 23.5	1.00 (ref.)	
AG/AA	(24) 12	(21) 10.5	0.881 (0.438 - 2.269)	1. 770
GG/AA	(2) 1	(4) 2	0.385 (0.068 - 2.194)	0.282
AA/AG	(60) 30	(69) 34.5	0.670 (0.401 - 1.1.120)	0.127
AG/AG	(26) 13.0	(22) 11.0	0.911 (0.460 – 1.804)	0.788
GG/AG	(1) 0.5	(4) 2	0.193 (0.021 - 1.781)	0.147
AA/GG	(17) 8.5	(22) 11	0.595 (0.285 – 1.246)	0.169
AG/GG	(9) 4.5	(6) 3	1.156 (0.384 – 3.475)	0.797
GG/GG	(0) 0.0	(5) 2.5		
MTR A2756G/ *TYMS* (1494 ins/del 6bp)				
AA/ +/+6bp	(32) 16	(37) 18.5	1.00 (ref.)	
AA/ -/+ 6bp	(72) 36	(67) 33.5	1.243 (.697-2.216)	0.462
AA/ -/- 6bp	(34) 17	(34) 17	1.156 (0.591 - 2.261)	0.671
AG/ -/- 6bp	(16) 8	(13) 6.5	1.423 (0.595 -3.402)	0.427
AG/ -/+ 6bp	(32) 16	(28) 14	1.321 (0.660 -2.644)	0.431
AG/ +/+6bp	(11) 5.5	(8) 4	1.590 (0.570 - 4.437)	0.376
GG/ +/+6bp	(1) 0.5	(3) 1.5	0.385 (0.038 -3.891)	0.419
GG/ +/- 6bp	(2) 1	(8) 4	0.289 (0.057 -1.461)	0.133
GG/ -/- 6bp	(0) 0	(2) 1	-	

Ref.: Reference category(double wild type genotype).

Table 5. Frequencies of the observed double compound genotypes of *TYMS* ins/del 6bp with each of *MTHFR* C677T, *MTHFR* A1298C and *MTRR* A66G compared with their wild type double compound genotypes in breast cancer patients and control females**.**

Compound genotype	No. of Cases (%)	No. of controls (%)	OR (95% CI)	*P*-value
TYMS ins-del6bp / *MTHFR* C677T				
+/+6bp/ CC	21(10.5)	19 (9.5)	1.00 (ref.)	
+/-6bp/ CC	45(22.5)	50 (25)	0.814(0.389-1.706)	0.586
+/+ 6bp/ TT	4(2)	8 (4)	0.452(0.117-1.747)	0.250
+/+6bp/ CT	19(9.5)	21(10.5)	0.819 (0.340-1.969)	0.655
+/- 6bp/ CT	45(22.5)	41(20.5)	0.993(0.469-2.105)	0.985
-/- 6bp/ CT	16(8)	20(10)	0.724(0.293-1.787)	0.483
+/-6bp/ TT	16(8)	12(6)	1.206(0.456-3.19)	0.705
-/- 6bp/ TT	6(3)	6(3)	0.905(0.249-3.289)	0.879
-/- 6bp/ CC	28(14)	23(11.5)	1.101(0.480-2.527)	0.820
TYMS ins-del6bp / *MTHFR* A1298C				
+/+ 6bp/ AA	18(9)	15(7.5)	1.00 (ref.)	
+/- 6bp/ AA	47(23.5)	46(23)	0.851 (0.384-1.889)	0.692
-/-6bp/ AA	25(12.5)	26(13)	0.801 (0.33-1.928)	0.621
-/- 6bp/ AC	17(8.5	18(9)	0.787 (3.303-2.042)	0.622
+/- 6bp/ AC	45(22.5)	40(20)	0.937 (0.418-2.101)	0.875
+/+ 6bp/ AC	22(11)	23(11.5)	0.797 (0.324-1.962)	0.622
-/- 6bp/ CC	8(4)	5(2.5)	1.333(0.360-4.945)	0.667
+/- 6bp/ CC	14(7)	17(8.5)	0.686 (0.256-1.837)	0.454
+/+ 6bp/ CC	4(2)	10(5)	0.333(0.087-1.282)	0.110
TYMS ins-del6bp / *MTRR* A66G				
+/+ 6bp/ AA	22(11)	37(18.5)	1.00 (ref.)	
+/- 6bp/ AA	43(21.5)	67(33.5)	1.079(0.562-2.072)	0.818
-/-6bp/ AA	22(11)	34(17)	1.088(0.513-2.309)	0.826
-/- 6bp/ AG	20(10)	13(6.5)	2.587(1.078-6.208)	0.033
+/- 6bp/ AG	49(24.5)	28(14)	2.943(1.457-5.944)	0.003
+/+ 6bp/ AG	18(9)	8(4)	3.784(1.412-10.966)	0.008
-/- 6bp/ GG	8(4)	2(1)	6.727(1.309-34.572)	0.022
+/- 6bp/ GG	14(7)	8(4)	2.943(1.065-8.132)	0.037
+/+ 6bp/ GG	4(2)	3(1.5)	2.242 (0.459-10.966)	0.319

Ref.: Reference category (double wild type genotype); OR: Odds Ratio; CI: confidence interval according to multinomial logistic regression. No.: number

Table 6. Frequencies of the observed double compound genotypes of *MTHFR* C677T/A, *MTHFR* A1298C and *MTRR* A66G compared with their wild type double compound genotypes in the breast cancer patients and the control females**.**

Compound Genotype	No. of Cases (%)	No. of Control females (%)	OR (95% CI)	*P*-value
MTHFR C677T / *MTHFR* A1298C				
CC/AA	28 (14)	28 (14)	1.00 (ref.)	
CC/AC	41 (20.5)	35 (17.5)	1.17 (0.587-2.338)	0.654
CC/CC	25 (12.5)	29 (14.5)	0.86 (0.408- 1.823)	0.689
CT/AA	40 (20)	38 (19)	1.53 (0.530- 2.092)	0.884
CT/AC	39 (19.5)	41 (20.5)	0.95 (0.480-1.883)	0.886
CT/CC	1 (0.5)	3 (1.5)	0.33 (0.033- 3.402)	0.613
TT/AA	22 (11)	21 (10.5)	1.05 (0.473- 2.320)	0.909
TT/AC	4 (2)	5 (2.5)	0.80 (0.194- 3.294)	0.757
TT/AC	ND (0)	ND (0)		
MTHFR C677T / *MTRRA66G*				
CC/AA	42 (21)	62 (31)	1.00 (ref.)	
CC/AG	40 (20)	25 (12.5)	2.36 (1.252-4.457)	0.008
CC/GG	12 6)	5 (2.5)	3.54 (1.162-10.797)	0.026
CT/AA	34 (17)	55 (77.5)	0.91 (0.511-1.630)	0.757
CT/AG	33 (16.5)	20 (10)	2.44 (1.234-4.806)	0.010
CT/GG	13 (6.5)	7 (3.5)	2.74 (1.010-7.444)	0.048
TT/AA	11 (5.5)	21 (10.5)	0.77 (0.338-1.770)	0.543
TT/AG	14 (7)	4 (2)	5.17 (1.590-16.784)	0.006
TT/GG	1 (0.5)	1 (0.5)		
MTHFR A1298C / *MTRRA66G*				
AA/AA	42 (21)	60 (30)	1.00 (ref.)	
AA/AG	36 (18)	24 (12)	2.14 (1.119-4.104)	0.22
AA/GG	12 (6)	3 (1.5)	5.71 (1.519-21.502)	0.10
AC/AA	34 (17)	58 (29.5)	0.84 (0.470-1.494)	0.548
AC/AG	39 (19.5)	14 (7)	3.98 (1.924-8.232)	0.000
AC/ GG	11 (5.5)	9 (4.5	1.75 (0.665-4.584)	0.258
CC/AA	11 (5.5)	20 (5.5)	0.79 (0.341-1.810)	0.571
CC/AG	12 (6)	11 (5.5	1.56 (0.628-3.865)	0.338
CC/GG	3 (1.5)	1 (0.5)	4.29 (0.31-42.630)	0.214

NO: Number; ref: Reference category (double wild type genotype); OR: Odds Ratio; CI: confidence interval according to multinomial logistic regression; ND: not detected in this study

4. Discussion

In this case-control study, the associations between five SNPs in the folate/one-carbon metabolism and the risk of female breast cancer in Jordan are examined. this study reports for the first time that there is a direct association between the risk of female breast cancer in Jordan and the mutant homozygous genotype GG of the SNP *MTR* A2756G (rs1805087). This is in agreement with previously reported association of this SNP with the susceptibility of different cancers, and is also in agreement with the role of MTR enzyme in activating MTRR that is essential for the synthesis of the universal one carbon donor SAM, that affects DNA methylation and gene expression (Krushkal *et al*., 2016).

The fact that that the homozygous genotype *MTR* 2756GG increased the risk of breast cancer in Jordanian females by more than four folds (GG: OR=4.360; CI=1.213-15.666, p= 0.011), while its heterozygous genotype had no such risk for breast cancer, indicates a recessive role of the mutant *MTR* 2756G towards its wild type allele in being a risk factor for breast cancer.

However, in the post-menopausal cases, *MTR* 2756G mutant allele as well as its homozygous and heterozygous genotypes were positively associated with breast cancer, which indicated that the menopausal status of Jordanian women has a significant modifying effect on their risk of breast cancer. This observed positive association between *MTR* 275G with breast cancer was in agreement with the role of wild type MTR in DNA synthesis, repair, and methylation (Krushkal *et al*., 2016).

The observed lack of associations between the risk of breast cancer and each of the single alleles of the other examined four SNPs in both groups of cases as well as the separated pre- and post-menopausal breast cancer cases, indicated that the menopausal status of Jordanian women had no effect on the association between any of the other four examined SNPs and the risk of breast cancer.

Despite the observed lack of association between the risk of breast cancer with each individual SNPs *TYMS* (1494 ins/del 6) and *MTRR* A66G, the results show a significant association between their compound double heterozygous genotypes with the risk of breast cancer, which could be related to an additive effect of both altered MTRR and TYMS enzymes. MTRR function is to regenerate the active form of MTR that is involved in DNA methylation, while TYMS enzyme is directly involved in DNA synthesis. The alteration of both enzymes in these double heterozygotes seemed to cause perturbation in both DNA synthesis, repair, and gene expression that is expected to lead to pleiotropic cellular effects that may end up with carcinogenesis (Choi and Mason, 2000).

The observed lack of significant association between *MTHFR* C677T and the risk of breast cancer in the Jordanian females was different from the results reported previously in Jordan (Awwad *et al.*, 2015), which suggested a positive association between *MTHFR* C677T and breast cancer. Such difference may be due to the differences in the design of the two studies; unlike this current study, Awwad *et al*., (2015) used 150 female cases and 150 age-matched healthy individuals at Al-Basheer hospital, which is located in the central part of Jordan. Besides, there is still some doubt regarding their control group, which were defined as "150 age-matched healthy individuals". Furthermore, their sample collection was limited to 9 months between the 15th of March till 21st of December 2014, which may not be significantly random and representative of the Jordanian population, as much as this study's 200 samples, which were collected from two different hospitals in the central and the northern parts of Jordan over a period of more than two years.

In this study, the observed lack of association between *MTHFR* C677T and the risk of breast cancer in Jordanians is similar to those reported in Saudi (Alshatwi, 2010), Greek (Kalemi *et al.*, 2005), Japanese (Ma *et al.*, 2009) and Brazilian populations (Batschauer *et al.*, 2011), but it is different from those reported in Turks (Ergul *et al*., 2003; Deligezer *et al*., 2005), Chinese (Gao *et al*., 2009), and the Americans (Chen *et al.*, 2005). Similarly, the observed absence of association between the risk of breast cancer and *MTHFR* A1298C alleles and genotypes in this study is in harmony with those found in Saudis (Alshatwi, 2010), Polish (Lissowska *et al.*, 2007), Chinese (Gao *et al*., 2009) and Russian populations (Vainer *et al*., 2010), but it is contrary to the results reported in the Turkish (Ergul *et al*., 2003) and the American (Chen *et al*., 2005) populations.

There is a lack of association between the risk of breast cancer in the carriers of *MTHFR* C677T and *MTHFR* A1298C as well as their double heterozygous genotype *MTHFR* 677 CT / 1298AC, although these genotypes lead to the reduction in the MTHFR activity compared to homozygous wild-types (Narayanan *et al.*, 2004); however, such unexpected results may be explained by either the genetic backgrounds of our subjects and/or the compensation of folate-rich diet and supplementation by Jordanian women before and during pregnancies, which leads to the compensation of the plasma levels of the central metabolite 5, 10-methylene-THF in the folate/one-carbon metabolism. This is in harmony with the differences in the risk factors for breast cancer in different populations, which are thought to be affected by the different genetic backgrounds of the populations, as well as the difference in their life styles and diets (Alshatwi, 2010; Gao *et al.*, 2009; Ma *et al*., 2009; Ericson *et al*., 2007), in addition to the compensation for the lack of MTHFR catalytic activity through different side pathways within the folate/one-carbon metabolism that utilize MTHFD1 and TYMS enzymes (James and Hobbs, 2002). More studies of the compound genotypes of the folate-related genes, which need a larger number of cases, will allow for a better understanding of the link between folate metabolism and the risk of breast cancer in Jordan.

5. Conclusions

This study shows that *MTR* A2756G (rs1805087) homozygous mutant genotype *MTR* 2756GG is significantly associated with the risk of breast cancer in Jordanian females. Furthermore, the menopausal status of these females influences the risk of breast cancer in the females heterozygous to *MTR* A2756AG genotype. In addition, this study found out that the compound double heterozygous genotypes between *TYMS* (1494 ins/del 6), *MTRR* A66G and *MTHFR* C677T) are significantly associated with the risk of breast cancer in Jordan, which indicates that the folate/one-carbon SNPs constituted potential contributing risk factors for breast cancer in Jordanian females.

Acknowledgments

The authors acknowledge the kindness of the participating patients and control females. This study was supported by Grants from the Deanship of Research at Jordan University of Science and Technology and the Deanship of Scientific Research and Higher Studies at Yarmouk University (Irbid, Jordan).

Conflicts of Interest

The authors declare no conflict of interest.

References

Al-Refai EA, Sadiq MF, Khassawneh MY and Amjad DA. 2009. Effect of methotrexate on the survival of human lymphocyte cultures carrying MTHFR 677 (C>T) and MTHFR 1298 (A>C) mutations. *Drug Chem Toxicol*, **32 (2)**:103-107.

Al-Sweedan SA, Jaradat S, Iraqi M and Beshtawi M. 2009. The prevalence of factor V Leiden (G1691A), prothrombin G20210A and methylenetetrahydrofolate reductase C677T mutations in Jordanian patients with beta-thalassemia major. *Blood Coagul Fibrinolysis*, **20 (8)**:675-678.

Alshatwi AA. 2010. Breast cancer risk, dietary intake, and methylenetetrahydrofolate reductase (MTHFR)single nucleotide polymorphisms. *Food Chem Toxicol*, **48 (7)**:1881-1885.

Awwad N, Yousef AM, Abuhaliema A, Abdalla I and Yousef M. 2015. Relationship between Genetic Polymorphisms in MTHFR (C677T, A1298C and their Haplotypes) and the Incidence Of Breast Cancer among Jordanian Females--Case-Control Study. *Asian Pac J Cancer Prev*, **16 (12)**:5007-5011.

Balaghi M and Wagner C. 1993. DNA methylation in folate deficiency: use of CpG methylase. *Biochem Biophys Res Commun*, **193 (3)**:1184-1190.

Batschauer AP, Cruz NG, Oliveira VC, Coelho FF, Santos IR, Alves MT, Fernandes AP, Carvalho MG and Gomes KB. 2011. HFE, MTHFR, and FGFR4 genes polymorphisms and breast cancer in Brazilian women. *Mol Cell Biochem*, **357 (1-2)**:247-253.

Chen J, Gammon MD, Chan W, Palomeque C, Wetmur JG, Kabat GC, Teitelbaum SL, Britton JA, Terry MB, Neugut AI and Santella RM. 2005. One-carbon metabolism, MTHFR polymorphisms, and risk of breast cancer. *Cancer Res*, **65 (4)**: 1606-1614.

Choi SW and Mason JB. 2000. Folate and carcinogenesis: an integrated scheme. *J Nutr*, **130 (2)**:129-132.

Deligezer U, Akisik EE and Dalay N. 2005. Homozygosity at the C677T of the MTHFR gene is associated with increased breast cancer risk in the Turkish population. *In Vivo*, **19 (5)**:889-893.

DeVos L, Chanson A, Liu Z, Ciappio ED, Parnell LD, Mason JB, Tucker KL and Crott JW. 2008. Associations between single nucleotide polymorphisms in folate uptake and metabolizing genes with blood folate, homocysteine, and DNA uracil concentrations. *Am J Clin Nutr*, **88 (4)**:1149-1158.

Duthie SJ. 1999. Folic acid deficiency and cancer: mechanisms of DNA instability. *Br Med Bull*, **55 (3)**:578-592.

Duthie SJ, Narayanan S, Brand GM, Pirie L and Grant G. 2002. Impact of folate deficiency on DNA stability. *J Nutr*, **132 (8 Suppl)**:2444S-2449S.

Eid SS and Shubeilat T. 2005. Prevalence of factor V Leiden, prothrombin G20210A, and MTHFR G677A among 594 thrombotic Jordanian patients. *Blood Coagul Fibrinolysis*, **16 (6)**:417-421.

Ergul E, Sazci A, Utkan Z and Canturk NZ. 2003. Polymorphisms in the MTHFR gene are associated with breast cancer. *Tumour Biol*, **24 (6)**:286-290.

Ericson U, Sonestedt E, Gullberg B, Olsson H and Wirfalt E. 2007. High folate intake is associated with lower breast cancer incidence in postmenopausal women in the Malmo Diet and Cancer cohort. *Am J Clin Nutr*, **86 (2)**:434-443.

Ferlay J, Soerjomataram I, Dikshit R, Eser S, Mathers C, Rebelo M, Parkin DM, Forman D and Bray F. 2015. Cancer incidence and mortality worldwide: sources, methods and major patterns in GLOBOCAN 2012. *Int J Cancer*, **136 (5)**:E359-386.

Friso S, Choi SW, Girelli D, Mason JB, Dolnikowski GG, Bagley PJ, Olivieri O, Jacques PF, Rosenberg IH, Corrocher R and Selhub J. 2002. A common mutation in the 5,10-methylenetetrahydrofolate reductase gene affects genomic DNA methylation through an interaction with folate status. *Proc Natl Acad Sci U S A*, **99 (8)**:5606-5611.

Frosst P, Blom HJ, Milos R, Goyette P, Sheppard CA, Matthews RG, Boers GJ, den Heijer M, Kluijtmans LA, van den Heuvel LP, and et al. 1995. A candidate genetic risk factor for vascular disease: a common mutation in methylenetetrahydrofolate reductase. *Nat Genet*, **10 (1)**:111-113.

Gao CM, Kazuo T, Tang JH, Cao HX, Ding JH, Wu JZ, Wang J, Liu YT, Li SP, Su P, Keitaro M and Toshiro T. 2009. [MTHFR polymorphisms, dietary folate intake and risks to breast cancer]. *Zhonghua Yu Fang Yi Xue Za Zhi*, **43 (7)**:576-580.

James S, and Hobbs C. 2002. **Folate and Human Development,** edited by editor Massaro E, 43-70. Humana Press.

Jordan Cancer Registry MOH. 2016. "Cancer Inscidence in Jordan, Yearly Statitical Report (2013 Report), Page 46." accessed 15 Feb 2018.

Kalemi TG, Lambropoulos AF, Gueorguiev M, Chrisafi S, Papazisis KT and Kotsis A. 2005. The association of p53 mutations and p53 codon 72, Her 2 codon 655 and MTHFR C677T polymorphisms with breast cancer in Northern Greece. *Cancer Lett*, **222 (1)**:57-65.

Krushkal J, Zhao Y, Hose C, Monks A, Doroshow JH and Simon R. 2016. Concerted changes in transcriptional regulation of genes involved in DNA methylation, demethylation, and folate-mediated one-carbon metabolism pathways in the NCI-60 cancer cell line panel in response to cancer drug treatment. *Clinical Epigenetics*, **8**:73.

Lissowska J, Gaudet MM, Brinton LA, Chanock SJ, Peplonska B, Welch R, Zatonski W, Szeszenia-Dabrowska N, Park S, Sherman M and Garcia-Closas M. 2007. Genetic polymorphisms in the one-carbon metabolism pathway and breast cancer risk: a population-based case-control study and meta-analyses. *Int J Cancer*, **120 (12)**:2696-2703.

Ma E, Iwasaki M, Junko I, Hamada GS, Nishimoto IN, Carvalho SM, Motola J, Jr., Laginha FM and Tsugane S. 2009. Dietary intake of folate, vitamin B6, and vitamin B12, genetic polymorphism of related enzymes, and risk of breast cancer: a case-control study in Brazilian women. *BMC Cancer*, **9**:122.

Mfady DS, Sadiq MF, Khabour OF, Fararjeh AS, Abu-Awad A and Khader Y. 2014. Associations of variants in MTHFR and MTRR genes with male infertility in the Jordanian population. *Gene*, **536 (1)**:40-44.

Narayanan S, McConnell J, Little J, Sharp L, Piyathilake CJ, Powers H, Basten G and Duthie SJ. 2004. Associations between two common variants C677T and A1298C in the methylenetetrahydrofolate reductase gene and measures of folate metabolism and DNA stability (strand breaks, misincorporated uracil, and DNA methylation status) in human lymphocytes in vivo. *Cancer Epidemiol Biomarkers Prev*, **13 (9)**:1436-1443.

Pardini B, Kumar R, Naccarati A, Prasad RB, Forsti A, Polakova V, Vodickova L, Novotny J, Hemminki K and Vodicka P. 2011. MTHFR and MTRR genotype and haplotype analysis and colorectal cancer susceptibility in a case-control study from the Czech Republic. *Mutat Res*, **721 (1)**:74-80.

Qublan HS, Eid SS, Ababneh HA, Amarin ZO, Smadi AZ, Al-Khafaji FF and Khader YS. 2006. Acquired and inherited thrombophilia: implication in recurrent IVF and embryo transfer failure. *Hum Reprod*, **21 (10)**:2694-2698.

Sadiq MF, Al-Refai EA, Al-Nasser A, Khassawneh M and Al-Batayneh Q. 2011. Methylenetetrahydrofolate reductase polymorphisms C677T and A1298C as maternal risk factors for Down syndrome in Jordan. *Genet Test Mol Biomarkers*, **15 (1-2)**:51-57.

Ulrich CM, Bigler J, Velicer CM, Greene EA, Farin FM and Potter JD. 2000. Searching expressed sequence tag databases: discovery and confirmation of a common polymorphism in the thymidylate synthase gene. *Cancer Epidemiol Biomarkers Prev*, **9 (12)**:1381-1385.

Vainer AS, Boiarskikh UA, Voronina EN, Selezneva IA, Sinkina TV, Lazarev AF, Petrova VD and Filipenko ML. 2010.

[Polymorphic variants of folate metabolizing genes (C677T and A1298C MTHFR, C1420T SHMT1 and G1958A MTHFD) are not associated with the risk of breast cancer in West Siberian Region of Russia]. *Mol Biol (Mosk)*, **44 (5)**:816-823.

Waly M, Arafa M, Jriesat S, Sallam S, and Al-Kafajei A. 2012. Folate and vitamin B12 deficiency is associated with colorectal cancer in Jordan. *Inter J Nutr Pharmacol Neurol Dis*., **2 (1)**:57-60.

Wang P, Li S, Wang M, He J and Xi S. 2017. Association of MTRR A66G polymorphism with cancer susceptibility: Evidence from 85 studies. *J Cancer*, **8 (2)**:266-277.

Weisberg I, Tran P, Christensen B, Sibani S and Rozen R. 1998. A second genetic polymorphism in methylenetetrahydrofolate reductase (MTHFR) associated with decreased enzyme activity. *Mol Genet Metab*, **64 (3)**:169-172.

World Medical A. 2013. World Medical Association Declaration of Helsinki: ethical principles for medical research involving human subjects. *JAMA*, **310 (20)**:2191-2194.

Zhang JG, Liu JX, Li ZH, Wang LZ, Jiang YD and Wang SR. 2007. Dysfunction of endothelial NO system originated from homocysteine-induced aberrant methylation pattern in promoter region of DDAH2 gene. *Chin Med J (Engl)*, **120 (23)**:2132-2137.

JJBS

Volume 12, Number 1,March 2019
ISSN 1995-6673
Pages 99 - 106

Jordan Journal of Biological Sciences

The Role of the Overexpression of *Suaeda maritima* Choline Monooxygenase and Betaine Aldehyde Dehydrogenase *cDNAs* in the Enhancement of Salinity Tolerance in Different Strains of *E.coli*

Shrikanth Saraswathi Krishnamurthi[1,3*], Sindhu Kuttan[1], Sankararamasubramanian Meenakshisundram[1], Thajuddin Nooruddin[3*] and Ajay Parida[1, 2*]

[1]*Department of Molecular Biology and Biotechnology, M.S. Swaminathan Research Foundation, Taramani Institutional Area, Chennai 600 113;*

[2]*Institute of Life Science, Bhubaneswar 751 023;* [3]*Department of Microbiology, Bharathidasan University, Tiruchirapalli 620 024, India*

Received May 17, 2018; Revised August 4, 2018; Accepted August 12, 2018

Abstract

Heterologous expression of genes in to *Escherichia coli* helps establish the function of the encoded proteins in complex pathways of higher organisms. This methodology is particularly important in the case of plants where the whole genome sequence information is unavailable. Choline monooxygenase (CMO) and betaine aldehyde dehydrogenase (BADH) are two key enzymes of the glycine betaine biosynthetic pathway in *Suaeda maritima,* a halophyte found growing in the Pichavaram mangroves in Tamil Nadu. The present research is conducted to study the function of *SmCMO* and *SmBADH cDNAs* involved in glycine betaine biosynthetic pathway in *Suaeda maritima* in providing NaCl stress adaptability to *E. coli.* Three different *E. coli* strains namely DH5α, MC4100 and BL21 (DE3) are used for the study. Stability of pET32a*SmCMO+pET32aSmBADH* double recombinants and subsequent analyses for salinity tolerance in each of the strains were performed using *pET32a* protein expression vector. BL21 (DE3) double recombinants showed the maximum level of NaCl tolerance in both Minimal and LB media when compared with that of the other two strains as well as with non-recombinant BL21 (DE3) cells. This study enabled the functional characterization of *S. maritima* glycine betaine pathway genes as well as the additive effect of the *cDNAs* in conferring NaCl tolerance.

Keywords: Salinity, CMO, BADH, Glycine betaine, Osmoprotectants, *E. coli.*

1. Introduction

Living organisms, whether single-celled bacteria or eukaryotic multi-cellular plants and animals, have evolved various mechanisms to cope with extreme environmental conditions. Mangroves represent those plant communities that have developed morphological as well as physiological mechanisms to withstand harsh environmental conditions. They survive under high salinity, light and temperature, as well as heavy metal polluted soils that are considered unsuitable for the survival of other plants (Cheeseman *et al.* 1997). Previous studies have shown that genes isolated from mangroves and mangrove associated halophytes that were transferred to crop plants have been effective in conferring tolerance to abiotic stresses in crop plants (Rathinasabapathi, 2000; Ashraf and Foolad, 2007; Prashanth *et al.* 2008, Yamanaka *et al.* 2009).

Suaeda maritima is herbaceous, succulent, facultative annual halophyte which is native to saline soils of arid and semiarid regions exhibiting a wide range of stress adaptability, and can serve as a potential model for studying the oxidative-stress response in mangroves (Jithesh *et al.* 2006). *S. maritima* is a salt accumulator, and is known to accumulate osmolytes such as proline and glycine betaine (GB) (Moghaeib *et al.* 2004) that helps maintain osmotic equilibrium within the cells and with the external environment. Other species that accumulate GB include halophytic plants such as *Suaeda fruticosa* (Khan *et al.* 2000), *Suaeda aralocaspica, Bienertia sinuspersici* (Park *et al.* 2009) *Salicornia dolichostachya* (Katschnig *et al.* 2013), *Inula crithmoides (*Domenech *et al.* 2016) and halotolerant microbes such as *Ectothiorhodospira halochloris* (Peters and Truper, 1992), *Actinopolyspora halophilia (*Nyyssola *et al.* 2000*), Halomonas elongata* (David *et al.* 2000), *Aphanothece halophytica* (Waditee *et al.* 2003), and *Vibrio sp.* (Yancey *et al.* 1982; Dagmar *et al.* 2005).

Glycine betaine (GB) is also synthesized by most bacteria (Le Rudulier *et al.* 1984), cyanobacteria (Reed *et al.* 1986) and plants (Storey and Jones, 1977; Rhodes and Hanson, 1993). GB acts as a non-toxic cytoplasmic osmolyte, and hence plays a significant role in stress

* Corresponding author. e-mail: ajaydirector18@gmail.com; nthaju2002@yahoo.com; shrimicro3@gmail.com.

adaptation in plants (McNeil *et al.* 1999; Chen and Murata, 2011). Among higher plants, GB is synthesized from choline in a two-step oxidation reaction catalyzed first by a ferredoxin (Fd)-dependent choline monooxygenase (CMO) in to betaine aldehyde (Brouquisse *et al.*1989), followed by a NAD^+-dependent betaine aldehyde dehydrogenase (BADH) to give rise to GB (Weigel *et al.* 1986; Sakamoto and Murata, 2002). GB accumulates in the cytoplasm of plants, where it provides osmotic adjustment (Shabir *et al.* 2013).

Under osmotic stress, most bacteria accumulate organic solutes together with K^+ in their cytoplasm to build up the internal osmotic strength and thereby prevent osmotic dehydration of the cells (Epstein, 1986). *E. coli* display high versatility in the synthesis and uptake of osmoprotectants depending on the classes of compounds present in the growth medium. Betaines such as GB, proline betaine (stachydrine) and λ-butyrobetaine and other osmolytes such as proline, trehalose and glutamic acid when added in low concentrations stimulate the growth of *E. coli* and other enteric bacteria (Larsen *et al.* 1987; Incharoensakdi *et al.* 2000).

In *E. coli*, four genes, *betA*, *betB*, *betI* and *betT* have been associated with GB synthesis and accumulation, subsequently conferring osmotolerance (ability to grow in the presence of ≥ 0.5 M NaCl) when choline is supplied to the growth medium. *BetA* codes for choline dehydrogenase (CDH), *betB* codes for betaine aldehyde dehydrogenase (BADH), *betI* codes for a putative regulatory protein, and *betT* codes for a high affinity choline transporter (Strom *et al.* 1986).The *E. coli* CDH is a membrane bound, oxygen-dependent flavoprotein independent of soluble cofactors, and contains an N-terminal FAD-binding region (Lamark *et al.* 1991). CDH also catalyzes the oxidation of betaine aldehyde to GB *in vitro*, as it has a lower affinity for betaine aldehyde than betaine aldehyde dehydrogenase (Lamark *et al.* 1992). Due to the O_2 requirement of CDH, *E. coli* can utilize choline only under aerobic growth conditions. The *E. coli* BADH is a soluble enzyme with a high affinity for betaine aldehyde, and has a strong preference for NAD^+ as electron acceptor (Boyd *et al.* 1991). The *betT* gene is a choline transporter located upstream to the operon and the entire *bet* gene cluster is regulated by the presence of oxygen, choline, and the occurrence of osmotic stress (Andresen *et al.* 1988; Lamark *et al.* 1996).

The present study is conducted to understand the roles if any, of CMO and BADH proteins of *S. maritima* in providing NaCl stress adaptability to *E. coli* in which the *cDNAs* were introduced. As mentioned earlier, *E. coli* itself is a GB accumulator, and can tolerate high salt concentrations. However, there is a difference between plants and bacteria with respect to the synthesis of GB in the first of the two catalytic steps and in the kinetics of the two principal enzymes involved. Therefore, introducing heterologous genes into *E. coli* necessitates a thorough study of its growth responses in the presence of NaCl at different concentrations and also with respect to differences in genotypes of the strains. The present study intends to first screen the NaCl tolerance of three strains DH5α, MC4100 and BL21(DE3) and assay for the stability or successful retention of plasmids in double recombinants (transformation of *pET32a+SmCMO* as well as *pET32a+ SmBADH* in the same cell).

2. Materials and Methods

2.1. Bacterial Strains

E.coli BL21(DE3), DH5α and MC4100 bacterial strains are used for this study and the genotypes of strains are listed (Supplementary Table 1). The bacterial strains were grown overnight in Luria-Bertani (LB) broth, and were then plated in LB agar. For checking the viability of the strains, they were maintained in both Minimal Medium 63 and LB medium with different concentration of NaCl.

Table 1. Growth response of different *E. coli* strains in the presence of NaCl in M63 Medium.

Strains of *E. coli*		Control w/ o NaCl	0.1M NaCl	0.25M NaCl	0.5M NaCl	0.75M NaCl	1.0M NaCl
BL21(DE3)	1	++++	++++	++++	++++	----	----
	2	++++	++++	++++	++++	----	----
	3	++++	++++	++++	++++	----	----
	4	++++	++++	++++	++++	----	----
DH5α	1	++--	++--	+---	----	----	----
	2	++--	+---	+---	----	----	----
	3	++--	++--	+---	----	----	----
	4	++--	++--	+---	----	----	----
MC4100	1	++++	++++	++++	++--	----	----
	2	++++	++++	++++	+---	----	----
	3	++++	++++	++++	++--	----	----
	4	++++	++++	++++	+---	----	----

Representation of ++++ indicates very good growth; +++- indicates good growth; ++-- indicates moderate growth; +--- indicates poor growth; ---- indicates no growth.

2.2. Growth Kinetics

Ten mL of each LB was inoculated with a loopful of each of the strains and was incubated at 37°C at 180 rpm for twelve to sixteen hours. 2.5 mL aliquots from each of the overnight grown cultures were then transferred to 250mL flasks containing 100mL of pre-warmed LB. At approximately fifteen-minute intervals starting from the time of inoculation, 1mL each of the samples were aseptically transferred, and their absorbance at 600nm (A_{600}) was recorded using a Lambda 3B spectrophotometer. When the growth reached the exponential phase (at ~20 minutes), 2mL each of the samples was taken at thirty-minute intervals. One mL was used for plating, and the remaining 1mL was used for recording the absorbance. Serial dilutions of each of the samples were then prepared and 0.1mL from each of the 10^{-4}, 10^{-5}, and 10^{-6} dilutions was plated onto LB-agar plates and incubated at 37°C.

2.3. Cloning of SmCMO and SmBADH ORFs into E. coli Protein Expression Vector

The full-length cDNA sequences of CMO and BADH (NCBI accession nos. JX629239 and JX629240 respectively) previously isolated by RT-PCR and cloned in T/A cloning vector, were analyzed *insilico* using *webcutter2*.0. Primers with restriction sites were designed

based on the web cutter analyses and the MCS of the cloning vector *pET32a* (Amp$^+$) (Novagen Inc., Germany). The ORF of CMO and BADH were amplified using primers with *Bam H1* and *Xho1* overhangs, digested with *BamH1/Xho1* restriction sites (Supplementary Table 2) and cloned onto *pET32a* at the same sites. The clones were named *pET32a+SmCMO* and *pET32a+SmBADH* as 1.3kb and 1.5 kb respectively and 1 Kb Marker was used.

Table 2. Growth response of different *E. coli* strains in the presence of NaCl in LB Medium.

Strains of *E. coli*		Control (W/O NaCl)	0.1M NaCl	0.25M NaCl	0.5M NaCl	0.75M NaCl	1.0M NaCl
BL21(DE3)	1	++++	++++	++++	++++	++--	----
	2	++++	++++	++++	+++-	+---	----
	3	++++	++++	++++	+++-	++--	----
	4	++++	++++	++++	+++-	+---	----
DH5α	1	++++	++++	++++	+---	+---	----
	2	++++	++++	+++-	+---	----	----
	3	++++	++++	+++-	++--	----	----
	4	++++	++++	++++	----	----	----
MC4100	1	++++	++++	++++	++--	+---	----
	2	++++	++++	++++	++--	+---	----
	3	++++	++++	++++	++--	----	----
	4	++++	++++	++++	++--	----	----

Representation of ++++ indicates very good growth; +++- indicates good growth; ++-- indicates moderate growth; +--- indicates poor growth; ---- indicates no growth

2.4. Competent Cell Preparation

A single *E. coli* colony of each of the BL21(DE3), DH5α and MC4100 cells was inoculated into 10mL each of LB liquid medium containing ampicillin (0.1 %), and was grown overnight at 37ºC at 180 rpm. One hundred (100) µL each of the overnight grown culture was then inoculated into 100mL LB liquid medium, and was incubated at 37ºC at 180 rpm for two to three hours until the absorbance reached 0.4. It was then kept on ice for fifteen to twenty minutes. Cells were then centrifuged at 5000 rpm for ten minutes at 4ºC. The supernatant was discarded, and the pellet was suspended in 1.5mL of freshly-prepared ice cold TSS. Two hundred (200) µL of competent cells were aliquoted in sterile microfuge tubes. The competent cells were frozen in liquid nitrogen and were stored at -80ºC until use (Chung *et al.* 1989).

2.5. Transformation

Two hundred (200) µL of BL21 (DE3), DH5α and MC4100 competent cells, 50ng each plasmid were added and incubated in ice for thirty minutes. Heat shock was given to the cells at 42ºC for ninety seconds and they were immediately kept in ice for five minutes. Eight hundred (800) µL of LB liquid medium was added and kept at 37ºC at 180 rpm for one hour. One hundred (100) µL of the cells was spread plated on to LB agar containing ampicillin (0.1 %), and the plates were incubated at 37ºC overnight (Maniatis *et al.* 1989).

2.6. Colony PCR

The colonies from the plates were picked and colony PCR was performed. The PCR reaction was carried out under the following conditions (initial denaturation 94°C - 3 min; denaturation 94°C - 30 sec; annealing 62°C - 45 sec; extension 72°C - 90 sec for 30 cycles and final extension 72°C - 7 min).The products were visualized on a 0.8 % agarose gel, and were observed under UV. The positive colony obtained as a result of colony-PCR was transformed to specific selective competent cells, and were then plated on ampicillin amended plates.

2.7. Effect of NaCl on the growth of BL21 Transformants

Overnight grown cultures of BL21 (DE3) transformed with *pET32aSmCMO, pET32aSmBADH* and *pET32aSmCMO+BADH* were plated onto LB agar containing different concentrations of NaCl (Control, 100mM, 200mM, 300mM, 400mM and 500mM). The media was also amended with 100µg/mL ampicillin, 1mM IPTG and 100µM choline chloride. BL21 cells transformed with *pET32a* without an insert served as the control. The plates were incubated at 37ºC overnight and were observed for colony formation.

2.8. IPTG Induction

The transformed BL21 (DE3) cells were inoculated into the 10mL LB containing ampicillin (100µg/mL media), and were incubated at 37ºC at 180 rpm overnight. From the overnight grown culture 1mL was added to a flask containing 10mL LB broth with ampicillin (100ug/mL media), and was kept at 37ºC at 180 rpm. When the absorbance reached 0.6, 1mL was taken in an microfuge tube as control. Nine (9) µL of 1M IPTG (1mM final concentration) and 0.5M NaCl concentration was added to the remaining culture, and it was incubated at 37ºC at 180 rpm. One mL culture was withdrawn every three hours. The cells collected at different intervals were then treated with SDS PAGE sample buffer, and were loaded onto 12 % SDS gel. The gel was run at constant 50V. The gel was removed from the glass plate and washed thrice with Milli-Q water. The gel was soaked in staining solution (mix well before use) for twelve hours/overnight in the gel-rocker. The staining solution was removed, and the gel was rinsed twice in Milli-Q water. It was allowed to destain until the background was clear (10-60 min). The bands were then visualized and documented.

3. Results and Discussion

3.1. Growth Response of E. coli Strains

E. coli is known to display innate mechanisms to cope with NaCl stress, including that of GB accumulation. In order to take into account the basal tolerance to NaCl, experiments using three strains of *E.coli* namely DH5α, MC4100 and BL21 (DE3) in nutrient-rich LB medium as well as Minimal medium were carried out in the presence of different concentrations of NaCl.

3.2. Minimal Medium (M63) with Different NaCl Concentrations

The evaluation of three different *E. coli* strains for growth in a Minimal medium containing different

concentrations of NaCl (Control, 0.1, 0.25, 0.5, 0.75, 1M) resulted in varying responses among the strains (Table 1). Interestingly, DH5α was not able to tolerate even 0.25M of NaCl in the growth medium. BL21 (DE3) cells were able to tolerate the maximum NaCl concentration (0.5M) and was the best growing strains among the three tested in the present study. MC4100 showed poor growth response at 0.5M NaCl.

3.3. Luria Bertanni Medium (LB) with Different NaCl Concentrations

In the LB medium with different NaCl concentrations (Control, 0.1, 0.25, 0.5, 0.75, 1M), DH5α showed good growth up to 0.5M NaCl unlike in the M63 medium. MC4100 did not grow well in the LB medium as observed in the case of the M63 medium, while BL21 (DE3) could grow well at concentrations of NaCl up to 0.75M (Table 2).

3.4. E. coli BL21(DE3) showing maximum level of NaCl Tolerance

The comparison of the growth response of *E. coli* strains MC4100, DH5α and BL21(DE3) revealed that BL 21(DE3), a widely used strain for protein expression studies grew well in the LB medium and Minimal medium. The same couldn't be said as DH5α and MC4100 showed preference for Minimal medium. Although BL21(DE3) responded well in terms of growth in both the LB as well as the Minimal media, its NaCl tolerance was observed to be better in the LB medium (Figures 1 and 2).

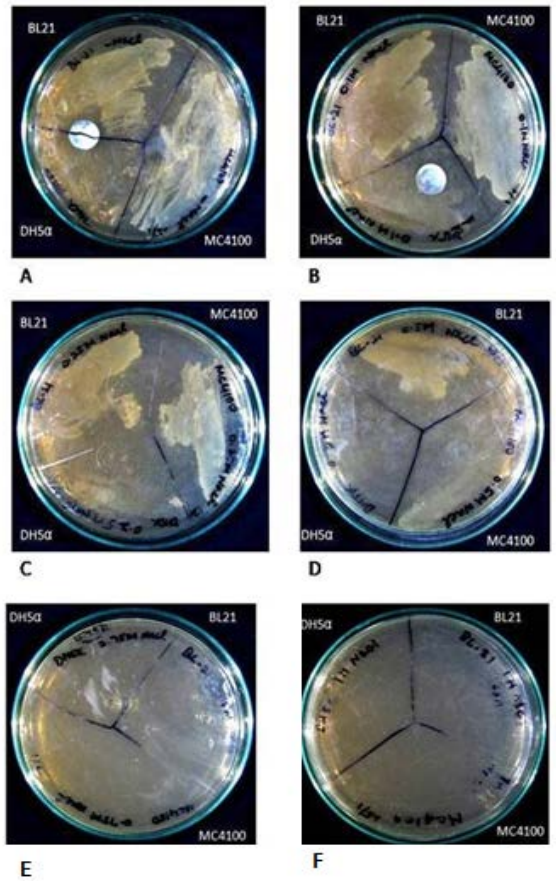

Figure 1. Growth response of *E. coli* strains DH5α, MC4100 and BL21(DE3) in M63 medium added with NaCl at different concentrations [A - Control (without NaCl); B in 0.1M; C in 0.25M; D in 0.5M; E in 0.75M; F in 1M].

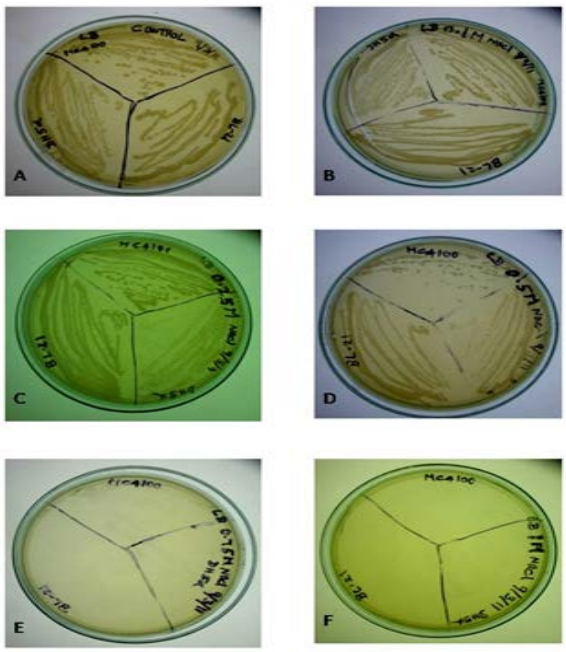

Figure 2. Growth response of E.coli strains DH5α, MC4100 and BL21(DE3) in LB medium added with NaCl at different concentrations [A - Control (without NaCl); B in 0.1M; C in 0.25M; D in 0.5M; E in 0.75M; F in 1M].

The difference in growth response could be attributed to genotype differences and the consequent mechanisms that help in achieving tolerance in these strains. It may also be noted that BL21 (DE3) cells are devoid of two proteases (Yadava *et al.* 2005), and such a genotype can possibly aid in protecting proteins from salt-induced misfolding and subsequent degradation (Paliy and Gunasekara, 2007).

Further screening of BL21 (DE3) for NaCl tolerance (Table 3) to narrow down the range of NaCl concentration revealed that the maximum level of tolerance that could be repeated consistently was 0.5M. Moderate to poor growth was observed at higher concentrations. Absorbance (at 600nm) of the culture was maximal at six hours (corresponding to the late log phase of growth- Supplementary Figure 1) at 0.7M NaCl after which the values declined (Figures 3 and 4).

Table 3. Growth response of *E. coli* strain BL 21(DE3) between 0.4M to 1M NaCl concentration at different time intervals in LB medium.

Strain of *E .coli*	**NaCl Concentration (Molar)**	**0 hr**	**1 hr**	**3 hrs**	**6 hrs**
BL21(DE3)	Control (W/0 NaCl)	++++	++++	++++	++++
	0.4	+++-	++++	++++	++++
	0.5	+++-	+++-	+++-	+++-
	0.6	++--	++--	++--	++--
	0.7	++--	+---	++--	++--
	0.8	----	----	----	----
	0.9	----	----	----	----
	1.0	----	----	----	----

Representation of ++++ indicates very good growth; +++- indicates good growth; ++-- indicates moderate growth; +--- indicates poor growth; ---- indicates no growth.

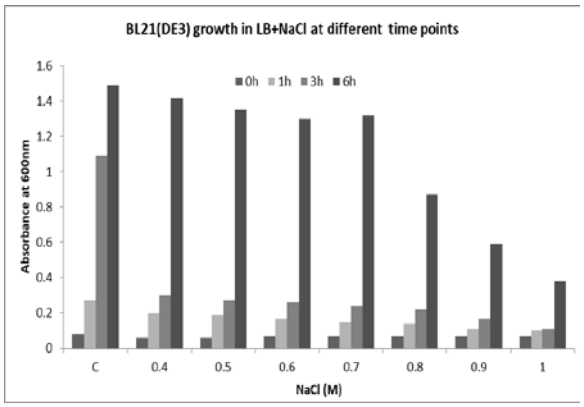

Figure 3. Growth response of *E. coli* strain BL21 (DE3) between 0.4M to 1M NaCl concentrations in LB medium.

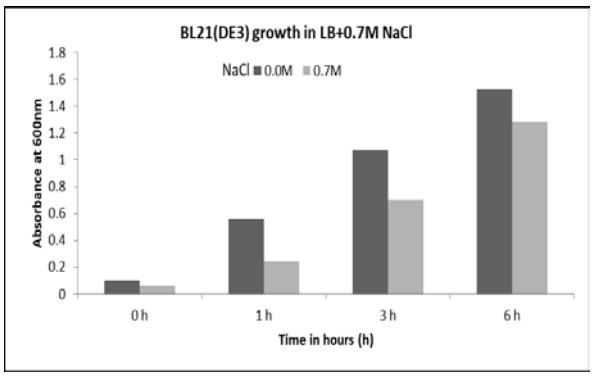

Figure 4. Growth of response of *E. coli* strain BL21 (DE3) at different time intervals in LB medium with 0.7M NaCl.

3.5. Evaluation of Plasmid Stability in the Three E. coli Strains

The ability of bacterial cells to take up plasmids could differ significantly based on media composition, pH, and temperature (Hanahan, 1983; Inoue *et al.* 1990). In the present study, two constructs (*pET32a+SmCMO* and *pET32a+SmBADH* referred to, henceforth, as p*SmCMO* and p*SmBADH* for simplicity) were used together at equimolar concentrations to transform the three tested *E. coli* strains and resulted in good transformation efficiency. The possibility of these two constructs co-existing and replicating in the same host was assayed by PCR using corresponding gene-specific primers.

From the results, it is interesting to note that DH5α was able to retain both the plasmids in maximum number of colonies than in BL21 (DE3) or MC4100. It is possible that this particular strain has a genotype which is more suited for the maintenance of plasmids. BL21 (DE3) and MC4100 were examined for the presence of double recombinants at various time points of growth. However, the PCR experiment for the detection of double recombinants at regular intervals during the growth phase did not result in the detection of bands, and hence they were not included in this report (data not shown). Transformation experiments were also repeated to confirm the study's observations. It was found that the initial results were consistently repeated. It is interesting to note that the overnight grown cultures or colonies that were subcultured as patches lost one of the plasmid constructs as compared to the early or mid-log phase fresh cultures, even in the presence of ampicillin selection in the growth medium (Figures 5 and 6). In order to avoid plasmid loss due to frequent sub-culturing experiments to assay for salt tolerance in BL21(DE3), double recombinants were performed only with fresh glycerol stocks of early log phase cultures stored at -80°C (Figure 7a and b).

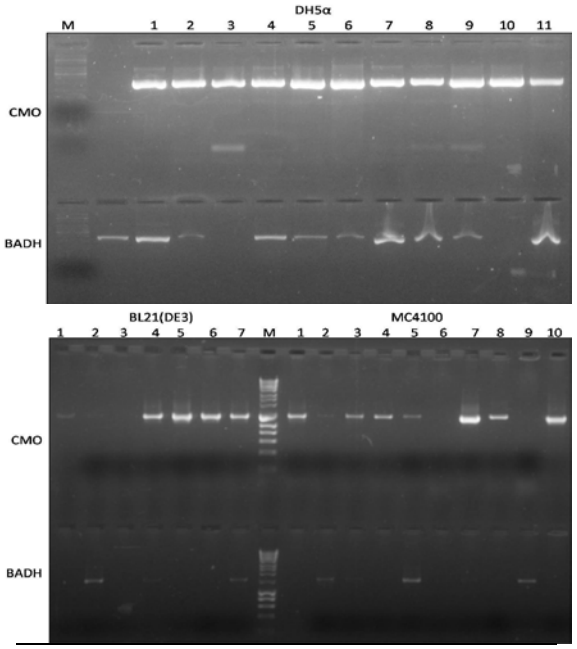

Strains of *E.coli*	Positives (Lane Nos.) for CMO&BADH
BL21(DE3)	2,4,7
DH5α	1,4,5,7,8,9
MC4100	2,3,5,7,

Figure 5. Identification of positive transformants (for both pET32a+ *SmCMO* and *pET32a+SmBADH*) using gene specific primers.

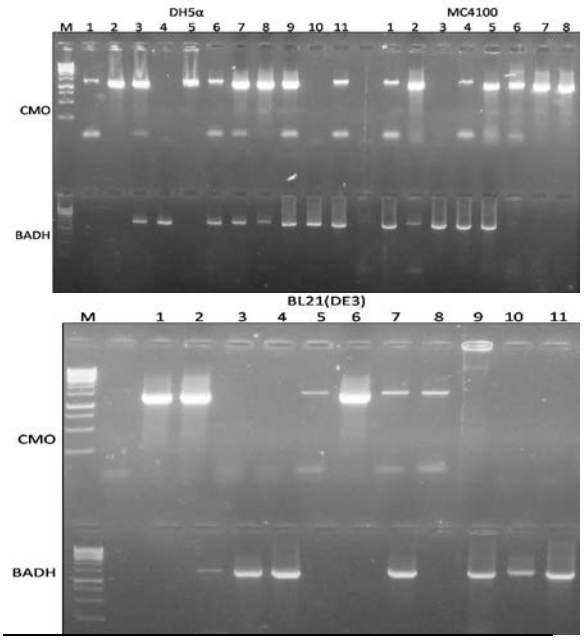

Strains of *E. coli*	Positives (Lane Nos.) for CMO&BADH
BL21(DE3)	7
DH5α	3,6,7,8,9
MC4100	1,3,4,6,7

Figure 6. Identification of positive transformants (for both pET32a+*SmCMO* and pET32a+*SmBADH*) using gene specific primers - from overnight cultures from plates.

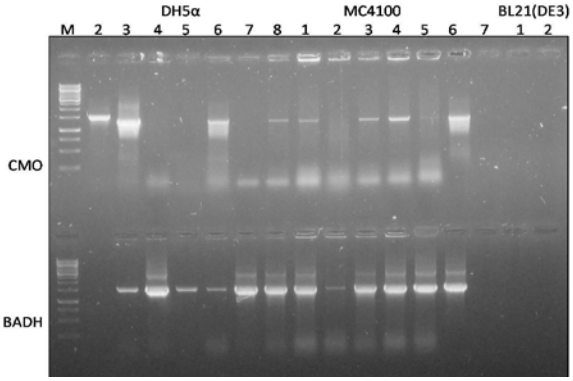

Strains of *E. coli*	Positives (Lane Nos.) for CMO&BADH
BL21(DE3)	Nil
DH5α	3,8
MC4100	1,3,6,7

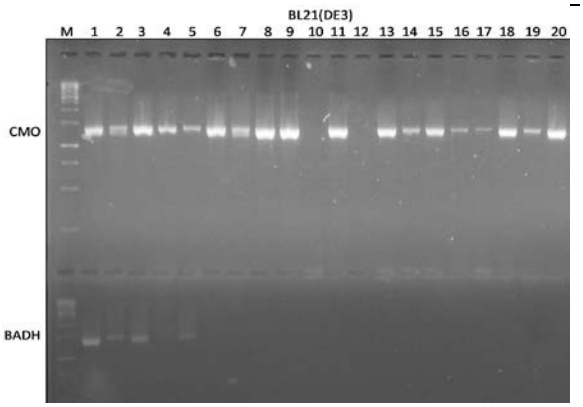

Strains of *E. coli*	Positives (Lane Nos.) for CMO&BADH
BL21(DE3)	1*,2*,3*

Figure 7. Identification of positive transformants (for both ET32a+*SmCMO* and pET32a+*SmBADH*) using gene specific primers - Top gel performed using batch cultures **(a)**; Bottom panel performed using 3h culture taken from 20 fresh transformants (colonies).

*Positive cultures were maintained as glycerol stocks for further experiments **(b)**.

3.6. Sodium Chloride Tolerance of BL21 (DE3) Cells in the Presence of pSmCMO and pSmBADH

Plasmid constructs for the both the cDNAs involved in GB biosynthetic pathway in *S. maritima* were transferred to competent BL21 (DE3) cells separately (*pSmCMO*, p*SmBADH*) as well as in combination (*pSmCMO+pSmBADH)*. Growth inhibition at higher concentrations of NaCl (0.7M) in IPTG-induced recombinant BL21 (DE3) was observed in the present study in comparison with the uninduced and non-recombinant cells (Figure 8). The results suggest a toxic effect of the recombinant proteins primarily due to high concentrations of NaCl. However at 0.5M NaCl, tolerance was better in the induced recombinants, both in isolation as well as in combination of the individual plasmids (Figure 9).

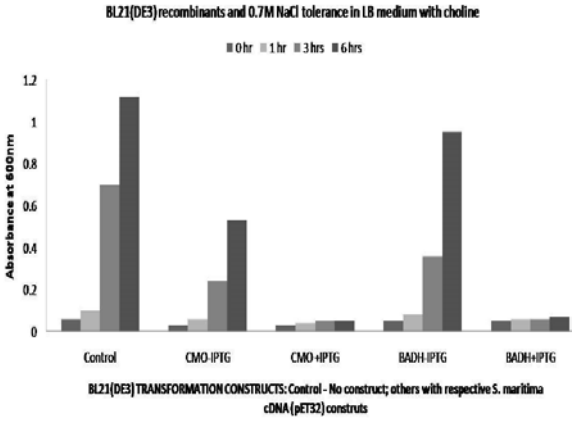

Figure 8. Growth response of BL21 (DE3) with different plasmid constructs in 0.7M NaCl containing LB medium supplemented with choline in the presence and absence of IPTG.

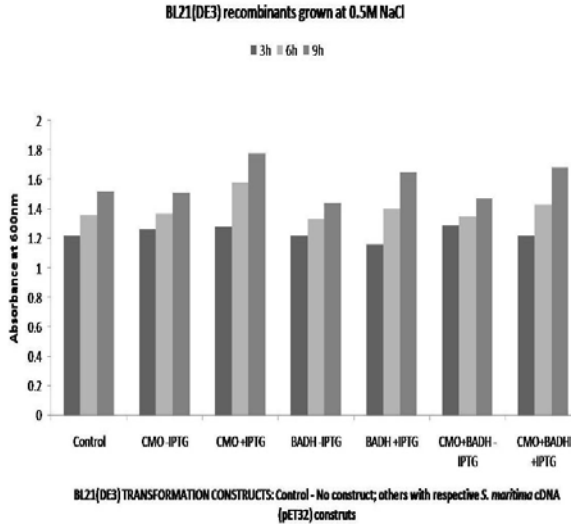

Figure 9. Growth response of BL21 (DE3) with different plasmid constructs in 0.5M NaCl containing LB medium in the presence and absence of IPTG**.**

SDS-PAGE of the proteins purified from BL21(DE3) recombinants containing p*SmCMO* and p*SmBADH* in isolation or in combination resulted in higher induction of the CMO polypeptide in case of the *pSmCMO* only recombinant, while the other recombinants were not induced at higher levels. *pSmCMO* expressing BL21(DE3) cells showed a better tolerance to NaCl at all the time points tested. This observation is consistent with earlier reports (Hibino *et al*. 2002) where *E. coli* BL21 cells transformed with spinach CMO accumulated more GB suggesting that the expressed protein was able to better utilize the externally supplied choline. Although in recombinants with both the constructs, BADH at about 80kDa was found to be expressed more, while it was not clear whether CMO was expressed or not, since a band was visible in this molecular weight range in all the protein samples (Figure 10), possibly because of its plasmid being lost or expressed inefficiently due to the less utilization of externally supplied choline. Interestingly, these results show that some of the host proteins were repressed in the induced recombinants.

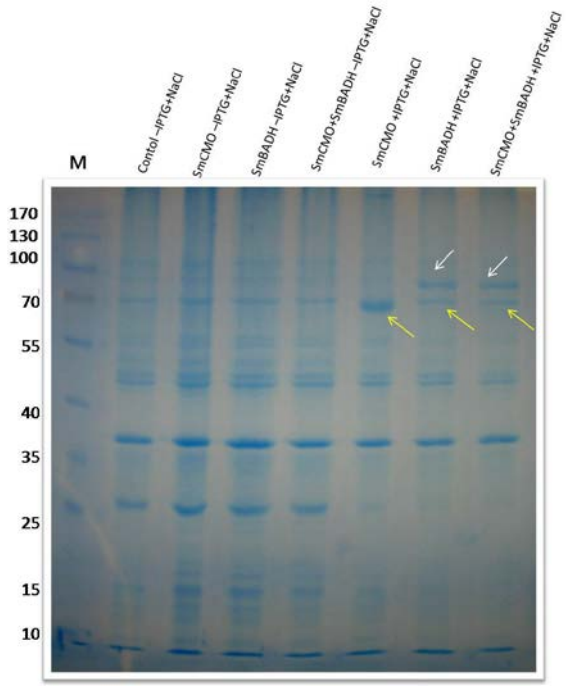

Figure 10. SDS PAGE of BL21(DE3) recombinants with different plasmid constructs in 0.5M NaCl containing LB medium in the presence and absence of IPTG. Control – non recombinant. Yellow arrow indicates *SmCMO* polypeptide; White arrow indicates *SmBADH*; M-marker.

4. Conclusion

The natural sodium chloride tolerance in *E. coli* is possibly determined by the genotype of the strains, as there is a difference in NaCl-tolerance levels between the DH5α and BL21 (DE3) cells in the LB media, with the difference being more marked in Minimal media. The stability or retention of the two plasmid in the same cell may also depend on the genotype. DH5α, which is generally used for plasmid maintenance, performed better in the present study. Growth of BL21 (DE3) recombinants for *pSmCMO and pSmBADH* proteins, both in isolation and in combination, was inhibited at 0.7M NaCl. This suggests the toxicity of the recombinant proteins when the cells are exposed to high concentrations of NaCl. Sodium chloride tolerance of induced recombinant BL21 (DE3) was better at 0.5M compared to the non-recombinant and uninduced recombinant controls. However, the difference was significant enough to conclusively suggest an additive effect of the cloned proteins from *S. maritima* GB biosynthetic pathway.

Acknowledgements

The researchers extend their cordial thanks to Professor M.S. Swaminathan for providing facilities and for the constant support to carry out this research. Dr. N. Thajuddin expresses his appreciation for the UGC, New Delhi for BSR one-time grant (F.19-156/2015(BSR). Thanks also go to Ashok Kumar and Lakshmi Priya, MSSRF for giving suggestions and helping in the current research work.

Conflict of Interest

The authors have no conflict of interest.

References

Andresen PA, Kaasen I, Styrvold OB, Boulnois G and Strom AR. 1988. Molecular cloning, physical mapping and expression of the bet genes governing the osmoregulatory choline-glycine betaine pathway of *Escherichia coli*. *J. Gen. Microbiol.*, **134**:1737-1746.

Ashraf M and Foolad MR. 2007. Roles of glycine betaine and proline in improving plant abiotic stress resistance. *Environ. Exp. Bot.*, **59**:206-216.

Boyd LA, Adam L, Pelcher LE, McHugen A, Hirji R and Selvaraj G. 1991. Characterization of an *Escherichia coli* gene encoding betaine aldehyde dehydrogenase (*BADH*): structural similarity to mammalian *ALDHs* and a plant *BADH*. *Gene*,**103**: 45-52.

Brouquisse R, Weigel P, Rhodes D, Yocum CF and Hanson AD. 1989. Evidence for a ferredoxin-dependant choline monooxygenase from spinach chloroplast stroma. *Plant Physiol.***, 90**: 322-329.

Cheeseman JM, Herendeen LB, Cheeseman AT and Clough BF. 1997. Photosynthesis and photoprotection in mangroves under field conditions. *Plant Cell Environ.*, **20**:579-588.

Chen THH and Murata N. 2011. Glycinebetaine protects plants against abiotic stress: mechanisms and biotechnological applications. *Plant Cell Environ.*, **34**:1-20

Chung CT, Suzzanne LN and Roger HM. 1989. One-step preparation of competent Escherichia coli: transformation and storage of bacterial cells in the same solution. *Proc. Natl. Acad. Sci. U S A*, **86**:2172-2175.

David C, Carmen V, Susanne K, Maria Jesus M, Antonio V, Erhard B and Joaquin JN. 2000. Genes for the synthesis of the osmoprotectant glycine betaine from choline in the moderately halophilic bacterium *Halomonas elongata* DSM 3043. *Microbiology*, **146**:455-463.

Domenech LLP, Tifrea A, Grigore MN, Boscaiu M and Vicente O. 2016. Proline and glycine betaine accumulation in two succulent halophytes under natural and experimental conditions. *Plant Biosystems*, **150(5)**:904-915.

Epstein W. 1986. Osmoregulation by potassium transport in *Escherichia coli*. *FEMS Microbiol. Rev.*, **39**:73-78.

Hanahan D. 1983. Studies on transformation of *Escherichia coli* with plasmids. *J. Mol. Biol.*, **166**:557-580.

Hibino T, Waditee R, Araki E, Ishikawa H, Aoki K, Tanaka Y and Takabe T. 2002. Functional characterization of choline monooxygenase an enzyme for betaine synthesis in plants. *J. Biol. Chem.*, **277(44)**:41352-41360.

Incharoensakdi A, Nobuyuki M, Takashi H, Yu Ling M, Hiroshi I, Akira H, Tohru F, Tetsuko T and Teruhiro T. 2000. Overproduction of spinach betaine aldehyde dehydrogenase in *Escherichia coli:* structural and functional properties of wild-type, mutants and *E. coli* enzymes. *Eur. J. Biochem.* **267**:7015-7023.

Inoue H, Nojima H and Okayama H. 1990. High efficiency transformation of *Escherichia coli* with plasmids. *Gene*, **96**:23-28.

Jithesh MN, Prashanth SR, Sivaprakash KR and Parida A. 2006. Antioxidative response mechanisms in halophytes: their role in stress defence. *J Genet*, **85(3):**237-254.

Kapfhammer D, Karatan E, Pflughoeft,KJ and Watnick PI. 2005. Role for glycine betaine transport in Vibrio cholerae osmoadaptation and biofilm formation within microbial communities. *Appl. Environ. Microbiol.*, **71(7):**3840-3847

Katschnig D, Broekman R and Rozema J. 2013. Salt tolerance in the halophyte *Salicornia dolichostachya* moss: growth, morphology and physiology. *Environ Exp Bot.,* **92**:32-42.

Khan MA, Ungar IA and Showalter AM. 2000. The effect of the salinity on the growth, water status, and ion content of a leaf succulent perennial halophyte, *Suaeda fruticosa (L)* Forssk. *J Arid Environ.*, **45**:73-84.

Lamark T, Kaasen I, Eshoo MW, Falkenberg P, McDougall J and Strom AR. 1991. DNA sequence and analysis of the bet genes encoding the osmoregulatory choline glycine betaine pathway of *Escherichia coli*. *Mol Microbiol.,* **5**:1049-1064.

Lamark T, Rokenes TP, McDougall J and Strom AR. 1996. The complex *bet* promoters of *Escherichia coli*: regulation by oxygen (*ArcA*), choline (*BetI*), and osmotic stress. *J Bacteriol.,* **178(6):**1655-1662.

Lamark T, Styrvold OB and Strom AR. 1992. Efflux of choline and glycine betaine from osmoregulation cells of *Escherichia coli*. *FEMS Microbiol. Lett.*, **96**:149-154.

Larsen I, Sydnes K, Landfald B, Strom AR. 1987. Osmoregulation in *Escherichia coli* by accumulation of organic osmolytes: betaines, glutamic acid, and trehalose. *Arch Microbiol.,* **147**: 1-7.

Le Rudulier D, Strom AR, Dandekar AM, Smith LT and Valentine RC. 1984. Molecular biology of osmoregulation. *Sci.,* **224**:1064-1068.

Maniatis T, Fritsch EF and Sambrook J. 1989**. Molecular Cloning: a Laboratory Manual**. Cold Spring Harbor Laboratory Press, *Cold Spring Harbor, New York*.

McNeil SD, Nuccio ML and Hanson AD. 1999. Betaines and related osmoprotectants. targets for metabolic engineering of stress resistance. *Plant Physiol.*,**120**:945-949.

Moghaieb REA, Saneoka H and Fujita K. 2004. Effect of salinity on osmotic adjustment, glycinebetaine accumulation and the betaine aldehyde dehydrogenase gene expression in two halophytic plants, *Salicornia europaea*and *Suaeda maritima*. *Plant Sci.,***166**:1345-1349.

Nyyssölä A, Kerovuo J, Kaukinen P, Von Weymarn N and Reinikainen T. 2000. Extreme halophiles synthesize betaine from glycine by methylation. *JBiol Chem.,* **275**:22196-22201

Paliy O and Gunasekara TS. 2007. Growth of *E. coli* BL21 in minimal media with different gluconeogenic carbon sources and salt contents. *Appl Microbiol Biotechnol.,* **73**:1169-1172.

Park J, Okita TW and Edwards GE. 2009. Salt tolerant mechanisms in single-cell C4 species *Bienertia sinuspersici* and *Suaeda aralocaspica* (Chenopodiaceae). *Plant Sci.,* **176**:616-626.

Peters P and Truper HG. 1992. Transport of glycine betaine in the extremely haloalkaliphilic sulphurbacterium *Ectothiorhodospira halochloris*. *J Gen Microbiol.,* **138**:1993-1998.

Prashanth SR, Sadhasivam V and Parida A. 2008. Over expression of cytosolic copper/zinc superoxide dismutase from a mangrove plant *Avicennia marina* in indica rice var *Pusa Basmati-1* confers abiotic stress tolerance. *Transgenic Res.,* **17(2)**:281-291.

Rathinasabapathi B. 2000. Metabolic engineering for stress tolerance: installing osmoprotectant synthesis pathways. *Ann. Bot.,* **86(4)**:709-716.

Reed RH, Borowitzka LJ, Mackay MA, Chudek JA, Foster R, Warr SRC, Moore DJ and Stewart WDP. 1986. Organic solute accumulation in osmotically stressed cyanobacteria. *FEMS Microbiol Rev.*, 2 (1-2):51-56,

Rhodes D and Hanson AD. 1993. Quaternary ammonium and tertiary sulfonium compounds in higher plants. *Ann Rev Plant Physiol Plant Mol Biol.,* **44:**357-384.

Sakamoto A and Murata N. 2002. The role of glycine betaine in the protection of plants from stress: clues from transgenic plants. *Plant Cell Environ.,* **25**:163-171.

Shabir HW, Naorem BS, Athokpam H and Javed IM. 2013. Compatible solute engineering in plants for abiotic stress tolerance - role of glycine betaine. *Curr. Genomics*, **14**:157-165.

Storey R and Jones RGW. 1977. Quaternary ammonium compounds in plants in relation to salt resistance. *Phytochem.,* **16**:447-453.

Strom AR, Falkenberg Pand Landfald B. 1986. Genetics of osmoregulation in *Escherichia coli*: uptake and biosynthesis of organic osmolytes. *FEMS Microbiol Rev.,* **39**:79-86.

Waditee R, Tanaka Y, Aoki K, Hibino T, Jikuya H, Takabe T and Takabe T. 2003. Isolation and functional characterization of N-methyltransferase that catalyze betaine synthesis from glycine in a halotolerant photosynthetic organism *Aphanothece halophytica*. *J Biol Chem.,* **278**:4932-4942.

Weigel P, Elizabeth AW and Andrew DH. 1986. Betaine aldehyde oxidation by spinach chloroplast. *Plant Physiol.,* **82(3):**753-759.

Yadava RS, Kumar R and Yadava PK. 2005. Expression of *lexA* targeted ribozyme in *Escherichia coli BL21* (DE3) cells. *Mol Cell Biochem.,* **271**:197-203.

Yamanaka T, Miyama M and Tada Y. 2009. Transcriptome profiling of the mangrove plant *Bruguiera gymnorhiza* and identification of salt tolerance genes by *Agrobacterium* functional screening. *Biosci.Biotechnol.Biochem.,* **73**:304-310.

Yancey PH, Clark ME, Hand SC, Bowlus RD and Somero GN. 1982. Living with water stress: evolution of osmolytes systems. *Sci.,* **217**:1214-1222.

JJBS

Volume 12, Number 1,March 2019
ISSN 1995-6673
Pages 107 - 117

Jordan Journal of Biological Sciences

Parentage Analysis of the Progenies of the Reciprocal Crosses of *Pangasianodon hypophthalmus* (Sauvage, 1878) and *Clarias gariepinus* (Burchell, 1822) using Cytochrome b Gene

Okomoda V. Tosin[1], Koh I. C. Chong[2], Hassan Anuar[2], Amornsakun Thumronk[3] and *Shahreza Md Sheriff[2,4]

[1]*Department of Fisheries and Aquaculture, University of Agriculture, Makurdi, Nigeria*

[2]*School of Fisheries and Aquaculture Sciences, Universiti Malaysia Terengganu, Malaysia*

[3]*Department of Technology and Industries, Prince of Songkla University, Pattani campus Thailand,* [4]*Institute of Tropical Aquaculture, Universiti Malaysia Terengganu, Malaysia*

Received June 6, 2018; Revised June 26, 2018; Accepted June 29, 2018

Abstract

In this study, parentage analysis of the progenies from reciprocal crosses of *Pangasianodon hypophthalmus* (PH) and *Clarias gariepinus* (CG) was accomplished by sequencing the cytochrome b gene and running phylogenetic analysis. The result obtained showed that the nucleotide composition of the cytochrome b gene of the reciprocal hybrid crosses exhibited high (99 %) similarity with those of the maternal parents notwithstanding the different morphology within the hybrid pool (i.e. Panga-like and Clarias-like). The analysis of 1076bp of the cytochrome b gene using three methods for inferring molecular relationships (Maximum Likelihood, Neighbour Joining, and Maximum Parsimony) revealed two main clusters. The upper cluster was a mix of *C. gariepinus* and the two distinct progenies of ♀CG × ♂PH (i.e. Panga-like and Clarias-like), while the lower cluster was a mix of the *P. hypophthalmus* and the progenies of ♀PH × ♂CG (i.e. Panga-like only). Hence, despite, phenotypic differences within the hybrid pool, progenies still inherit cytochrome b gene from the maternal parent alone. As a result, the direction of crosses of the reciprocal crosses could be accurately determined.

Keywords: Asian catfish, African catfish, Cytochrome b, Hybrid morphotype.

1. Introduction

The main aim of hybridization between different fish groups or species is to produce offsprings that perform better than the parental species (Bartley *et al.,* 2001; Okomoda *et al.,* 2017). However, unintended consequences have been experienced as a result of accidental backcrossing, hence, threatening the diversity of many freshwater fish species (Epifanio and Nielsen, 2000; Perry *et al.,* 2002; Senanan *et al.,* 2004; Na-Nakorn *et al.,* 2004). Aside from the fear of genetic homogenization of farmed and natural fish stocks (Hashimoto et al. 2010); hybrids may compete successfully with the native parental lineages in several ways (Ryman and Utter, 1987; Allendorf *et al.,* 2001; Rosenfield *et al.,* 2004), hence, the need for characterization.

The efficacy of molecular markers in the determination of the hybridization status, direction of crosses, and genetic introgression cannot be over emphasized (Forbes and Allendorf, 1991; Cianchi *et al.,* 2003; Hänfling *et al.,* 2005). This is because most hybrids inherit part of the genetic makeup of both species (Wilkins, *et al.,* 1994). As a result, the hybridization status of different crosses has been well investigated using nuclear markers since inheritance of this kind of DNA is from both parents (Rieseberg *et al.,* 1990; Sang *et al.,* 1995; Buckler *et al.,* 1997; Odorico and Miller, 1997). Similarly, morphological and cytogenetic analysis has been widely exploited for the same purpose. It is important to note that these methods command the same level of accuracy and at a very lower cost compared to the molecular characterization method (Hashimoto et al. 2010). However, they cannot be used to determine the direction of the hybridization of the crosses.

Although the potential of erythrocyte characterization for directional cross discrimination have been demonstrated in the earlier study by Okomoda *et al.,* (2018a), the outlined limitations of this approach largely reduce their usability in a wide array of species or studies. The most accurate method still remains the characterization of the mitochondrial DNA (mtDNA). This is because the mtDNA is primarily matrilineally inherited. As a result, their analysis can conveniently identify the maternal origin of the hybrids, and hence the direction of crosses (Pitts, 1995). The mitochondrial cytochrome b gene has particularly gained recognition as an important index in the comparisons of closely related taxa such as between populations or species (Degani 2004; Pfrender, *et*

* Corresponding author. e-mail: shahreza@umt.edu.my.

al., 2004; Perdices, *et al.*, 2005). However, it is conserved enough for clarifying deeper phylogenetic relationships (Allegrucci, *et al.*, 1999; Cunha, *et al.*, 2002; Sulaiman, *et al.*, 2006; Feulner, *et al.*, 2007).

While mtDNA has been exploited for the characterization of hybrids, the phylogenetic relationships between progenies were seldom analysed. This is particularly important in distant crosses which lead to the production of ploidy polymorphism of the hybrid progenies (i.e. different cytogenetic characteristics within the hybrid pool). A good example of such cross is the study on the hybridization between *Pangasianodon hypophthalmus* (Sauvage, 1878) and *Clarias gariepinus* (Burchell, 1822) where three distinct morphotypes were observed (Okomoda *et al.*, 2017, 2018a, 2018b) with different cytogenetic characteristics (Okomoda *et al.*, 2018c). Understanding the various levels of genetic relationships between hybrids and pure crosses could significantly aid in the development of management guidelines for commercial use and for conservation purposes (Birstein *et al.*, 2005; Freyhof *et al.*, 2005; Ludwig, 2008). Haven established the hybridization status of the reciprocal crosses between *P. hypophthalmus* and *C. gariepinus* in the study by Okomoda *et al.*, (2018b, 2018c), this study was designed for parentage determination and to establish phylogenetic relationship between pure and reciprocal progenies of the fishes using the cytochrome b gene.

2. Materials and Methods

Progenies of pure and reciprocal crosses between of *C. gariepinus*, *P. hypophthalmus* used in this study were obtained using the method previously described by Okomoda *et al.*, (2017, 2018 b, c). In brief, mature *P. hypophthalmus* and *C. gariepinus* were spawned by induced breeding using the Ovaprim® hormone (0.5mL/kg). Eggs and sperm were mixed to produce pure *C. gariepinus* (♀CH × ♂CH), pure *P. hypophthalmus* (♀PH × ♂PH), and the reciprocal crosses Clariothalmus (♀CG × ♂PH) and Pangapinus (♀PH × ♂CG). The progenies obtained from six different breeding trials were then cultured for one month in fibreglass tanks. At this point, two morphotypes were conspicuous in the Clariothalmus (Clarias-like and Panga-like), while all Pangapinus were of one morphotype (Panga-like) (See figure 1). All groups were continuously fed with commercial diet (35 % CP), and water quality was maintained at optimum (temperature = 33.0 ± 1.6^{0}C; pH = 7.0 ± 0.41; conductivity = 251 ± 0.31mg l^{-1}; total dissolved solids = 78.0 ± 0.89 mg l^{-1}; dissolved oxygen = 4.7 ± 0.39 mg l^{-1}).

Fifty fishes comprised of *P. hypophthalmus* (10), Clarias-like Clariothalmus (10), Panga-like Clariothalmus (10), Pangapinus (10), and *C. gariepinus* (10) were randomly selected and preserved in 95 % ethanol contained in appropriately labelled 1.5mL tubes. DNA was extracted from the fins of these fishes using specified protocol for Vivantis Nuclear Acid extraction kit (according to manufacturer's instruction). Amplification of the Cytochrome b, was carried out by polymerase chain reaction (PCR) using the universal primers Cyt b 3F (5'-CCACCGTTGTTATTCAACTATAGAAA-3') and Cyt b 3R (5'-AGAATRCTAGCTTTGGGAG-3') which was described by Bowen *et al.*, (2008).

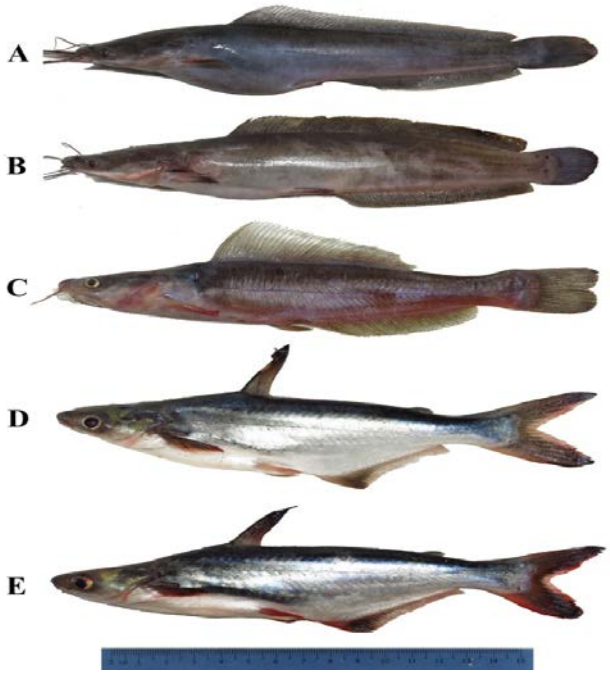

Figure 1. Morphology of (A) *Clarias gariepinus*; (B) Clarias-like Clariothalmus; (C) Panga-like Clariothalmus; (D) Pangapinus and (E) *Pangasianodon hypophthalmus*. (Source Okomoda *et al.*, 2018c)

A reaction volume of 25 µL was used containing 2.5 µL Easy *Taq* buffer, 2.0 µL dNTPs, 0.5 µL each of universal forward and reverse primer, 0.2µL *Taq* DNA polymerase (Easy *Taq*), 0.5µL template DNA, and 18. 8 µL sterile deionised water. Reactions were performed using an Eppendorf Mastercycler. The Cyt b PCR amplification was programed at 95^{0}C for two minutes, followed by thirty-five cycles of denaturation at 95^{0}C (thirty seconds), annealing temperature at 47^{0}C (forty-five seconds) and an extension of 72^{0}C (one minute), this was followed by a final single extension at 72^{0}C (seven minutes). An aliquot of the reaction was subjected to electrophoresis on a 1.0 % agarose gel. The gels were visualized using a gel documentation system (BIO RAD, USA).

PCR products were sent for sequencing at First Base Laboratories SDN BHD, Malaysia. All sequences were aligned and edited using ClustalW as implemented in MEGA version 6. Sequence ambiguities were resolved by comparing complementary strands of ten nucleotide sequences per group of fish. The identity of the sequences was confirmed using BLAST at the NCBI website (https://blast.ncbi.nlm.nih.gov/Blast.cgi?PROGRAM=blastnandGE_TYPE=BlastSearchandLINK_LOC=blasthome). The percentages of similarities of all the progenies with the available sequences on the NCBI website were gotten.

The relationship between the different groups of fish was examined using neighbour joining (Saitou and Nei 1987), maximum parsimony and maximum likelihood (Felsenstein 1983) methods (using MEGA version 6). The confidence of the branching patterns was assessed by 1000 bootstrap replicates in the NJ analysis (Hillis and Bull 1993). The out group used was *Cyprinus carpio* (NCBI

Accession number: AB158806), while *C. macrocephalus* (NCBI Accession number: KJ533248) and *Pangasius nasutus* (NCBI Accession number: HM236395) were used as the sister groups in this study.

3. Results

Amplification of the universal primers in relation to the mitochondrial cytochrome b gene showed bands of approximately 1300bp for all the groups of fish and their different morphotypes (Appendix 1). The partial sequences obtained for the cytochrome b revealed very high similarity between the nucleotide composition of the reciprocal crosses and the maternal parents irrespective of their morphotypes. Blast also showed that the target sequence was gotten as the nucleotide compositions were 99 % identical with available cytochrome b sequences in the GenBank for *Clarias gariepinus* (accession number KJ533253.1) and *Pangasianodon hypophthalmus* (accession number KM434895.1) (respectively for pure and reciprocal progenies with Clarias and Panga maternal origins) (Appendix 2, 3, 4, 5 and 6). The results obtained by sequencing allowed the analysis of 1076bp of the Cyt b gene. Similar genetic pattern were obtained from the three methods used for inferring molecular relationships in this study (Maximum likelihood, Neighbour Joining, and Maximum Parsimony Respectively for Figure 2, Appendix 7 and 8). From the result obtained, two main groups were clearly defined. The upper group was a mix of *C. gariepinus*, Clarias-like Clariothalmus and Panga-like Clariothalmus with three haplotypes. The lower group, on the other hand, was a mix of the Pangapinus and the *P. hypophthalmus* with six observed haplotypes. The variations in the difference haplotypes occurred in three bases or less.

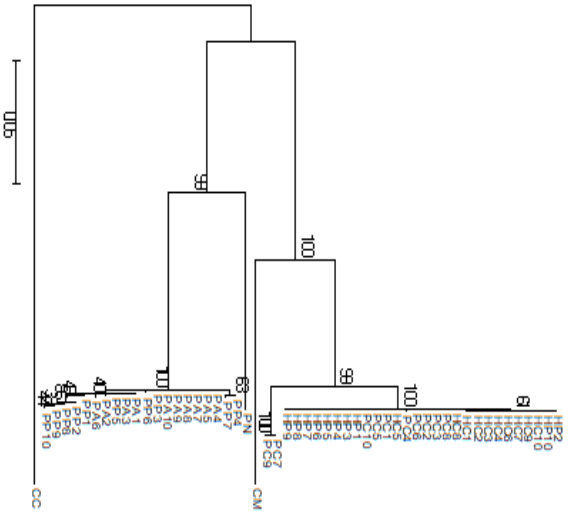

Figure 2. Phylogenetic relationships of the different progenies following Maximum likelihood analysis of 1076bp of the cytochrome b gene. PC1 - PC10 = *C. gariepinus*; HC1 – HC10 = Clarias-like Clariothalmus; HP1 – HP10 = Panga-like Clariothalmus; PA1 - PA10 = Pangapinus; PP1 - PP10 = *P. hypophthalmus*; CC = *Cyprinus carpio*; CM = *Clarias macrocephalus;* PN = *Pangasius nasutus.* (Support values are bootstrap values).

The genetic distances within haplotypes of the same groups in this study (i.e. pure and hybrid crosses from the same maternal origin) ranged between 0.000 - 0.056 (Table 1). However, the genetic distance between the pure P. hypophthalmus and C. gariepinus ranges from 0.472 - 0.506.

Table 1: Genetic distance range between pure and reciprocal crosses of *Pangasianodon hypophthalmus* and pure *Clarias gariepinus*.

	PC	HC	HP	PA	PP
PC	0.000 – 0.056				
HC	0.000 – 0.056	0.000 – 0.056			
HP	0.000 – 0.056	0.000 – 0.054	0.000 – 0.056		
PA	0.472 – 0.502	0.475 – 0.504	0.472 – 0.506	0.010 – 0.051	
PP	0.472 – 0.506	0.470 – 0.491	0.472 – 0.494	0.000 – 0.052	0.000 – 0.050

Keys: PC = *C. gariepinus*; HC1 = Clarias-like Clariothalmus; HP1 = Panga-like Clariothalmus; PA1 = Pangapinus; PP1 = *P. hypophthalmus*.

4. Discussion

Different researchers had justified the need to discriminate reciprocal crosses of different species because hybrid progenies could display different biological and zootechnical characteristics (Tave, 1993; Toledo- Filho *et al.*1998; Porto-Foresti *et al.* 2008). More so, information on the directionality of mating can have significant effects on a number of factors including spatial, temporal, behavioural, physiological, and stock composition of the hybrid progenies (Pitts, 1995; Scribner *et al.*, 2001). This assumption is validated by the results of early studies which show differences in performance not only between the reciprocal crosses of *P. hypophthalmus* and *C. gariepinus*, but also between progenies of the hybrid Clariothalmus (i.e Clarias-like and Panga-like) (Okomoda *et al.*, 2018b, 2018c). Similarly, Dunham et al. (1982) had justified molecular discrimination of F1 progenies of the hybrids ♀*Ictalurus punctatus* × ♂*I. furcatus* and ♀*I. furcatus* × ♂*I. punctatus* on the bases of differential growth performances.

The cytochrome b gene is a highly conserved region (Moritz *et al.*, 1987; Olufeagba and Okomoda 2016); hence, the universal primer used in this study uniformly amplified 1300bp in all the progenies tested as expected. The observation of the very high similarity between the progenies of the reciprocal crosses and their maternal parent confirms the direction of crosses. Similarly, the phylogenetic analysis shows two separate groups of the test progenies in direction of the maternal origin. Observations of previous studies using different mtDNA genes are in line with the findings of this study. do-Prado *et al.*, (2011) had used 16S mitochondrial genes to discriminate reciprocal hybrids 'pintachara' and 'cachapinta' by the identification of the maternal parent of these crosses. The efficacy of differentiating reciprocal hybrids of *Leporinus macrocephalus* and *L. elongatus* using 16S mitochondrial DNA had also been reported by

Hashimoto *et al*., (2010). In addition, Olufeagba and Okomoda (2016) confirmed the maternal origin of the hybrid ♀ *C. gariepinus* × ♂ *C. batrachus* with the cytochrome b gene. Waldbrieser and Bosworth (2008) were able to discriminate reciprocal crosses of channel catfish (*I. punctatus*) and blue catfish (*I. furcatus*) hybrid using the mitochondrial cytochrome c oxidase 1 gene.

On the whole, mitochondrial DNA have proven to be a very effective molecular tool in the identification of the parental status of hybrids since it is cytoplasmically housed and only inherited from the mother to the offspring, and has no paternal contribution (Moritz *et al*., 1987; Wyatt *et al*., 2006). Hence, the pattern of genetic homogenization between progenies from the same maternal parent and distinct groups observed for the different maternal origins clearly shows the direction of crosses of the progenies. In line with this, Nazia *et al*., (2010) had earlier stated that high levels of genetic homogenization are large because of the common origin or the ongoing gene flow. Notwithstanding, different haplotype groups with close genetic distances were observed within the two main groups in this study. This observed variation within the progenies with similar maternal origins may have resulted from the different population of broodstocks used for the six different trials of breeding. Similar assumption has been advanced by several authors for the observation of haplotypes in fishes from different populations (e.g. Windsor and Hutchinson1995; Williams, *et al*., 1997; Doupe' and Lymbery 1999; Cross 2000; Englbrecht, *et al*., 2002; Frost et al. 2006; Norfatimah *et al*., 2009; Nazia *et al*., 2010).

Although *C. gariepinus* and *P. hypophthalmus* belong to different families, the phylogenetic analysis of the mitochondrial cytochrome b showed a considerably close genetic distance between these two species. Pardo *et al*., (2005) and Azevedo *et al*., (2008), have earlier hypothesized that close genetic distances between different fish families could explain the feasibility of hybridization between them. This assumption may be the reason for the successful hybridization of *C. gariepinus* and *P. hypophthalmus*. Although the hybridization status of the reciprocal crosses produced in this study were earlier confirmed using morphological (Okomoda *et al*., 2018b) and cytogenetic tools (Okomoda *et al*., 2018c), the direction of hybridization or cross combination could not be determined. The use of erythrocyte characterization had also been advanced in previous studies by the authors of this research, but with some limitations (Okomoda *et al*., 2018a). However, the characterization of the mitochondrial DNA still remains the most accurate and unambiguous tool for directional cross determination.

Acknowledgements

The authors are indebted to the School of Fisheries and Aquaculture Science, Universiti Malaysia Terengganu, Malaysia for providing *C. gariepinus* and *P. hypophthalmus* broodstock used in this study. The researchers also acknowledge the help of all technical staffs of the PPSPA hatchery department and laboratory officers of AKUATROP during the breeding trial and lab work of this study respectively. This study is part of the first author's Ph. D thesis.

References

Allegrucci G, Caccone A and Sbordoni V. 1999. Cytochrome b sequence divergence in the European sea bass (*Dicentrarchus labrax*) and phylogenetic relationships among some Perciformes species. *J Zool Systematics Evolut Res.*, **37**: 149-156.

Allendorf FW, Leary RF, Spruell P and Wenburg JK. 2001. The problems with hybrids: setting conservation guidelines. *Trends in Ecol Evolut.*, **16**: 613–622.

Azevedo MFC, Oliveira C, Pardo BG, Martínez P and Foresti F. 2008. Phylogenetic analysis of the order Pleuronectiformes (Teleostei) based on sequences of 12S and 16S mitochondrial genes. *Genet Mol Biol.*, **31(1)**: 284-292.

Bartley DM, Rana K and Immink AJ. 2001. The use of inter-specific hybrids in aquaculture and fisheries. *Rev Fish Biol Fisher.*, **10 :** 325–337.

Birstein VJ, Ruban G, Ludwig A, Doukakis P and DeSalle R. 2005. The enigmatic Caspian Sea Russian sturgeon: how many cryptic forms does it contain? *System Biodivers.*, **3:** 203–218

Buckler ES, Ippolito, A and Holtsford TP. 1997. The evolution of ribosomal DNA: divergent paralogues and phylogenetic implications. *Genet.*, **145:** 821–832.

Cianchi R, Ungaro A, Marini M and Bullini L. 2003. Differential patterns of hybridisation between the swallowtails *Papilio machaon* and *P. hospiton* from Sardinia and Corsica Islands (Lepidoptera, Papilionidae). *Mol Ecol.*, **12 :** 1461–1471.

Cunha C, Mesquita N and Dowling TE. 2002. Phylogenetic relationships of Eurasian and American cyprinids using cytochrome b sequences. *J Fish Biol.*, **61:** 929-944.

Degani G. 2004. Application of RAPD and cytochrome b sequences to the study of genetic variations in F1 and F2 generations of two different strains of guppy (*Poecilia reticulata*, Peter1854). *Aquaculture Res.*, **35:** 807-815.

do-Prado FD, Hashimoto DT, Mendonca FF, Senhorini JA, Foresti F and Porto-Foresti F. 2011. Molecular identification of hybrids between Neotropical catfish species *Pseudoplatystoma corruscans* and *Pseudoplatystoma reticulatum*. *Aquaculture Res.*, **42:** 1890-1894

Dunham RA, Smitherman RO, Brooks MJ, Benchakan M and Chappell JA. 1982. Paternal predominance in reciprocal channel–blue hybrid catfish. *Aquaculture*, **29:** 389–396.

Epifanio J and Nielsen J. 2000. The role of hybridization in the distribution, conservation and management of aquatic species. *Rev Fish Biol Fisher*., **10:** 245–251.

Felsenstein J. 1983. Parsimony in systematics: biological and statistical issues. *Ann Rev Ecol Systematics*, **14:** 313-333.

Feulner PGD, Kirshbaum F, Mamonekene V, Ketmaier V and Tierdemann R. 2007. Adaptive radiation in African weakly electric fish (Teleostei: Mormyridae: Campylomormyrus): a combined molecular and morphological approach. *J Evolut Biol*., **20:** 403-414.

Forbes SH and Allendorf FW. 1991. Associations between mitochondrial and nuclear genotypes in cutthroat trout hybrid swarms. *Evolution* **45:** 1332–1349.

Freyhof J, Lieckfeldt D, Pitra C and Ludwig A. 2005. Molecules and morphology: evidence for introgression of mitochondrial DNA in Dalmatian cyprinids. *Mol Phylogenet Evol*., **37:** 347–354.

Ha¨nfling B, Bolton P, Harley M and Carvalho G. 2005. A molecular approach to detect hybridisation between crucian carp (*Carassius carassius*) and nonindigenous carp species (*Carassius spp*. and *Cyprinus carpio*). *Freshwater Biol*., **50:** 403–417.

Hashimoto DT, Mendonça FF, Senhorini JA, Bortolozzi J, de Oliveira C, Foresti F and Porto–Foresti F. 2010. Identification of hybrids between Neotropical fish *Leporinus macrocephalus* and *Leporinus elongatus* by PCR–RFLP and multiplex–PCR: Tools for genetic monitoring in aquaculture. *Aquaculture*, **298:** 346–349.

Hillis DM and Bull J. 1993. An empirical test of bootstrapping as a method for assessing confidence limits in phylogenetic analysis. *Systematic Biol.,* **42:** 182-192.

Ludwig A. 2008. Identification of Acipenseriformes species in trade. *J Appl Ichthyol.,* **24(S1):**2–19

Moritz C, Dowling TE, Brown WM. 1987. Evolution of animal mitochondrial DNA: relevance for population biology and systematic. *Ann Rev Ecol, Evolut Systematics*, **18:** 269–292.

Na-Nakorn U, Kamonrat W and Ngamsiri T. 2004. Genetic diversity of walking catfish, *Clarias macrocephalus*, in Thailand and evidence of genetic introgression from introduced farmed *C. gariepinus*. *Aquaculture*, **240:** 145–163.

Nazia AK, Suzana M, Azhar H, Nguyen Thuy TT and Siti Azizah MN. 2010. No genetic differentiation between geographically isolated populations of *Clarias macrocephalus* Gunther in Malaysia revealed by sequences of mtDNA Cytochrome b and D-loop gene regions. *J Appl Ichthyol.,* **26:** 568–570.

Odorico, DM and Miller DJ. 1997. Variation in the ribosomal internal transcribed spacers and 5_8s rDNA among five species of Acropora (Cnidaria; Scleractinia): patterns of variation consistent with reticulate evolution. *Mol Biol Evolut.,* **14:** 465–473.

Okomoda VT, Koh ICC and Shahreza MS. 2017. First report on the successful hybridization of *Pangasianodon hypophthalmus* (Sauvage, 1878) and *Clarias gariepinus* (Burchell, 1822). *Zygote* **25 (4):** Pp 443-452.

Okomoda VT, Koh ICC, Hassan A, Amornsakun T and Shahreza MS. 2018b. Morphological characterization of the progenies of pure and reciprocal crosses of *Pangasianodon hypophthalmus* (Sauvage, 1878) and *Clarias gariepinus* (Burchell, 1822). *Scientific Reports* **8:** 3827**.**

Okomoda VT, Koh ICC, Hassan A, Amornsakun T and Shahreza MS. 2018c. Performance and characteristics of the progenies from the crosses of *Pangasianodon hypophthalmus* (Sauvage, 1878) and *Clarias gariepinus* (Burchell, 1822). *Aquaculture* **489 (3):** 96-104.

Okomoda VT, Koh ICC, Hassan A, Amornsakun T, Khairul ABK, Rajamad RY, Shuhaimi AD, Shafiq MR and Shahreza MS. 2018a. Erythrocyte characteristics of the progenies of pure and reciprocal crosses of *Pangasianodon hypophthalmus* (Sauvage, 1878) and *Clarias gariepinus* (Burchell, 1822). *Comp Clin Pathol.,* **27:** 301-312.

Olufeagba SO and Okomoda VT. 2016. Parentage determination of the hybrids between *Clarias batrachus* and *Clarias gariepinus* using Cytochrome B. *Banat's J Biotechnol.,* **14 (1):** 55-59

Pardo BG, Machordom A, Foresti F, Porto-Foresti F, Azevedo MFC, Bañon R, Sánchez L and Martinez P. 2005. Phylogenetic analysis of flatfishes (order Pleuronectiformes) based on mitochondrial 16S rDNA sequences. *Sci Mar.*, **69:** 531-543.

Perdices A, Sayanda D and Coelho MM. 2005. Mitochondrial diversity of Opsariichthys bidens (Teleostei, Cyprinidae) in three Chinese drainages. *Mol Phylogen Evolut.,* **37:** 920-927.

Perry WL, Lodge DM and Feder JL. 2002. Importance of hybridization between indigenous and nonindigenous freshwater species: an overlooked threat to North American biodiversity. *Syst. Biol.,* **51:** 255–275.

Pfrender ME, Hicks J and Lynch M. 2004. Biogeographic patterns and current distribution of molecular-genetic variation among populations of speckled dace, *Rhinichthys osculus* (Girard). *Molecular Phylogen Evolut.,* **30:** 490-502.

Pitts CS. 1995. Inter-specific hybridization in the fish family Cyprinidae. PhD thesis, University of Hull 103pp

Porto–Foresti F, Hashimoto DT, Alves AL, Almeida RBC, Senhorini JA, Bortolozzi J and Foresti F. 2008. Cytogenetic markers as diagnoses in the identification of the hybrid between Piaucu (*Leporinus macrocephalus*) and Piapara (*Leporinus elongatus*). *Gene Mol Biol.,* **31(Suppl.):** 195–202.

Rieseberg LH, Beckstromsternberg S and Doan K. 1990. *Helianthus annuus* ssp. texanus has chloroplast DNA and nuclear ribosomal RNA genes of *Helianthus debilis* ssp. cucumerifolius. *Proceedings of the National Academy of Sci USA*, **87:** 593–597.

Rosenfield JA, Nolasco S, Lindauer S, Sandoval C and Kodric-Brown A. 2004. The role of hybrid vigor in the replacement of Pecos pupfish by its hybrids with sheepshead minnow. *Conser Biol.*, **18:** 1589– 1598.

Ryman N and Utter F. ed. 1987. **Population Genetics and Fishery Management**. - University of Washington Press, Seattle, WA.

Saitou N and Nei M. 1987. The neighbor-joining method: a new method for reconstructing phylogenetic tress. *Mol Biol Evolut.*, **4:** 406-425.

Sang T, Crawford DJ and Stuessy TF. 1995. Documentation of reticulate evolution in peonies (Peonia) using internal transcribed spacer sequences of nuclear ribosomal DNA: implications for biogeography and concerted evolution. *Proceedings of the National Academy of Sci, USA,* **92:** 6813–6817.

Senanan W, Kapuscinski AR, Na-Nakorn U and Miller LM. 2004. Genetic impacts of hybrid catfish farming (*Clarias macrocephalus* x *C. gariepinus*) on native catfish populations in central Thailand. *Aquaculture* **235:** 167–184.

Strathmann RR. 1981. On the barriers to hybridization between *Strongylocentrotus droebachiensis* and *S. pallidus*. *J Exp Mar Biol Ecol.*, **55:** 39–47.

Sulaiman ZH, Hui TH, Lim KKP and Ng PKL. 2006. Mitochondrial DNA sequence analyses in Bornean sucker fishes (Balitoridae: Teleostei: Gastromyzontinae). *Integrative Zool.*,**1:** 12-14

Tave D. 1993. **Genetics for Fish Hatchery Managers**. *2nd Ed, Van Nostrand Reinhold New York*, **415p**.

Toledo–Filho SA, Almeida–Toledo LF, Foresti F, Calcagnotto D, Santos SBAF and Bernardino, G. 1998. Programas geneticos de selecao, hibridacao e endocruzamento aplicados a piscicultura. *Cadernos de Ictiogenetica 4, CCS/USP, Sao Paulo, SP, Brazil*, **56pp.**

Waldbrieser GC and Bosworth BG. 2008. Utilization of a Rapid DNA-Based Assay for Molecular Verification of Channel Catfish, Blue Catfish, F1 Hybrids, and Backcross Offspring at Several Life Stages. *North Am J Aquaculture*, **70:** 388–395.

Wilkins NP, Courtney HP and Curatolo A. 1994. Recombinant genotypes in backcrosses of male Atlantic salmon x brown trout hybrids to female Atlantic salmon. *J Fish Biol.,* **43,** 393–399.

Wyatt PMW, Pitts CS and Butlin RK. 2006. A molecular approach to detect hybridization between bream *Abramis brama*, roach *Rutlius rutilus* and rudd *Scardinius erythrophthalmus*. *J Fish Biol.*. **69:** 52–71.

Appendix

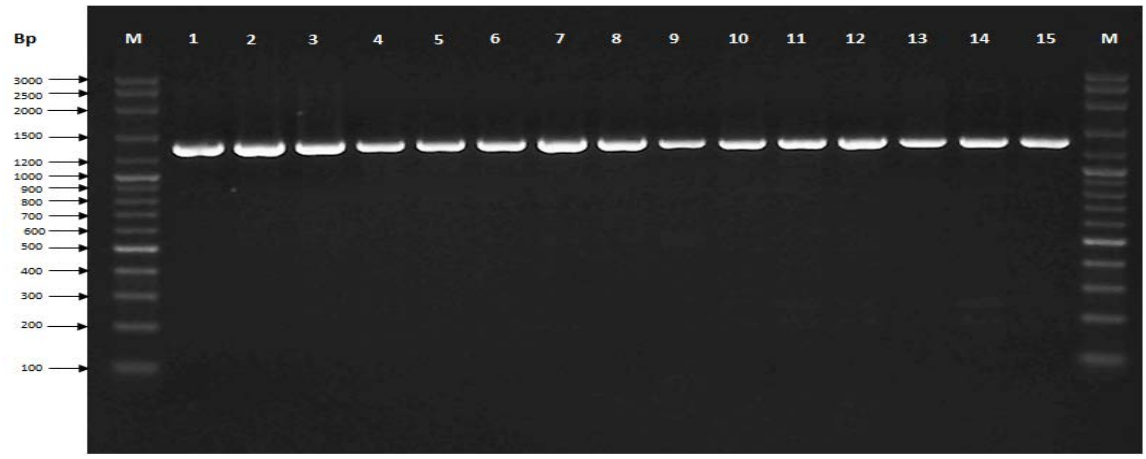

Appendix 1. Agarose gel showing the amplified PCR products of the Cyt B of the progenies of pure and reciprocal crosses of *Pangasianodon hypophthalmus* and pure *Clarias gariepinus*. M: Marker; Lane 1-3: *C. gariepinus*; Lane 4-6: Clarias-like Clariothalmus; Lane 7-9: Panga-like Clariothalmus; Lane 10-12: Pangapinus: Lane 13-15: *P. hypophthalmus*.

Download GenBank Graphics

Clarias gariepinus isolate BCG2 cytochrome b gene, partial cds; mitochondrial

Sequence ID: KJ533253.1 Length: 1114 Number of Matches: 1

Range 1: 39 to 1114 GenBank Graphics Next Match Previous Match

Score	Expect	Identities	Gaps	Strand
1982 bits(1073)	0.0	1075/1076(99%)	0/1076(0%)	Plus/Plus

```
Query  1     CGACGCACTCATCGACCTTCCCGCCCCCTCTAATATCTCCGCATGATGAAACTTTGGCTC  60
Sbjct  39    CGACGCACTCATCGACCTTCCCGCCCCCTCTAATATCTCCGCATGATGAAACTTTGGCTC  98
Query  61    ACTACTATTACTATGTCTTGGAGTACAAATCCTCACAGGACTATTCCTAGCCATACACTA  120
Sbjct  99    ACTACTATTACTATGTCTTGGAGTACAAATCCTCACAGGACTATTCCTAGCCATACACTA  158
Query  121   CACTTCTGATATCTCAACCGCATTCTCATCAGTAGTACACATCTGCCGAGACGTCAACTA  180
Sbjct  159   CACTTCTGATATCTCAACCGCATTCTCATCAGTAGTACACATCTGCCGAGACGTCAACTA  218
Query  181   CGGATGAATCATCCGAAACCTTCACGCCAACGGAGCATCCTTCTTCTTCATCTGCATCTA  240
Sbjct  219   CGGATGAATCATCCGAAACCTTCACGCCAACGGAGCATCCTTCTTCTTCATCTGCATCTA  278
Query  241   CCTTCACATTGGCCGTGGTCTGTACTATGGCTCATACCTATACAAAGAGACCTGAAACAT  300
Sbjct  279   CCTTCACATTGGCCGTGGTCTGTACTATGGCTCATACCTATACAAAGAGACCTGAAACAT  338
Query  301   CGGCGTCGTACTACTCCTTTTAGTAATAATAACAGCCTTCGTAGGATACGTACTACCATG  360
Sbjct  339   CGGCGTCGTACTACTCCTTTTAGTAATAATAACAGCCTTCGTAGGATACGTACTACCATG  398
Query  361   AGGACAAATATCCTTCTGAGGTGCCACAGTAATCACAAACCTCTTATCAGCCGTACCCTA  420
Sbjct  399   AGGACAAATATCCTTCTGAGGTGCCACAGTAATCACAAACCTCTTATCAGCCGTACCCTA  458
Query  421   CATAGGAGATGCCCTAGTCCAATGAATCTGAGGAGGCTTCTCCGTAGACAATGCAACACT  480
Sbjct  459   CATAGGAGATGCCCTAGTCCAATGAATCTGAGGAGGCTTCTCCGTAGACAATGCAACACT  518
Query  481   TACACGATTCTTCGCATTCCACTTCCTCCTACCATTCACAATCATCGCAGCTACAATTCT  540
Sbjct  519   TACACGATTCTTCGCATTCCACTTCCTCCTACCATTCACAATCATCGCAGCTACAATTCT  578
Query  541   ACACGCACTATTCCTACACGAAACAGGATCAAACAACCCAATTGGACTAAACTCCGACGC  600
Sbjct  579   ACACGCACTATTCCTACACGAAACAGGATCAAACAACCCAATTGGACTAAGCTCCGACGC  638
Query  601   AGACAAAATCTCATTCCACCCATATTTCTCCTACAAAGACCTACTAGGATTTATCATTCT  660
Sbjct  639   AGACAAAATCTCATTCCACCCATATTTCTCCTACAAAGACCTACTAGGATTTATCATTCT  698
Query  661   ATTAACAGCCCTCGCATCTCTAAGCCTATTCTCCCCAAACCTTCTAGGCGACCCAGAAAA  720
Sbjct  699   ATTAACAGCCCTCGCATCTCTAAGCCTATTCTCCCCAAACCTTCTAGGCGACCCAGAAAA  758
Query  721   CTTCACCCCCGCCAACCCCCTAGTAACTCCACCTCACATCAAACCAGAATGATACTTCCT  780
Sbjct  759   CTTCACCCCCGCCAACCCCCTAGTAACTCCACCTCACATCAAACCAGAATGATACTTCCT  818
Query  781   ATTCGCATACGCCATCCTCCGATCCATCCCAAACAAACTAGGCGGAGTATTAGCACTATT  840
Sbjct  819   ATTCGCATACGCCATCCTCCGATCCATCCCAAACAAACTAGGCGGAGTATTAGCACTATT  878
Query  841   ATTCTCCATCCTAGTACTAATAGTAGTAGCACTACTACACCTCTCAAAACAACAGGGCCT  900
Sbjct  879   ATTCTCCATCCTAGTACTAATAGTAGTAGCACTACTACACCTCTCAAAACAACAGGGCCT  938
Query  901   AACCTTCCGACCTTTATCCCAAATCTTATTCTGAACCCTAGTAGCAGATGTAATAATCTT  960
Sbjct  939   AACCTTCCGACCTTTATCCCAAATCTTATTCTGAACCCTAGTAGCAGATGTAATAATCTT  998
Query  961   AACATGAATCGGCGGCATACCAGTAGAACATCCGTTCATCATTATCGGACAAATCGCCTC  1020
Sbjct  999   AACATGAATCGGCGGCATACCAGTAGAACATCCGTTCATCATTATCGGACAAATCGCCTC  1058
Query  1021  CATCCTCTACTTCTCCCTATTCCTCATCTTAAACCCACTAGCAGCCTGACTAGAAA  1076
Sbjct  1059  CATCCTCTACTTCTCCCTATTCCTCATCTTAAACCCACTAGCAGCCTGACTAGAAA  1114
```

Appendix 2. Aligned *Clarias gariepinus* cytochrome b sequence showing 99 % similarity with *Clarias gariepinus* isolate BCG2 cytochrome b gene, partial cds; mitochondrion (GenBank Accession Number KJ533253.1).

Appendix 3. Aligned Clarias-like Clariothalmus cytochrome b sequence showing 99 % similarity with *Clarias gariepinus* isolate BCG2 cytochrome b gene, partial cds; mitochondrion (GenBank Accession Number KJ533253.1).

Download GenBank Graphics

Clarias gariepinus isolate BCG2 cytochrome b gene, partial cds; mitochondrial

Sequence ID: KJ533253.1 **Length:** 1114 **Number of Matches:** 1

Range 1: 39 to 1114 GenBank Graphics Next Match Previous Match

Score	Expect	Identities	Gaps	Strand
1982 bits(1073)	0.0	1075/1076(99%)	0/1076(0%)	Plus/Plus

```
Query  1     CGACGCACTCATCGACCTTCCCGCCCCCTCTAATATCTCCGCATGATGAAACTTTGGCTC  60
             ||||||||||||||||||||||||||||||||||||||||||||||||||||||||||||
Sbjct  39    CGACGCACTCATCGACCTTCCCGCCCCCTCTAATATCTCCGCATGATGAAACTTTGGCTC  98

Query  61    ACTACTATTACTATGTCTTGGAGTACAAATCCTCACAGGACTATTCCTAGCCATACACTA  120
             ||||||||||||||||||||||||||||||||||||||||||||||||||||||||||||
Sbjct  99    ACTACTATTACTATGTCTTGGAGTACAAATCCTCACAGGACTATTCCTAGCCATACACTA  158

Query  121   CACTTCTGATATCTCAACCGCATTCTCATCAGTAGTACACATCTGCCGAGACGTCAACTA  180
             ||||||||||||||||||||||||||||||||||||||||||||||||||||||||||||
Sbjct  159   CACTTCTGATATCTCAACCGCATTCTCATCAGTAGTACACATCTGCCGAGACGTCAACTA  218

Query  181   CGGATGAATCATCCGAAACCTTCACGCCAACGGAGCATCCTTCTTCTTCATCTGCATCTA  240
             ||||||||||||||||||||||||||||||||||||||||||||||||||||||||||||
Sbjct  219   CGGATGAATCATCCGAAACCTTCACGCCAACGGAGCATCCTTCTTCTTCATCTGCATCTA  278

Query  241   CCTTCACATTGGCCGTGGTCTGTACTATGGCTCATACCTATACAAAGAGACCTGAAACAT  300
             ||||||||||||||||||||||||||||||||||||||||||||||||||||||||||||
Sbjct  279   CCTTCACATTGGCCGTGGTCTGTACTATGGCTCATACCTATACAAAGAGACCTGAAACAT  338

Query  301   CGGCGTCGTACTACTCCTTTTAGTAATAATAACAGCCTTCGTAGGATACGTACTACCATG  360
             ||||||||||||||||||||||||||||||||||||||||||||||||||||||||||||
Sbjct  339   CGGCGTCGTACTACTCCTTTTAGTAATAATAACAGCCTTCGTAGGATACGTACTACCATG  398

Query  361   AGGACAAATATCCTTCTGAGGTGCCACAGTAATCACAAACCTCTTATCAGCCGTACCCTA  420
             ||||||||||||||||||||||||||||||||||||||||||||||||||||||||||||
Sbjct  399   AGGACAAATATCCTTCTGAGGTGCCACAGTAATCACAAACCTCTTATCAGCCGTACCCTA  458

Query  421   CATAGGAGATGCCCTAGTCCAATGAATCTGAGGAGGCTTCTCCGTAGACAATGCAACACT  480
             ||||||||||||||||||||||||||||||||||||||||||||||||||||||||||||
Sbjct  459   CATAGGAGATGCCCTAGTCCAATGAATCTGAGGAGGCTTCTCCGTAGACAATGCAACACT  518

Query  481   TACACGATTCTTCGCATTCCACTTCCTCCTACCATTCACAATCATCGCAGCTACAATTCT  540
             ||||||||||||||||||||||||||||||||||||||||||||||||||||||||||||
Sbjct  519   TACACGATTCTTCGCATTCCACTTCCTCCTACCATTCACAATCATCGCAGCTACAATTCT  578

Query  541   ACACGCACTATTCCTACACGAAACAGGATCAAACAACCCAATTGGACTAAACTCCGACGC  600
             |||||||||||||||||||||||||||||||||||||||||||||||| ||||||||||||
Sbjct  579   ACACGCACTATTCCTACACGAAACAGGATCAAACAACCCAATTGGACTAAGCTCCGACGC  638

Query  601   AGACAAAATCTCATTCCACCCATATTTCTCCTACAAAGACCTACTAGGATTTATCATTCT  660
             ||||||||||||||||||||||||||||||||||||||||||||||||||||||||||||
Sbjct  639   AGACAAAATCTCATTCCACCCATATTTCTCCTACAAAGACCTACTAGGATTTATCATTCT  698

Query  661   ATTAACAGCCCTCGCATCTCTAAGCCTATTCTCCCCAAACCTTCTAGGCGACCCAGAAAA  720
             ||||||||||||||||||||||||||||||||||||||||||||||||||||||||||||
Sbjct  699   ATTAACAGCCCTCGCATCTCTAAGCCTATTCTCCCCAAACCTTCTAGGCGACCCAGAAAA  758

Query  721   CTTCACCCCCGCCAACCCCCTAGTAACTCCACCTCACATCAAACCAGAATGATACTTCCT  780
             ||||||||||||||||||||||||||||||||||||||||||||||||||||||||||||
Sbjct  759   CTTCACCCCCGCCAACCCCCTAGTAACTCCACCTCACATCAAACCAGAATGATACTTCCT  818

Query  781   ATTCGCATACGCCATCCTCCGATCCATCCCAAACAAACTAGGCGGAGTATTAGCACTATT  840
             ||||||||||||||||||||||||||||||||||||||||||||||||||||||||||||
Sbjct  819   ATTCGCATACGCCATCCTCCGATCCATCCCAAACAAACTAGGCGGAGTATTAGCACTATT  878

Query  841   ATTCTCCATCCTAGTACTAATAGTAGTACCACTACTACACCTCTCAAAACAACAGGGCCT  900
             ||||||||||||||||||||||||||||||||||||||||||||||||||||||||||||
Sbjct  879   ATTCTCCATCCTAGTACTAATAGTAGTACCACTACTACACCTCTCAAAACAACAGGGCCT  938

Query  901   AACCTTCCGACCTTTATCCCAAATCTTATTCTGAACCCTAGTAGCAGATGTAATAATCTT  960
             ||||||||||||||||||||||||||||||||||||||||||||||||||||||||||||
Sbjct  939   AACCTTCCGACCTTTATCCCAAATCTTATTCTGAACCCTAGTAGCAGATGTAATAATCTT  998

Query  961   AACATGAATCGGCGGCATACCAGTAGAACATCCGTTCATCATTATCGGACAAATCGCCTC  1020
             ||||||||||||||||||||||||||||||||||||||||||||||||||||||||||||
Sbjct  999   AACATGAATCGGCGGCATACCAGTAGAACATCCGTTCATCATTATCGGACAAATCGCCTC  1058

Query  1021  CATCCTCTACTTCTCCCTATTCCTCATCTTAAACCCACTAGCAGCCTGACTAGAAA  1076
             ||||||||||||||||||||||||||||||||||||||||||||||||||||||
Sbjct  1059  CATCCTCTACTTCTCCCTATTCCTCATCTTAAACCCACTAGCAGCCTGACTAGAAA  1114
```

Appendix 4. Aligned Panga-like Clariothalmus cytochrome b sequence showing 99 % similarity with *Clarias gariepinus* isolate BCG2 cytochrome b gene, partial cds; mitochondrion (GenBank Accession Number KJ533253.1).

Download GenBank Graphics

Pangasianodon hypophthalmus isolate PSH02 cytochrome b (Cytb) gene, partial cds; mitochondrial

Sequence ID: KM434895.1 Length: 1139 Number of Matches: 1

Range 1: 42 to 1117 GenBank Graphics Next Match Previous Match

Score	Expect	Identities	Gaps	Strand
1982 bits(1073)	0.0	1075/1076(99%)	0/1076(0%)	Plus/Plus

```
Query  1     CGACGCACTAATTGACCTTCCTGCCCCATCCAATATTTCCGCATGATGAAACTTTGGTTC  60
             ||||||||||||||||||||||||||||||||||||||||||||||||||||||||||||
Sbjct  42    CGACGCACTAATTGACCTTCCTGCCCCATCCAATATTTCCGCATGATGAAACTTTGGTTC  101

Query  61    CCTACTATTATTATGCCTTATAGTACAGATCCTAACAGGACTTTTCCTAGCCATACATTA  120
             ||||||||||||||||||||||||||||||||||||||||||||||||||||||||||||
Sbjct  102   CCTACTATTATTATGCCTTATAGTACAGATCCTAACAGGACTTTTCCTAGCCATACATTA  161

Query  121   TACCTCAGACATCTCTACTGGCTTCTCATCCGTAGCCCACATCTGTCGAGATGTAAATTA  180
             |||||||||||||||||| ||||||||||||||||||||||||||||||||||||||||
Sbjct  162   TACCTCAGACATCTCTACTGCCTTCTCATCCGTAGCCCACATCTGTCGAGATGTAAATTA  221

Query  181   CGGATGAGTCATCCGCAACTTACATGCCAACGGAGCTTCATTCTTTTTCATCTGTATTTA  240
             ||||||||||||||||||||||||||||||||||||||||||||||||||||||||||||
Sbjct  222   CGGATGAGTCATCCGCAACTTACATGCCAACGGAGCTTCATTCTTTTTCATCTGTATTTA  281

Query  241   CCTACACATCGGACGAGGATTATATTATGGCTCTTACTTATATAAAGAAACCTGAAATAT  300
             ||||||||||||||||||||||||||||||||||||||||||||||||||||||||||||
Sbjct  282   CCTACACATCGGACGAGGATTATATTATGGCTCTTACTTATATAAAGAAACCTGAAATAT  341

Query  301   TGGAGTAGTACTTCTCCTATTAGTTATAATAACCGCCTTCGTCGGATATGTTTTACCATG  360
             ||||||||||||||||||||||||||||||||||||||||||||||||||||||||||||
Sbjct  342   TGGAGTAGTACTTCTCCTATTAGTTATAATAACCGCCTTCGTCGGATATGTTTTACCATG  401

Query  361   AGGTCAAATATCATTTTGAGGCGCCACAGTAATCACAAATCTCCTATCAGCTGTCCCTTA  420
             ||||||||||||||||||||||||||||||||||||||||||||||||||||||||||||
Sbjct  402   AGGTCAAATATCATTTTGAGGCGCCACAGTAATCACAAATCTCCTATCAGCTGTCCCTTA  461

Query  421   CATAGGAGATATACTAGTACAATGAATTTGAGGTGGCTTCTCCGTAGACAATGCAACACT  480
             ||||||||||||||||||||||||||||||||||||||||||||||||||||||||||||
Sbjct  462   CATAGGAGATATACTAGTACAATGAATTTGAGGTGGCTTCTCCGTAGACAATGCAACACT  521

Query  481   AACACGATTCTTCGCATTTCACTTCCTACTTCCATTCGTAATTGTCGCAGCCACAGTATT  540
             ||||||||||||||||||||||||||||||||||||||||||||||||||||||||||||
Sbjct  522   AACACGATTCTTCGCATTTCACTTCCTACTTCCATTCGTAATTGTCGCAGCCACAGTATT  581

Query  541   ACATGCCTTATTCCTACACGAAACAGGCTCCAATAACCCAATTGGCCTAAACTCCGACGC  600
             ||||||||||||||||||||||||||||||||||||||||||||||||||||||||||||
Sbjct  582   ACATGCCTTATTCCTACACGAAACAGGCTCCAATAACCCAATTGGCCTAAACTCCGACGC  641

Query  601   AGACAAAATCTCCTTCCACCCATACTTCTCCTATAAAGATGTATTAGGATTCATAATCCT  660
             ||||||||||||||||||||||||||||||||||||||||||||||||||||||||||||
Sbjct  642   AGACAAAATCTCCTTCCACCCATACTTCTCCTATAAAGATGTATTAGGATTCATAATCCT  701

Query  661   CCTCACAGCCCTCGCATCTTTAGCCCTCTTCTCACCAAACCTTTTAGGAGATCCAGAAAA  720
             ||||||||||||||||||||||||||||||||||||||||||||||||||||||||||||
Sbjct  702   CCTCACAGCCCTCGCATCTTTAGCCCTCTTCTCACCAAACCTTTTAGGAGATCCAGAAAA  761

Query  721   CTTCACCCCAGCCAACCCATTAGTAACACCGCCCCACATCAAACCAGAATGATACTTCCT  780
             ||||||||||||||||||||||||||||||||||||||||||||||||||||||||||||
Sbjct  762   CTTCACCCCAGCCAACCCATTAGTAACACCGCCCCACATCAAACCAGAATGATACTTCCT  821

Query  781   ATTTGCATATGCCATCCTACGATCAATCCCAAATAAGCTAGGAGGGGTCCTGGCCCTACT  840
             ||||||||||||||||||||||||||||||||||||||||||||||||||||||||||||
Sbjct  822   ATTTGCATATGCCATCCTACGATCAATCCCAAATAAGCTAGGAGGGGTCCTGGCCCTACT  881

Query  841   ATTCTCCATCCTAGTATTAATAGTTGTTCCCCTATTACACACCTCTAAACAACAAGGCCT  900
             ||||||||||||||||||||||||||||||||||||||||||||||||||||||||||||
Sbjct  882   ATTCTCCATCCTAGTATTAATAGTTGTTCCCCTATTACACACCTCTAAACAACAAGGCCT  941

Query  901   CACTTTCCGCCCCCTCTCCCAATTCCTATTCTGAGCCCTAGTAGCAGACGTAGCCATTCT  960
             ||||||||||||||||||||||||||||||||||||||||||||||||||||||||||||
Sbjct  942   CACTTTCCGCCCCCTCTCCCAATTCCTATTCTGAGCCCTAGTAGCAGACGTAGCCATTCT  1001

Query  961   CACTTGAATTGGCGGTATACCAGTCGAACACCCATTCATCATTATCGGACAAATCGCCTC  1020
             ||||||||||||||||||||||||||||||||||||||||||||||||||||||||||||
Sbjct  1002  CACTTGAATTGGCGGTATACCAGTCGAACACCCATTCATCATTATCGGACAAATCGCCTC  1061

Query  1021  CATTTTATATTTTCTCTTCTTCCTAGTCCTAAACCCCCTAGCAGGATGACTAGAAA  1076
             ||||||||||||||||||||||||||||||||||||||||||||||||||||||||
Sbjct  1062  CATTTTATATTTTCTCTTCTTCCTAGTCCTAAACCCCCTAGCAGGATGACTAGAAA  1117
```

Appendix 5. Aligned Pangapinus cytochrome b sequence showing 99 % similarity with *Pangasianodon hypophthalmus* isolate PSH02 cytochrome b (Cytb) gene, partial cds; mitochondrial sequence (GenBank Accession Number KM434895.1).

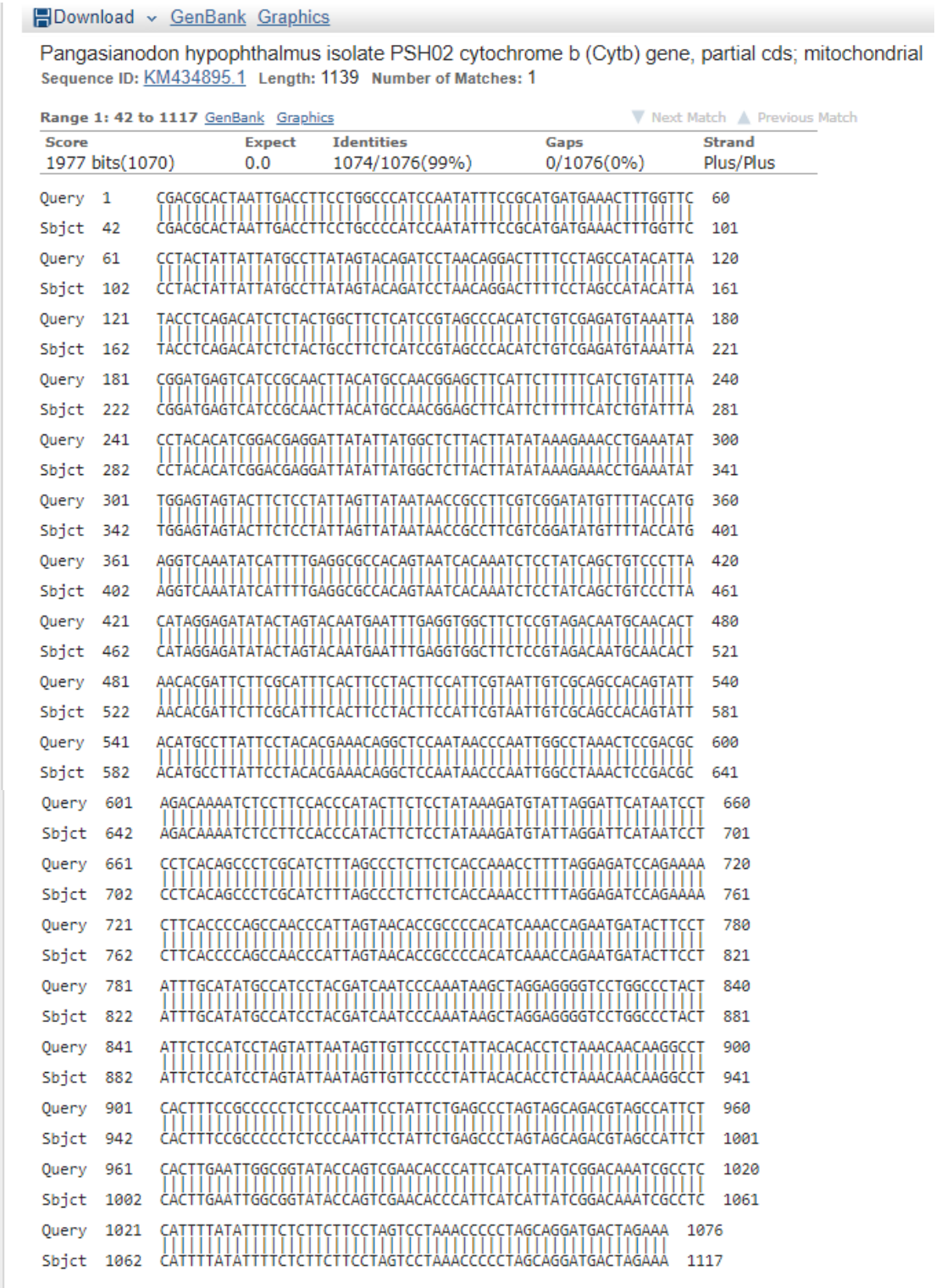

Download GenBank Graphics

Pangasianodon hypophthalmus isolate PSH02 cytochrome b (Cytb) gene, partial cds; mitochondrial

Sequence ID: KM434895.1 Length: 1139 Number of Matches: 1

Range 1: 42 to 1117 GenBank Graphics Next Match Previous Match

Score	Expect	Identities	Gaps	Strand
1977 bits(1070)	0.0	1074/1076(99%)	0/1076(0%)	Plus/Plus

```
Query  1     CGACGCACTAATTGACCTTCCTGGCCCATCCAATATTTCCGCATGATGAAACTTTGGTTC  60
             ||||||||||||||||||||| ||||||||||||||||||||||||||||||||||||
Sbjct  42    CGACGCACTAATTGACCTTCCTGCCCCATCCAATATTTCCGCATGATGAAACTTTGGTTC  101

Query  61    CCTACTATTATTATGCCTTATAGTACAGATCCTAACAGGACTTTTCCTAGCCATACATTA  120
             ||||||||||||||||||||||||||||||||||||||||||||||||||||||||||||
Sbjct  102   CCTACTATTATTATGCCTTATAGTACAGATCCTAACAGGACTTTTCCTAGCCATACATTA  161

Query  121   TACCTCAGACATCTCTACTGGCTTCTCATCCGTAGCCCACATCTGTCGAGATGTAAATTA  180
             |||||||||||||||||| ||||||||||||||||||||||||||||||||||||||||
Sbjct  162   TACCTCAGACATCTCTACTGCCTTCTCATCCGTAGCCCACATCTGTCGAGATGTAAATTA  221

Query  181   CGGATGAGTCATCCGCAACTTACATGCCAACGGAGCTTCATTCTTTTTCATCTGTATTTA  240
             ||||||||||||||||||||||||||||||||||||||||||||||||||||||||||||
Sbjct  222   CGGATGAGTCATCCGCAACTTACATGCCAACGGAGCTTCATTCTTTTTCATCTGTATTTA  281

Query  241   CCTACACATCGGACGAGGATTATATTATGGCTCTTACTTATATAAAGAAACCTGAAATAT  300
             ||||||||||||||||||||||||||||||||||||||||||||||||||||||||||||
Sbjct  282   CCTACACATCGGACGAGGATTATATTATGGCTCTTACTTATATAAAGAAACCTGAAATAT  341

Query  301   TGGAGTAGTACTTCTCCTATTAGTTATAATAACCGCCTTCGTCGGATATGTTTTACCATG  360
             ||||||||||||||||||||||||||||||||||||||||||||||||||||||||||||
Sbjct  342   TGGAGTAGTACTTCTCCTATTAGTTATAATAACCGCCTTCGTCGGATATGTTTTACCATG  401

Query  361   AGGTCAAATATCATTTTGAGGCGCCACAGTAATCACAAATCTCCTATCAGCTGTCCCTTA  420
             ||||||||||||||||||||||||||||||||||||||||||||||||||||||||||||
Sbjct  402   AGGTCAAATATCATTTTGAGGCGCCACAGTAATCACAAATCTCCTATCAGCTGTCCCTTA  461

Query  421   CATAGGAGATATACTAGTACAATGAATTTGAGGTGGCTTCTCCGTAGACAATGCAACACT  480
             ||||||||||||||||||||||||||||||||||||||||||||||||||||||||||||
Sbjct  462   CATAGGAGATATACTAGTACAATGAATTTGAGGTGGCTTCTCCGTAGACAATGCAACACT  521

Query  481   AACACGATTCTTCGCATTTCACTTCCTACTTCCATTCGTAATTGTCGCAGCCACAGTATT  540
             ||||||||||||||||||||||||||||||||||||||||||||||||||||||||||||
Sbjct  522   AACACGATTCTTCGCATTTCACTTCCTACTTCCATTCGTAATTGTCGCAGCCACAGTATT  581

Query  541   ACATGCCTTATTCCTACACGAAACAGGCTCCAATAACCCAATTGGCCTAAACTCCGACGC  600
             ||||||||||||||||||||||||||||||||||||||||||||||||||||||||||||
Sbjct  582   ACATGCCTTATTCCTACACGAAACAGGCTCCAATAACCCAATTGGCCTAAACTCCGACGC  641

Query  601   AGACAAAATCTCCTTCCACCCATACTTCTCCTATAAAGATGTATTAGGATTCATAATCCT  660
             ||||||||||||||||||||||||||||||||||||||||||||||||||||||||||||
Sbjct  642   AGACAAAATCTCCTTCCACCCATACTTCTCCTATAAAGATGTATTAGGATTCATAATCCT  701

Query  661   CCTCACAGCCCTCGCATCTTTAGCCCTCTTCTCACCAAACCTTTTAGGAGATCCAGAAAA  720
             ||||||||||||||||||||||||||||||||||||||||||||||||||||||||||||
Sbjct  702   CCTCACAGCCCTCGCATCTTTAGCCCTCTTCTCACCAAACCTTTTAGGAGATCCAGAAAA  761

Query  721   CTTCACCCCAGCCAACCCATTAGTAACACCGCCCCACATCAAACCAGAATGATACTTCCT  780
             ||||||||||||||||||||||||||||||||||||||||||||||||||||||||||||
Sbjct  762   CTTCACCCCAGCCAACCCATTAGTAACACCGCCCCACATCAAACCAGAATGATACTTCCT  821

Query  781   ATTTGCATATGCCATCCTACGATCAATCCCAAATAAGCTAGGAGGGGTCCTGGCCCTACT  840
             ||||||||||||||||||||||||||||||||||||||||||||||||||||||||||||
Sbjct  822   ATTTGCATATGCCATCCTACGATCAATCCCAAATAAGCTAGGAGGGGTCCTGGCCCTACT  881

Query  841   ATTCTCCATCCTAGTATTAATAGTTGTTCCCCTATTACACACCTCTAAACAACAAGGCCT  900
             ||||||||||||||||||||||||||||||||||||||||||||||||||||||||||||
Sbjct  882   ATTCTCCATCCTAGTATTAATAGTTGTTCCCCTATTACACACCTCTAAACAACAAGGCCT  941

Query  901   CACTTTCCGCCCCCCTCTCCCAATTCCTATTCTGAGCCCTAGTAGCAGACGTAGCCATTCT  960
             ||||||||||||||||||||||||||||||||||||||||||||||||||||||||||||
Sbjct  942   CACTTTCCGCCCCCCTCTCCCAATTCCTATTCTGAGCCCTAGTAGCAGACGTAGCCATTCT  1001

Query  961   CACTTGAATTGGCGGTATACCAGTCGAACACCCATTCATCATTATCGGACAAATCGCCTC  1020
             ||||||||||||||||||||||||||||||||||||||||||||||||||||||||||||
Sbjct  1002  CACTTGAATTGGCGGTATACCAGTCGAACACCCATTCATCATTATCGGACAAATCGCCTC  1061

Query  1021  CATTTTATATTTTCTCTTCTTCCTAGTCCTAAACCCCCTAGCAGGATGACTAGAAA  1076
             ||||||||||||||||||||||||||||||||||||||||||||||||||||||
Sbjct  1062  CATTTTATATTTTCTCTTCTTCCTAGTCCTAAACCCCCTAGCAGGATGACTAGAAA  1117
```

Appendix 6. Aligned *Pangasianodon hypophthalmus* cytochrome b sequence showing 99 % similarity with *Pangasianodon hypophthalmus* isolate PSH02 cytochrome b (Cytb) gene, partial cds; mitochondrial sequence (GenBank Accession Number KM434895.1).

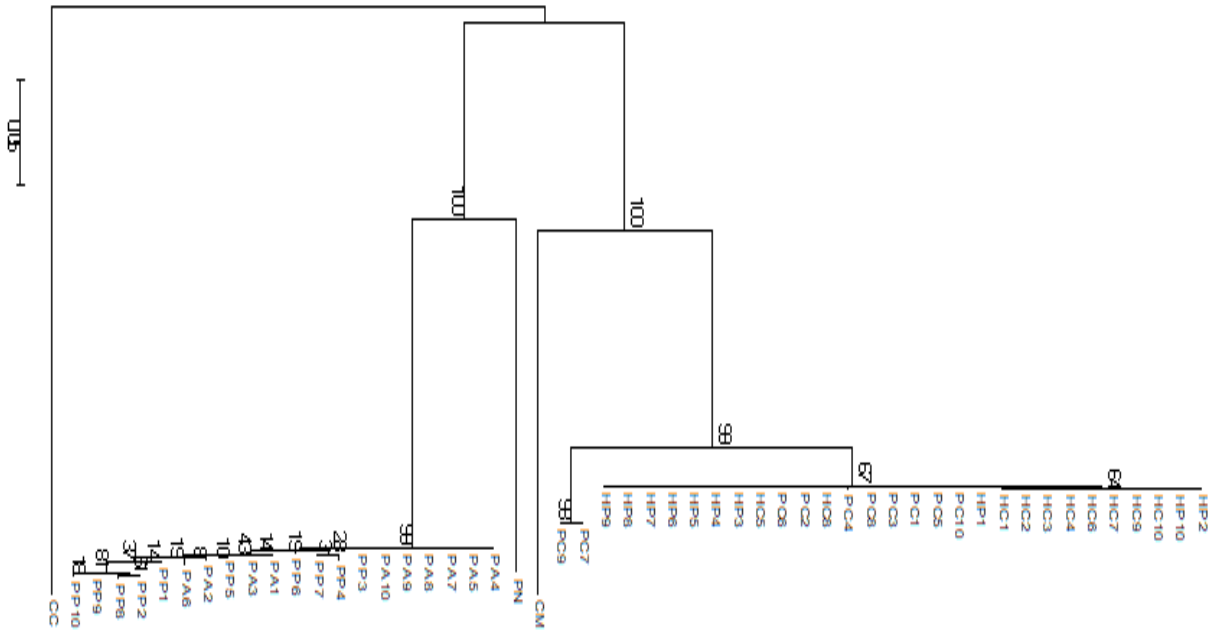

Appendix 7. Phylogenetic relationships of the different progenies following Neighbour joining analysis of 1076bp of the cytochrome b gene. PC1 - PC10 = *C. gariepinus*; HC1 – HC10 = Clarias-like Clariothalmus; HP1 – HP10 = Panga-like Clariothalmus; PA1 - PA10 = Pangapinus; PP1 - PP10 = *P. hypophthalmus*; CC = *Cyprinus carpio*; CM = *Clarias macrocephalus;* PN = *Pangasius nasutus.* (Support values are bootstrap values).

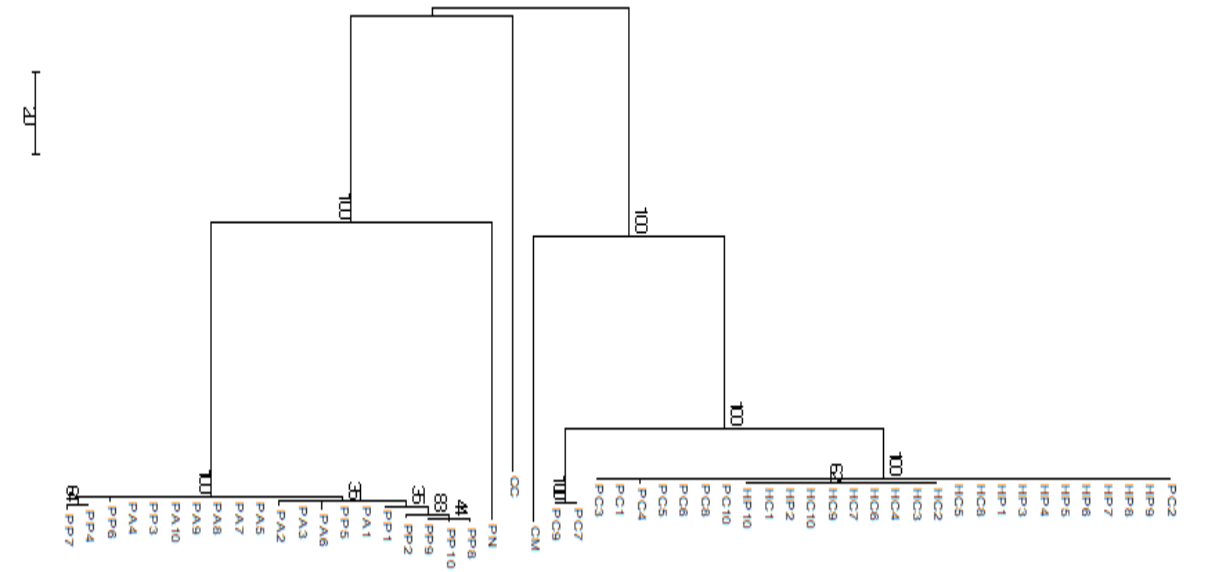

Appendix 8. Phylogenetic relationships of the different progenies following Maximum Parsimony analysis of 1076bp of the cytochrome b gene. PC1 - PC10 = *C. gariepinus*; HC1 – HC10 = Clarias-like Clariothalmus; HP1 – HP10 = Panga-like Clariothalmus; PA1 - PA10 = Pangapinus; PP1 - PP10 = *P. hypophthalmus*; CC = *Cyprinus carpio*; CM = *Clarias macrocephalus;* PN = *Pangasius nasutus.* (Support values are bootstrap values).

JJBS

Volume 12, Number 1,March 2019
ISSN 1995-6673
Pages 119 - 122

Jordan Journal of Biological Sciences **Short Communication**

Effects of Hypersaline Conditions on the Growth and Survival of Larval Red Drum-(*Sciaenops ocellatus*)

Irma Kesaulya[1,2,3,*] and Robert Vega[1,2]

[1]*Department of Life Science, Texas A&M University Corpus Christi, 6300 Ocean Drive, 78412;*

[2]*Texas Parks and Wildlife Department Coastal Fisheries Division CCA Marine Development Center,4300 Waldron Road Corpus Christi, Texas 78418, USA;*

[3]*Fisheries and Marine Science Faculty, Pattimura University, Kampus Poka Jl. Martha Alfons-Poka 97233. Ambon-Maluku, Indonesia. (present address).*

Received May 24, 2018; Revised July 23, 2018; Accepted August 12, 2018

Abstract

Texas bays and estuaries experience salinity fluctuations (e.g., droughts, reduced freshwater inflows and hurricanes) caused by natural weather and climate change. This could have impacts on red drum *Sciaenops ocellatus* (Linnaeus) early life stages beacause red drum spend their early life stage at the shallow bays and estuarine waters of Texas Bay. The purpose of the present study is to evaluate the impact of high salinity concentrations on the survival, growth and development of red drum eggs and larvae. Red drum brood stocks were collected from wild stocks throughout the lower Texas coast and were held in hatchery tanks (13,250 L) until spawning. The water quality conditions were maintained at a salinity of 38ppt and seawater temperature of 25°C. The red drum eggs were hatched at a wide range of salinity treatments (28-48ppt). Egg hatch-out rates and larvae growth were reduced at the lowest (28ppt) and highest (48ppt) salinity treatments. Hypersalinity (≥ 40ppt) and a temperature of 25ºC affected the hatching success of red drum eggs. The percentage of egg hatching success and length of larvae were reduced in both lower (28ppt) and/or hypersalinity (48ppt). This study shows that red drum eggs can hatch within a wide range of salinities with best hatch-out and growth rates occurring between 33 – 43ppt. It also suggests that climate change that produces global warming can keep the increasing environmental salinity of the Texas bay which might have an impact on the development of the early stages of the red drum in their natural environment.

Keywords: Estuary, early life stages, hypersalinity,hatching success,red drum, Texas Bay.

1. Introduction

The red drum *Sciaenops ocellatus* (Linneaus) is an important commercial and recreational sciaenid that ranges from Tuxpan, Mexico in the Gulf of Mexico to Massachusetts in the Atlantic Ocean (Pattilo *et al*., 1997). In Texas, red drum was recognized as being overfished in the mid-1970's which prompted state regulators to implement progressively restrictive rules to reduce fishing harvest levels (Swingle, 1990). The sale of wild- caught red drum was prohibited in 1981 (Matlock, 1990a), and as an alternative fisheries management tool hatchery production of juvenile red drum at state-operated facilities was initiated in Texas for stock enhancement purposes (Matlock, 1990b; McEachron *et al*., 1995; Blaxter, 2000). These measures were taken in order to reduce fishing pressures and supplement wild stock populations through the stock enhancement.

Red drum is a quasi-catadromous sciaenid (Rounsefell, 1975). The adult red drum migrate from estuaries to the near shore gulf to spawn during the fall (September – November) (Matlock, 1990a). Currents carry eggs and larvae into shallow bays and estuarine nurseries (Peters and McMichael, 1987; Holt *et al*., 1989; Comyns *et al*., 1991; Holt *et al.*, 1985 and Rooker *et al*., 1997). Red drum juveniles and sub-adults remain in estuaries for three-five years (Miles, 1950) before migrating offshore as adults (Swingle, 1990). In the shallow bays and estuaries, the temperature and salinity conditions can fluctuate within and between the seasons. Early life stages (age/size dependent) of red drum vary in their ability to tolerate shifts in environmental variables (Neill, 1990). Conditions beyond the environmental thresholds of tolerance may cause deformities, low hatching rates, reduced growth, and a decreased larva survival (Kucera *et al*., 2002). Knowing how early life stages of fishes cope with non-optimal conditions is an important consideration for their effective management (Holt and Holt, 2002).

Salinity in Texas bays and estuaries varies from brackish to hypersaline depending on the hydrographic condition such as freshwater inflow, tides, evaporation and currents (Holt and Holt, 2002). The coastal waters near passes are characterized by a wind-driven surface current, and can vary greatly in salinity (Ponwith and Neill, 1995). According to Buskey *et al*. (2001), mean salinities for Matagorda Bay in north of Corpus Christi and Upper Laguna Madre, south of Corpus Christi are 18 to 24ppt and

* Corresponding author. e-mail: irma_kesaulya@yahoo.com.

40 to 50ppt respectively. High temperatures during the summer months can cause drought conditions due to increased evaporation rates.

Several studies investigating the effects of seawater salinity on the early development and larvae growth of different fishes had been conducted. However, to the researchers' knowledge, information on the early life development of the red drum in higher salinity (> 40ppt) as it occurs in their natural environment along the south Texas coast is still limited. Determining the effect of hypersalinity (> 40ppt) on hatching success rates of red drum may provide better habitat management and an insight into the successful early development of red drum in hypersaline Texas bays.

The purpose of the present study is to evaluate the impact of high salinity concentrations on the survival, growth, and development of red drum eggs and larvae.

2. Materials and Methods

All experiments were performed at the laboratory of the Texas Parks and Wildlife Department Coastal Conservation Association, Marine Development Center (MDC) hatchery in Corpus Christi, Texas, USA during November 2013. Red drum brood stocks were collected from wild stocks throughout the lower Texas coast and were transported to the MDC. Broodstocks were held in hatchery tanks (13,250 L) and were subjected to a photoperiod and temperature cycle of 150 days to induce spawning (Arnold *et al*., 1976). During the spawning time, water quality conditions were maintained at a salinity of 38ppt and a seawater temperature of 25°C. A fiberglass egg collector (230 L) lined with a 300 µm mesh bag was connected to each brood tank. Seawater was moved by means of a mechanical air-lift from the brood tanks to the egg collectors via a surface skimmer located inside each tank. The spawned eggs came from five parental fish (3 females and 2 males) kept in the tank. After spawning, eggs flowed from the brood tanks to the collectors and were concentrated into 100 mL graduated-cylinders and volumetrically enumerated. Viable eggs floated to the surface within one-five minutes, and non-viable eggs sank to the bottom of the cylinder. Fertilized eggs were transported to the laboratory/aquariums for experiment.

Fifteen aquariums sized 48x34x30 cm were used for the experiment and were filled with the filtered seawater. Those aquariums were set up randomly for three replicates of each salinity of 28, 33, 38, 43, 48ppt (5ppt increments). Treatment of salinities was obtained using deionized freshwater to lower salinities or by adding artificial sea salt to increase salinity, while the salinity of 38ppt was a control salinity. The room temperature was set up at 27°C during the experimenta and the water temperature in all fifteen aquariums were kept at 25°C. Salinity, temperature and pH parameters were measured at the beginning and the end of the experiments using Hydrometer Model YSI 556 MPS meter. Aeration was provided to each aquarium. A photoperiod of twelve hours of light and twelve hours of dark was maintained during the trials.

A subsample of 130 eggs was examined using a dissecting microscope (4x, magnification) with an ocular micrometer to measure the egg diameter and oil globule to the nearest 1 µm. Fertilized eggs were placed into plastic egg containers that had two sides in openings condition covered only by a net of a 300 µm mesh size to facilitate seawater flow through the containers. Three egg containers were placed in each aquarium and 130 fertilized eggs were stocked in each egg container. A total of nine egg containers (1,170 eggs) per salinity treatment were tested. All the eggs were in the embryo stage. Egg distribution into the containers was completed within one hour, and the experimental trials were conducted for thirty-six hours. The hatching success of eggs was determined after exposure. All yolk-sac larvae from each container were collected by pouring them unto a plastic tray for enumeration. Larval characteristics were determined by the number of eggs hatched (%), normal and deformity of larvae were counted for each container, and a sub-sample of thirty larvae from each container were measured in terms of the total length (TL) using Micron 1 Imagine software. Larvae were measured from the tip of the snout to the end of the notochord to the nearest 0.01 mm (Zacharia and Kakati, 2004). The hatching rate was calculated by dividing the number of larvae by the total number of eggs in a container. Descriptive statistical analysis was performed using Excel 2010. All data were analyzed using SPSS® software. A one-way ANOVA (α = 0.05) was used to analyze salinity effects on the larval length between and within the test salinities and was followed by post hoc test in the ANOVA to test the difference between mean of red drum yolk sac larvae and TL at different salinities. Salinity was an independent variable, whereas the dependent variable was the TL of larval.

3. Results

Mean seawater temperature (± SD) and pH in all tanks during the experiment were 24.65±0.22ºC and 8.08±0.03 respectively. Mean salinity for each treatment was 28.41±0.20, 33.33±0.28, 38.14 ±0.999, 43.21 ± 0.16 and 48.4±0.22ppt. The ranges of salinity selected below 43ppt were representative of conditions occurring in coastal waters during the normal spawning season of red drum and the high salinity (≥ 43ppt) was representative of lower Texas coast bay conditions.

The fertilized red drum eggs contain one oil globule. Diameters of 100 fertilized eggs ranged between 0.91 and 0.99mm, and the mean ± SD diameter was 0.96± 0.03mm and with an average of oil globules ranged from 0.17–0.20mm with the mean ± SD diameter was 0.23± 0.02mm. Those numbers indicated that the eggs were almost of uniform size, and based on the visual observations using microscope, those eggs were all in a normal condition; that they were spherical and transparent with buoyancy (Song *et al*., 2013). Salinity affected both egg hatching and development (length) of yolk-sac larvae (Table 1). Successful hatching occurred at all the salinities tested, but the lowest rate occurred at the 48ppt treatment. Red drum eggs held at the 38ppt showed the highest percentage of hatching success, and the longest in TL of larvae compared to other salinity treatments. Mean TL of yolk sac larvae reared in the lower (28ppt) and higher (48ppt) salinities was shorter in length than in other salinities (Table 1), and the average TL of yolk-sac larvae was 2.525±0.133mm.

Table 1. Number of viable larvae, hatching success (%) of red drum eggs and mean total length (TL) of red drum larvae maintained at different salinities

Salinity (ppt)	n±SD	Egg hatch (%)	n	Mean TL±SD (mm)
28	66±2.7	61	30	2.426 ± 0.092
33	71±9.5	69	30	2.591 ± 0.075
38	87±1.4	76	30	2.659 ± 0.059
43	66±6.6	63	30	2.620 ± 0.057
48	52±3.1	48	30	2.410 ± 0.099

The one-way ANOVA results show that the TL of yolk sac larvae are affected both by the lowest (28 ppt) and by the highest (48ppt) salinity treatments ($P < 0.05$).

The post hoc test shows that the TL of yolk-sac larvae differ significantly among salinities, and they can be divided into two groups. Yolk-sac larvae from lower (28ppt) and hyper salinity (48ppt) have no significance difference, but they are significantly different ($P < 0.05$) with the other treatments (33, 38 and 43ppt).

4. Discussion

Salinity is an important environmental factor for the hatching of red drum eggs and larval survival (Holt *et al*., 1981), and it can affect fish egg fertilization rates, reduce hatchability rates, change buoyancy (Holliday, 1969), cause morphological deformities and decrease larvae survival rates (Kucera *et al*., 2002). Moreover, it was a significant factor affecting energy in juvenile red drum development (Norris, 2016). Red drum spawn during the fall along the Texas coast and tidal currents carry the eggs and larvae into estuarine nursery grounds (Holt *et al*., 1985, Rooker *et al*., 1997) that have salinity varying from brackish to hypersaline (Holt and Holt, 2002).

In this study, red drum eggs were hatched at a wide range of salinity treatment. Egg hatch-out rates and larvae growth were reduced at the lowest and highest salinity treatment. Hypersalinity (≥ 40ppt) and a temperature of 25ºC affected the hatching success of red drum eggs. The brood fish for this study were growing at the salinity of 38ppt and 24ºC, and the results show that the highest percentage of hatching success was in the 38ppt. Early life stage development of other sciaenid fish such as Greenback flounder (*Rhombosolea tapirina*), summer flounder (*Paralichthys dentatus*), and Southern flounder (*Paralichthys lethostigma*) was affected by salinity concentrations (Smith *et al.*, 1999; Specker *et al*., 1999; Hart and Purser, 1995; Lee *et al*., 1984). Holt *et al*. (1981) and Lee *et al*., (1984), investigated the early life history stages of red drum as affected by different temperature and salinity combinations from 22-33ºC and 20-40ppt. Hatching occurs within twenty-eight to twenty-nine hours when water is maintained at a 22ºC, and it takes a slightly longer time in cooler water and a slightly shorter time in warmer waters.

The salinity of the water in which the parents lived affected the response of developing cyprinodont fish to salinity (Kinne and Kinne, 1962). Other studies have demonstrated that the larvae of another sciaenid spotted seatrout (*Cynoscion nebulosus*) hatched from eggs spawned at high salinities are more tolerate for higher salinities than larvae hatched from the eggs spawned at lower salinities (Holt and Holt, 2002; Kucera *et al*., 2002). The seatrout seemed to be better suited to conditions that were typical of their habitats. This study demonstrated that the percentage of egg hatching success and length of larvae were reduced in both lowest (28ppt) and/or hypersalinity (48ppt). As described by Bakun (1996) for marine fishes, it seems that the success of other salinity treatments is associated more with mean conditions than extreme conditions. Less saline seawater has lower density and red drum egg yolks are absorbed faster by the larva to maintain their position in the water column (Ponwith and Neill, 1995) and there may not be enough energy left for larval growth. If red drum yolk-sac larvae are unable to survive through their first feeding stage, this may be a contributing factor to year-class strength. The salinity tolerances observed provide additional information about the survival of red drum in the early life stages.

5. Conclusion

This study demonstrates that red drum eggs can hatch within a wide range of salinities with the best hatch-out and growth rates occurring between 33 – 43ppt. Because Texas bays and estuaries experience salinity fluctuations caused by natural weather events (e.g., droughts, reduced freshwater inflows, and hurricanes), this might leave an impact on red drum early life stages in their wild population.

Acknowledgments

Grateful acknowledgement is made to the staffs at Texas Parks and Wildlife Department Coastal Fisheries Division, and the CCA Marine Development Center in Corpus Christi. Special thanks go to Ivonne Blandon, Rodney Gomez, and his team for providing the red drum eggs and other supporting facilities used in this study. This study was conducted with the funding for IK by a Fulbright-DIKTI 2013 scholarship.

References

Arnold CR, Lasswell JL, Bailey WH, Williams TD and Fable WA. Jr. 1976. Methods and techniques for spawning and rearing spotted sea-trout (*Cynoscion nebulosus*) in the laboratory. *Proc. a. Conf. SEast. Ass. Fish & Wildlife Agency*, **30**: 167-178

Bakun A.1996. **Patterns in the Ocean - Ocean Processes and Marine Population Dynamics**. California Sea Grant College Program, La Jolla, CA; pp 174-177.

Blaxter JH. 2000. The enhancement of marine fish stocks. In: Southward AJ, Tyler PA, Young CM, and Fuiman LA. (Eds.), **Advances in Marine Biology**. Academic Press, New York; pp 2-47.

Buskey EJ, Liu H, Collumb C and Bersano JGF. 2001. The decline and recovery of a persistent Texas brown tide algal bloom in the Laguna Madre (Texas, USA). *Estuaries***, 24**: 337-346.

Comyns BH, Lyczkowski-Shultz J, Nielend DL and Wilson CA. 1991. Reproduction of red drum, *Sciaenops ocellatus* in The North Central Gulf of Mexico: Seasonality and spawner biomass. U.S. Department Commerce, National Oceanic and Atmospheric Administration Technical Report National Marine Fisheries Service. Silver Spring, Maryland 95; pp 17–26.

Hart PR and Purser GJ. 1995. Effects of salinity and temperature on eggs and yolk sac larvae of the greenback flounder (*Rhombosolea tapirina* Gunther, 1862). *Aquaculture***, 136:** 221-230.

Holiday FGT. 1969. The effects of salinity on eggs and larvae of teleosts. In: Hoar WS, Randall DJ. (Eds.), **Fish Physiology** vol 1. Academic Press, New York; pp 47-65.

Holt GJ and Holt SA. 2002. Effects of variable salinity on reproduction and early life stages of spotted seatrout. In **Biology of the Spotted Seatrout.** CRC Press; pp 135-145.

Holt SA, Holt GJ and Arnold CR.1989. Tidal stream transport of larval fishes into non-stratified estuaries. *Rapp P V Reun Cons Int Explor Mer*., **191**: 100-104.

Holt SA, Holt GJ and Arnold CR.1985. Diel periodicity of spawning in sciaenids. *Mar. Ecol. Prog. Ser***., 27:** 1-7

Holt GJ, Godbout R and Arnold CR. 1981. Effect of temperature and salinity on eggs hatching and larval survival of red drum *Sciaenopsocellata*. *Fish Bull*.**,79**: 569-573.

Kinne O and Kinne EM. 1962. Rates of development in embryos of cyprinodont fish exposed to different temperature-salinity-oxygen condition. *Can J Zool*.**, 40**: 231-253.

Kucera CJ, Faulk CK and Holt GJ. 2002. The effect of spawning salinity on eggs of spotted seatrout (*Cynoscion nebulosus*, Cuvier) from two bays with historically different salinity regimes. *J Exp Mar Bio Ecol***., 272**: 147-158.

Lee WY, Holt GJ and Arnold CR. 1984. Growth of Red Drum Larvae in the Laboratory. *Trans Am Fish Soc*., **11:** 245-246.

Matlock GC. 1990a. The life history of red drum. In: **Red Drum Aquaculture**, **Proceedings of a Symposium of the Culture of Red Drum and Other Warm Water Fishes**. Galveston, Texas, Texas A&M University Sea Grant College Program.

Matlock GC. 1990b. Preliminary results of red drum stocking in Texas. In: **Marine farming and enhancement. Proceedings of the 15th U.S. Japan Meeting on Aquaculture**. U.S. Department of Commerce, National Oceanic and Atmospheric Administration, National Marine Fisheries Service, NOAA Technical Report NMFS 85, Washington, D.C.; pp 11-15.

McEachron LW, McCarty CE and Vega RR. 1995. Beneficial uses of marine fish hatcheries: enhancement of red drum in Texas coastal waters. In: Schramm HL, Piper RG (Eds), **Uses and Effects of Cultured Fishes in Aquatic Ecosystems**. Am. Fish.Soc., Symp.15, Bethesda, Maryland; pp 161-166.

Miles DW. 1950. The life histories of spotted seatrout, *Cynoscion nebulosus*, and the redfish, *Sciaenops ocellatus*. **Texas, Game Fish Community**, **Rockport, Texas, 49**: pp 66-103.

Neill WH. 1990. Environemtal requirements of red drum. In: Chamberlain GW, Miget RJ, Haby MG (Eds.), **Red Drum Aquaculture**.Texas A&M Sea Grant College Program No. TAMU-SG-90-603: pp 22-24.

Norris BJ. 2016. The effect of pH and salinity of juvenile hatchery reared red drum (*Sciaenops ocellatus*). MSc Thesis, Texas A&M University, Corpus Christy, USA.

Pattillo ME, Czapla TE, Nelson DM and Monaco ME.1997. Distribution and abundance of fishes and invertebrates in Gulf of Mexico estuaries, Vol II: Species life history summaries. **Estuarine Living Marine Resources Program Report 11**. National Oceanic and Atmospheric Administration/National Ocean Service Strategic Environmental.

Peters KM and McMichael RH. 1987. Early life history of the red drum, *Sciaenops ocellatus* (Pisces: Sciaenidae), in Tampa Bay, Florida. *Estuaries*, **10:** 92-107.

Ponwith BJ and Neill WH. 1995. The influence of incubation salinity on the buoyancy of red drum eggs and yolk sac larvae. *J Fish Bio*.**, 46:** 955-960.

Rooker JR, Holt GJ and Holt SA. 1997. Condition of larval and juvenile red drum (*Sciaenops ocellatus*) from estuarine nursery habitats. *Mar Bio*.,**127**: 387-394.

Rounsefell GA. 1975. Ecology, utilization and management of marine fishes. C.V. Mosby Co. St. Louis; pp 516.

Smith TIJ, Denson MR, Heyward LD, Jenkins WE and Carter LM. 1999. Salinity effects on early life stages of southern flounder *Paralichthys lethostigma*. *J World Aqua Soc***., 30**: 236-244.

Song YB, Lee CH, Kang HC, Kim HB and Lee YD. 2013. Effect of Water Temperature and Salinity on the Fertilized Egg Development and Larval Development of Sevenband Grouper, *Epinephelus septemfasciatus*. *Dev Reprod*., **17**: 369-377.

Specker JL, Schhreiber AM, McArdle ME, Poholek A, Henderson J and Bengtson DA.1999. Metamorphosis in summer flounder: effects of acclimation to low and high salinities. *Aquaculture***, 176:** 145-154.

Swingle WE. 1990. Status of the commercial and recreational fishery, In Chamberlain GW, Miget RJ, Haby MG (Eds.), **Red Drum Aquaculture**. Texas A&M Sea Grant College Program No. TAMU-SG-90-603; pp 22-24.

Zacharia S and Kakati VS. 2004. Optimal salinity and temperature for early developmental stages of *Penaeus merguiensis* De man. *Aquaculture*, 232: 373-382.

Subscription

Jordan Journal of
Biological Sciences

An International Peer – Reviewed Research Journal

Published by the Deanship of Scientific Research, The Hashemite University, Zarqa, Jordan

Name: ..... الاسم:

Specialty: ..... التخصص:

Address: ..... العنوان:

P.O. Box: ..... صندوق البريد:

City &Postal Code:..... المدينة: الرمز البريدي:

Country: ..... الدولة:

Phone: ..... رقم الهاتف

Fax No.: ..... رقم الفاكس:

E-mail: ..... البريد الإلكتروني:

Method of payment: ..... طريقة الدفع:

Amount Enclosed: ..... المبلغ المرفق:

Signature: ..... التوقيع:

Cheque should be paid to Deanship of Research and Graduate Studies – The Hashemite University.

I would like to subscribe to the Journal

For

- ☐ One year
- ☐ Two years
- ☐ Three years

One Year Subscription Rates

	Inside Jordan	Outside Jordan
Individuals	JD10	$70
Students	JD5	$35
Institutions	JD 20	$90

Correspondence

Subscriptions and sales:

Prof. Khaled H. Abu-Elteen
The Hashemite University
P.O. Box 330127-Zarqa 13115 – Jordan
Telephone: 00 962 5 3903333 ext. 4399
Fax no. : 0096253903349
E. mail: jjbs@hu.edu.jo

المجلة الأردنية للعلوم الحياتية
Jordan Journal of Biological Sciences (JJBS)

http://jjbs.hu.edu.jo

المجلة الأردنية للعلوم الحياتية: مجلة علمية عالمية محكمة ومفهرسة ومصنفة، تصدرعن الجامعة الهاشمية وبدعم من صندوق البحث العلمي والابتكار – وزراة التعليم العالي والبحث العلمي.

ترسل البحوث الى العنوان التالي:

رئيس تحرير المجلة الأردنية للعلوم الحياتية

الجامعة الهاشمية

ص.ب , 330127 , الزرقاء, 13115 , الأردن

هاتف: 0096253903333 فرعي 4357

E-mail: jjbs@hu.edu.jo, Website: www.jjbs.hu.edu.jo

المملكة الأردنية الهاشمية

المجلة الأردنية

للعلوم الحياتية

مجلة علمية عالمية محكمة

تصدر بدعم من صندوق دعم البحث العلمي و الابتكار

http://jjbs.hu.edu.jo/